Georgia Water Resources Institute
Annual Technical Report
FY 2002

Introduction

The GWRI mission is to foster the creation of partnerships, resources, and knowledge base necessary to address current water resources challenges in the state of Georgia, the U.S., and the world. Specific GWRI goals include:

a) Develop new research methods and scientific knowledge to support sustainable river basin planning and management;

b) Educate scientists, engineers, and water professionals in state-of-the-science methods and their potential applications; and

c) Disseminate useful information to policy makers, water managers, industry stakeholders, citizen groups, and the general public.

In keeping with the above-stated mission and goals, during Fiscal Year 2002, the Georgia Water Resources Institute (GWRI) was involved in a wide range of activities at the state, national and international levels. The following sections summarize these activities as they pertain to research, education, technology transfer, and professional and policy impact.

RESEARCH PROJECTS:

Reservoir Shoreline Erosion and Sedimentation Analysis: Lake Hartwell, SC/GA, sponsored by GWRI/USGS104B;

Developing a Regional Water Management and Planning Initiative Model: Using Regional Leadership Summits to Address Water Resource Challenges in the Flint River Watershed, GA, sponsored by GWRI/USGS104B;

Investigation of Chlorination and Ozonation of Antibiotics Detected in Georgia Waters, sponsored by GWRI/USGS104B;

Mid Infrared Water Quality Sensors for the Detection of Organic Pollutants, sponsored by GWRI/USGS104G;

Nile Decision Support System, sponsored by the Food and Agriculture Organization of the United Nations (FAO/UN);

INFORM: Integrated Forecast and Reservoir Management System for Northern California, sponsored by NOAA, California Energy Commission, and CalFed;

EDUCATION AND TECHNOLOGY TRANSFER:

USGS Graduate Student InternshipGroundwater Modeling for Coastal Aquifers;

Georgia Water Resources Conference, co-sponsorship and electronic proceedings development;

Hydrologic Engineering for Dam Design, continuing education course;

Nile Decision Support Tool Software Training Workshops, sponsored by the Food and Agriculture Organization (FAO) of the United Nations, Dar Es Salaam, Tanzania, and Entebbe, Uganda;

PROFESSIONAL AND POLICY IMPACT:

GWRIs involvement in Africa (Nile DST) and California (INFORM) has the potential for significant policy impact. The Nile DST has now been disseminated to all 10 Nile countries (Burundi, Congo, Egypt, Eritrea, Ethiopia, Kenya, Rwanda, Sudan, Tanzania, and Uganda) and is used to generate the information base for policy dialogue among the Nile partners. In the course of FY 2002, GWRI personnel worked closely with country ministers, heads of agencies, engineers, and scientists to support their information needs.

In the US, INFORM is a project that is motivated by the water and energy shortages in California. INFORM brings together all relevant agencies and stakeholder groups associated with the Sacramento and American Rivers in Northern California. Participating agencies include the National Weather Service, the US Army Corps of Engineers, the US Bureau of Reclamation, the Sacramento Flood Control Authority, US EPA, California Department of Water Development, and the California Energy Commission. The project aims at developing the institutional framework and technical tools necessary to support integrated river basin management.

Research Program

Toxic Metalloid (As, Se, Sb) Enrichment from Coal-Fired Power Plants in the Chattahoochee-Apalachicola (ACF) & Etowah-Coosa (ACT) Rivers

Basic Information

Title:	Toxic Metalloid (As, Se, Sb) Enrichment from Coal-Fired Power Plants in the Chattahoochee-Apalachicola (ACF) & Etowah-Coosa (ACT) Rivers
Project Number:	2002GA5B
Start Date:	3/1/2002
End Date:	2/28/2003
Funding Source:	104B
Congressional District:	
Research Category:	None
Focus Category:	Water Quality, Toxic Substances, Geochemical Processes
Descriptors:	None
Principal Investigators:	Philip Nissen Froelich

Publication

1. Lesley, Michael P., 2002, "The Fluxes and Fates of Arsenic, Selenium, and Antimony from Coal Fired Power Plants to Rivers," Geochemistry, School of Earth and Atmospheric Sciences, Georgia Tech, Atlanta, GA, 133 pages.

The Fluxes and Fates of Arsenic, Selenium, and Antimony from Coal Fired Power Plants to Rivers

School of Earth and Atmospheric Sciences
Georgia Institute of Technology

prepared by:
Michael Patrick Lesley
Philip N. Froelich, Jr.

sponsored by:
Georgia Water Resources Institute
and
The U.S. Geological Survey

October 2002

ACKNOWLEDGEMENTS

I believe the completion of this thesis is due more to those around me than myself. I did the leg work, but you all pulled me through. I would like to thank the members of my thesis reading committee, Dr. Philip (Flip) N. Froelich, Dr. Ellery Ingall, Dr. Martial Taillefert, and Dr. Herb Windom for their advice and insight during this process. In particular, I would like to extend Flip a huge thanks. He has put up with me for two years and has driven me to produce a solid piece of science that I am very proud of.

I am extremely grateful to my wife Becca who has *also* put up with me for two years, and who has given up more than one Friday night to help me in the lab.

I would like to thank my fellow geochemistry graduate students (especially Jean Fracois Kopervnijak and Poloumi Sanigrahi) for their fellowship, advice, and support.

There are two people without whom this project would not have been completed. They are Dr. Stephany Rubin-Mason and Chris Bartley. Chris provided *all* the nutrient data for this project. He got up early with me for sampling trips, and worked late analyzing samples after I was able to go home. For this, I am grateful. Stephany has been a constant source of encouragement and advice. She has taught me more about the lab and doing science than I thought I would ever know. Stephany and Chris, I can't thank you enough.

And a final dubious thanks to the Foster Falls copperhead population, who got me busted for skipping school and who gave Flip verbal ammunition for a lifetime.

TABLE OF CONTENTS

CHAPTER

I INTRODUCTION

LIST OF TABLES

LIST OF FIGURES

LIST OF SYMBOLS

ppb	part per billion (µg / L)
ΔG_f	Gibbs Free Energy of Formation
ICP-MS	Inductively Coupled Plasma-Mass Spectrometry
C	Analyte Concentration
m	Slope of the Calibration Curve
R_s	Ratio of Analyte to Internal Standard
A	Isotopic Abundance of Analyte in Nature
C_{sus}	Concentration of Metalloids in Suspended Solids
C_{ex}	Metalloid Concentration of Filter Extract
M_{sed}	Mass of Sediment per Volume Water
F	Volume River Water Through Filter
E_{eff}	Metalloid Escape Efficiency
B	Mass of Coal Burned per Unit Time
R	Metalloid Release in Mass per Unit Time
Q	Stream Flow
F_{ss}	Suspended Sediment Metalloid Flux

SUMMARY

The toxic metalloids arsenic (As), selenium (Se) and antimony (Sb) are mobilized to their local aquatic environments during coal combustion. Measurements above and below power plants on the Chattahoochee River have allowed the quantification of this flux. From this flux I have been able to estimate the escape efficiency of As, Se, and Sb from power plants to rivers. Mass balance modeling has shown that the aqueous input from fly ash effluent is not sufficient to balance downstream loss. I hypothesize that this extra input is in the form of ash that sluices out of the holding ponds when they are released to rivers.

I have estimated the partitioning of As, Se, and Sb between the aqueous, suspended sediment, and biologic systems as the contaminant plume moves downstream. Calculations show that bio-removal of metalloid elements is the dominant metalloid sink in contaminated rivers.

This study compares estimates of metalloid release to EPA Toxic Release Inventories (TRI) and the PISCES model. My findings show that TRI estimates are too low by a factor of two or more. The PISCES model predicts that the majority of Se and Sb in coal are lost to the atmosphere via stack gas. Aqueous escape efficiency estimates show that Se and Sb are partitioned both onto fly ash and lost via stack gas.

Finally, a before / after comparison of metalloid flux has been made based on historic and recent samples of a large coal fired power plant that has been converted from a wet ash disposal system to a dry ash disposal system.

CHAPTER I

INTRODUCTION

1.1 Rationale and Objectives

The majority of electrical power in the United States is generated by power plants burning coal. With many nuclear power plants reaching the end of their projected lifetimes, the lack of new construction of nuclear power plants, the lack of funding for other renewable energy sources, and large US coal reserves (200-300 years at current rates of usage), this percentage will increase in the next 25-50 years. Coal combustion is a notoriously dirty process. Much attention has been paid to the airborne effects of coal combustion and to methods to control airborne pollutants. The effect of coal combustion on the aquatic environments immediately surrounding coal fired power plants (CFPPs) has received far less attention.

Work in the 1980's by Froelich (1985) showed enrichment in the metalloid element Germanium (Ge) in waters receiving ash pond effluent from coal fired power plants. It follows that these waters should also be enriched in the other toxic metalloids Arsenic (As), Selenium (Se,) and Antimony (Sb). The objective of this research has been to quantify the flux of metalloids from coal fired power plants to local receiving waters, to trace the fates of metalloids downstream through inorganic and biologic reactions, and to evaluate the accuracy of US EPA methods and estimates.

1.2 Clean versus Dirty Rivers

1.2.1 Natural Backgrounds

The metalloid concentration in contaminated rivers can be orders of magnitude higher than in rivers not impacted by anthropogenic change. The typical concentration ranges in clean rivers of As, Se, and Sb are 0.5-2.0 ppb (Francesconi and Kuehnelt 2002), 0.1 ppb (this study), and <1.0 ppb (Filella et al. 2002), resepectively.

Metalloids in natural waters are the result of the weathering of rocks containing metalloid minerals. The high concentration of As in rocks is due to the substitution of As in the crystal lattices of silicate minerals, particularly in place of Si, Al, and Fe (Bhumbala and Keefer, 1994). Arsenic is commonly associated with pyrite, forming several arseno-sulfide (AsS) minerals; Arsenopyrite (FeAsS), Cobaltite (CoAsS), and Prousite (Ag_3AsS_3) (Francesconi and Kuehnelt 2002). High levels of Se in streams and rivers in the western United States have been associated with the weathering of certain Cretaceous and Tertiary age rock formations, particularly shales (Stephens and Waddel, 1998). Antimony in nature occurs mainly in the forms of Stibnite (Sb_2S_3) and Valentinite (Sb_2O_3) (Filella et al. 2002). These minerals are commonly associated with Barite bearing strata (Klien and Hulbut 1993).

1.2.2 Metalloid Uses and Sources of Contamination

Arsenic, selenium, and antimony have a wide variety of industrial uses. The manufacturing of commercial products is the main source of anthropogenic As to the environment, representing 40% of the total flux. (Bhumbala and Keefer 1994). One of the largest uses of As is in the wood preservative copper chromated arsenate (CCA). CCA treated wood is used ubiquitously in outdoor building. The US EPA is currently requesting a voluntary industry-wide effort to phase out CCA use in lumber for domestic use by 2004 (www.epa.gov/pesticides/citizens/1file.htm). Release of As from coal combustion by products represents the second highest (20%) flux to the environment. Between 4% and 40% of the As in coal ash is water extractable. 100% of ash borne As is extractable at pH < 7 (Bhumbala and Keefer 1994).

Selenium has been used as an agricultural supplement for animals since its discovery as an essential micronutrient in the 1960's. These practices led to concerns regarding the toxicity of Se metabolites in livestock urine and manure. Subsequent studies revealed concentrations as high as 7.3% Se in dry matter and 133 ppb in the aqueous phase in manure lagoons (Oldfield 1998). Concentrations of this magnitude present serious concerns regarding the possibility of groundwater Se contamination in aquifers beneath livestock waste lagoons.

Selenium has also been the culprit behind fish reproductive failures and population declines in freshwater lakes receiving ash pond effluent. In the 1980s an in depth study of Hyco Reservoir, a reservoir receiving ash pond effluent from the Roxboro CFPP revealed water concentrations reaching as high as 15 ppb in 1985 (Crutchfield 2000). Subsequent studies conducted after the Roxboro plant converted to dry ash disposal have shown a decline in Se concentrations to near background levels in both water and fish tissue samples.

Antimony is widely used industrially. Alloying lead with Sb greatly increases its hardness and mechanical strength in applications such as batteries, small arms bullets, and cable sheathing. Antimony trioxide (Sb_2O_3) has strong flame retardant properties and is widely used in plastics, adhesives, and cloth. Alloyed Sb is commonly reclaimed through recycling. However, recent trends towards the use of Sb in non-recyclable products such as paints, plastics, and adhesives have led to the release of more Sb to the environment (Filella et al. 2002).

1.3 Solubility and Stability

1.3.1 Speciation

This section discusses the major species of As, Se, and Sb found in nature. It includes Gibbs Free Energy of Formation (ΔG_f) values and Eh-pH diagrams for the major aqueous phases of these elements.

1.3.1.1 Redox Speciation

Arsenic has two major valence states, arsenite (As(III)) and arsenate (As(V)). As(-III) can be formed in certain reducing conditions, however, these conditions are not prevalent in natural systems. Table 1-1 contains ΔG_f in kcal / mol data for the major redox species of As in natural waters. This table contains data for a number of AsS compounds. These compounds are extremely important in reducing environments, such as swamps, where coal formation takes place. Figure 1-1 shows two Eh-pH diagrams. Figure 1-1A shows the As acid-base / redox speciation in a system with no S present. From the diagram it can be seen that in oxidizing / pH neutral waters the As(V) species $HAsO_4^{2-}$ dominates. This is of critical importance as As(V) species have a high affinity for Fe and Mg oxyhydroxide minerals. These relationships play a critical role in the

Table 1-1 Arsenic ΔG$_f$ values

Table 1-1 contains the ΔG$_f$ values for the major As redox species found in natural water systems. In the state column, “c” is crystalline and “aq” is aqueous. ΔG$_f$ is in units of kcal per mol.

Species	State	ΔG$_f$ (kcal/mol)
As	C	0.00
AsS	C	-16.80
As_2S_3	C	-40.30
As_2O_3	C	-137.66
H_3AsO_4	Aq	-183.08
$H_2AsO_4^-$	Aq	-180.01
$HAsO_4^{2-}$	Aq	-170.69
AsO_4^{3-}	Aq	-154.97
H_3AsO_3	Aq	-152.92
$H_2AsO_3^-$	Aq	-140.33
$HAsO_3^{2-}$	Aq	-125.31
AsO_3^{3-}	Aq	-107.00

Data from Brookins 1988

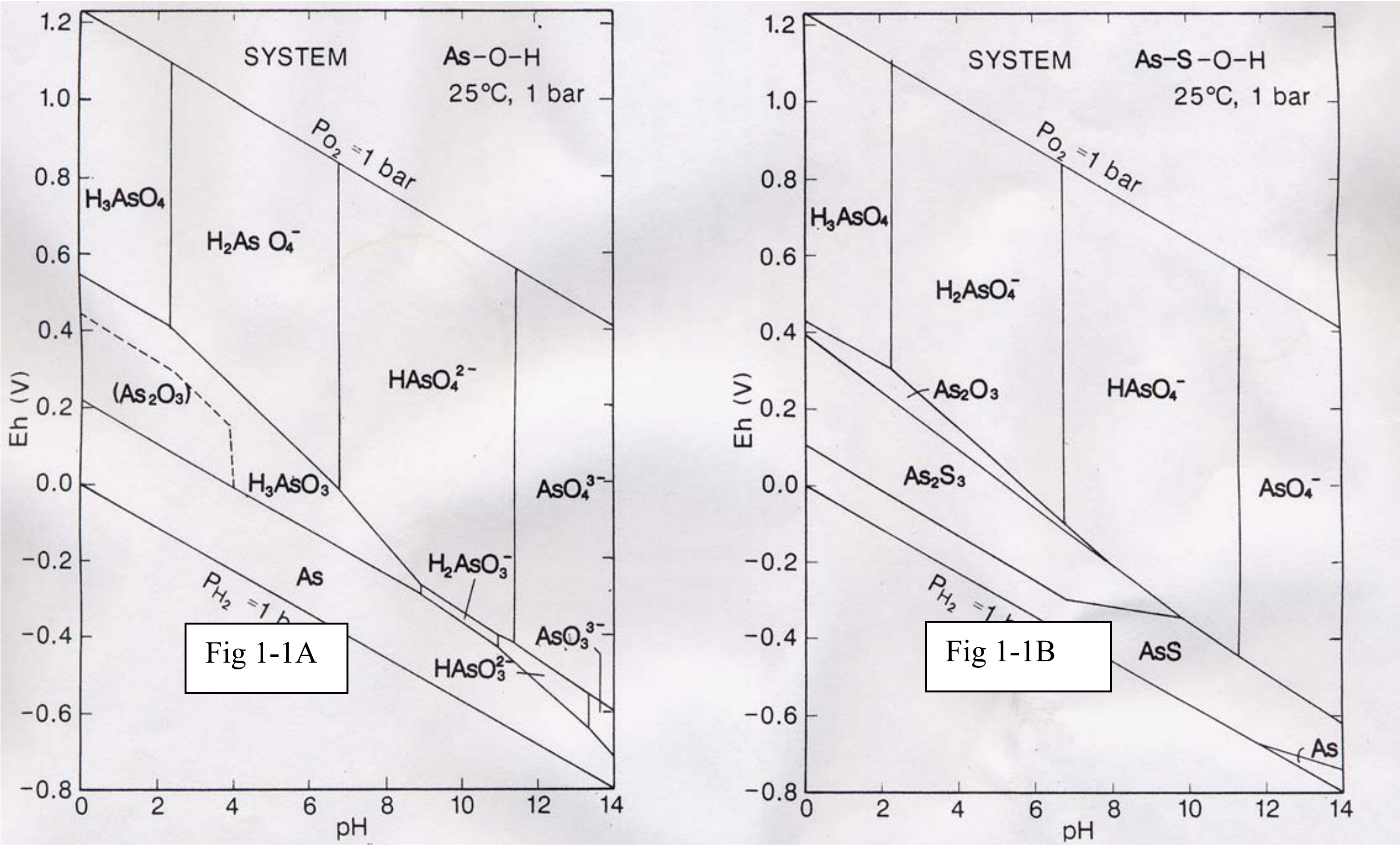

From Brookins 1988

Figure 1-1 As Eh-pH Diagram. Figure 1-1 A shows the Eh-pH diagram for the simple As acid-base system $\{As\}=10^{-6}$ $\{S\}=10^{-3}$. Figure 1-1 B shows the As acid-base system but includes sulfur species in reducing conditions.

mobility of As in the environment.

As (V) is less mobile and more strongly attracted to hydrous iron oxides than As (III). Through adsorption onto and co-precipitation with hydrous iron oxides much of the As (V) can be removed from a contaminated river (Mok and Wai 1994). If As is sorbed onto the surface of sediment suspended in streams, it can be transported to downstream to a reservoir where it settles. If the bottom waters of the reservoir become anoxic, insoluble Fe(III) can be reduced to soluble Fe (II). If this occurs the As (V) sorbed onto the Fe (III) minerals is mobilized into the bottom waters of the reservoir, usually in the reduced form of As (III). A similar phenomenon occurring in tube wells in Thailand and Nepal has been responsible for thousands of cases of chronic As poisoning. Agget and O'Brien (1985) discovered evidence of this phenomenon in anoxic sediments in Lake Ohakuri in New Zealand. They noted that while As (III) and As (V) were both mobilized to the water column from the dissolution of hydrous iron oxide bearing sediments, in sediments with appreciable amounts of S some of the As was sequestered through the precipitation of arsenopyrite (FeAsS) and orpiment (As_2S_3).

Selenium has oxidation states of Se (VI), Se (IV), Se (0) and Se (-II). However Se (-II) formation occurs outside the Eh-pH stability field for water. Table 1-2 contains the ΔG_f values for the major Se species in natural waters. Figure 1-2 shows the Eh-pH diagram for Se. The diagram shows that at neutral pH Se can exist in the +6, +4, and 0 valence states. Se (-II) can substitute for S(-II) in crystal lattices and in biological pathways (Brookins 1988). There is evidence that Se (IV) is more bioavailable because it is easier to reduce in cell pathways than Se (VI) . All Se that crosses the cell

Table 1-1 Selenium ΔG_f values

Table 1-2 contains the ΔG_f values for the major Se redox species found in natural water systems. In the state column, "c" is crystalline and "aq" is aqueous. ΔG_f is in units of kcal per mol.

Species	State	ΔG_f (kcal/mol)
Se^{2-}	Aq	30.90
HSe^{-}	Aq	1050.00
H_2Se	Aq	3.80
H_2Se0_3	Aq	-101.85
$HseO_3^{-}$	Aq	.98.34
SeO_3^{2-}	Aq	-88.38
$HSeO_4^{-}$	Aq	-108.08
SeO_4^{2-}	Aq	-105.47

Data from Brookins 1988

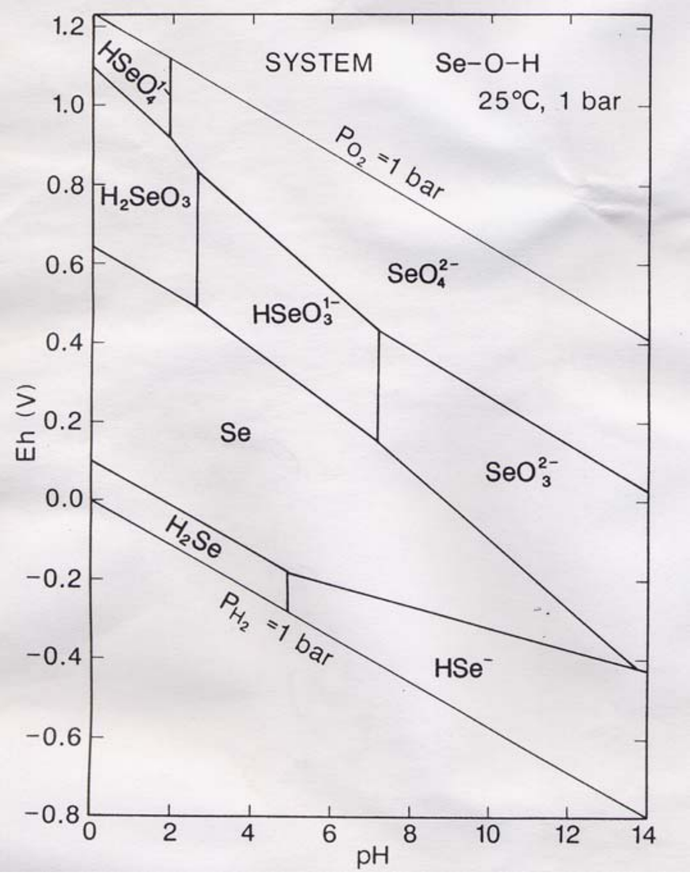

From Brookins 1988

Figure 1-2 Se Eh-pH Diagram. Figure 1-2 shows the Se Eh-pH diagram for the main inorganic Se species in natural waters. {Se}=10^{-6}

membrane is reduced to Se (-II). Se (IV) is the favored species for uptake as it is energetically favorable to reduce as compared to Se (VI).

Table 1-3 contains the ΔG_f data for the major Sb species in natural waters. Figure 1-3 shows the Eh-pH diagram for the Sb-S system in natural waters. From this diagram, thermodynamics predict that Sb (III) should be the dominant species in anoxic conditions and Sb (V) should be the dominant species in oxic waters. However, studies have shown Sb (III) present in oxic conditions and Sb (V) in anoxic conditions. This suggests that the controls on Sb speciation are kinetic as well as thermodynamic (Filella et al. 2002). Little is known about the uptake of Sb by organisms.

1.3.1.2 Organometalloid Speciation

Arsenic, selenium, and antimony are known to have organometallic speciation as well as redox speciation. In the case of As, there are mono and di-methylarseno acids for both the +3 and the +5 redox states (Newman et al. 1998): monomethylarsonic acid and dimethylarsinic acid (As (V)) and monomethylarsonous acid and dimethylarsenious acid (As (III)). While these compounds are the most widely occurring, arsenic organometallic speciation is not limited to simple methyl compounds. Arsenobetaine, aresenosugars and other larger organoarsenic compounds are produced by macrofauna. However, these compounds make up little of the total concentration of As in natural waters.

Like arsenic, selenium has a number of methyl and more complex organo species. Cooke and Bruland (1987) report nonvolatile seleno amino acids acids and a dimethylselenonium ion in addition to the volatile dimethylselenide and dimethyldiselenide species. They indicate that there is a biologically mediated pathway

Table 1-1 Antimony ΔG_f values

Table 1-2 contains the ΔG_f values for the major Sb redox species found in natural water systems. In the state column, “c” is crystalline and “aq” is aqueous. ΔG_f is in units of kcal per mol.

Species	State	ΔG_f (kcal/mol)
SbO+	aq	-42.33
SbO2-	aq	-81.31
Sb2S3	c	-41.49
Sb2S42-	aq	-23.78
HSbO2	aq	-97.39
Sb(OH)3	c	-163.77
Sb2O4	c	-190.18
Sb2O5	c	-198.18

Data from Brookins 1988

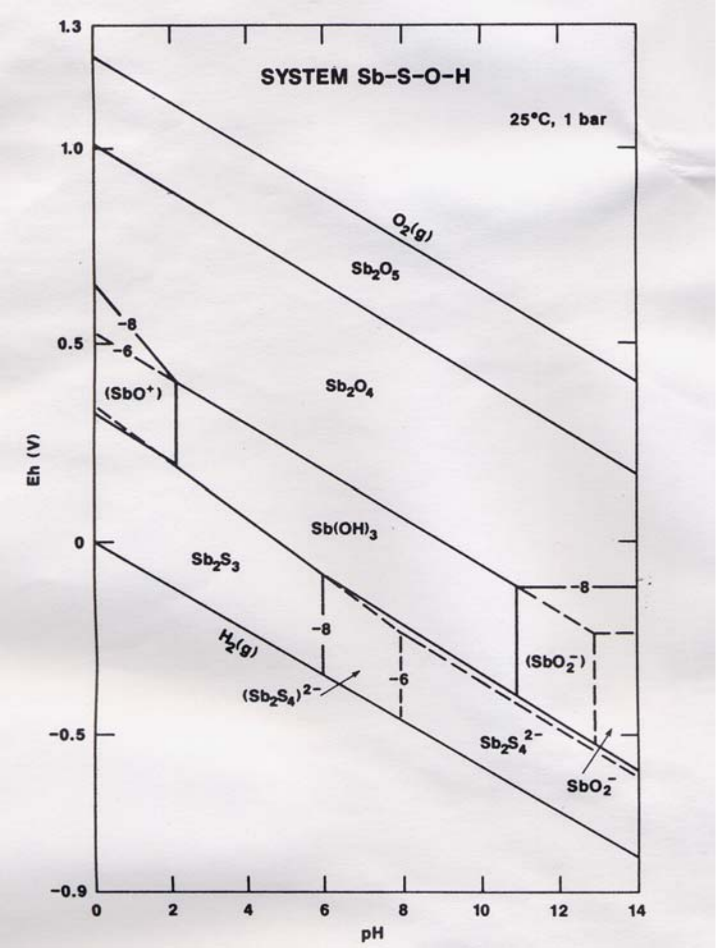

From Brookins 1988

Figure 1-3 Sb Eh-pH Diagram. Figure 1-3 shows the Eh-pH diagram for the main species of Sb-S system in natural waters. $\{Sb\}=10^{-6,-8}$ $\{S\}=10^{-3}$

from the dimethylselenonium ion to the volatile dimethyl selenide at neutral pH, and that this transformation may be an important process in the removal of Se from aqueous systems. Cutter and Bruland (1984) further distinguish that organo species of Se account for more than 80% of the total Se concentration in surface waters. They find that the maximum concentrations of reduced organo Se species (amino acids and sugars) in water column samples coincide with peaks in primary productivity, indicating that the formation of complex organo Se compounds is biologically mediated.

Evidence of biomethylation of Sb has been found in ocean water column studies (Andreae and Froelich 1984). However, these authors found no evidence of biomethylation by algae. This led them to hypothesize that biomethylation of Sb is a microbially mediated process. Recent studies show that certain fungi species can reduce and methylate Sb, releasing the volatile compound trimethylstibine in much the same manner some fungi species can reduce and methylate As to trimethylarsine (Andrewes et al. 2000).

1.3.2 Biotic Transformation

Recently much research has gone into the biotransformation of metalloids. This is due to the fact that metalloid toxicity depends greatly on speciation, and there is evidence that the organometallic species, produced exclusively biologically, may be more toxic to humans than inorganic species. There tend to be two classes of organisms that perform biological transformations, microbes and phytoplankton. Microbes, particularly in the case of As, seem to be responsible for the reduction of As (V) through respiration. Algae and plankton are responsible for both reduction and the production of methylated and more complex organic compounds.

Oremland et al. (2000) report that in high salinity stratified lakes arsenate respiration can become nearly as important as sulfur reduction in anoxic waters. Their study shows that as much as 14% of the annual respiration in the lake may be due to arsenate reduction. This is particularly important in saline environments where sulfate reducing bacteria are forced to expend large amounts of internal energy maintaining cellular electrolyte balances. In these environments As reduction, as compared to S reduction, can be energetically more favorable for a factor of 30. Microbial reduction has also been hypothesized as a process contributing to the presence of arsenite in oxic waters where arsenate should be the dominant inorganic species (Newman et al. 1998). Whether the significant concentration of arsenite in oxic waters is a result of extremely rapid microbial production, or if the oxidation of As (III) is a slow kinetically controlled process has yet to be determined.

Methylated As compounds can account for as much as 59% of the total As concentration in some waters (Anderson and Bruland 1991). Sanders (1982) states that in some environments reduction and methylation by phytoplankton can be responsible for as much as 80% of the As speciation. Peaks in arsenite and methylarsenic concentration in areas of high primary productivity in water column samples support this hypothesis (Andreae 1978).

The environmental chemistry of Se, an essential micronutrient, is profoundly impacted by biological transformations. As with arsenic species, the concentration of reduced and organo Se species in the water column peak in areas of primary production (Cutter and Bruland 1984, Takayanagi and Wong 1985). Recent research suggests that biological cycling of Se does not end with the release of methyl species followed by their degradation back to inorganic species. Baines et al. (2001) show that up to 53% of the organoselenides supplied to phytoplankton cultures were incorporated into biomass. The production of highly volatile organo Se compounds appears to be an extremely important factor in the flux of Se from the oceans to the atmosphere (Cooke and Bruland, 1987). It is this flux, and its subsequent transfer to the land via precipitation, that supplies the terrestrial biosphere with necessary Se.

Little is known about the biotransformations of Sb. Methlystibine species have been detected in natural systems, but their source is still unclear (Filella et al. 2002). Sb is not known to be used for respiration and is not known to be a micronutrient for any microbial or planktonic species.

Biotransformations can be a potentially useful tracer of the fate of fly ash effluent in river systems. Emissions from CFPPs are as inorganic metalloid species in the reduced form. The reduced metalloids should rapidly oxidize. If biological removal is a significant factor in the downstream fate of metalloids then the concentration of metalloid metabolites (oganometallic and reduced species) should increase downstream with a parallel decrease in oxidized metalloid concentrations.

1.4 Toxicity in Biota

1.4.1 Speciation

While arsenic is used in some microbial respiration and Se is an essential micronutrient, both are toxic in trace amounts. For both, toxicity depends largely on speciation. Arsenic (III) is commonly thought to be the more toxic of the inorganic As species. This is based mainly on median lethal dose tests. In reality there is no great difference in toxicity between As (III) and As (V) (Yamauchi and Fowler 1994). Methlylarsenic compounds are far less toxic than the inorganic species. In the past it has been thought that arsenic methylation was a detoxification pathway. Sordo et al. (2001) have shown that the metabolite dimethylarsonic acid (DMA) has the ability to damage DNA in human leukocytes. However, this is not a universal trait as susceptibility to DNA by DMA varied from individual to individual.

Little is known about the toxic effects of specific Se species. It stands to reason that, in excess amounts, Se (IV) will be more toxic than Se (VI) as it is more bioavailable.

1.4.2 Bioaccumulation

Both arsenic and selenium bioaccumulate up the food chain (Eisler 1994 and Crutchfield 2000). Arsenic bioaccumulation can cause damage to DNA (Eisler 1994 and Sordo et al. 2001) causing cancer and birth deformities. Exposure to high levels of As has been responsible for declines in fish and wildlife populations as well as birth abnormalities.

Se bioaccumulation, in association with coal fired power plants, was seen in Hyco reservoir, a reservoir that received fly ash effluent in the 1970's and 1980's. Se bioaccumulation was responsible for the decline in sport fish and bird populations as well as birth abnormalities. Due in part to this contamination, the Roxboro CFPP changed from a wet ash disposal system to a dry ash disposal system. With the cessation of ash pond effluent inputs to the local reservoir Se levels in water and animal tissues have returned to near baseline levels.

1.5 Coal and Coal Fired Power Plants

Metalloids are important trace elements in coal. Average metalloid concentrations in coal are shown in Table 1-4.

1.5.1 Behavior in Coal Fired Power Plants

In coals Arsenic, Selenium, and Antimony are all associated with the mineral pyrite (Zeng et al. 2001). Metalloids are liberated from coal during combustion regardless of combustion temperature or oxidation state (Yan et al. 2001). Arsenic is partitioned almost exclusively onto fly ash (Sandelin and Backman 2001) while Se and Sb are partitioned between fly ash and loss to the atmosphere via stack gas. (Yan et al. 2001). This difference in partitioning between As and Se and Sb is partly a thermodynamic consideration, but is also strongly impacted by the kinetics of escape from the pyrite melt during combustion (Zeng et al. 2001). Due to the reducing environment inside the combustor, metalloids in the ash and gas flow are typically found in the reduced form (Yan et al. 1999). Ash ponds are pH treated to trap toxic metals such as Cd, Zn, and Cu. At the pH>7 necessary to trap Cd, Zn, and Cu examination of the Eh-pH diagrams for As, Se, and Sb (Figs 1-1, 1-2, 1-3) show that the reduced, and therefore more mobile species

Table 1-4 Metalloid Concentrations in Coal

Table 1-4 shows the average weight concentration of metalloids in coal

Element	**Avg. Concentration (ppmw)**	**Range (ppmw)**
As[1]	10	0.5-80
Se[1]	1	0.2-1.5
Sb[2,3]	1	0.1-2

1-Sandelin and Backman 1999
2-Rubin 1999
3-Yan et al 2001

.

of the metalloids will be preserved. This facilitates the aquatic transport of metalloids from the ponds to local waters. It is possible that metalloid species can also be used as a tracer for ash pond effluent downstream, as one would expect to find the oxidized forms of these metalloids in an oxic stream flow.

CHAPTER II

METHODS AND MATERIALS

2.1 Materials

2.1.1 Reagents

All reagents used in this experiment are of trace metal grade. All standards are greater than or equal to 99% purity. Acid solvents are sub-boiling distilled by the manufacturer and are 99.9% impurity free. The distilled-deionized water (DDW, 18.3 MΩ) is produced in our lab. City water is distilled and allowed to cool. Once cool, the distilled water is passed first through a Barnstead-Thermolyne high-capacity cation exchange column. It is subsequently passed through two Barnstead Thermolyne ultra-pure cation exchange columns. This water is stored in HDPE carboys used exclusively for storing DDW. Table 2-1 contains a comprehensive list of reagents and manufacturers.

2.1.2 Inductively Coupled Plasma – Mass Spectrometer

In this study a Hewlett Packard HP-4500 Inductively Coupled Plasma – Mass Spectrometer (ICP-MS) is used exclusively for trace metal determination. This instrument uses a quadrapole mass filter that allows the near simultaneous determination of more than one analyte. The combination of ease of conversion between analytical methods, the ability to determine more than one isotope at a time, high sensitivity, and mass/charge (m/z) selectivity make this instrument ideal for studies such as this one.

2.1.3 Sampling and Storage Material

Samples taken in the field are stored in the vessels in which they are collected. Field collection vessels are 125 mL and 1 L high density polyethylene (HDPE) bottles manufactured by Nalgene. The bottles are cleaned by the method described in section 2.2.2.1. Water is drawn from the river using 50 mL Fortuna syringes. These are trace metal certified syringes with polyethylene bodies and polypropylene plungers. Gelman AcroDisc (GHP membrane, 0.45 μm pore size) syringe filters are used to filter samples in the field. These filters are not trace metal certified and are a potential source of error through surface exchange. Experiments were conducted to account for these possibilities. To test for filtrate loss a standard solution of known concentration was passed through a new AcroDisc and compared to an aliquot of the same solution not passed through the filter. There was a 3% loss of As, a 0.6% loss of Se, and a 0.3% loss of Sb as compared to the unfiltered solution. These losses are within the uncertainty of the experimental method and insignificant compared to the concentrations of the standards and samples. There is also the possibility of contamination though the leaching of metalloids from the filter. This phenomenon was consistently tested with field filter blanks. The metalloid concentrations in DDW passed through an AcroDisc in the field are the same (within error) as DDW and reagent blanks prepared in the lab under clean conditions. This confirms that there are no metalloids leaching from the AcroDiscs and validates cleanliness of the field methods.

Table 2-1 Analytical Reagents

Table 2-1. Analytical reagents. This table contains the instrumentation, reagents, and manufacturers used for elemental analysis during this study.

Element	Method	Reagents
As	Direct Aspiration / Nebulization ICP-MS	1, 2, Arsenic Standard (Aldrich), Yttrium Standard (Aldrich), Indium Standard (Aldrich)
Se	Direct Aspiration / Nebulization ICP-MS	1, 2, Selenium Standard (Greg Cutter), Yttrium Standard (Aldrich), Indium Standard (Aldrich)
Sb	Direct Aspiration / Nebulization ICP-MS	1, 2, Antimony Standard (Aldrich), Yttrium Standard (Aldrich), Indium Standard (Aldrich)

1 Optima HNO_3 (Fisher)

2 DDW

2.2 Methods

2.2.1 Cleaning

2.2.1.1 Sampling Materials

The bottles used for gathering and storing trace metal samples are new 125 mL high-density polyethylene (HDPE) bottles. Upon removal from their original packaging, they are rinsed with distilled-deionized water (DDW) to remove any particulate matter from the manufacturing process. They are then filled with 1 N HNO_3 and sonicated for 3-4 hours. After sonication the 1 N HNO_3 is removed and saved for use in later cleanings. The bottles, caps, and threads are then rinsed 3 times with DDW, once with 1% trace metal free HNO_3, followed with 3 more rinsings with DDW. After the last rinsing the bottles are filled with DDW and stored until use in the field.

New 1 L HDPE bottles are used to collect particulate samples. Prior to use, these bottles are partially filled with DDW and shaken vigorously to remove any particulate material. They are then filled with DDW and stored until use in the field. No other material used in the field was pre-cleaned.

2.2.1.2 Laboratory Materials

The autosampler vials used in direct aspiration / direct nebulization ICP-MS are cleaned using the same method for the 125 mL HDPE bottles. All standard solutions are placed in HDPE bottles that undergo similar treatment. All of the volumetric laboratory ware used in this study is plastic. Prior to use, the flasks are rinsed once with DDW, followed by a clean HNO_3 rinse, and finally a second DDW rinse. If they are not used immediately after cleaning the mouths of the flasks are covered with Parafilm to prevent contamination.

All standards and samples are prepared under a bench-top clean bench to avoid contamination by dust or sand in the air. Any micropipettes used to transfer standards or samples are equipped with new trace metal free tips prior to every use.

2.2.2 Sample Collection and Storage

Two types of samples were gathered during this study; filtered water samples used for metalloid analyses, and particulate samples used to determine the amount of suspended sediment in the river.

Filtered samples are taken by the following method. A 50 mL Fortuna syringe is filled with river water and emptied three times. An AcroDisc syringe filter is placed on the syringe luer tip. A small amount of river water is filtered through the syinge into a 125 mL trace metal cleaned bottle. The bottle is capped and the water swirled around. The water is dumped from the bottle into the cap, then poured over the threads. The process is repeated two more times. The syringe is then emptied and a fresh 50 mL aliquot of river water is collected. The entire volume of the syringe is passed through the filter and collected in the bottle. 500 µL of concentrated (69%-70%) Optima nitric acid is added to the sample. The amount of river water passed through the filter is recorded in order to calculate suspended metalloid concentrations.

Particulate samples are taken in cleaned 1 L bottles. The bottles, caps, and threads are rinsed three times with river water. The bottles are then immersed completely in the river and allowed to fill. Both filtered acidified samples and particulate grab samples must be stored in the cold and dark immediately after collection. A cooler filled with ice or ice packs is sufficient for this purpose.

Field filter blanks were taken to account for contamination in the field from dust or other debris and to test for leaching of metalloids from syringe filters.

2.2.3 Direct Aspiration / Direct Nebulization Inductively Coupled Plasma-Mass Spectrometry

Direct aspiration /direct nebulization inductively coupled plasma mass spectrometry (DA/DN ICP-MS) is used to analyze samples for total dissolved As, Se, and Sb. This method takes advantage of the quadrapole mass filter's ability to determine multiple analytes simultaneously. As and Se are determined by analysis of the ^{75}As and ^{77}Se isotopes respectively. Two Sb isotopes are analyzed; ^{121}Sb and ^{123}Sb, to cross check calculations. It is commonly thought that As and Se cannot be determined by ICP-MS due to isobaric interferences on their stable isotopes. I have determined that it is possible to analyze both these elements in low matrix samples when care is taken not to introduce interference by addition of specific reagents during the preparation stage. In the case of As, Cl^- cannot be present in the solution for analysis. In the torch, ^{40}Ar combines with ^{35}Cl and ^{38}Ar combines with ^{37}Cl to from the $ArCl^+$ ion of mass 75. This ion interferes with the only stable isotope of As. Workers using atomic absorption spectroscopy (AAS) to determine As have preserved and analyzed samples in HCl solutions. HNO_3 was used to preserve samples and as a matrix for standards to avoid this interference. The isobaric interferences for Se are more complicated. The major isotopes of Se, ^{76}Se, ^{78}Se, and ^{80}Se have interferences caused by the formation of Ar dimers ($^{40}Ar^{36}Ar$, $^{38}Ar^{38}Ar$, $^{38}Ar^{40}Ar$, $^{40}Ar^{40}Ar$) in the plasma torch. The only isotope without an Ar dimer interference is the rare (7.6%) ^{77}Se isotope. This however can have an interference caused by the combination ^{40}Ar and ^{37}Cl. Similar to the procedures used for arsenic analysis, the introduction of Cl must be avoided.

Internal standards are used to correct for instrument drift. It is possible that drift may not occur equally across the mass scale. This phenomenon is called differential mass drift. Samples are prepared volumetrically and an equal number of moles of the internal standard is added. All samples have an equal concentration of the internal standard. In this study 4.5 mL of sample is pipetted into an autosampler vial. 0.5mL of a 500 ppb internal standard solution is pipetted into the sample making the sample to exactly 10 ppb with respect to the internal standard. By calculating a ratio of the analyte counts to the internal standard counts it is possible to correct for any changes due to instrument drift. Correction of differential mass drift requires the use of multiple internal standards.

In this study, ^{89}Y is used as an internal standard for As and Se. Yttrium is extremely rare in nature, has no isobaric interferences, and has only one stable isotope, making it ideal for use as an internal standard for As and Se, which have masses of 75 and 77 respectively. Sb is standardized with ^{115}In. Indium is also extremely rare in nature but experiences isobaric interference from ^{115}Sn. However, the concentration of Sn in natural waters is in the 0-40 pM range (Byrd and Andrea, 1982) and ^{115}Sn is a tiny fraction of (0.34%) of the total concentration of Sn. The interference of ^{115}Sn on ^{115}In at 10 ppb In can be ignored.

Standards were prepared by serial dilution from commercially purchased primaries in the case of As and Sb. A 1000 ppm standard from Greg Cutter (Old Dominion University) was used for Se. All dilutions were done with 1% Optima HNO_3. First 0.1 L of a 1 ppm 2^o multi-element standard was prepared by diluting 100μL of a 1000 ppm As (Aldrich) standard, 100 μL of a 1000 ppm Se (Cutter) standard, and 99 μL of a 1010 ppm Sb (Aldrich) standard to 100 mL. A 100 ppb 3^o standard was prepared by diluting 10 mL of the 2^o to 100 mL. 1, 2, 4, 6, and 10 ppb working standards were made by diluting 100 μL, 200 μl, 400 μl, 600 μl, and 1 mL of the 2^o, respectively, to 100 mL. A 0.1 ppb working standard was made by diluting 100 μL of the 3^o standard to 100 mL. 0 ppb standard was prepared by transferring 100 mL of 1% Optima HNO_3 to the volumetric flask used to prepare the working standards and then transferred to its own bottle.

The 0, 0.1, 1, 2, 4, 6, and 10 ppb multi-element standards were used to make a 7 point calibration curve. The multi-element standards were spiked with the internal standard in the same manner as the samples. Calibration is done by plotting the ratio of the element to its internal standard versus the response. A typical set of calibration curves is shown in figure 2-1. The isotopic abundance of the isotope being analyzed is reflected in the concentrations shown on the x-axis. The analytical data are corrected for isotopic abundance to reflect the total metalloid concentrations in the samples. Concentration is calculated from the calibration curves using the following equation:

Eq. 2-1 Analyte Concentration in Samples

$$C = \frac{R_s}{m \times A}$$

C is the concentration of the analyte in the sample. R_s is the ratio of the analyte counts to internal standard counts measured for the sample. *m* is the slope of the calibration curve. A is the natural isotopic abundance of the analyte.

The detection limits of this method (3 times the standard deviation of the blank) for As, Se, and Sb are 0.006 ppb, 0.06 ppb, and 0.010 ppb respectively. Blank levels in DDW are 0.003 ppb for As, 0.04 ppb for Se, and 0.005 ppb for Sb. Precisions of 3.2% for As, 4.4% for Se, and 4.1% for Sb were obtained for samples having concentrations ≥ 0.1ppb (*n*=3). See Table 2-4 for reproducibility data.

The acquisition is made in peak jumping mode (m/z = 75 (As), 77 (Se), 89 (Y), 115 (In), 121 (Sb), and 123 (Sb)) with three points per peak. Dwell time is 0.5 s, with an acquisition time of 17 s. The detector is set to pulse counting mode. The peristaltic pump runs at 0.3 rps for a sample feed rate of 1 ml per minute. The autosampler program is as follows: DDW, reagent blank, 0-10 ppb standards (as listed above), samples, DDW. Between each sample and standard there is a 10s rinse with DDW and a 1 minute rinse with 1% Optima HNO_3. The plasma gas rate is 16 L / min, the auxiliary gas rate is 1 L / min, and the carrier gas rate is 1.15 L / min. See Table 2-3 for other ICP-MS instrument settings.

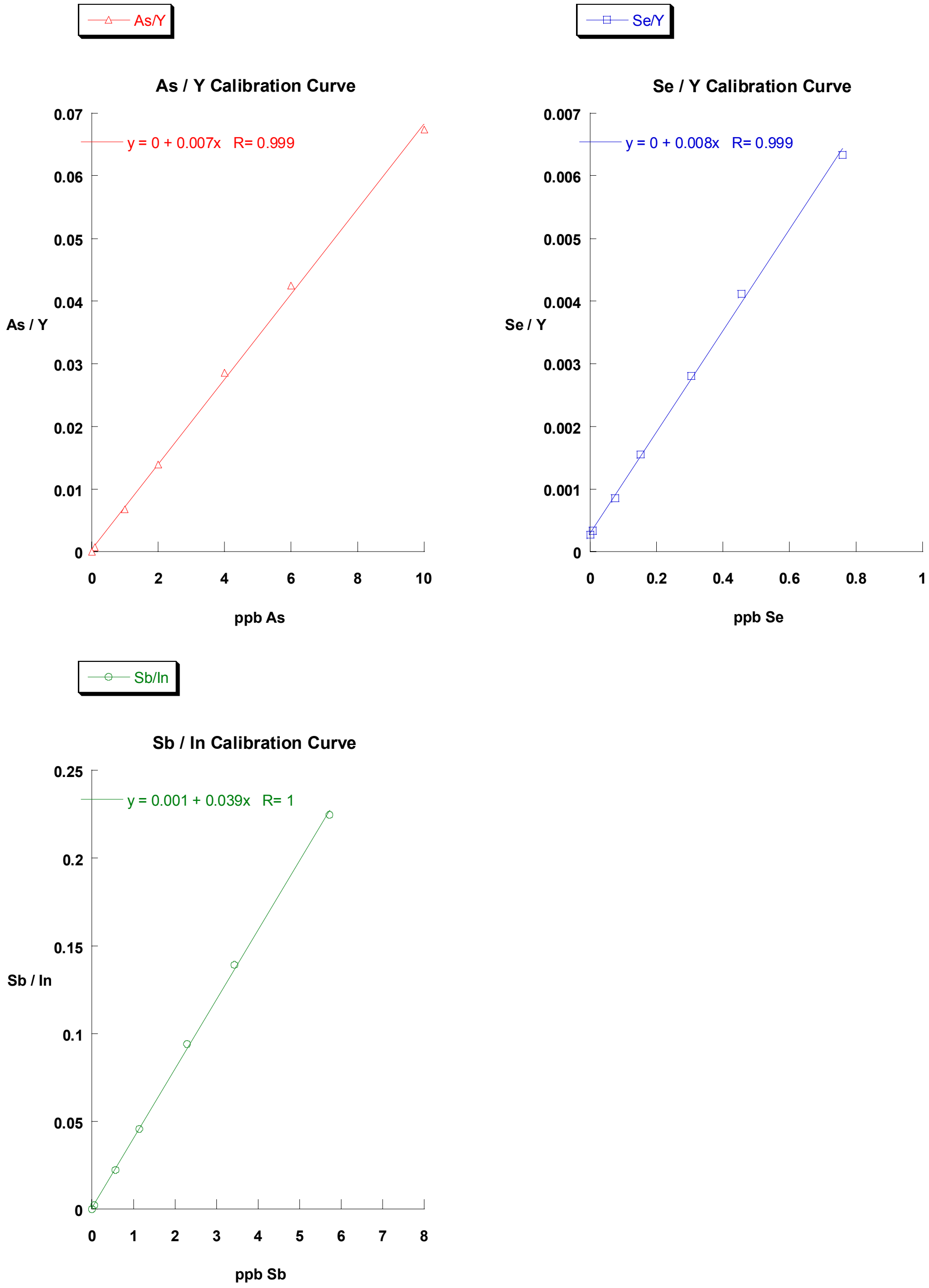

Figure 2-1 Metalloid Calibration Curves. Figure 2-1 shows a set of calibration curves for the multi-element standard. The x-axis is concentration in ppb. The y-axis is the count ratio of analyte to internal standard.

Table 2-3 ICP-MS Settings

Table 2-3. ICP-MS Settings. This is a table containing the settings of the ICP-MS instrument for a typical analysis run. These settings are particular to the HP-4500 and must be adjusted (re-tuned) each time the instrument is placed into standby mode.

Parameter	Setting	Parameter	Setting	Parameter	Setting
RF Power	1200 W	**Extract 1**	-250 V	**AMU Gain**	129
RF Matching	1.92 V	**Extract 2**	-100 V	**AMU Offset**	175
Sample Depth	5.5 mm	**Einzel 1,3**	-100 V	**Axis Gain**	1.001
Torch-H	-0.9 mm	**Einzel 2**	9.6 V	**Axis Offset**	-0.19
Torch-V	1.5 mm	**Omega Bias**	-50 V	**Plate Bias**	-4 V
Carrier Gas	1.15 L/min	**Omega (+)**	6 V	**Pole Bias**	0 V
Blend Gas	0 L/min	**Omega (-)**	-10 V	**Discriminator**	12 mV
Peristaltic Pump	0.3 rps	**Quadrapole Focus**	7 V	**EM Voltage**	-1910 V
Spray Chamber Temp	2 C	**Ion Deflection**	50 V	**Last Dynode**	-337 V
Sample Rate	1 mL / min	**Peak Jumping (m/z)**	75, 77, 89, 115, 121,123	**Dwell Time**	0.5s
Acquisition Time	17 s	**Detector Mode**	Pulse Counting	**Plasma Gas**	16 L / min

Table 2-4 Reproducibility Results

This table is located on the following page. It shows the reproducibility results for the storage and analysis methods used in the study. It is based on the original concentration calculated immediately after sample collection and a second quantification after some months of storage. “m” is the slope of the calibration curve for the day of analysis. ** indicates that no internal standard was used for these analyses. Original Concentration is the pre-storage calculation of concentration. The reanalysis concentrations are the calculated concentrations, in duplicate, of the samples after storage. The final reproducibility is the average of the standard deviations of the pre and post storage sample analyses.

Table 2-4 Reproducibility Results

R-Number	Date Collected	Element	Blank (ppb)	m (CPS/ppb)	Original Analysis Concentration (ppb)	Re-analysis Concentration 1 (ppb)	Re-analysis Concentration 2 (ppb)	Standard Deviation (n=3) (%)
R-1025	5/21/2001	As	0.003	11212 **	1.37	1.32	1.42	3.6
		Se	0.047	8937 **	1.40	1.33	1.45	4.2
		Sb	0.002	35627 **	0.61	0.65	0.60	4.2
R-1043	8/6/2001	As	0.002	0.016	1.89	1.95	1.84	2.9
		Se	0.010	0.011	1.25	1.34	1.36	4.5
		Sb	0.001	0.046	0.68	0.64	0.63	4.0
R-1048	9/15/2001	As	0.003	0.011	5.60	5.47	5.82	3.1
		Se	0.035	0.007	3.01	3.17	2.89	4.6
		Sb	0.002	0.043	1.41	1.35	1.46	3.9
R-1054	11/9/2001	As	0.002	0.011	3.72	3.55	3.79	3.3
		Se	0.027	0.008	2.02	2.12	2.19	4.1
		Sb	0.005	0.042	1.11	1.02	1.06	4.1
R-1060	12/18/2001	As	0.004	0.010	1.73	1.76	1.84	3.2
		Se	0.031	0.007	0.98	0.95	1.03	4.3
		Sb	0.002	0.040	0.52	0.53	0.57	4.5
R-1067	3/6/2002	As	0.001	0.009	0.40	0.43	0.42	3.4
		Se	0.042	0.007	0.64	0.62	0.67	4.0
		Sb	0.002	0.035	0.24	0.23	0.25	4.1
R-1079	5/6/2002	As	0.003	0.009	0.94	0.88	0.92	3.1
		Se	0.025	0.007	0.56	0.54	0.59	4.5
		Sb	0.002	0.033	0.33	0.34	0.36	4.2
R-1085	6/5/2002	As	0.002	0.008	5.67	5.40	5.35	3.2
		Se	0.034	0.006	1.99	2.08	1.90	4.6
		Sb	0.003	0.034	1.07	1.03	0.99	4.0
Reproducibility (Average Std. Deviation from re-analysis)							As	3.2
							Se	4.4
							Sb	4.1

2.2.4 Hot Acid Extraction

The concentration of metalloids on suspended sediments is determined by acid extracting the sediments from AcroDisk Filters used in the field. Suspended sediments collected on filters are extracted by passing a solution of hot nitric acid through the filter. A 10% HNO_3 solution is heated to 60^o C and drawn into an acid cleaned syringe through an acid cleaned length of tygon tubing. The acid is passed through the filter at a rate of 1 mL/min and collected in an acid cleaned scintillation vial, diluted to 1% acid (10 x) with DDW, then analyzed by DA/DN-ICP-MS. The calculation for metalloid concentration in PPM(W) is as follows:

Eq. 2-2 Metalloid Concentration in Suspended Solids

$$C_{sus} = \frac{C_{ex}}{M_{sed} \times F}$$

C_{sus} is the concentration of metalloids on suspended solids in PPM(W). C_{ex} is the concentration of the filter extract. M_{sed} is the mass of suspended sediment in a volume of water, determined directly from a separate 1 L aliquot. F is amount of water passed through the filter in the field.

2.2.5 Nutrient Methods

Si is measured by spectrophotometery using the molybdate blue method. Dissolved reactive PO_4 is determined by using spectrophotmetery by the method of Murphy and Riley (1962). This method has a detection range of 0.03 – 5.00 μM with a precision of $\pm 0.31/n^{1/2}$ where n is the number of analysis. Nitrite is analyzed by spectophotometery after Murphy and Riley (1963). This method has a precision of $\pm 0.5/n^{1/2}$ where n is the number of analyses. Nitrite + nitrate was analyzed in the lab of Dr. Joe Montoya.

2.3 Sample Sites

2.3.1 The Etowah-Coosa-Oostanaula River System

This section provides specific details about the geographical area on the Etowah-Coosa-Oostanuala sampling transect.

2.3.1.1 Geology, Cities, and Coal Fired Power Plants

The Etowah-Coosa-Oostanaula (ECO) river system (Fig. 2-3) is located in northwestern Georgia. This study covers the Etowah River from its outlet (Allatoona Reservoir) at Allatoona Dam to Rome, GA. In Rome, the Etowah joins the Oostanaula River to become the Coosa River. From Rome, the Coosa flows southwest into Alabama. There are two major cities on the ECO transect, Cartersville and Rome, Georgia. Cartersville is located approximately 10 km (by river) west of Allatoona Dam. Rome is located approximately 85 km (by river) west of Allatoona Dam.

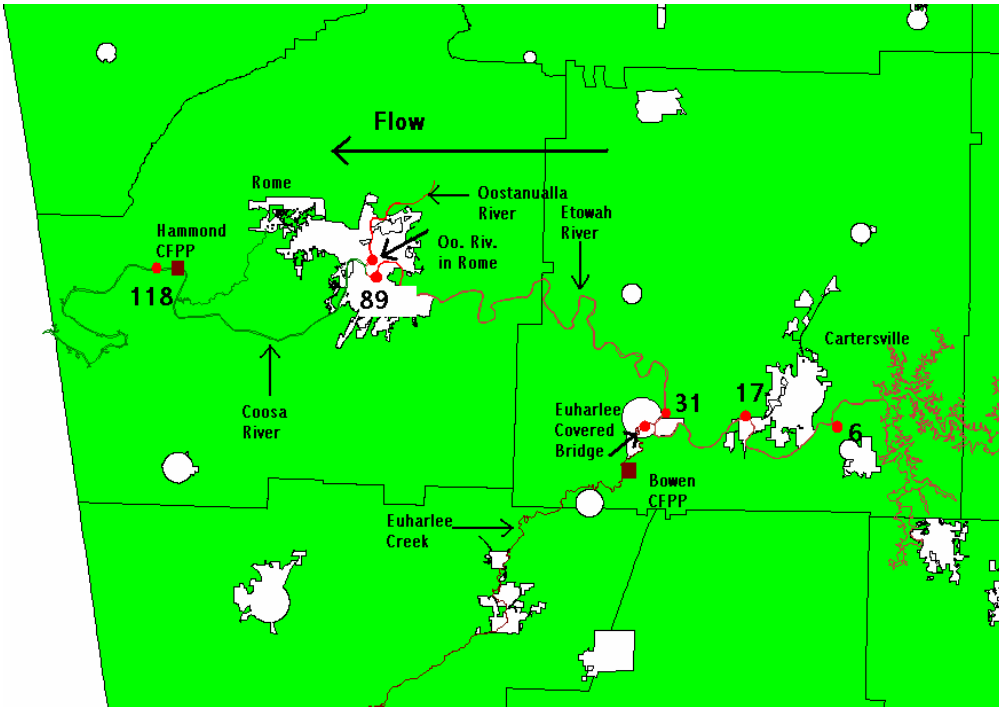

Figure 2-3 Etowah-Coosa-Oostanaula Sampling Area. Figure 2-3 shows the Etowah-Coosa-Oostanaula sampling area. Sample sites are indicated by orange circles. CFPP's are indicates by brown squares. The numbers next to the sample site markers are the km downstream (by river) of the site from the outlet at Allatoona Dam. The white areas are cities and towns.

In this area , the formation of particular interest is the Shady Dolomite, which outcrops in and around the Cartersville area. This formation contains veins and replacements of barite throughout its entire thickness. The barite is concentrated through weathering processes to the extent that the formation can contain 6-12% barite (Chowns 1983). The barite is strip mined and refined for use in making barium salt products. Of relevance to this study is the fact that barite is commonly associated with Sb minerals. The data gathered in this research suggest an input of metalloids to the Etowah River in the vicinity of these barite mines. We hypothesize that this input may be related to runoff from the mines and/or the barite bearing strata. Faulting processes heavily influence the stratigraphy and topography north of Rome.

There are two CFPPs on this transect of the ECO system, Plant Bowen and Plant Hammond. These two plants are radically different in both size and environmental impact. Plant Hammond (Figure 2-4) is a 800 MW plant while Plant Bowen (Figure 2-5) is a 3160 MW plant. Plant Hammond still uses wet ash disposal while evidence suggests that Plant Bowen has switched, at least partially, to a dry ash disposal system. While some ash is disposed of on site, about half is also being sold for other uses. A truck hauling ash from the ash field was followed to a housing development where the ash appeared to be used as ground fill beneath new houses. It is important to note that Plant Bowen is not situated directly on the Etowah River. A tributary stream (Euharlee Creek) receives any discharge from the fly ash settling pond and transports the resulting contaminants to the Etowah River.

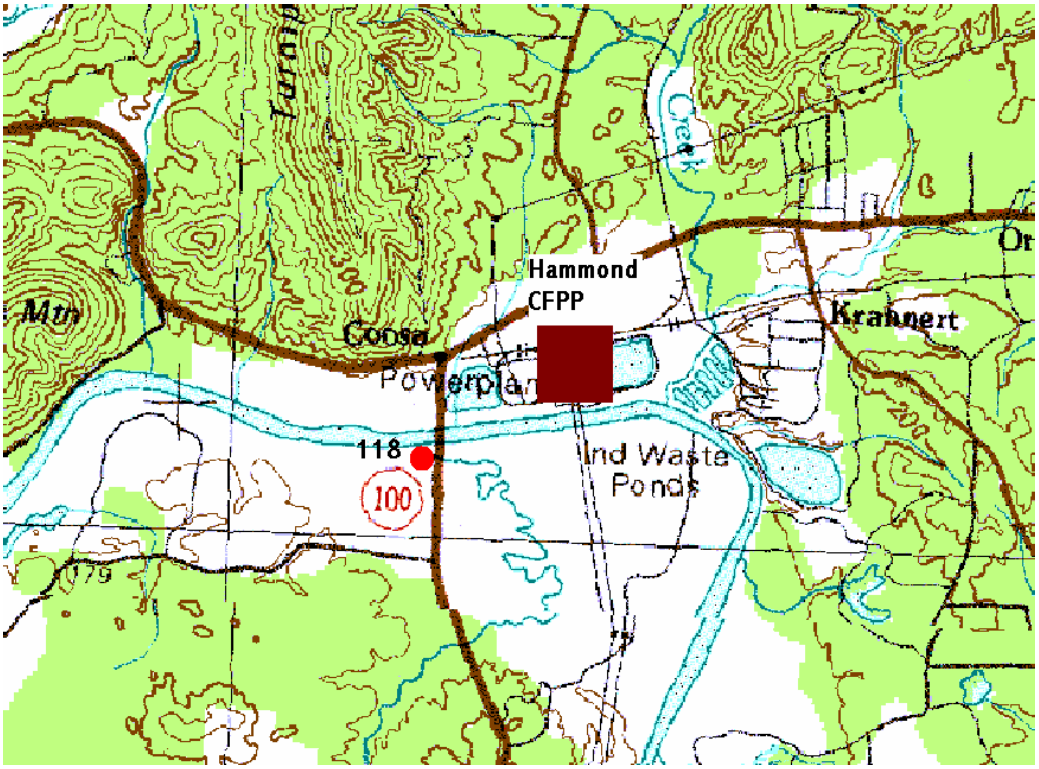

Figure 2-4 Plant Hammond Topography. Figure 2-4 shows the topography in the immediate vicinity of Plant Hammond. Sample sites are indicated by orange circles. CFPP's are indicated by brown squares. The numbers next to the sample site markers are the km downstream (by river) of the site from the outlet at Allatoona Dam. In this map the location of the site maker indicates the exact location of the sample site.

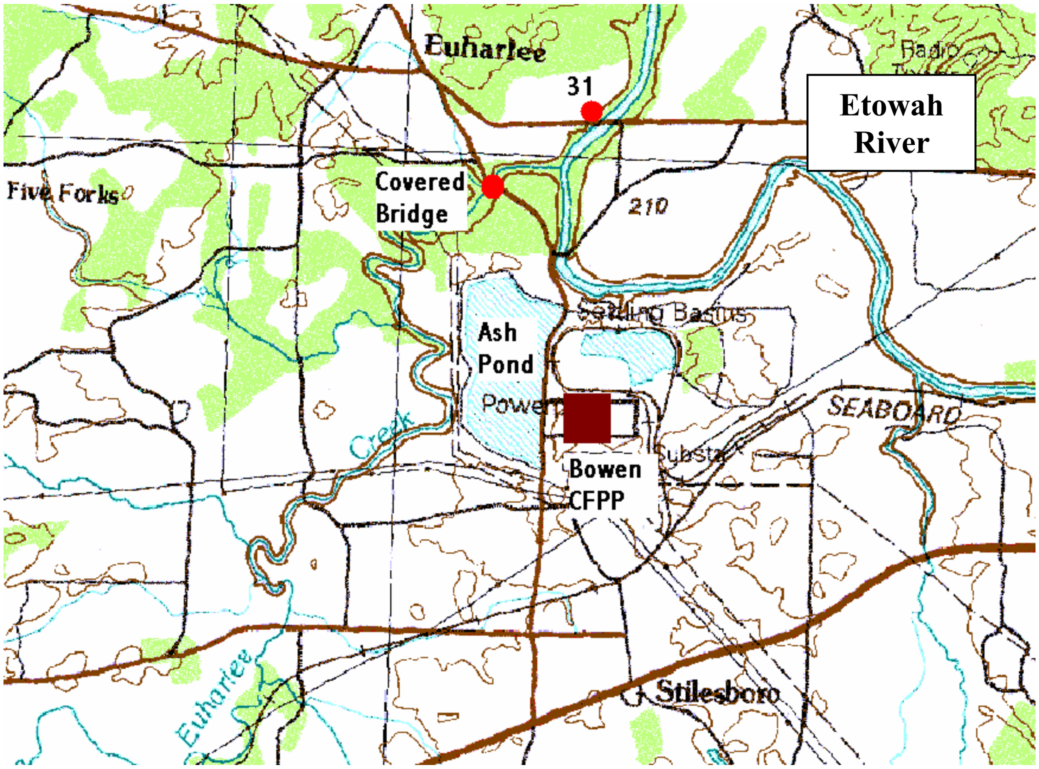

Figure 2-5 Plant Bowen Topography. Figure 2-5 shows the topography in the immediate vicinity of Plant Bowen. Sample sites are indicated by orange circles. CFPP's are indicated by brown squares. The numbers next to the sample site markers are the km downstream (by river) of the site from the outlet at Allatoona Dam. In this map the location of the site maker indicates the exact location of the sample site.

2.3.1.2 Sample Site Specifics The sample sites on this transect are taken above and below both power plants in order to assess the impact of the power plant on the rivers. There are seven sample sites on this transect, though only five of them fall on the Etowah or Coosa Rivers. Sample locations are named by their km marker downstream from the source reservoir (Fig 2-3). Sample site118 is located on the Coosa River downstream from Rome and Plant Hammond. A sample of the Oostanaula is collected in Rome upstream of the junction where the Etowah and the Oostanaula Rivers join to become the Coosa River. Sample site 89 is located on the Etowah River in Rome. Sample site 31 is located on the Etowah River downstream of Euharlee Creek. Any metalloid signal from Plant Bowen should be evident in waters taken at this location. There is a sample from Euharlee Creek. This allows confirmation that any increase in metalloid flux in the Etowah is due to input from Plant Bowen. Sample Site 17 is on the Etowah River, above Euharlee Creek, west of Carterville. It is this sample site that appears to be impacted by the barite strip mining southeast of Cartersville. Sample site 6 is located the Etowah River downstream of Allatoona Dam. This is considered the “clean” end member of the Etowah, as the river has not yet been impacted directly by effluent from fly ash ponds or barite mines. Specific driving directions to these locations as well as their latitude and longitude coordinates can be found in Appendix III.

2.3.2 The Chattahoochee River System

This section provides specific details about the geographical area on the Chattahoochee River sampling transect.

2.3.2.1 Geology, Cities, and Coal Fired Power Plants The section of the Chattahoochee River considered in this study begins at the outlet of Lanier Reservoir at Buford Dam and ends at the outlet of West Point Reservoir in West Point, Georgia (Fig. 2-6). There are several cities situated on the Chattahoochee in this transect, the largest of these being Atlanta, Georgia. The Chattahoochee flows through Atlanta for approximately 20 km (by river). In Atlanta the Chattahoochee is used for drinking water and also receives industrial, domestic, and sewage effluent. There is a small power plant, Plant McDonough (now Plant Atkinson), situated on the Chattahoochee in Atlanta. However, this plant has been converted to burn natural gas and is not considered in this study.

There are two major coal fired power plants on the river in this transect. They are Plant Wansley (1730 MW) (Fig 2-7) and Plant Yates (1250 MW) (Fig 2-8). Plant Yates is located 100 km downstream from Buford Dam. Plant Wansley is located 108 km downstream from Buford Dam. Both of these plants use wet ash disposal sytems.

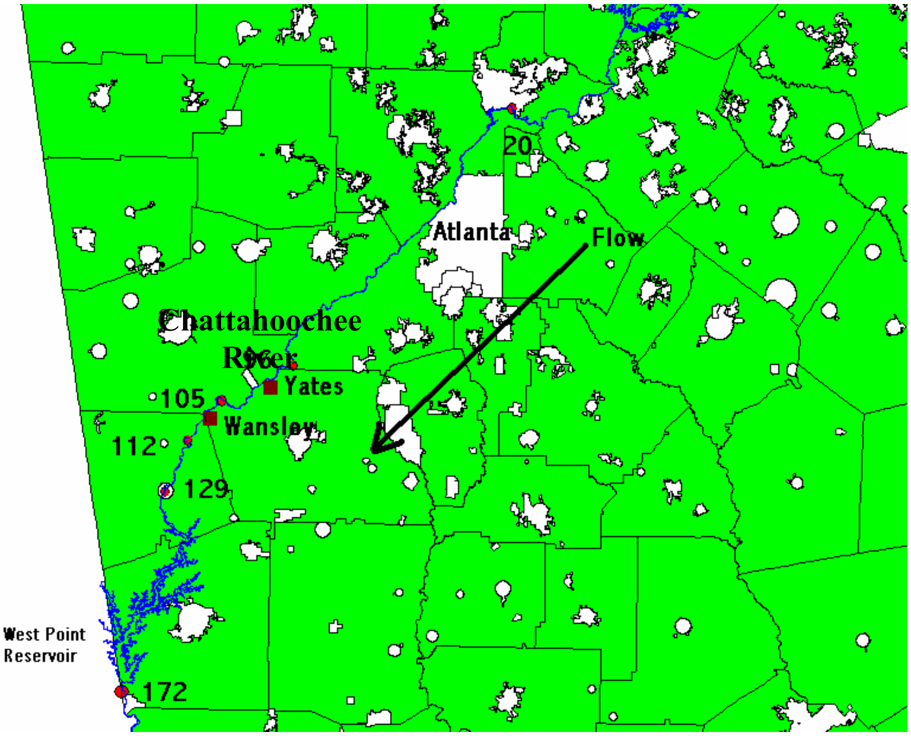

Figure 2-6 Chattahoochee Sampling Area. Figure 2-6 shows the Chattahoochee sampling area. Sample sites are indicated by orange circles. CFPP's are indicated by brown squares. The numbers next to the sample site markers are the km downstream (by river) of the site from the outlet at Buford Dam. The white areas are cities and towns.

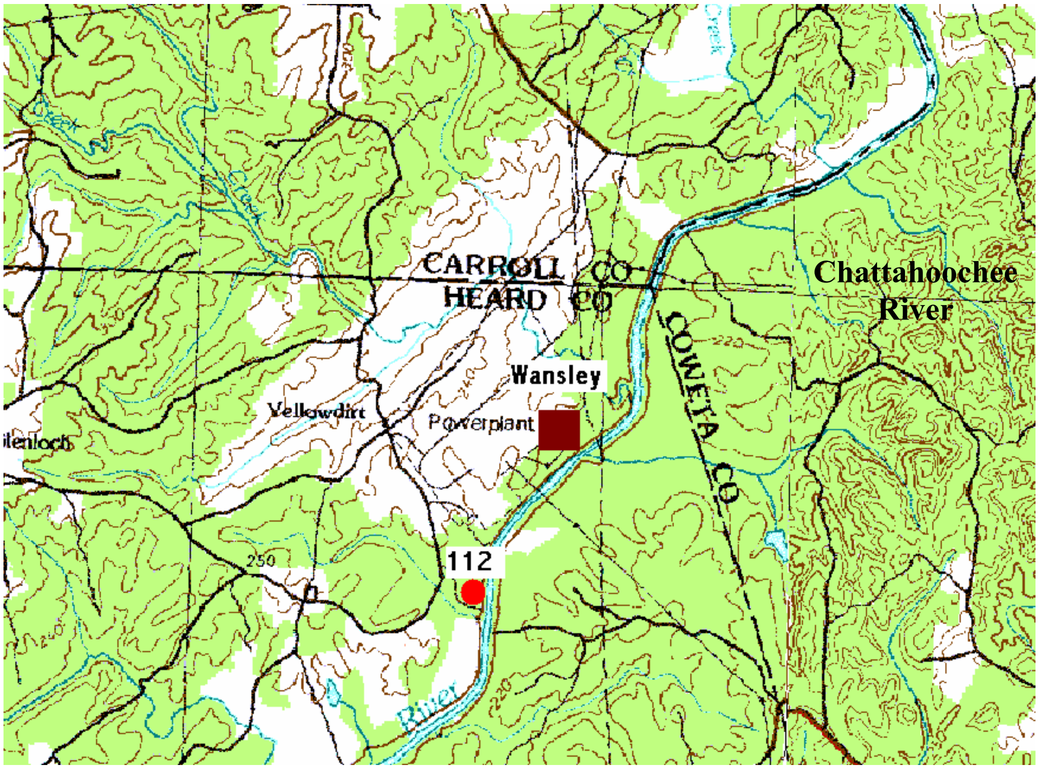

Figure 2-7. Plant Wansley Topography. Figure 2-7 shows the topography in the immediate vicinity of Plant Wansley. Sample sites are indicated by orange circles. CFPP's are indicated by brown squares. The numbers next to the sample site markers are the km downstream (by river) of the site from the outlet at Buford Dam. In this map the location of the site maker indicates the exact location of the sample site.

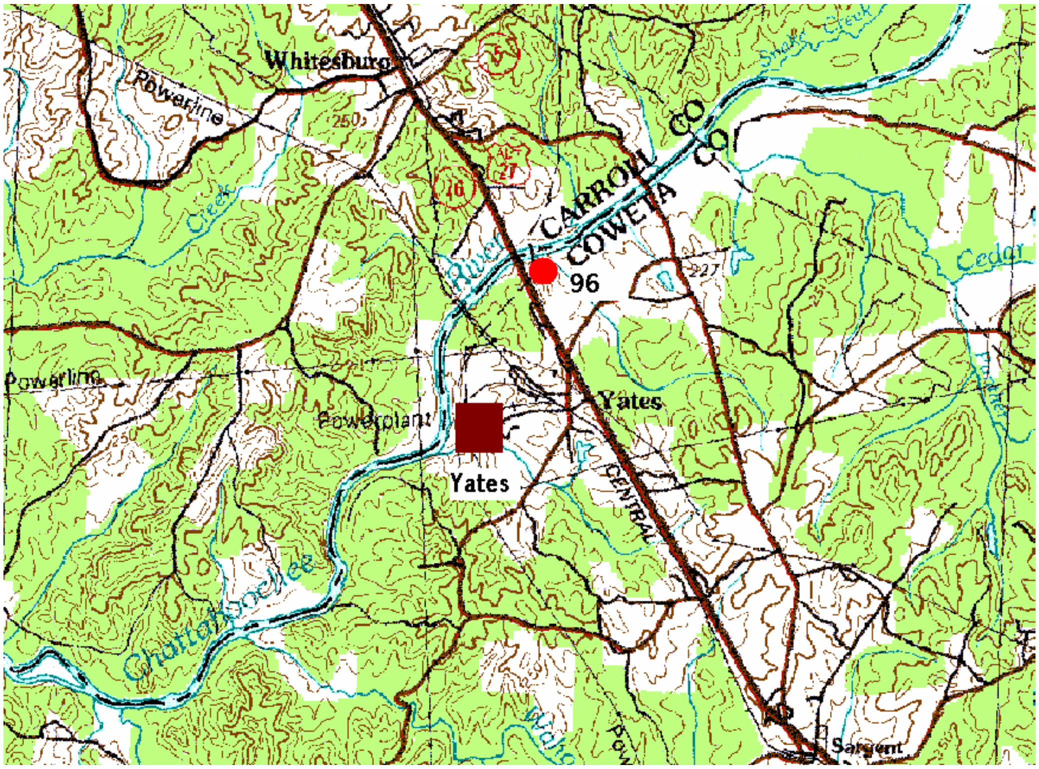

Figure 2-8 Plant Yates Topography. Figure 2-8 shows the topography in the immediate vicinity of Plant Yates. Sample sites are indicated by orange circles. CFPP's are indicated by brown squares. The numbers next to the sample site markers are the km downstream (by river) of the site from the outlet at Buford Dam. In this map the location of the site maker indicates the exact location of the sample site.

2.3.2.2 Sample Site Specifics Samples are taken above and below both power plants in order to assess the impact of these plants on the river receiving their ash pond effluent. There are six samples taken on this transect. They span the length of the river from Lanier Reservoir to West Point Reservoir, but focus on the last 72 km of the river Fig (2-6). A sample (sample site 172) is taken below West Point Reservoir to assess any changes in metalloid concentration from laucustrine processes. A sample is taken above West Point Reservoir (sample site 125) in order to gather information about the composition of the water flowing into West Point Lake. This site is also important because it gives a picture of metalloid behavior downstream of the power plants, but before the water is subject to any biological and chemical processes that may occur once water reaches the reservoir. A sample is taken approximately 4 km (by river) downstream of Plant Wansley (sample site 112). This sample has metalloid contamination from both power plants. A sample is taken upstream of Plant Wansley but downstream of Plant Yates (sample site 105). This allows separation, to some degree, the effect of the plants. Another sample is taken from upstream of both power plants (sample site 96). This gives a picture of the water composition immediately before the river is affected by power plant effluent. The sixth sample is taken far upstream approximately 20 km (by river) from the outlet of Buford Dam (sample site 20). This is considered the “clean” end member of the Chattahoochee. At this sample site the river has not been impacted directly by power plant pollution. Of note is the fact that this sample is taken at the main potable water intake facility for north Dekalb County, Georgia. Detailed driving directions to these sites can be found in Appendix III.

CHAPTER III

RESULTS

This chapter contains the analytical results of this project, presented as plots of downstream river transects. Appendices I and II contain the analytical data presented in these graphs. The dissolved and suspended metalloid and nutrient concentration data are presented in Appendix I. Flux calculation data are presented in Appendix II.

Figures 3-1 and 3-2 show average annual dissolved metalloid concentration profiles and the locations of important landmarks and features on the Chattahoochee (Fig 3-1) and Etowah Rivers (Fig 3-2). In both figures the x-axis is kilometers downstream of the river source reservoir. The y-axis is the dissolved metalloid concentration.

3.1 River Metalloid Profiles

This section discusses general trends in the metalloid profiles of the Etowah and Chattahoochee Rivers during the year of this study. While the degree of metalloid enrichment and loss varies from month to month, the general trends remain the same.

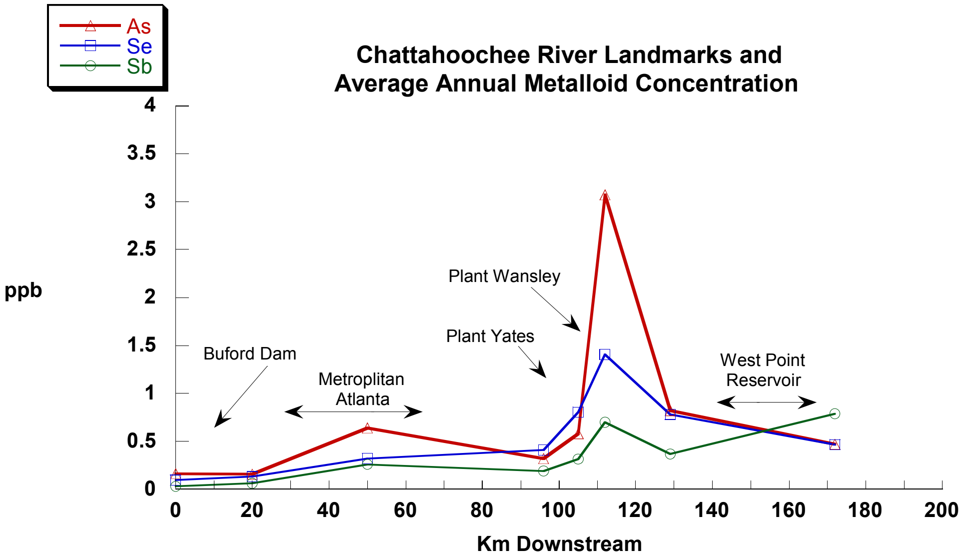

Figure 3-1. Chattahoochee River landmarks and typical (annual average) metalloid concentrations

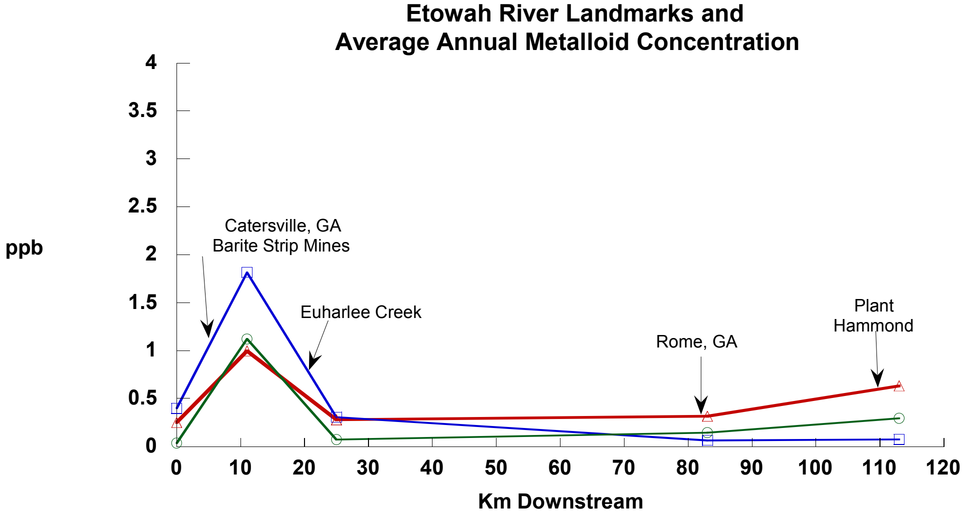

Figure 3-2. Etowah River landmarks and typical (annual average) metalloid concentrations.

3.1.1 Metalloid Concentration Profiles

The analytical data discussed in this section is located in Appendix I. The average annual metalloid concentrations in the Etowah River at its spill way from Allatoona Dam are 0.25 ppb As, 0.40 ppb Se, and 0.04 ppb Sb. An increase in total dissolved metalloid concentrations to 1.00 ppb As, 1.82 ppb Se, and 1.12 ppb Sb is found in the Etowah River (Fig. 3-7, 3-8) above Euharlee Creek (sample site 10). Downstream of Plant Hammond (km 112), As, Se, and Sb concentrations increase to 0.63 ppb, 0.8 ppb, and 0.30 ppb respectively. This is a marked increase compared to the concentrations of 0.32 ppb As, 0.63 ppb Se, and 0.15 ppb Sb found 30 km (by river) east in Rome, GA. We attribute the input of metalloids at km 10 to barite open pit quarries south of Cartersville, GA. Barite deposits are commonly associated with Sb bearing minerals. Fly ash leachate from Plant Hammond is believed to be the source of metalloid input at km 112.

Metalloid concentrations in the Chattahoochee River (Figs. 3-9 - 3-16) increase below Plants Yates and Wansley. The upstream concentrations of As, Se, and Sb are 0.16 (± 0.07) ppb, 0.13 (± 0.05) ppb, and 0.06 (±0.06) ppb respectively at Holcomb Bridge above Atlanta (sample site 20). Downstream of Atlanta but upstream of the power plants (sample site 96), the As, Se, Sb concentrations are 0.32 (±0.09) ppb, 0.41 (±0.26) ppb, and 0.20 (±0.06) ppb respectively, a two fold increase in As and a three fold increase in both Se and Sb relative to those at Holcomb Bridge. However, downstream of Plants Yates and Wansley (sample site 112) the average concentrations of As, Se, and Sb increase to 3.07 (± 2.6) ppb, 1.41 (±0.82) ppb, and 0.70 (±0.41) ppb respectively. This represents a 19 fold increase in As concentration, 11 fold increase in Se concentration, and 12 fold increase in Sb concentration compared to above Atlanta. Compared to concentrations immediately above the plants (sample site 96), there are ten fold, three fold, and four fold increases in As, Se, and Sb respectively.

Evidence that this increase in concentration is due to fly ash leachate can be found in the ratios of the metalloid concentrations in the rivers downstream of the power plants. The concentration of As, Se, and Sb in coal is in the preceding order, with As being the most abundant. The Se/As and Sb/As ratios in average coals are 0.1. The input fluxes from the power plants (3.1.3) reflect the ratios of metalloid concentration found in coal. It stands to reason that the rivers impacted by CFPP discharge will also reflect these concentration ratios, as found on the Chattahoochee River (Se/As=0.27, Sb/As=0.13). These ratios are within the bounds of the common metalloid concentrations in coal (Table 1-4) This theory can be applied to the question of the source of the increased concentrations at sample site 10 on the Etowah River. In both transects the element of metalloid of highest concentration is Se, which is not consistent with ash pond effluent (3.2).

3.1.2 Metalloid Flux Profiles

The data discussed in this section is located in Appendix II. Dissolved metalloid fluxes (Figure 3-3) are calculated using USGS river flow data (l/s) and analytical concentration data (mg/l). Multiplying the flow at a site by the metalloid concentration at

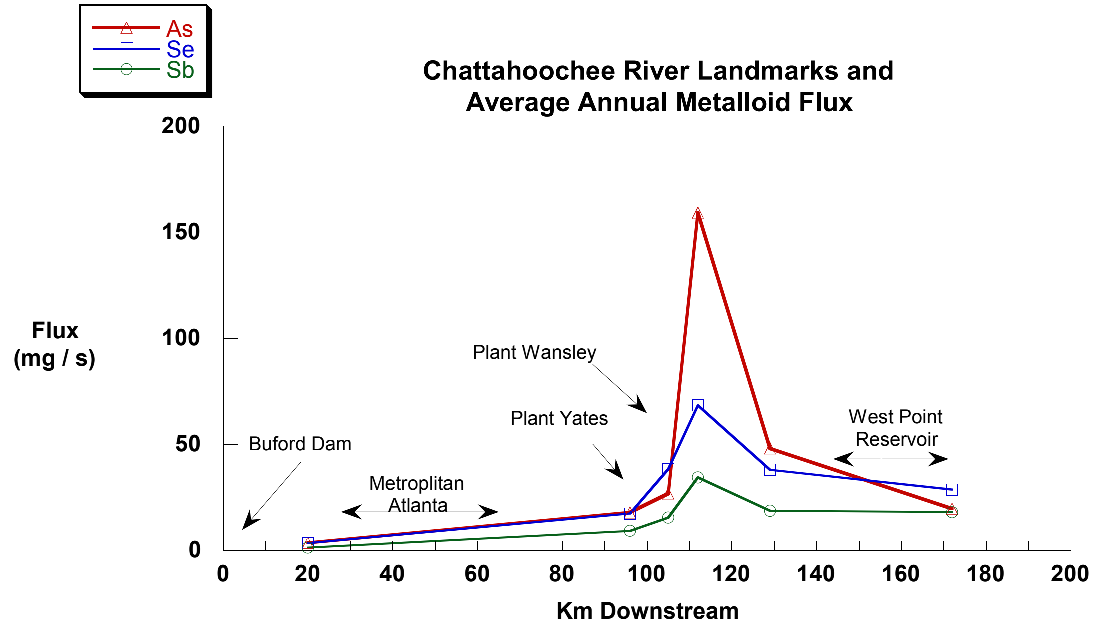

Figure 3-3. Chattahoochee River annual average metalloid flux

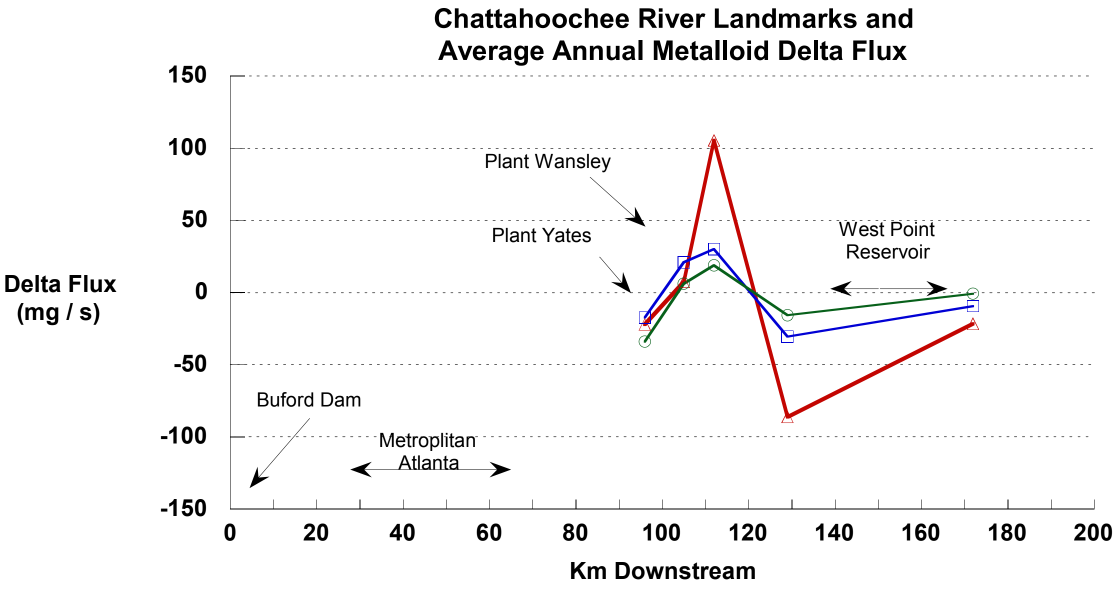

Figure 3-4. Chattahoochee River annual average metalloid Δ Flux

the site at the time of sampling yields metalloid flux, in units of mass per unit time (mg/s). Unlike concentration, which is a volume-dependant quantity, fluxes permit evaluations of the mass transport of metalloids through the river at the time and location of sampling.

On the Etowah River (Fig. 3-7, 3-8) there are two stretches of the river that show increasing metalloid fluxes. They occur at km 10 and km 112. The increase in flux at km 10 is attributed to the Cartersville barite mines. The increased fluxes at km 112 are the result of fly ash leachate from the Plant Hammond ash ponds.

On the Chattahoochee River (Figs. 3-9 - 3-16) there is an increase in metalloid flux beginning after sample site 95. This is presumably due to discharge from ash ponds. The same reasoning regarding the source of the increased metalloid concentrations on the Chattahoochee and Etowah Rivers can be applied to the flux calculations. However, there is also a sharp drop in flux from km 112 to km 125. This indicates that dissolved metalloids in the river are being removed from the system. The mechanism behind this loss and the fate of the metalloids in the river will be discussed in Chapter IV.

3.1.3 Delta Flux (Δ Flux) Profiles

The *Δ Flux data discussed in this section is located in Appendix II.* Delta flux (Δ Flux) is a measurement of the net loss or gain of dissolved metalloids over a stretch of river. Δ Fluxes are calculated by taking the difference of the downstream and upstream fluxes between any two points on a river. In profile (Figure 3-4) Δ Flux is displayed at the downstream sample site. The Δ Flux shown at km 96 is calculated using flux data from sample site 20 and sample site 96. A positive Δ Flux indicates an input of metalloids to the river. A negative Δ Flux indicates a loss of metalloids from the river.

In the Etowah River (Fig. 3-7, 3-8) the Δ Flux profiles show an input of metalloids at km 10 and 112. These positive Δ Fluxes are a result of effluent from tthe barite mines and Plant Hammond respectively.

On the Chattahoochee (Figs. 3-9 - 3-16) there is a input of metalloids from km 95 to km 109. The sources of the metalloid input are the ash ponds associated with Plants Yates and Wansley. Downstream of km 109 there is loss of metalloids from the river. The mechanisms behind this loss and the fate of the metalloids in the rivers will be discussed in Chapter IV.

3.1.4 Suspended Sediment Load and Metalloid Concentration Profiles

The suspended sediment data discussed in this section is located in Appendix I. The suspended sediment profiles (Fig. 3-6) and the suspended sediment metalloid concentration profiles (Fig. 3-5) show the concentration of metalloids on particles suspended in the river flow. Suspended sediment profile collections were begun in November 2001, thus there are no suspended sediment profiles for the Etowah River. The suspended sediment profiles in the Chattahoochee River (Figs. 3-9 - 3-16) show an increase in sediment metalloid loading downstream of the Plants Yates and Wansley. This is presumably due to two processes. The first is the input of solid ash material from the ash ponds to Chattahoochee from the ponds. The second is the sorption of dissolved

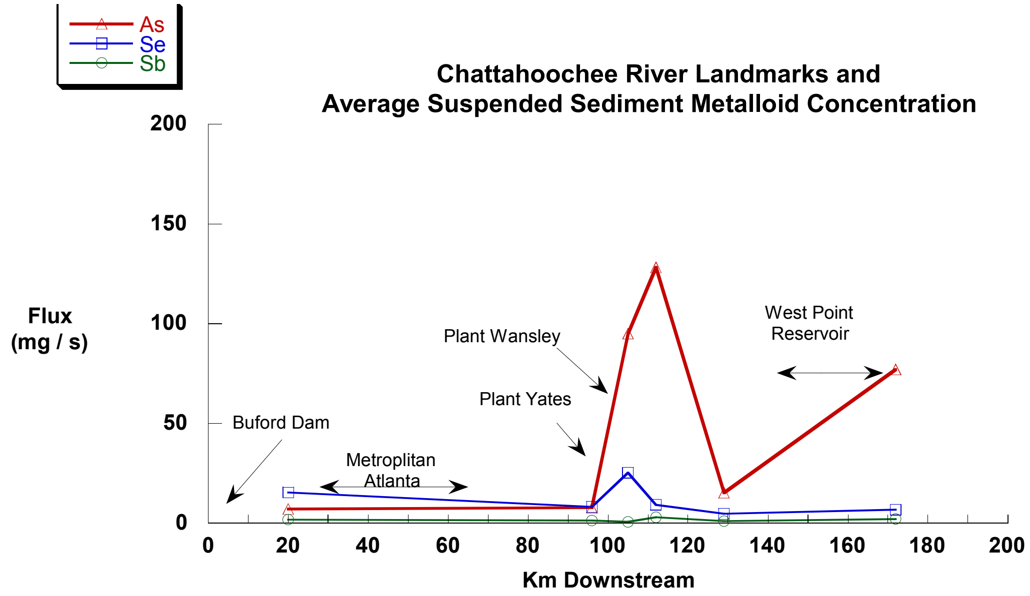

Figure 3-5. Chattahoochee River average annual suspended sediment metalloid concentration

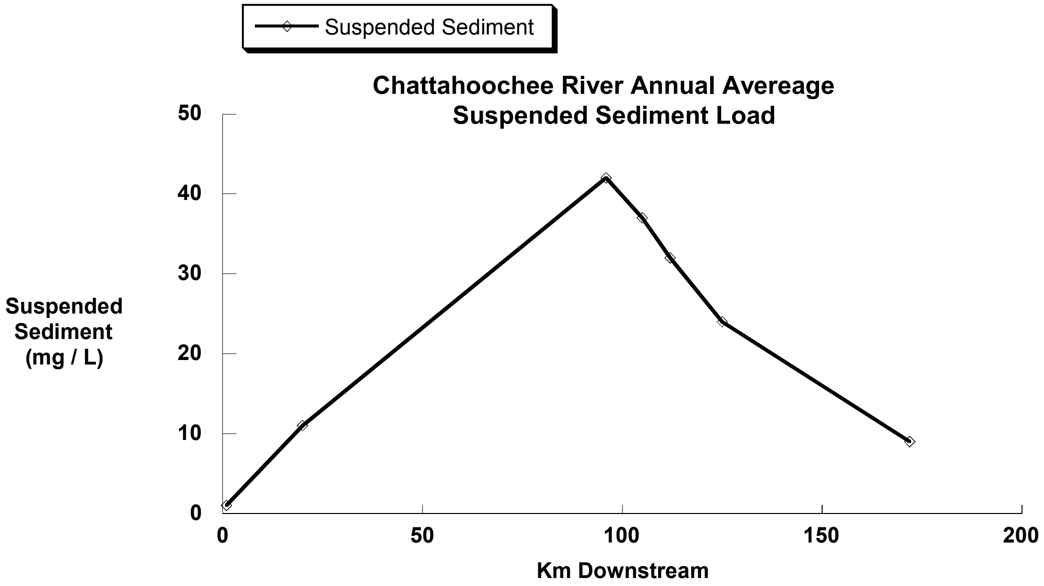

Figure 3-6. Chattahoochee River average annual suspended sediment load

As, Se, and Sb onto sediment suspended particles. Downstream of Yates and Wansley the suspended sediment metalloid concentrations decrease in a manner similar to the metalloid concentrations and fluxes. This is presumably due to the exchange processes that occur in river systems, i.e. the settling of metalloid laden sediment and the suspension of “clean” unaffected sediment from further downstream.

3.2 The Etowah River and Plant Bowen

In the late 1980’s and early 1990’s Froelich noted that Euharlee Creek, a tributary to the Etowah River that received ash pond effluent from Bowen CFPP was more contaminated with the metalloid Ge than any stream on the the planet. Presumably this Ge contamination was associated with the other more abundant and toxic metalloids As, Se, and Sb. It was the goal of this study to use the flux from plant Bowen as an integral part of the escape efficiency calculation. Transects of the Etowah above and below the mouth of Euharlee Creek (km 24 on figures 3-7 and 3-8) indicate there is no longer an appreciable flux of metalloids into the Etowah from Euharlee Creek and Plant Bowen. This is different from expectations based on the previous Etowah River transects. In the middle and late 1990’s plant Bowen switched, at least partially, to dry ash disposal. During dry ash disposal, ash sluiced from the bag house and precipitator is allowed to dry and stored on site or sold for other industrial use. Because the ash is stored dry the sorbed metalloids do not enter the aqueous phase and cannot be transported to local rivers. The fly ash sold off site is used for many industrial purposes including the production of dry wall and concrete. The author followed an ash truck from the Bowen site to a housing development where the ash was used as landfill beneath a new house. Georgia Power has informed the author that Bowen currently sells 50% of its ash, and wishes to eventually sell all ash produced at the plant.

Etowah River transects also reveal a surprising peak in metalloid flux at km 11 on figures 3-7 and 3-8. This peak is not located near a power plant, nor do the metalloid ratios (Se/As = 1.85, Sb/As = 1.12) agree with those in rivers clearly impacted by coal fired power plants (Se/As = 0.27, Sb/As = 0.13) (4.1.1). Research into the geology and history of the area shows that Cartersville area is actively involved in the barite ($BaSO_4$) mining industry. Barite is commonly associated with Sb (Klien and Halibut 1993) minerals such as stibnite and presumably other metalloid minerals. The abundance of barite nodules in the strata cut by the river in this area leads us to believe that this anomalous peak is the result of the weathering of barite bearing strata and minerals and water draining from water logged abandoned quarries.

Figures 3-7 – 3-16. Metalloid profiles vs. km downstream for each sampling transect.

Concentration of As, Se, and Sb in ppb (µg / L)

Flux of As, Se, and Sb in mg / s

Suspended sediment concentrations of As, Se, and Sb in ppm (mg / kg) and suspended sediment load in mg / L

Delta Flux of As, Se, and Sb in mg / s

On each graph, As is represented by red open triangles; Se by blue open squares; and Sb by green open circles. On the suspended sediment graphs suspended sediment load is represented by black open diamonds.

On the Delta (Δ) Flux plots, Δ Flux is displayed at the downstream sampling site. The Δ Flux at km 96 is calculated by subtracting the flux at km 20 from the flux at km 96. This Δ Flux is then displayed at km 96 in profile. This system is used for every station on every Δ Flux profile.

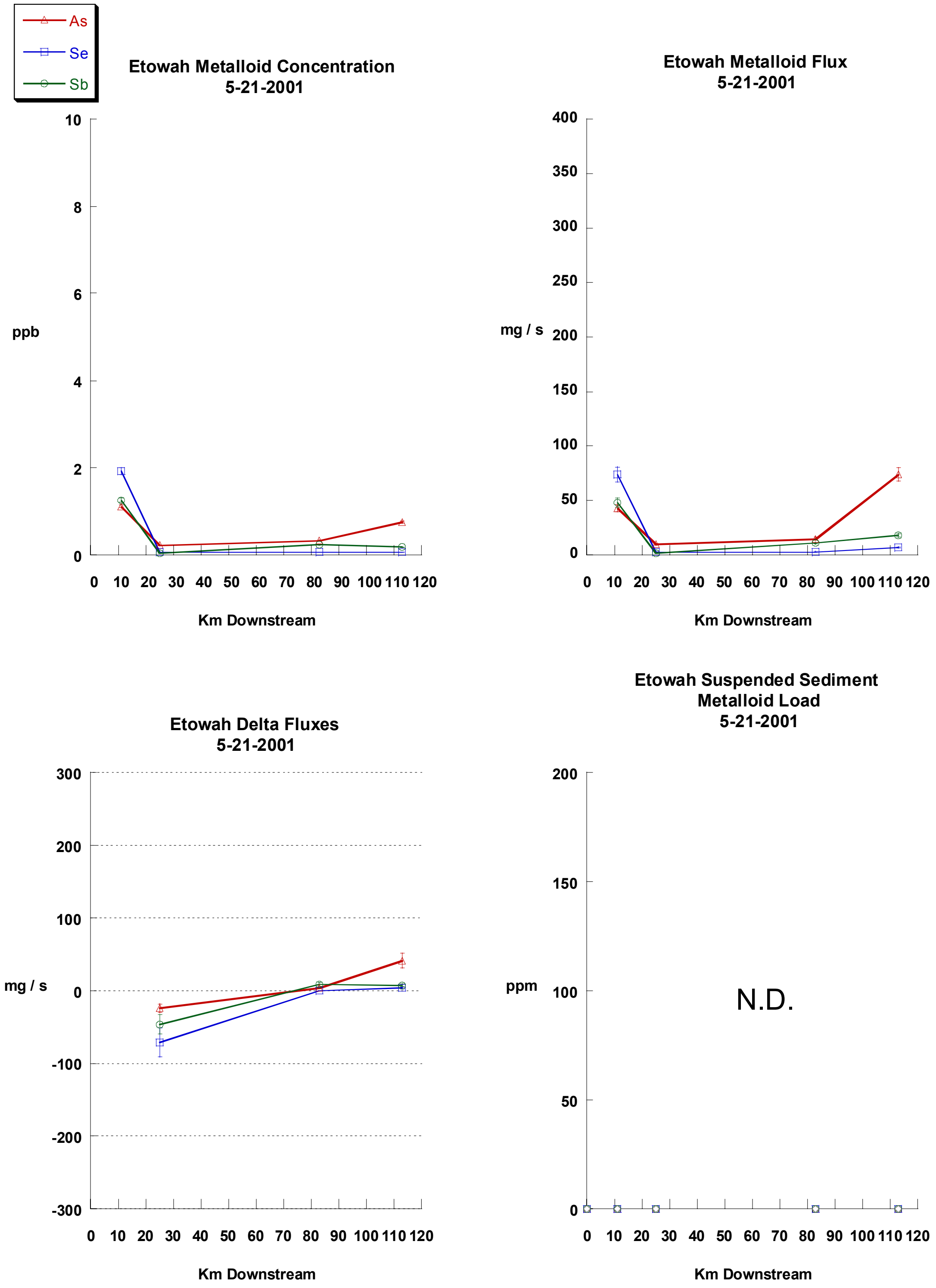

Figure 3-7. Etowah River Metalloid Data, 21 May 2001

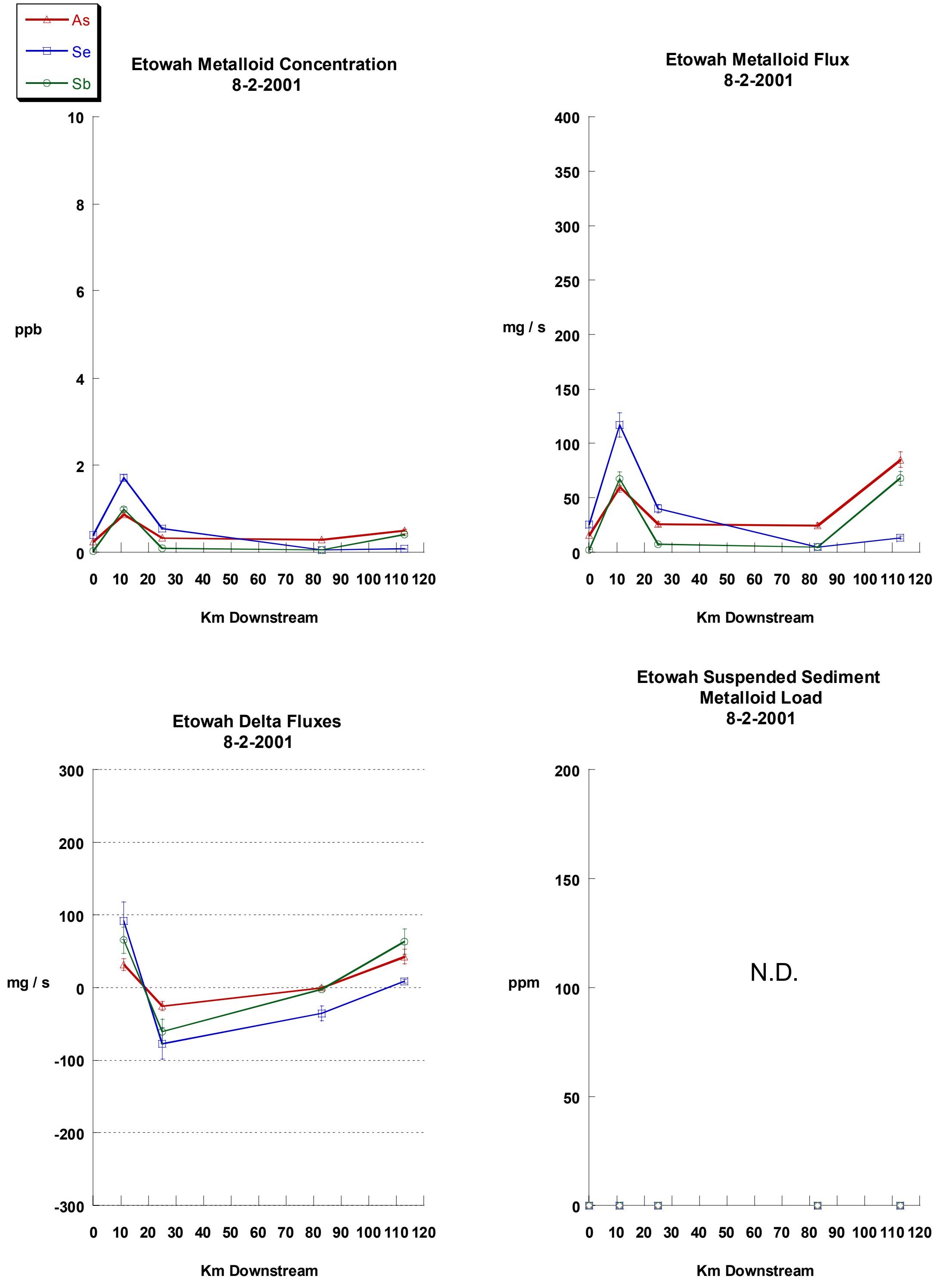

Figure 3-8. Etowah River Metalloid Data, 2 August 2001

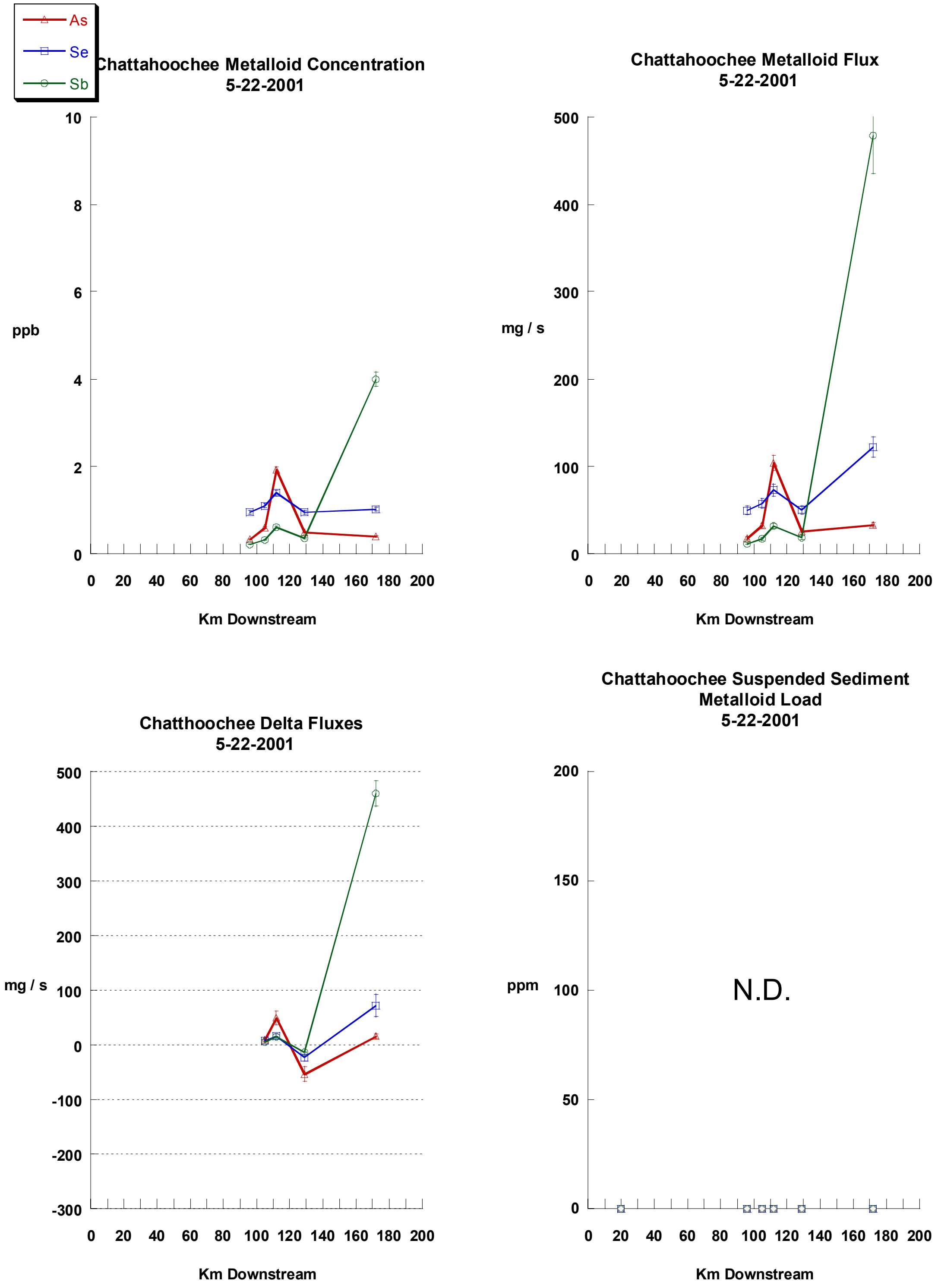

Figure 3-9. Chattahoochee River Metalloid Data, 22 May 2001

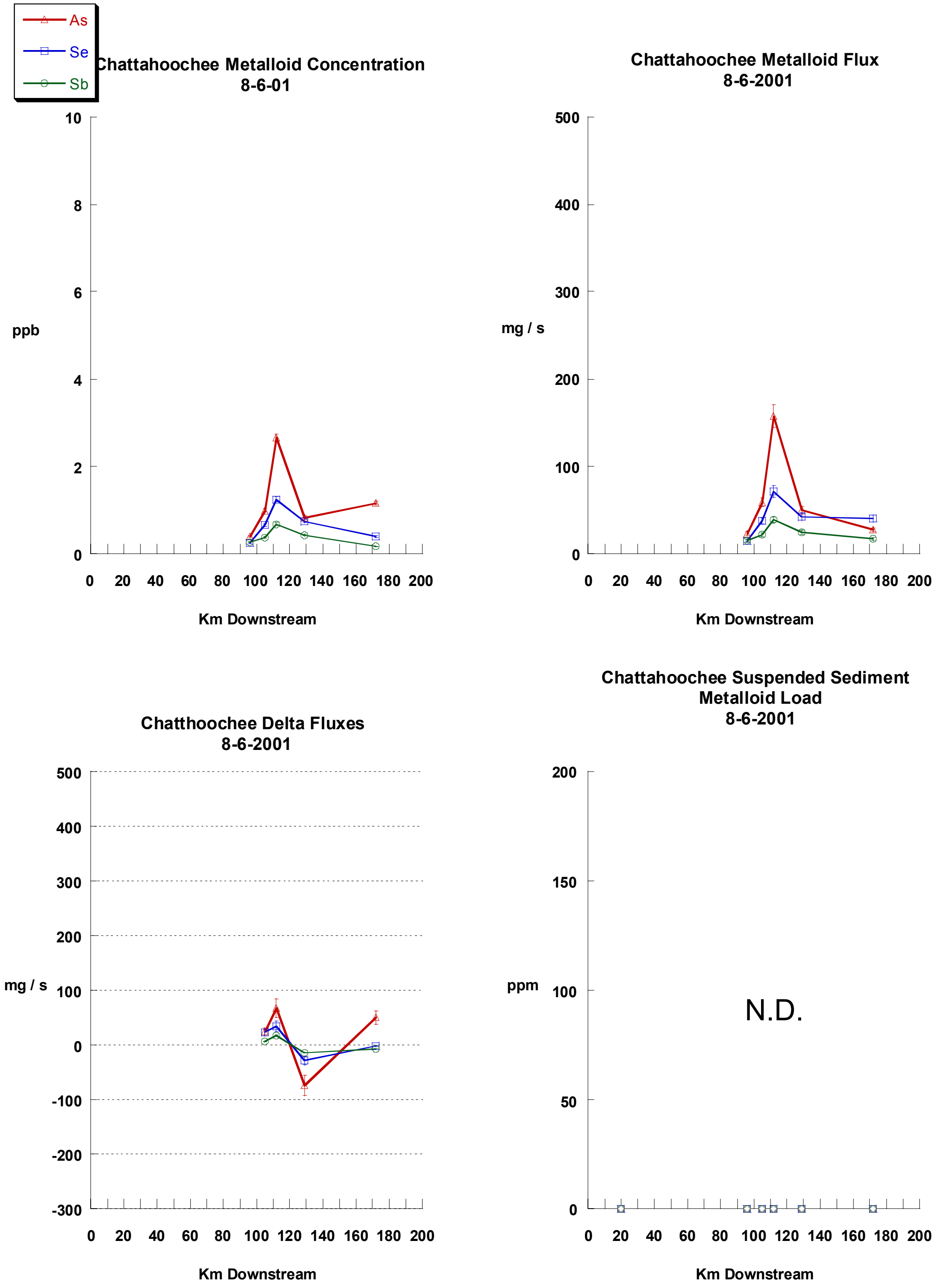

Figure 3-10. Chattahoochee River Metalloid Data, 6 August 2001

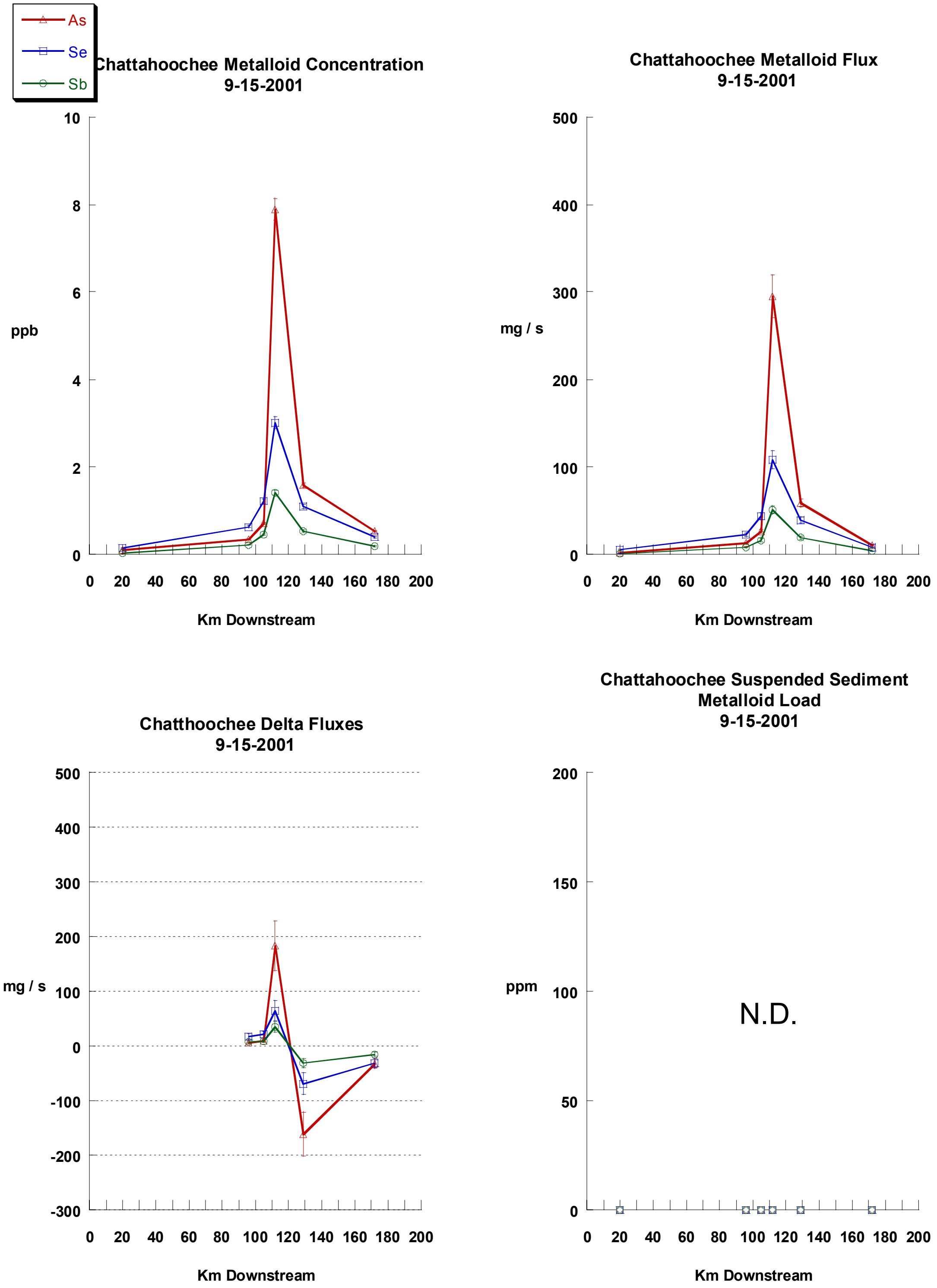

Figure 3-11. Chattahoochee River Metalloid Data, 15 September 2001

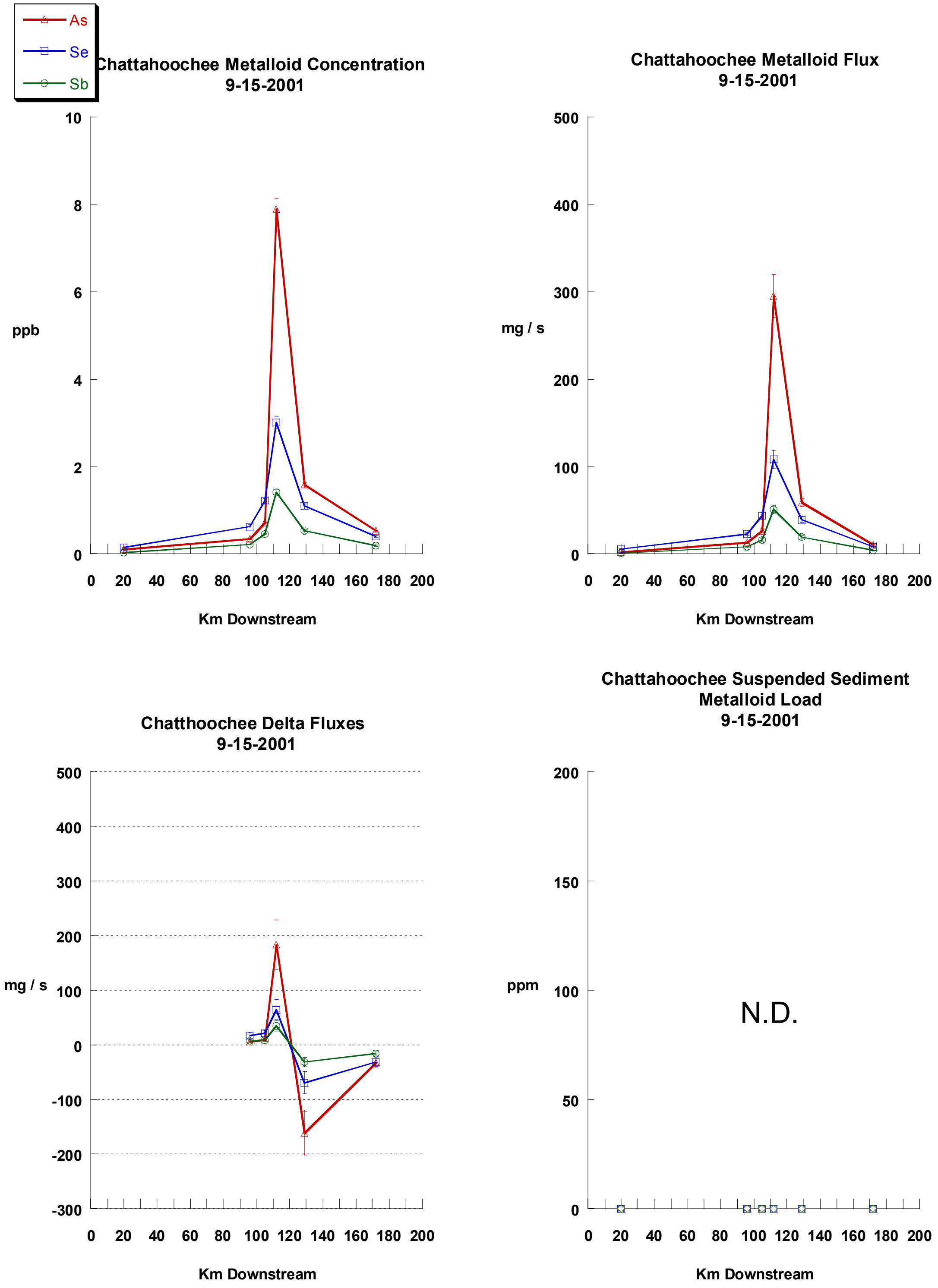

Figure 3-12. Chattahoochee River Metalloid Data, 9 November 2001

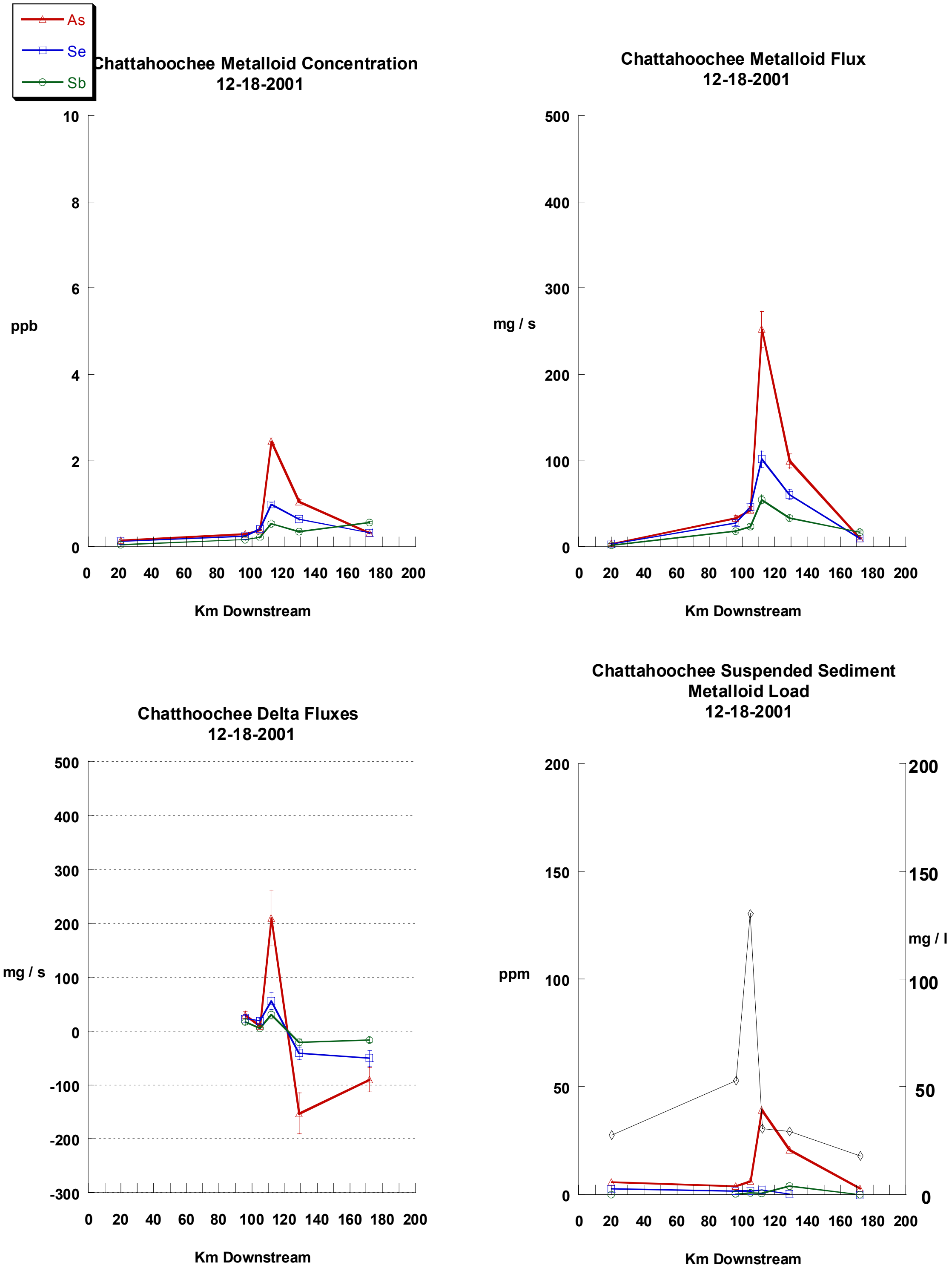

Figure 3-13. Chattahoochee River Metalloid Data, 18 December 2001

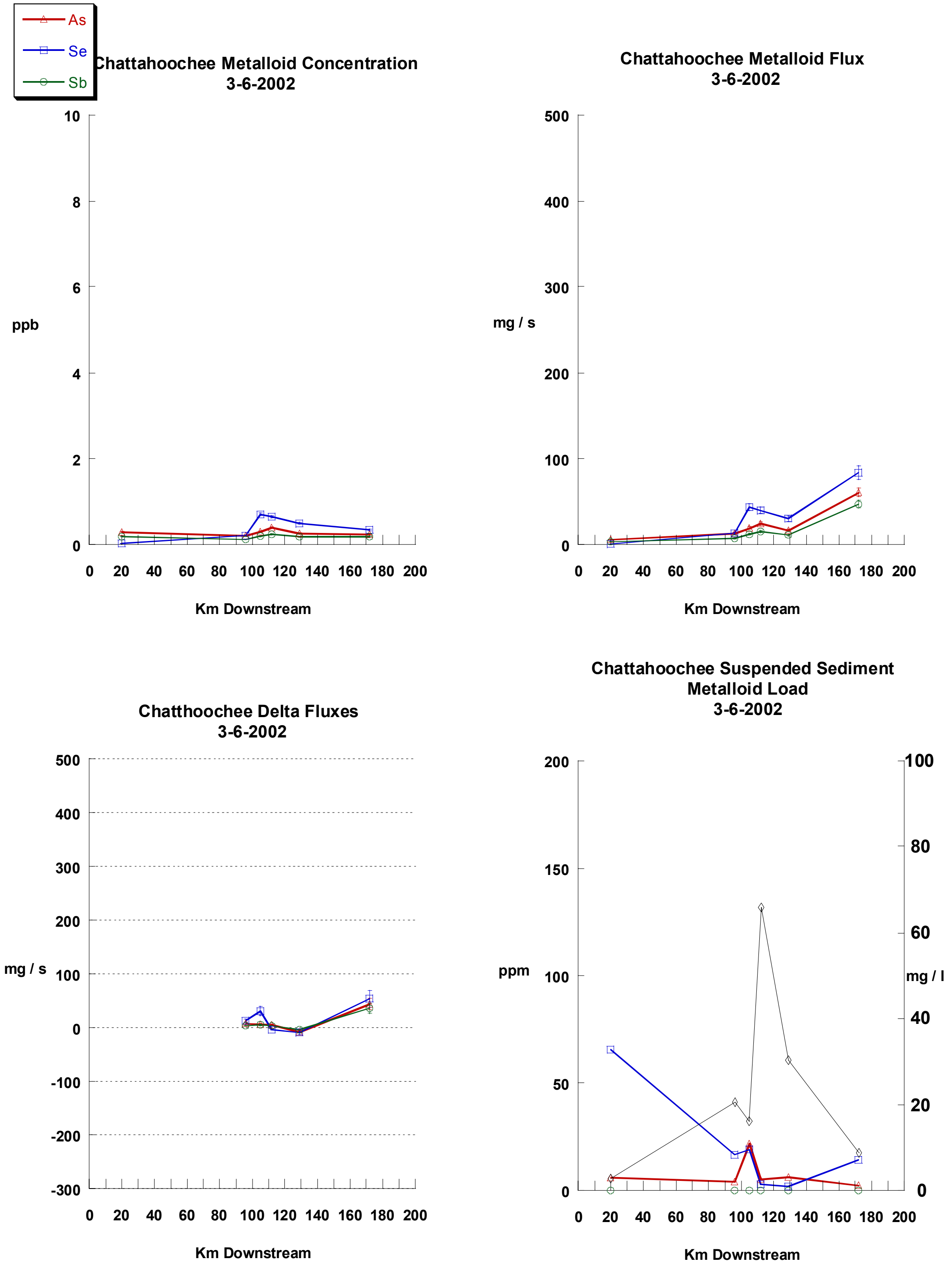

Figure 3-14. Chattahoochee River Metalloid Data, 6 March, 2002

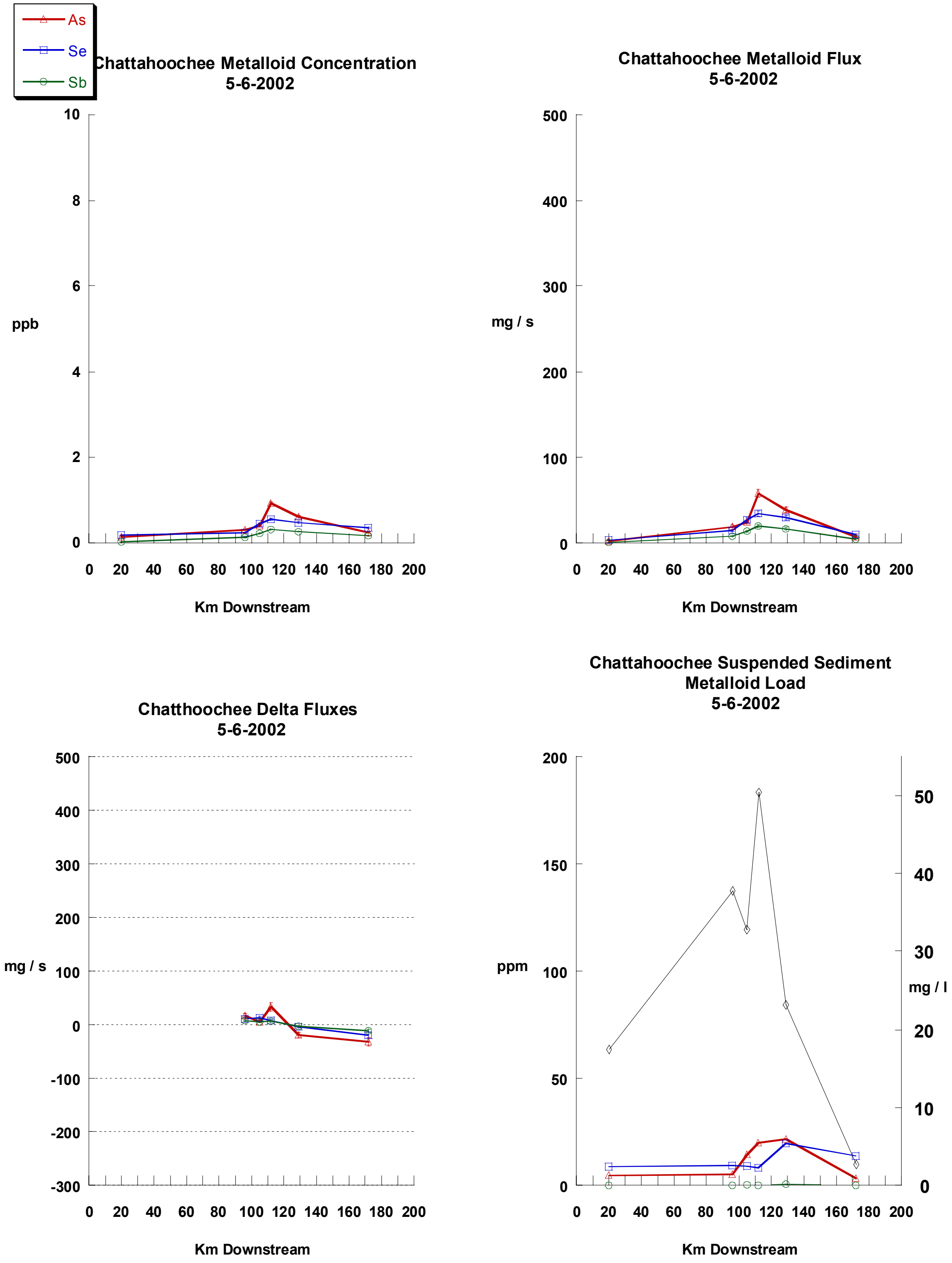

Figure 3-15. Chattahoochee River Metalloid Data, 6 May 2002

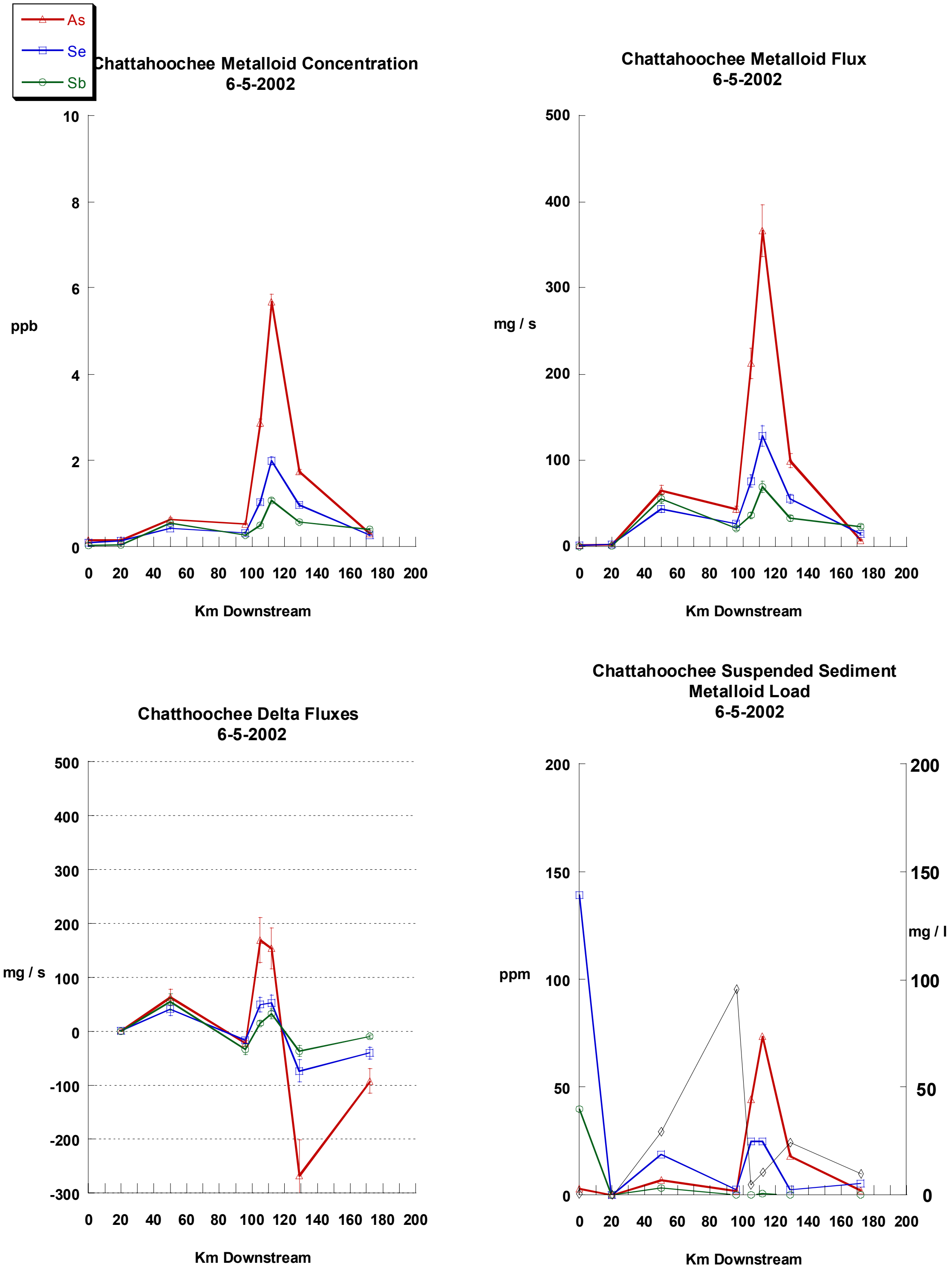
Chattahoochee Metalloid Concentration
6-5-2002

Chattahoochee Metalloid Flux
6-5-2002

Chatthoochee Delta Fluxes
6-5-2002

Chattahoochee Suspended Sediment
Metalloid Load
6-5-2002

Figure 3-16. Chattahoochee River Metalloid Data, 5 June 2002

3.3 River Nutrient Profiles

This section discusses the Chattahoochee River nutrient profiles gathered during this study. Although the magnitude of the increases and decreases in river nutrients change from transect to transect, the general trends are the same. These trends are discussed below.

Five nutrients were analyzed during this research: dissolved reactive phosphate (PO_4^{3-}), nitrite (NO_2^-), ammonia (NH_4^-), silica (Si^-), and nitrite + nitrate ($NO_2^- + NO_3^-$). Average annual concentrations are shown in Fig. 3-17. Daily transect data is shown in Figs. 3-18 – 3-22. All nutrient profiles show an increase in nutrient concentration from above Atlanta to above Plants Yates and Wansley. Below Yates and Wansley all nutrient concentrations decrease. This decrease is similar to the observed decreases in all metalloid profiles across the same stretch of river.

Phosphate, ammonia, nitrite, and nitrate are nutrients essential to the growth and sustenance of photosynthetic communities. All can be limiting nutrients depending on the prevailing environmental conditions. These nutrients are released into the environment in and around major metropolitan areas. Phosphate is a major constituent in laundry detergent. The state of Georgia does not have regulations governing phosphates in detergents. The nitrogenous nutrients are by products of wastewater treatment. One of the major wastewater treatment plants for Atlanta discharges treated water to Utoy Creek, a tributary of the Chattahoochee in Atlanta. Silica is a ubiquitous nutrient in aquatic environments. It is mobilized into the aquatic environment through the weathering of silicate rocks and minerals. The data indicate that the decreases in nutrient concentration across the stretch of the Chattahoochee River where Plants Yates and Wansley are sited is most likely a result of biological activity. This important has implications for the fate of metalloids in the environment, as will be discussed in Chapter IV.

Figures 3-13 – 3-17. Nutrient profiles vs. km downstream for each sampling trip arranged clockwise starting in the top left hand corner.

Dissolved Reactive Phosphate (PO_4) in units of μM

Ammonia (NH_4) in units of μM

Nitrite + Nitrate (NO_2 + NO_3)

Silica (Si) in units of μM

Nitrite (NO_2) in units of μM

On the graph of NO_2 + NO_3 and Si, NO_2 + NO_3 is represented by black open squares. Si is represented by green open inverted triangles.

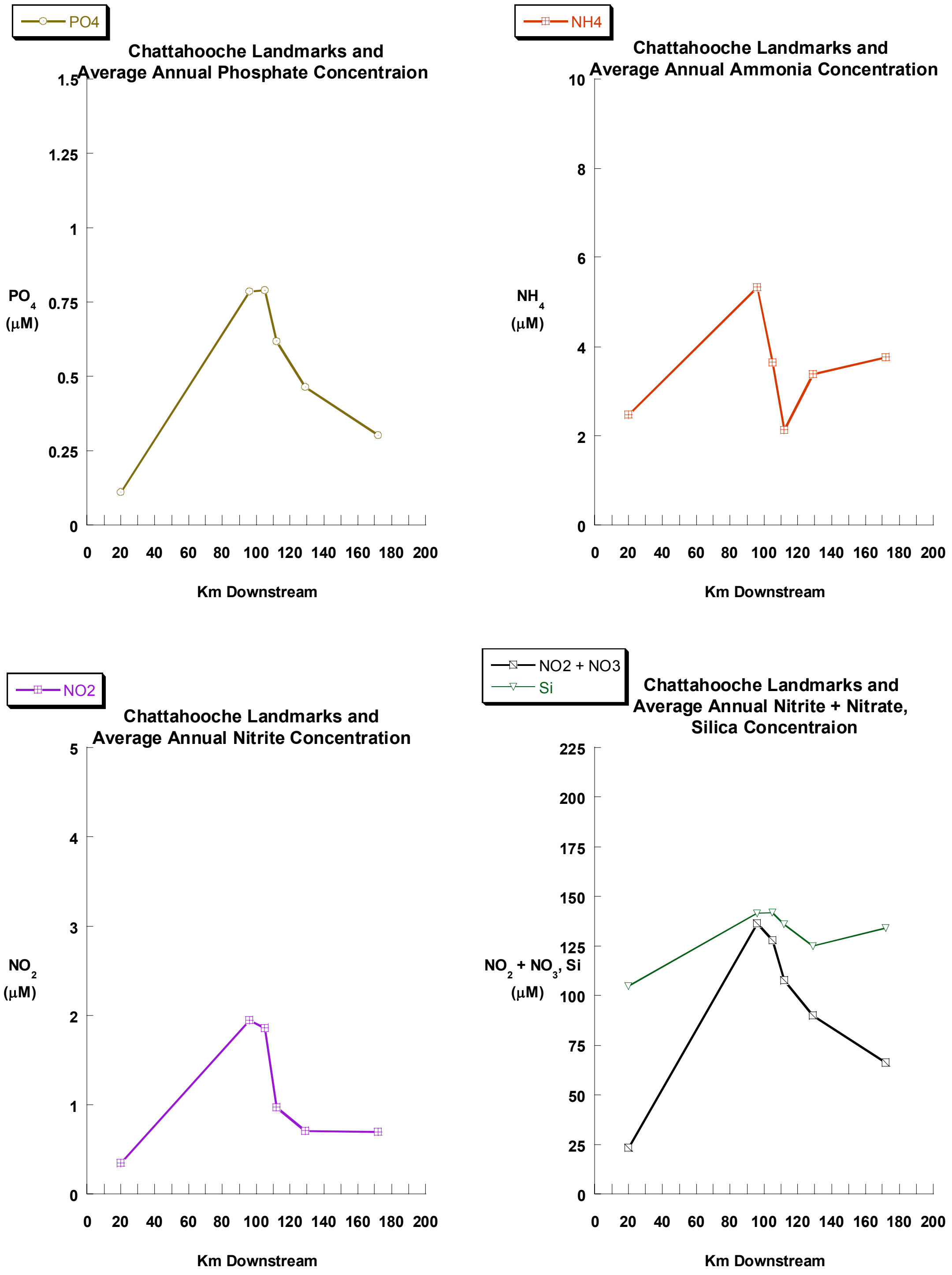

Figure 3-17. Chattahoochee River average annual nutrient concentrations

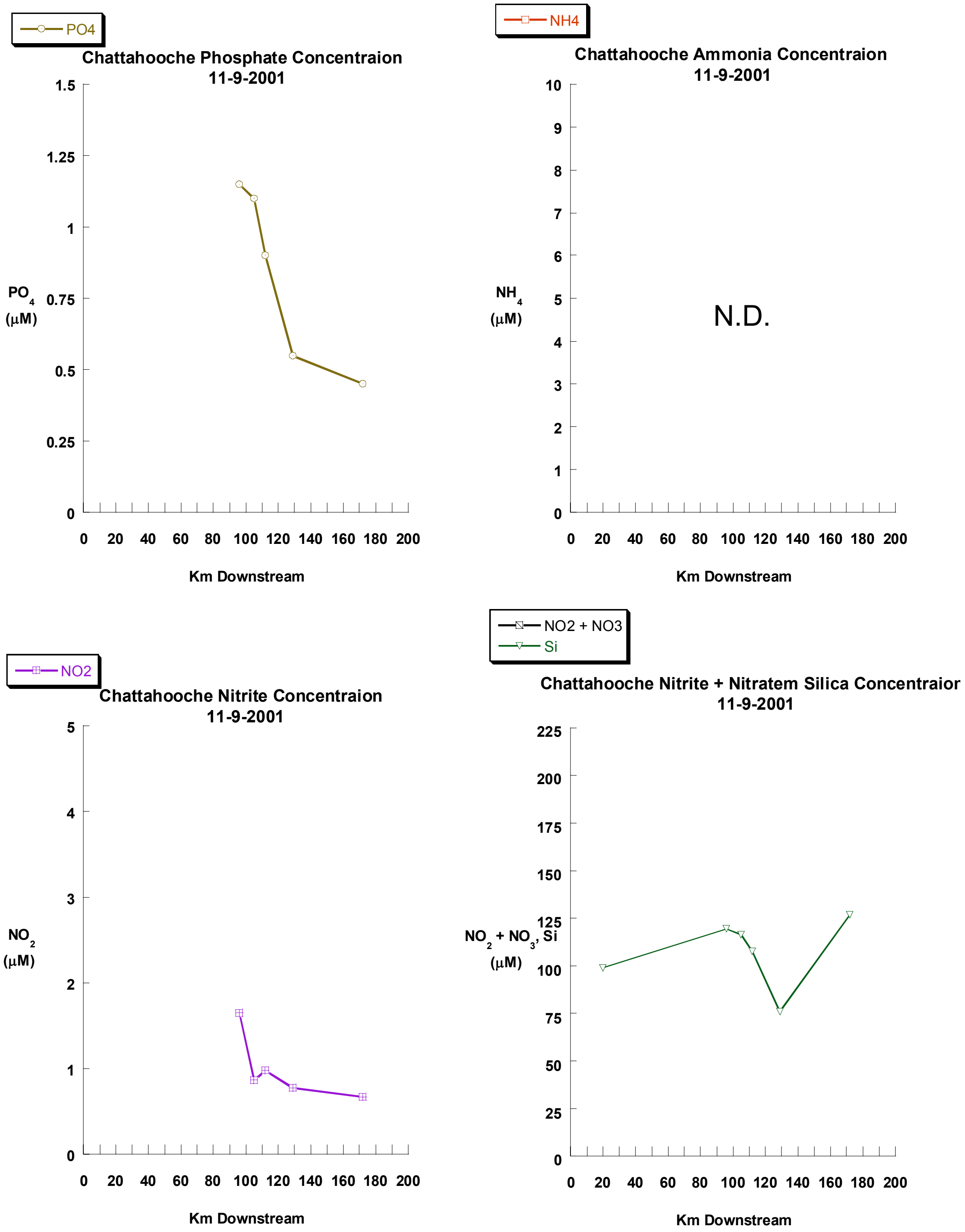

Figure 3-18. Chattahoochee River Nutrient Data, 9 November 2001

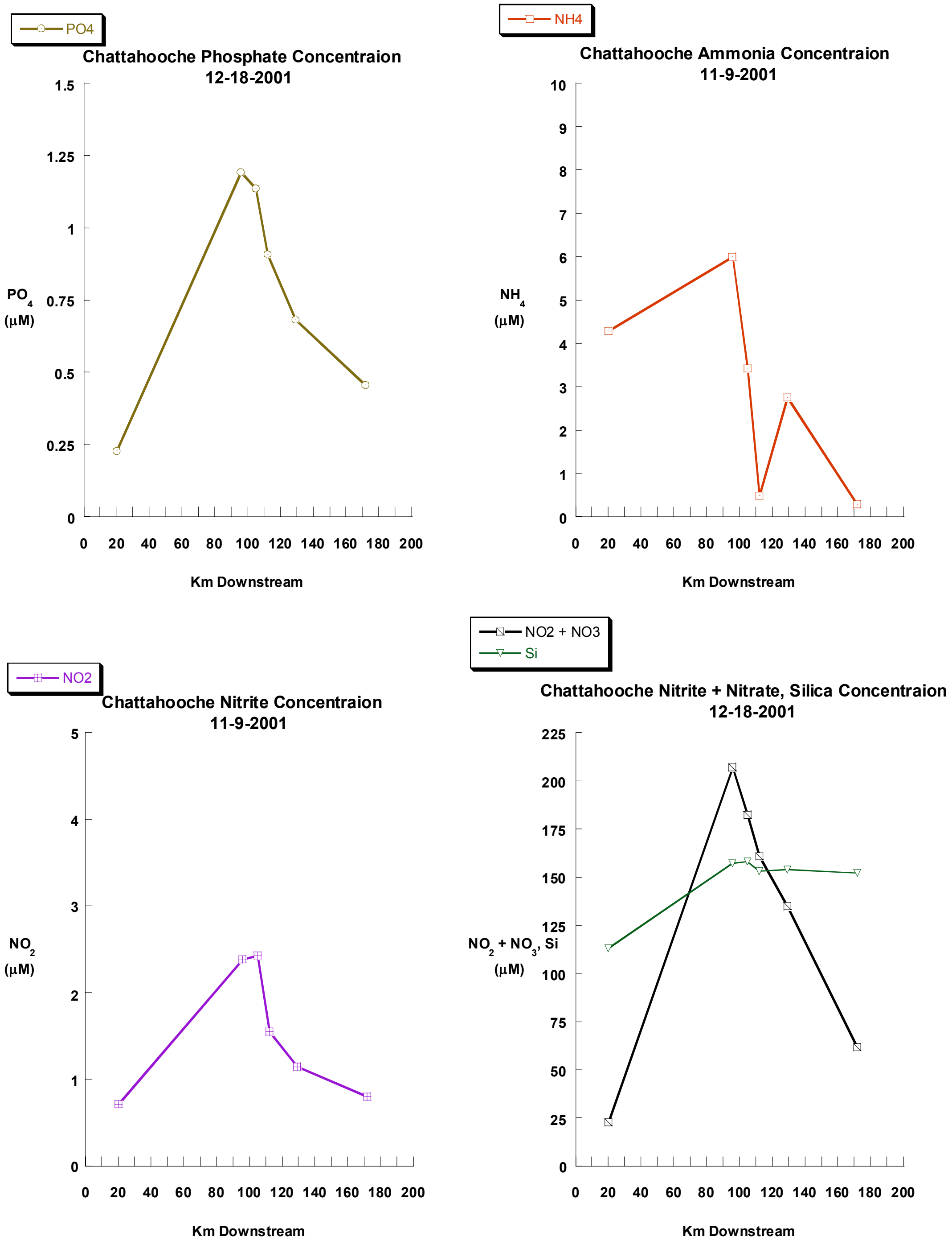

Figure 3-19. Chattahoochee Nutrient Data, 18 December 2001

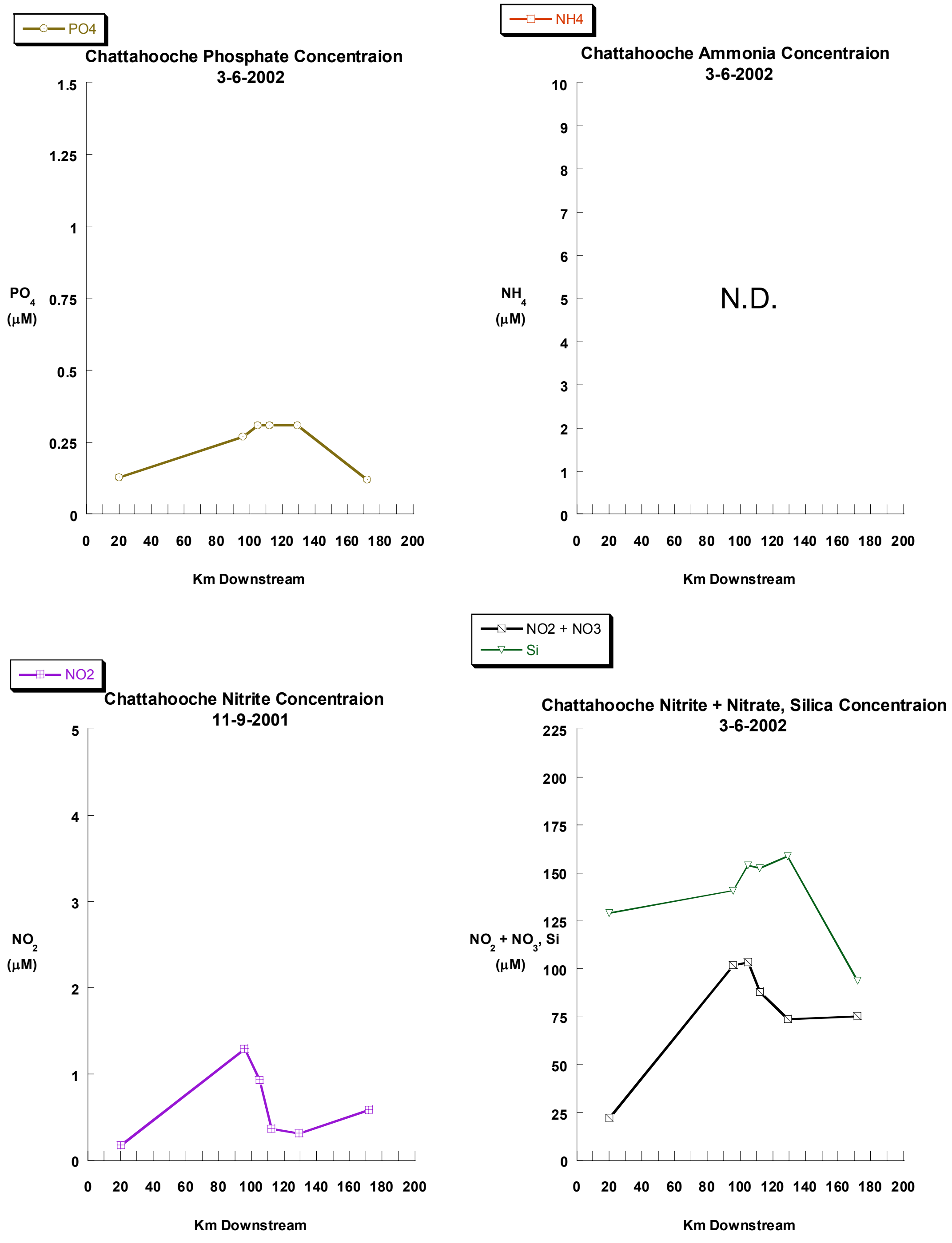

Figure 3-20. Chattahoochee River Nutrient Data, 6 March 2002

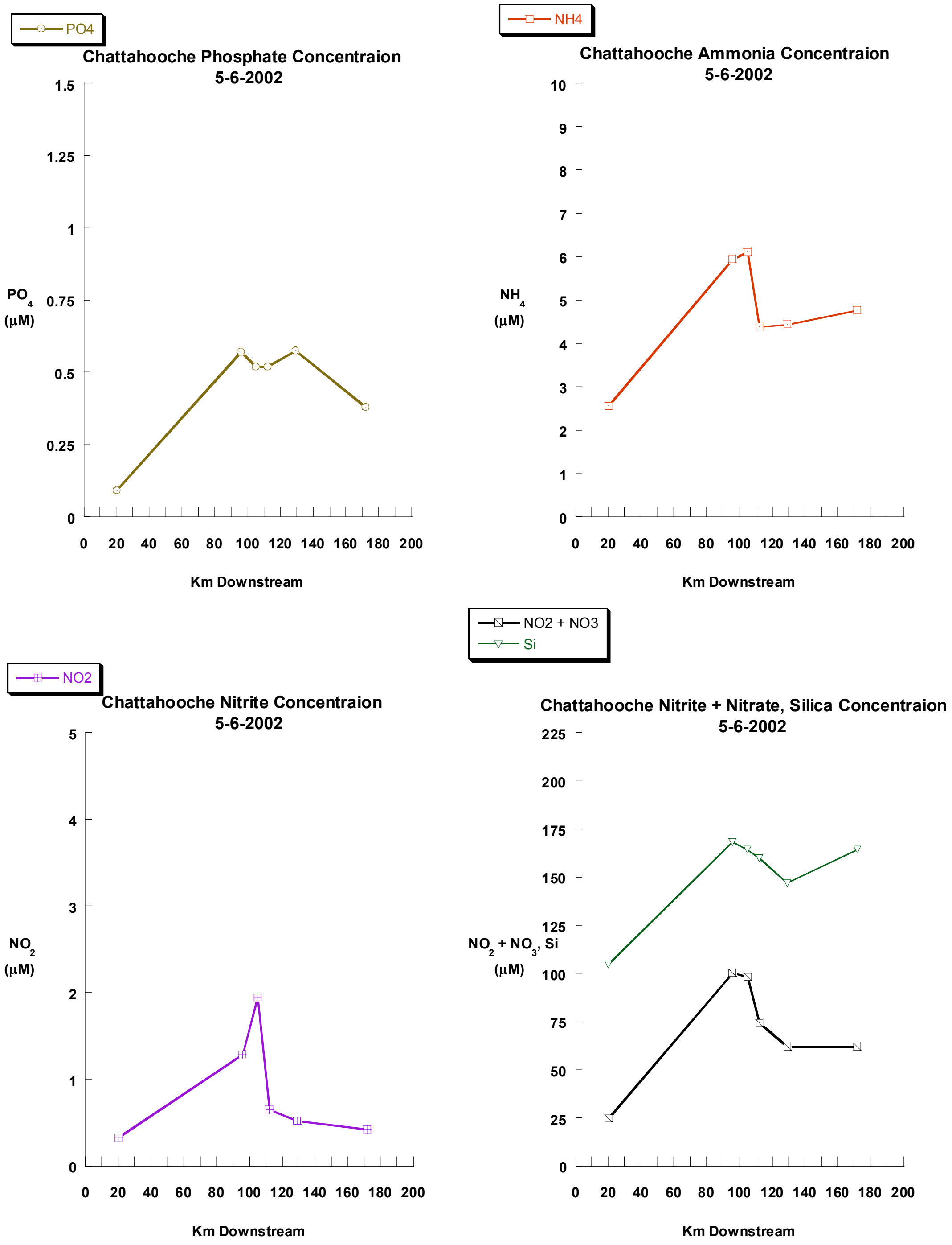

Figure 3-21. Chattahoochee River Nutrient Data, 6 May 2002

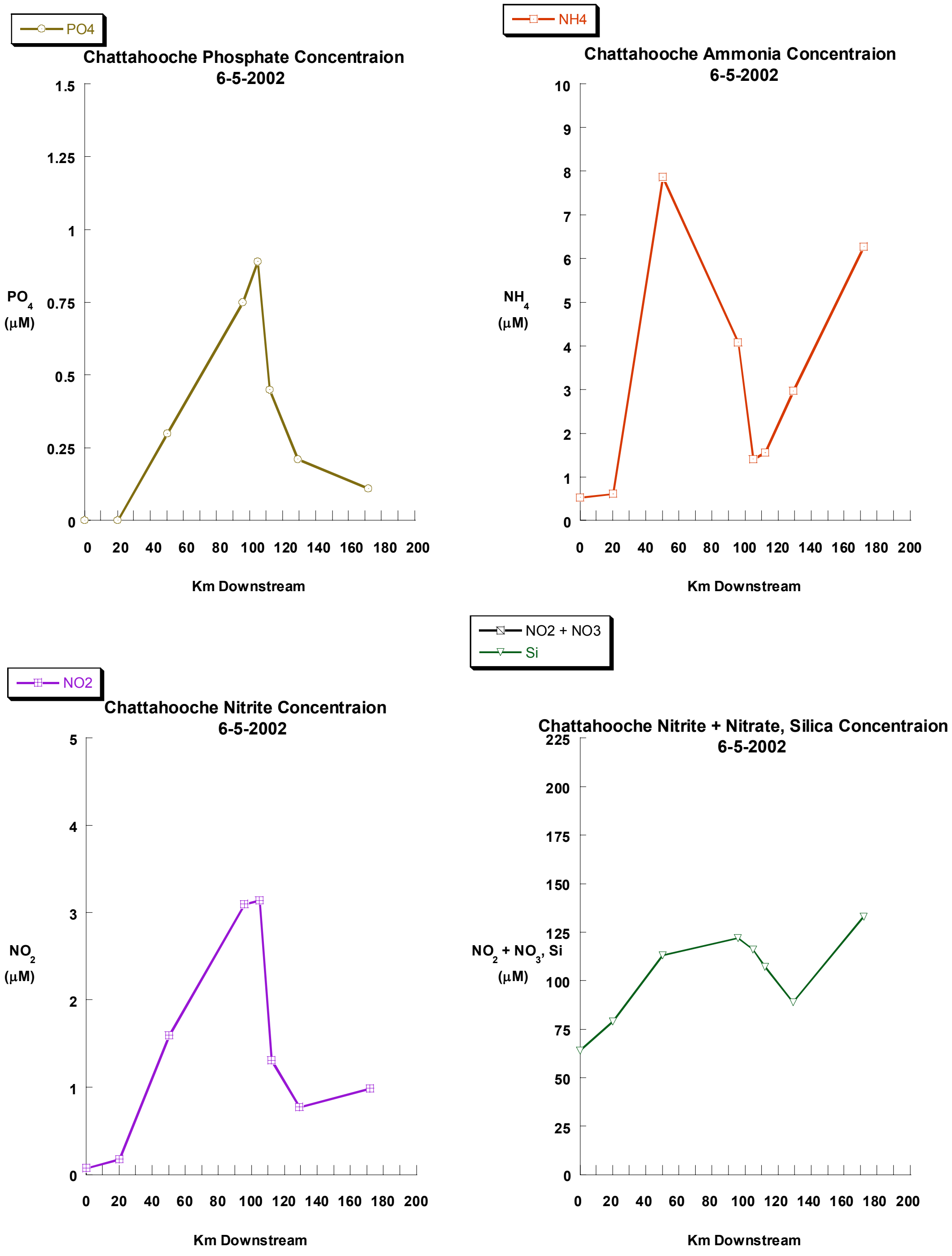

Figure 3-22. Chattahoochee River Nutrient Data, 5 June 2002

CHAPTER IV

DISCUSSION

This chapter discusses the implications of the data presented in the results section. I first focus on quantifying metalloid release from coal fired power plants. I follow with a discussion of the fate of metalloid contaminants in river systems.

4.1 Delta Fluxes

4.1.1 Ash Pond Effluent Evidence

Several conclusions can be drawn from examination of the Δ Flux data gathered during this study. Of critical import is evidence that the signal I have discovered can be attributed to ash pond effluent as opposed to a natural source or effluent from another type of industrial facility.

Table 1-4 contains the average concentrations of metalloids in coal and the reported ranges of those concentrations from the literature. If the peak in Δ Flux below plants Yates and Wansley is from ash pond effluent, then metalloid ratios in the receiving waters should reflect the ratios of the metalloid concentrations found in average coals. Figures 4-1a and b are "Redfield" style plots that show the ratios of Se and Sb to As in the Δ Fluxes calculated during this study. In both the Se / As and Sb / As plots there is a linear relationship. This relationship is expected if CFPP effluents discharge approximately constant As/Se/Sb ratios with time. The mass ratios of Se to As and Sb to As from the plots is 0.27 ppb / ppb and 0.13 ppb / ppb respectively. The metalloid

Table 4-1 Bowen Ash Pond Samples

Table 4-1 shows the metalloid concentration in historic ash pond samples (Froelich) taken from the Plant Bowen ash pond.

Location	Element	ppb	Se / As	Sb / As
Plant Bowen Fly Ash and Water Discharge (R-655)	As Se Sb	242.5 69.4 57.8	0.29	0.24
Plant Bowen Ash Pond Effluent (R-662)	As Se Sb	61.3 12.7 13.4	0.21	0.22

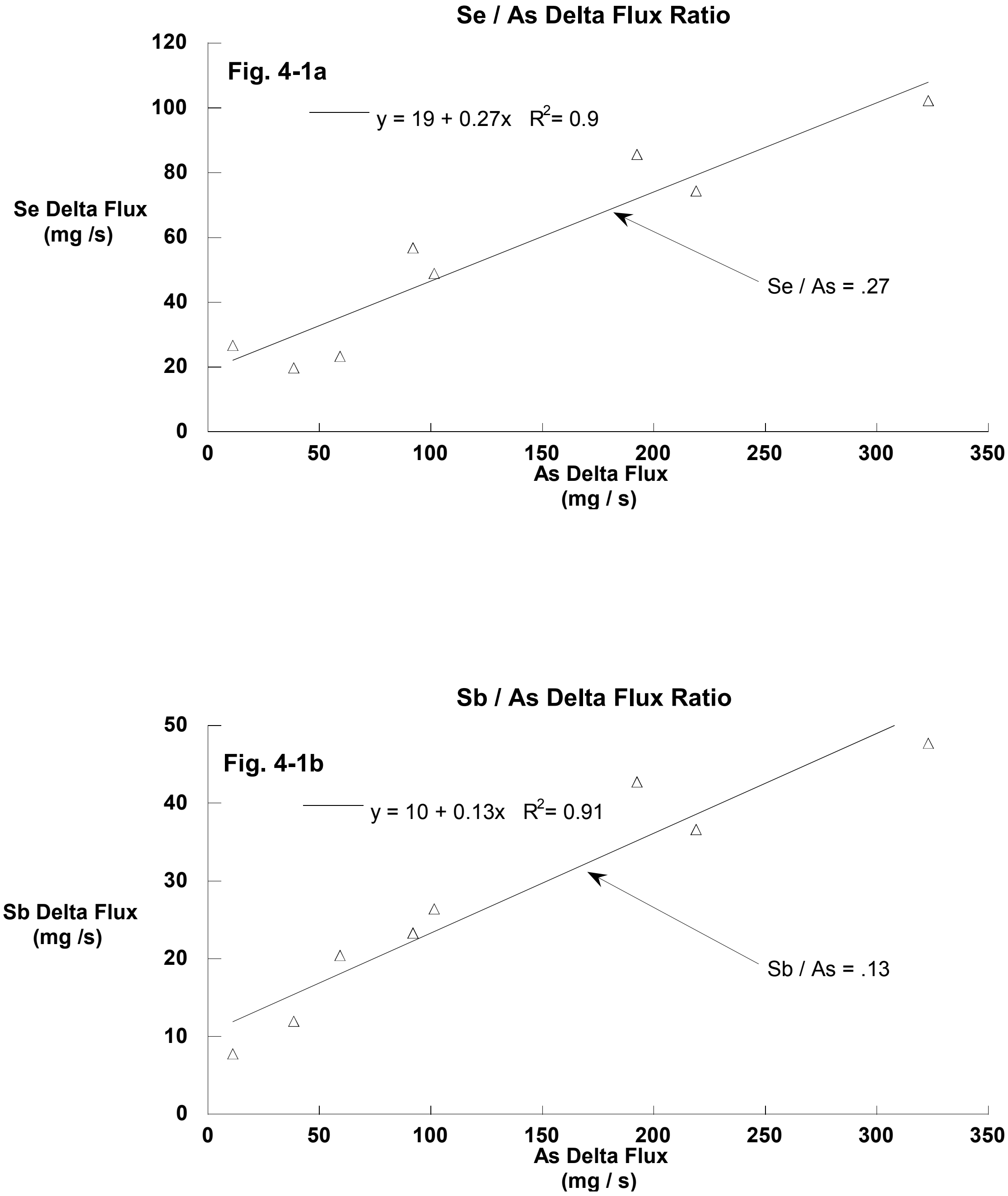

Figure 4-1 Δ Flux Metalloid Ratios. Figures 4-1a & b show the Se / As and Sb / As ratios of the Δ Fluxes calculated during this study.

concentrations in historic samples from the Plant Bowen ash pond (Table 4-1) show similar mass ratios (particularly Se / As) as compared to the Δ flux mass ratios. The mass ratios of Se to As and Sb to As calculated from the average values are both 0.1 (Table 1-4). In the case of the Sb / As ratio this is in close agreement with the ratio calculated from the Δ Fluxes. In all cases the differences in mass ratios fall within the ranges predicted by the concentration variability in coal. The positive intercepts of the Δ Flux plots (Se / As = 19 mg / s, Sb / As = 10 mg / s) suggest that As, Se, and Sb are removed from solution in the ash ponds at different rates (Fig. 4-1). Arsenic is apparently more efficiently. The lower intercept of the Sb line suggests that it is removed more efficiently than Se.

Some thermodynamic considerations may be used to explain these differential removal rates. The Eh-pH diagrams for arsenic, selenium, and antimony (Figs 1-1 through 1-3) show that in oxic river waters the oxidized species (As (V), Se (VI) and Sb (V)) will be the dominant inorganic forms of these elements. Although they are released from the ash ponds in their reduced states, thermodynamics predicts that they should oxidize to their higher valence states. This theory is supported by the rapid removal of As as compared to Se, and Sb. Arsenic (V) is strongly attracted to the iron oxyhydroxide clays which are suspended in the Chattahoochee River. Mass balance modeling supports this hypothesis. Little is known about the sorption characteristics of Se and Sb to mineral surfaces, however this data suggests that either the oxidation or the sorption processes of these elements is slower than As and may be kinetically limited as opposed to thermodynamically controlled.

4.1.2 Escape Efficiency

Using Δ Flux and CFPP coal flow data “escape efficiency” of the metalloid elements from coal fired power plants can be estimated. Escape efficiency is a measure of the steady-state fraction of the metalloids in fired coal that escapes into the aqueous phase from power plants.

Table 4-3 shows the peak Δ Flux calculations below plants Wansley and Yates on the dates sampled during this study. In order to estimate the escape efficiency, integrated Δ Fluxes over the period of the study must be calculated. The integrated Δ Fluxes over the time period of this study are the average of the highest Δ Flux values for each sampling trip. They are 130 mg / s, 55 mg / s, and 27 mg / s for As, Se and Sb respectively (See Table 4-3). Coal flow data obtained from Georgia Power (www.southernco.com/fuelservices/gapower.htm) states that Yates and Wansley together burn 5.6×10^9 kg of coal a year. The escape efficiency is the ratio of the Δ Flux (mass metalloid / time) to the coal flux (mass coal / time). This ratio yields a result with the dimensions of mass metalloid released / mass coal burned, or the mass metalloid released to the aquatic environment for every kilogram of coal burned. The escape efficiencies for As, Se, Sb are 0.73 mg / kg, 0.30 mg / kg, and 0.15 mg / kg respectively. Based on the average metalloid concentration in coal (Table 1-4) 7.3% of the As, 30% of the Se, and 15% of the Sb in combusted coal is released aquatically every year.

Table 4-2 Metalloid Δ Fluxes

Table 4-2 shows the peak Δ Fluxes in mg /s at the peak below Plants Yates and Wansley. These are the sums of the Δ Fluxes below Yates and the Δ Fluxes below Wansley. This permits the calculation of a “universal escape efficiency based on more than one power plant.

Peak Δ Fluxes (mg / s)									
	5/22/2001	**8/6/2001**	**9/15/2001**	**11/9/2001**	**12/18/2001**	**3/6/2002**	**5/6/2002**	**6/5/2002**	**Integrated**
As	59	92	192	102	219	11	39	323	130
Se	23	57	86	49	74	27	20	102	55
Sb	20	23	43	26	37	8	12	48	27

Eq. 4-1 Metalloid Release

$$E_{eff} \times B = R$$

Equation 4.1 is used to calculate the rate of release of a metalloid element into the environment based on the escape efficiency and the amount of coal burned per unit time. E_{eff} is the metalloid escape efficiency in units of mg metalloid released / kg coal burned. B is the amount of coal burned per unit time. R is the rate of metalloid release in units of mg per unit time. Using the escape efficiency of 0.73 mg / kg for As and the estimated 5.6×10^9 kg coal burned by plants Wansley and Yates I calculate that 4.1×10^9 mg or 4.1 tons arsenic is released in to the Chattahoochee River every year. Similar calculations for Se and Sb reveal that 1.7 tons of Se and 0.87 tons of Sb are released annually to the aquatic environment. Over a 20-year period, approximately the lifetime of these power plants, this is equivalent to 81 tons As, 34 tons Se, and 17 tons Sb discharged into the Chattahoochee River.

4.2 The Fate of Metalloids in Rivers

While there is clearly a source of metalloids to the Chattahoochee River from plants Yates and Wansley, there is also a loss of metalloids from the dissolved phase downstream of the power plants. The same calculations used to determine the integrated peak Δ Flux can be used to quantify the amount of metalloids lost downstream.

Table 4-4 shows the Δ Flux values between the sampling site below Wansley and Yates (sample site 112) and the sampling site in Franklin, GA (sample site 125). The Δ Flux values show a decrease in metalloid flux between the site below Yates and Wansley and the site in Franklin. Treating this data in the same manner as the peak Δ Flux data yield integrated values of –103 mg / s As, -35 mg /s Se, and –18 mg / s Sb. Assuming that this loss rate is the same over the last 20 years, these loss fluxes represent a removal of 65 tons As, 22 tons Se, and 11 tons Sb. These removal fluxes represent 80% of the As input and 65% of the Se and Sb inputs from the power plants. Plots (Fig. 4-3) of peak Δ Flux (Table 4-3) vs. metalloid loss flux (Table 4-4) confirm the integrated loss estimates. There is a linear relationship between the Δ Flux and the loss flux. The slope of -1.2 for each of the loss plots indicates that metalloid input is 1.2 times greater than the loss and that 80% of the input flux is lost from the aqueous phase. For As, this agrees exactly with the integrated estimate. For Se and Sb there is close agreement with the integrated loss estimate. The question now becomes the fate of the metalloids in contaminated river systems. I hypothesize that there are two fates for these metalloids. The first is incorporation into the planktonic and benthic biologic systems through incidental uptake.

Table 4-3 Metalloid Loss Fluxes

Table 4-3 shows the metalloid loss fluxes between the sample site below Wansley and Yates and the sample site in Franklin. A large fraction of the metalloid input from the ash pond effluents is lost over this 17 km length of river.

Metalloid Loss Fluxes (mg / s)									
	5/22/2001	8/6/2001	9/15/2001	11/9/2001	12/18/2001	3/6/2002	5/6/2002	6/5/2002	average
As	-54	-74	-161	-90	-153	-8	-19	-267	-103.134
Se	-23	-29	-69	-28	-41	-10	-5	-73	-34.661
Sb	-13	-14	-32	-19	-21	-4	-3	-36	-17.7918

Table 4-4 Phosphate Loss Fluxes

Table 4-4 shows the loss flux of phosphate between the sample sites below Wansley and Yates and the sample site in Franklin.

PO_4^{3-} Loss Fluxes (mg / s)					
11/9/2001	12/18/2001	3/6/2002	5/6/2002	6/5/2002	Integrated
-1123.12	-2783.22	-16.70	333.17	-1621.20	-1042.21

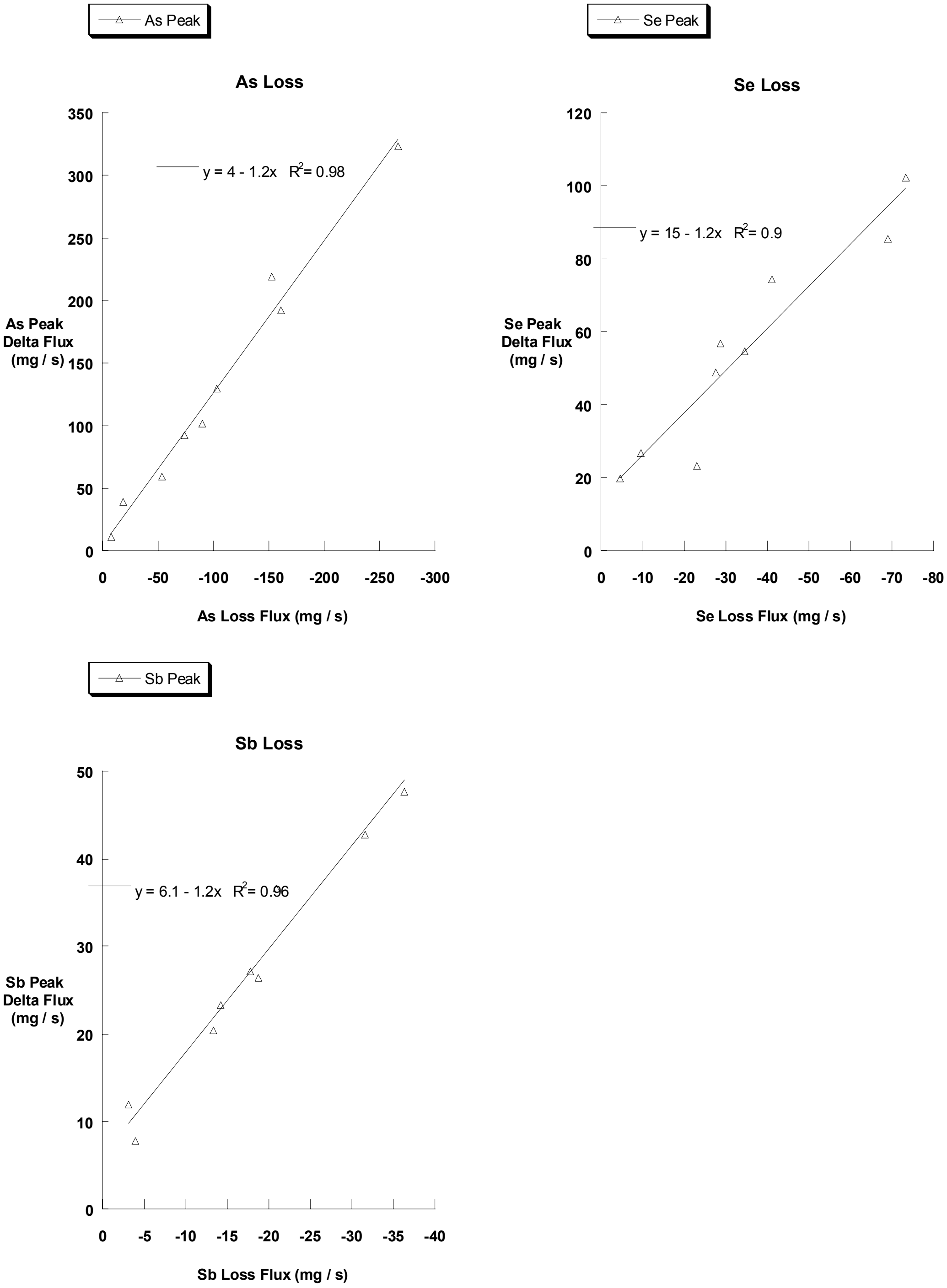

Figure 4-2Metalloid Loss Factors. Figure 4-2 shows the loss factors for As, Se, and Sb. A negative *loss* factor indicates that input is greater than loss.

The second is sorption onto suspended sediment particles followed by transport downstream.

4.2.1 Biological Uptake

All of the Chattahoochee nutrient profiles (Figs. 3-17 – 3-22) show dramatic increases in nutrient concentration between Atlanta (sample site 20) and sample site 96, above Yates and Wansley. Between this sample site and the site below Yates and Wansley (sample site 112) there is a drop in the concentration of all the nutrients analyzed during this study. This may be due to either dilution or biological uptake. Analyses of USGS stream flow data reveal that there is insufficient increase in water flow in the Chattahoochee over this stretch of river to explain the dilution of nutrients. This clearly suggests that aquatic flora and fauna are taking up nutrients.

It is known that metalloids can be incidentally incorporated into biomass in place of nutrient elements. Two well-documented examples are the substitution of Ge (germanic acid) for Si (silicic acid) in diatom shells and the incidental uptake of As (arsenate) into P (phosphate) biochemical pathways. There is also evidence for the uptake of Se in to the biochemical pathways for S. All profiles of Si and PO_4^{3-} (Figs. 3-17 – 3-22) show decreasing concentrations across the stretch of river where the CFPPs are sited. These two facts coupled with concurrent decreases in NO_2^-, NO_3^-, and NH_4^+ suggest increases in phytoplankton are occurring in the river. The magnitude of the nutrient uptake suggests that a large percentage of the metalloid loss flux could be due to loss into aquatic and benthic organisms. Table 4-5 shows the loss of PO_4^{3-} between Wansley and Yates and Franklin. If biological uptake is a factor in the loss of As from the river one would expect to see a relationship between PO_4^{3-} loss and As loss (Figure 4-4). With only 5 data points a definitive quantitative relationship cannot be made between these two loss fluxes. However, the estimated 6.5 atoms of As uptake for 100 atoms of PO_4^{3-} uptake appear reasonable, particularly in a PO_4^{3-} limited system.

4.2.2 Sorption onto Sediments

Suspended sediment profiles of the Chattahoochee River (Figs. 3-9 through 3-16) show an increase in the mass of metalloids on suspended sediments. This is presumably due to effluent from ash ponds. The concentrations of metalloids in the suspended phase show the same characteristic order (Se / As = 0.16, Sb / As = 0) found in the river. This is farther evidence that this loading is due to CFPPs and is not carried down the river from further upstream. As the metalloid concentrations in the river increase the mass of metalloids on suspended particles will also increase in an attempt to maintain equilibrium between the metalloids in the dissolved phase and in the particulate phase.

Mass balance modeling has revealed that the power plants also discharge solid ash material in the effluent from ash ponds. In the case of Plant Yates the metalloid discharge in the ash phase is greater than in the dissolved phase.

Using river flow data and suspended sediment data it is possible to calculate the flux of metalloids on suspended sediments. By comparing up and downstream fluxes, i.e. calculating a Δ Flux for suspended sediment metalloids, it is possible to estimate partitioning between metalloid loss into the biological system and sorption onto suspended sediments. The sediment flux calculation is as follows:

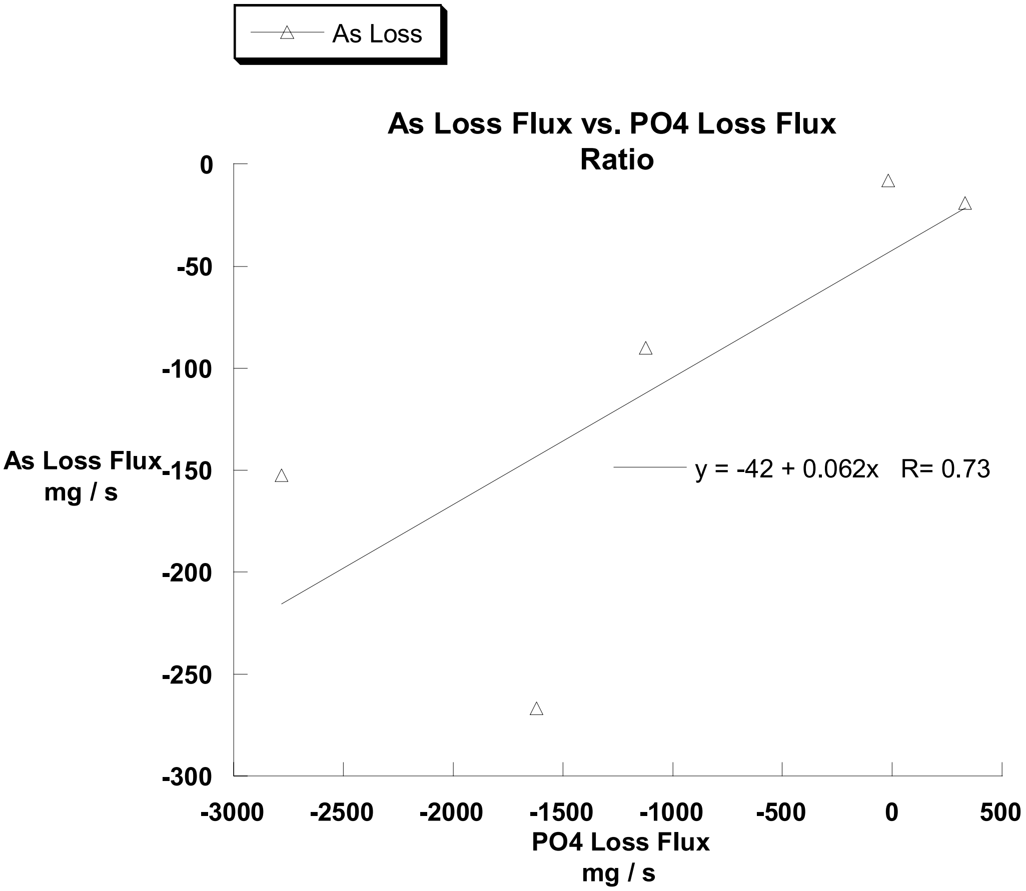

Figure 4-3 As / PO_4 Loss Ratio. Figure 4-3 shows the ratio of As loss and PO_4 loss between site 112 and site 129.

Eq. 4-2

$$M_{sed} \times Q \times C_{sed} = F_{ss}$$

M_{sed} is the mass of sediment per volume water (kg / L). Q is the river flow in L / s. C_{sed} is the metalloid concentration on the suspended sediment (mg / kg). F_{ss} is the flux of metalloids on suspended sediments in units of mg suspended metalloid / s. Table 4-5 contains the suspended metalloid Δ Fluxes as between the sample site above Wansley and Yates and the peak suspended metalloid concentration. With the exception of 5/6/2002 the peak concentration is at the site below Wansley and Yates. On this day the peak concentration suspended metalloid concentration was recorded in Franklin, GA.

From the values in this table the integrated suspended sediment Δ Flux can be calculated. They are 49 mg / s, 8 mg / s, and 0 mg / s for As, Se and Sb respectively. It is important to notice that the integrated value for Se is skewed by the high flux on 5/6/2002. This table shows that there is little change in the particulate flux of Se and Sb across the power plants. Along with the thermodynamic considerations put forth earlier (4.1.1), this suggests that the riverine chemistry of these elements is different than that of As.

Figures 4-5 – 4-7 are box models of metalloid fluxes through the Chattahoochee River system. These models show the two main metalloid reservoirs in the Chattahoochee system: the dissolved phase, and the suspended phase. The most important fluxes into, out of, and between these systems are the input of dissolved and solid metalloid phases from ash ponds, sorption of metalloids onto material suspended in the stream flow, desorption of metalloids off of suspended material, the settling of

Table 4-4 Peak Sediment Delta Fluxes

Table 4-4 shows the peak sediment Δ Fluxes for the Chattahoochee River below plants Wansley and Yates

Peak Sediment Delta Flux (mg / s)						
	11/9/2001	**12/18/2001**	**3/6/2002**	**5/6/2002**	**6/5/2002**	**Integrated**
As	39	101	16	55	35	49
Se	0	0	0	39	0	8
Sb	0	1	0	2	0	0

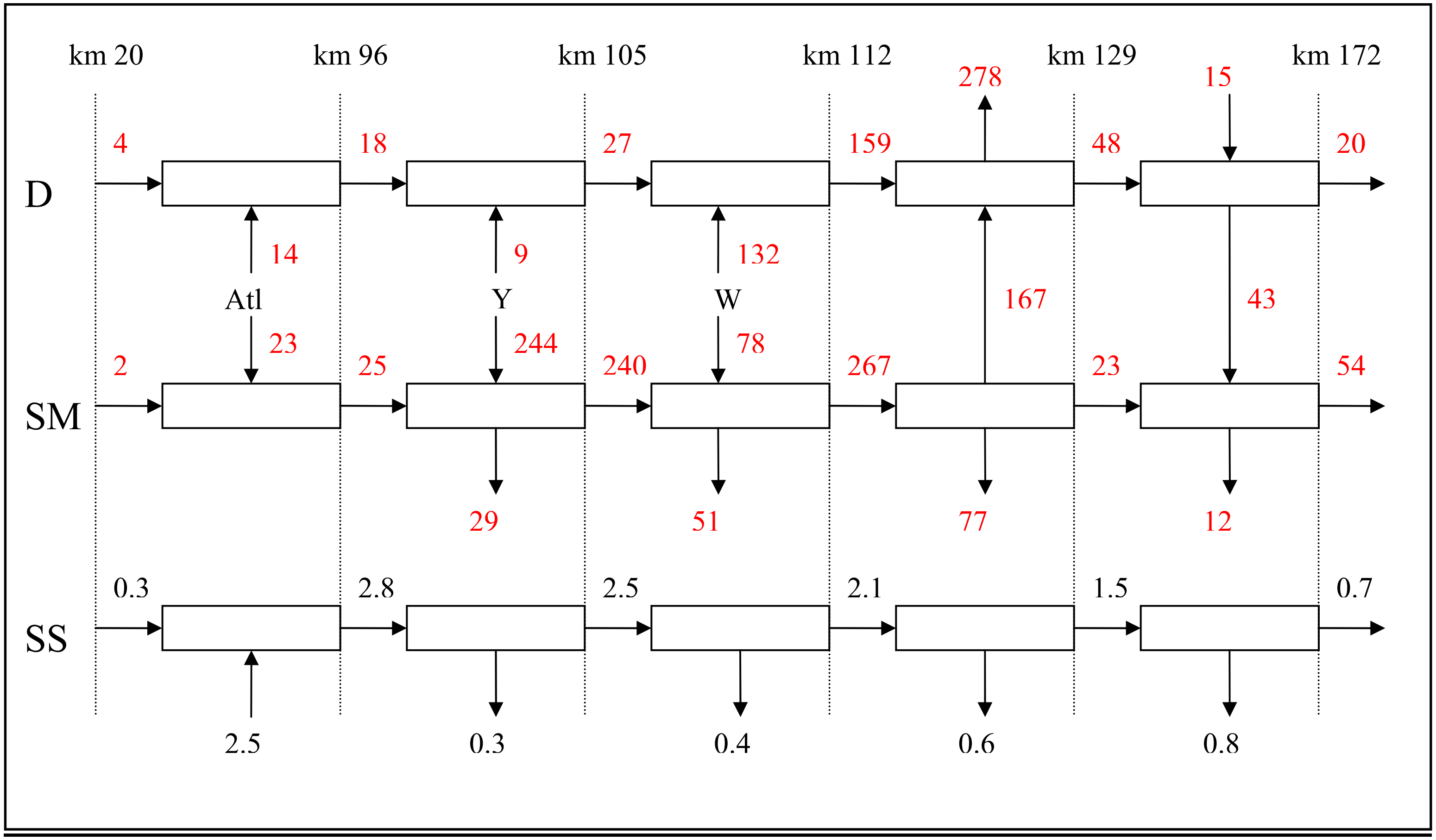

Figure 4-4 Chattahoochee River Arsenic Box Model. Figure 4-4 shows a box model of metalloid fluxes on the Chattahoochee River system. D is the dissolved phase. SM is the suspended material phase. SS shows the input and settling of suspended sediment in the river. Atl is Atlanta, GA; Y is Plant Yates; and W is Plant Wansley. D and SM Fluxes are in mg / s. SS Fluxes are in kg / s.

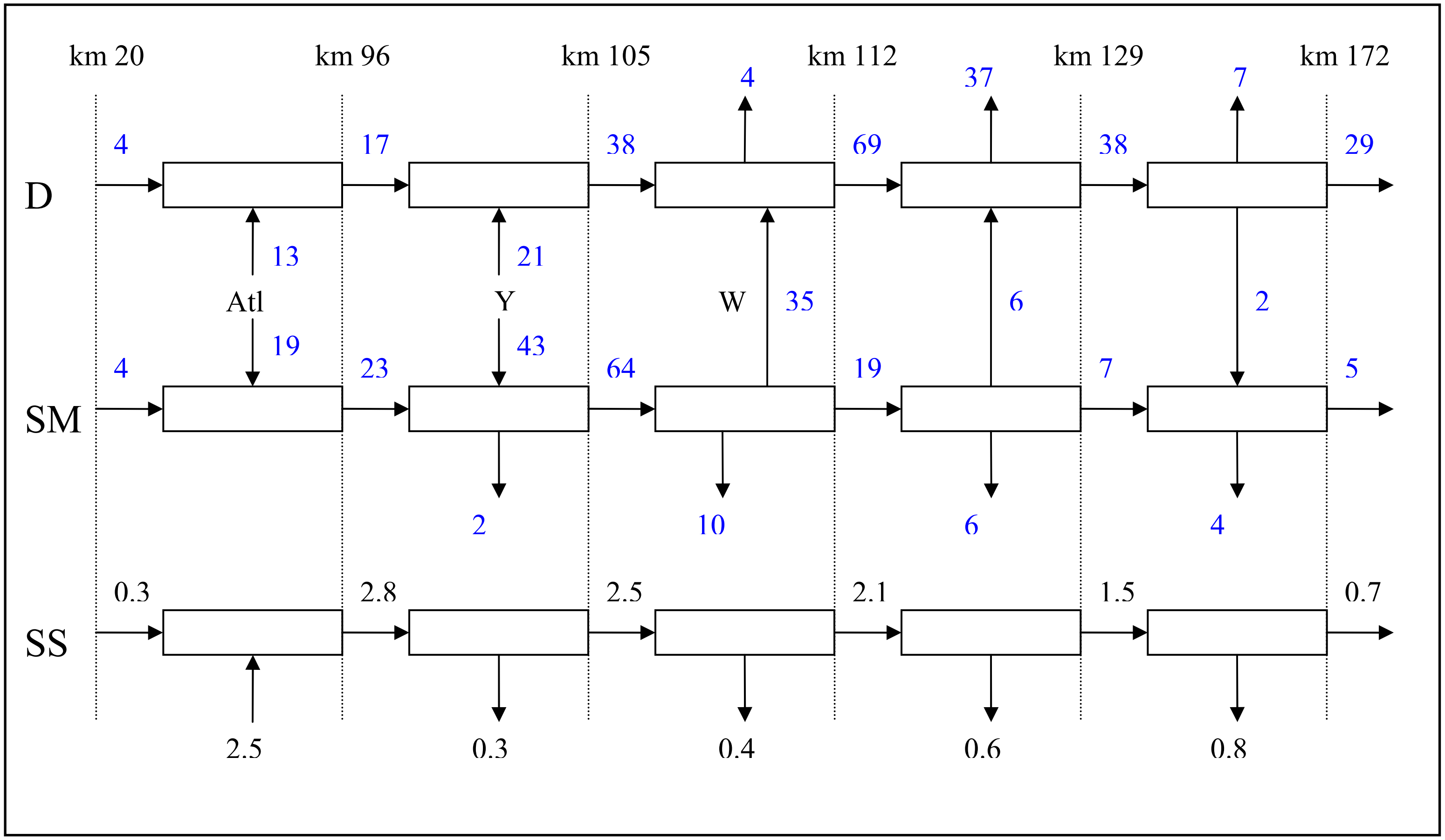

Figure 4-5 Chattahoochee River Selenium Box Model. Figure 4-5 shows a box model of metalloid fluxes on the Chattahoochee River system. D is the dissolved phase. SM is the suspended material phase. SS shows the input and settling of suspended sediment in the river. Atl is Atlanta, GA; Y is Plant Yates; and W is Plant Wansley. D and SM Fluxes are in mg / s. SS Fluxes are in kg / s.

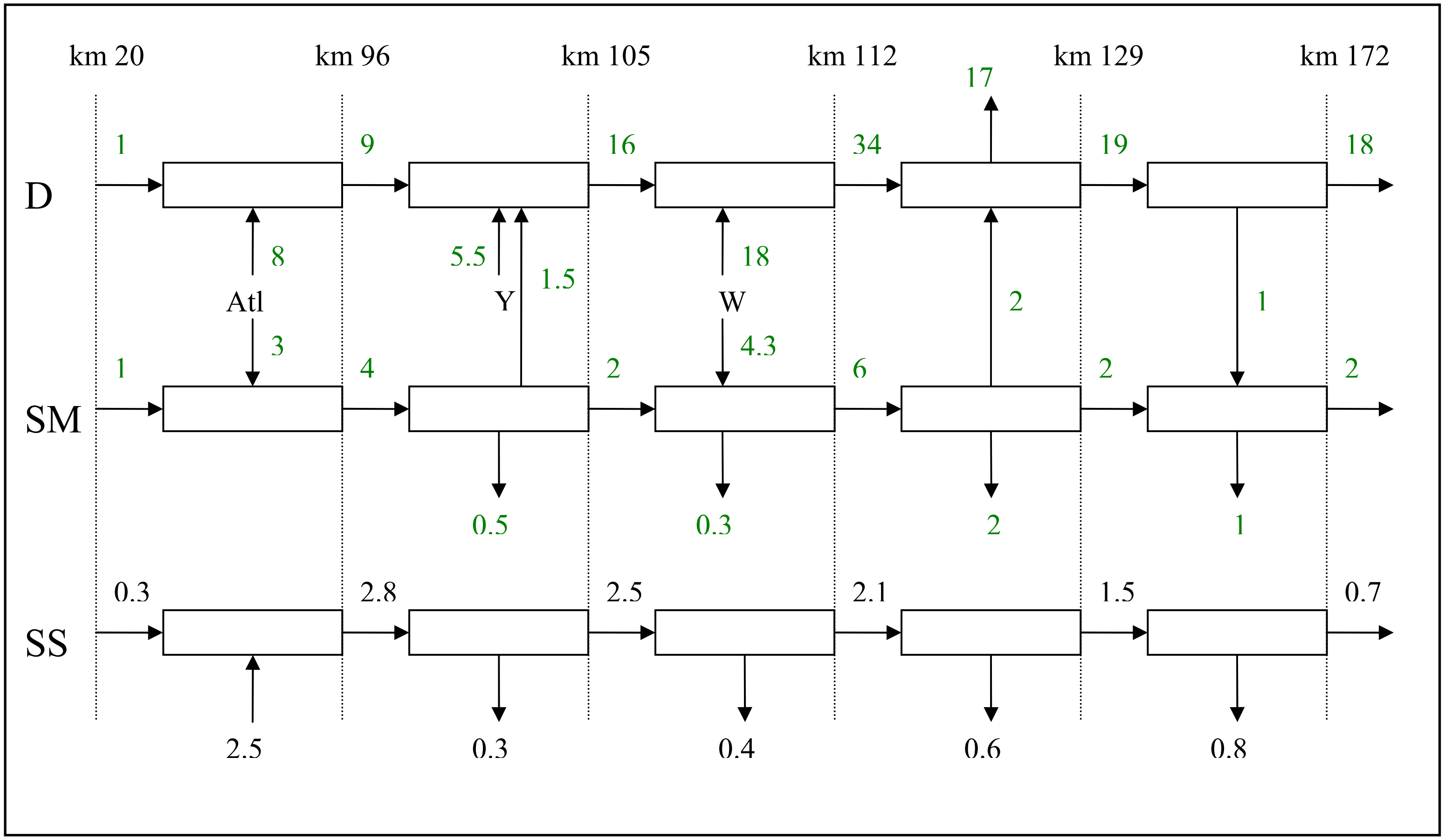

Figure 4-6 Chattahoochee River Antimony Box Model. Figure 4-6 shows a box model of metalloid fluxes on the Chattahoochee River system. D is the dissolved phase. SM is the suspended material phase. SS shows the input and settling of suspended sediment in the river. Atl is Atlanta, GA; Y is Plant Yates; and W is Plant Wansley. D and SM Fluxes are in mg / s. SS Fluxes are in kg / s.

suspended material onto the bed of the Chattahoochee River, and uptake of metalloids by micro and macro organisms. It is important to note that these models represent year long net fluxes and may not accurately describe the short term cycling of metalloids between the reservoirs.

Dissolved and suspended fluxes are calculated using the methods described previously (3.1.2 and 4.2.2). The rate of setting of metalloid laden sediment is calculated by multiplying concentration of metalloids on the sediment (mg / kg) by the loss of sediment (kg / s) in the river (SS out arrows in Figs. 4-5 through 4-7) to obtain the rate in units of mg / s.

The models reveal that the input of solid ash material from the ash pods is major source of metalloid contamination in the Chattahoochee River. In the case of arsenic, the suspended metalloid flux from CFPPs to the river is greater than the dissolved flux by a factor of two. The models also reveal that biological uptake is the principal metalloid sink in contaminated systems. The rates of biological uptake of As, Se, and Sb are 278 mg / s, 48 mg /s, and 17 mg / s respectively. Over the year of this study these fluxes represent biological uptake of 8.7 tons arsenic, 1.5 tons selenium, and 0.5 tons antimony. The models also show that the settling of metalloid laden sediment is an important process. This is of concern due to the fact that the sediment is eventually transported downstream to the upper reaches of West Point Lake, an important drinking water source for west central Georgia, and a popular sport fishing locale.

4.3 Toxic Release Inventories and the PISCES Model

4.3.1 Toxic Release Inventories

Beginning in 1998, coal fired electric plants are required to report their toxic releases. The reporting and the subsequent release of data is done through the US Environmental Protection Agency's (EPA) Toxic Release Inventory (TRI) program. In the case of CFPP's, TRI requirements are based on the size and power output of the power plant. Arsenic is required to be reported for plants 400 MW and larger; Se, for 1200 MW and larger; and Sb, for 4500 MW plants and larger (Rubin, 1999). Under these guidelines, Arsenic TRI reports would be required by every power plant in this study. Selenium TRI's would be required for Plants Bowen, Wansley and Yates. The 4500 MW requirement for Sb reporting in the TRI is larger than the rating of any of the power plants in this study.

Table 4-7 contains the TRI information for the power plants this study. It shows the TRI estimates for As, Se, and Sb for the years 1998, 1999, and 2000. The lag between the collection year and the publication of the data is approximately two years. The data for the year 2001 will be available in 2003. The latest year available at this writing is 2000. These TRI estimates can be compared to my estimated aquatic releases based on the mass of coal burned per year at each power plant and the escape efficiency calculated in section 4.1.2. This table shows that with the exception of the Yates Arsenic estimate for the year 2000 all of the TRI estimates are lower that the escape efficiency estimate by a factor of two or greater. It is interesting to note that the As estimates for Yates and Wansley increase from zero or near zero in the years before 2000 to approximately 1500 kg per year emission into the aqueous phase in the 2000 reporting year. I believe this reflects a change in the methods used for estimating the partitioning of toxic releases to the environment. It is of note that due to analytical uncertainty and the ±5% uncertainty in the USGS river flow data there is a ±25% uncertainty in my escape efficiency estimate for arsenic, a ± 28% uncertainty for selenium, and a ±28% uncertainty for antimony. The 1474 kg arsenic release estimate from Plant Yates (2000) falls within this uncertainty. None of the other TRI estimates for any of these plants are within the escape efficiency uncertainty. It is also of note that a TRI for Sb is not required for these plants. While there is comparatively little known about this element and its riverine chemistry, it is known to be toxic and shown here to be released to the environment in significant amounts from coal fired power plants.

4.3.2 The PISCES Model

The Power Plant Integrated Systems: Chemical Emissions Studies (PISCES) Model is a model that the US EPA allows the electrical industry to use to estimate its toxic releases. The PISCES model is a thermodynamic model if the CFPP combustor train that attempts to minimize Gibbs free energy through mass and energy balances. The data base contains equilibrium constants for 21 elements and a total of 698 species (Sandelin and Backman 2001). A study of two power plants was conducted by these workers. They compared the measured results of trace element partitioning during coal combustion and the results of the PISCES calculations. These results showed that the experimentally derived exclusive partitioning of As onto fly ash was largely adequately by the model. However, this study showed a large discrepancy between the Se

Table 4-5 TRI Aquatic and Total Release Reports

Power Plant **MW** **kg Coal / year**	**Element**	**CFPP Aquatic Release (This Study) 2001-02 (kg/yr)**	**1998 TRI Aquatic (Total) Estimate (kg/yr)**	**1999 TRI Aquatic (Total) Estimate (kg/yr)**	**2000 TRI Aquatic (Total) Estimate (kg/yr)**
Bowen	As	*5300*	0 (14500)	0 (11600)	0 (24200)
3160	Se	*2200*	0 (14250)	0 (13200)	8 (18800)
$7.27\text{x}10^9$	Sb	*1100*	NR*	NR	NR
Hammond	As	*1400*	NA**	NA	NA
800	Se	*570*	NR	NR	NR
$1.91\text{x}10^9$	Sb	*280*	NR	NR	NR
Wansley	As	2650	0 (16400)	0 (17500)	1474 (23600)
1730	Se	1100	507 (8100)	207 (7600)	209 (7800)
$3.64\text{x}10^9$	Sb	550	NR	NR	NR
Yates	As	1450	4 (110)	4 (9650)	1573 (13800)
1250	Se	600	NA	NA	NA
$2.00\text{x}10^9$	Sb	300	NR	NR	NR

*Not Required by TRI **Required by TRI but not available in published data

Data from www.epa.gov/tri/

Table 4-5 shows EPA TRI estimates as compared to the aquatic estimates from this study. Numbers in parenthesis indicate total release estimates. Numbers in italics indicate release estimates calculated from the Wansley / Yates escape efficiency estimate. These estimates may not be appropriate for Plants Bowen and Hammond.

partitioning of the model and the measured results. The model predicts that 100% of the Se in coal is lost from fired coal to the gas phase and lost via flue gas. Measurements show 75% of the Se is sorbed onto fly ash. Sandelin et al. (2000) attribute this discrepancy to the incomplete treatment of the thermodynamics for Se. This problem in the model for Se could be the source of the low TRI estimates for Se.

Another group of workers (Yan et al. 2001) have performed a similar experiment using a different model with a more extensive thermodynamic database (54 elements, 3200 species). The trace element partitioning results of their calculations agree with our results from Δ Flux calculations and escape efficiency estimates. They predict that As is partitioned almost exclusively onto fly ash while Se, and Sb are both sorbed onto fly ash and lost via stack gas. However, they do not quantify the exact Se and Sb partitioning. The larger thermodynamic database appears to make a difference in the models ability to correctly predict trace element fate during coal combustion.

However, we believe that it is not simply a matter of thermodynamics to predict trace element partitioning in CFPPs. The models used are equilibrium thermodynamic models. Within the confines of the boiler or the scrubber chambers an equilibrium model may be appropriate. As gases and ash move from one part of the plant to another they experience drastic changes in temperature, pressure, and gas and particulate phase chemistry. The temperature in the boiler is approximately 1200 K while the temperature in the particulate scrubber is only 300 K. The process occurring as the temperature drops 900 k are not thermodynamic equilibrium processes, they are kinetic processes. In order to have a complete understanding of the processes governing trace element partitioning during coal combustion detailed kinetic models and studies must be undertaken along with thermodynamic treatments.

CHAPTER 5

THE PLANT BOWEN ASH SPILL

On July 28, 2002 a 4 acre sink hole collapsed under the 250 acre ash pond at Plant Bowen. Over a 3 day period 2.2 million gallons of ash pond effluent and 1.87 million pounds of ash was discharged from this sinkhole to Euharlee Creek a tributary of the Etowah River above Rome GA's drinking water intake. I performed sampling transects on the 31st of July and the 1st of August to establish the fluxes of metalloids downstream, and to quantify the release of metalloids to the environment. The sampling transects for these days were slightly different than normally taken on the Etowah River. The sample sites and locations are described below.

Sample 1:Etowah River. Sample site is located below Allatoona Dam 0 km from the spillway.

Sample 2: Etowah above Euharlee Creek. Located off Euharlee road at a public fishing bank, 15 km from spillway.

Sample 3: Euharlee Creek. Sample taken at the Historic Covered Bridge in Euharlee, GA. Euharlee Creek enters the Etowah 24 km below the Allatoona spillway

Sample 4: Etowah River below Euharlee Creek. Sample collected 1 km downstream of Euharlee creek. Site is located 25 km from the spillway

Sample 5: Etowah River at Hardin Bridge. Sample collected below the one lane bridge on Hardin Bridge Road. Site is located 30 km from the Allatoona spillway

Sample 6: Etowah River at GA Hwy. 20 / 411. Sample is collected under the bridge over the river. Site is located 50 km from the Allatoona Spillway

Sample 7: Etowah River in Rome. Sample site is located in downtown Rome, GA just upstream of the Oostanuala entry to the Etowah. Site is located 83 km from the Allatoona spillway.

Table 5-1 Above Euharlee Creek Metalloid Concentrations

Above Euharlee				
Date	Sample	As (μg/L)	Se (μg/L)	Sb (μg/L)
07/31/2002	1	0.184	0.880	0.038
	2	0.347	0.916	0.142
08/01/2002	1	0.236	0.891	0.036
	2	0.288	0.854	0.250

Average	0.26	0.89	0.12
Std. Dev (±)	0.07	0.03	0.102
RSD (%)	26.56	2.92	87.55

Table 5-1 Analytical data for the metalloid concentrations above Euharlee Creek 7-31-01 and 8-01-02. The numbers below the chart are the average values, standard deviations and relative standard deviations for the metalloid concentrations.

Table 5-2 Below Euharlee Creek Metalloid Concentrations

Below Euharlee				
Date	Sample	As (µg/L)	Se (µg/L)	Sb (µg/L)
07/31/2002	4	1.188	1.300	0.362
	5	1.460	2.594	1.300
08/01/2002	4	0.564	1.358	0.484
	5	0.677	1.484	0.552
	6	0.424	1.105	0.251
	7	1.193	1.546	0.566

	As	Se	Sb
Average	0.92	1.57	0.57
Std. Dev (±)	0.42	0.53	0.37
RSD (%)	45.41	33.72	63.13

Table 5-1 Analytical data for the metalloid concentrations below Euharlee Creek 7-31-01 and 8-01-02. The number below the chart are the average values, standard deviations and relative standard deviations for the metalloid concentrations.

Figures 5-1a and 5-1b Etowah River Concentration Profiles

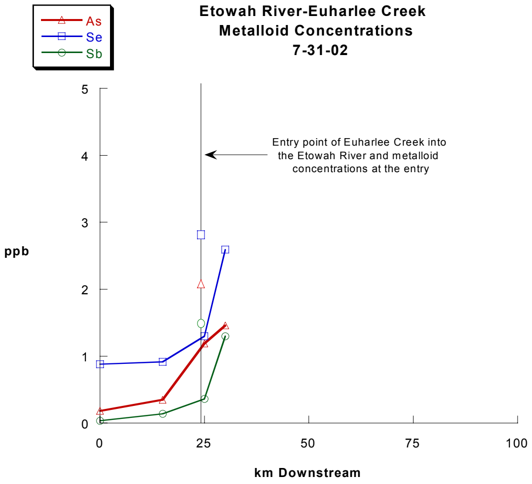

Figure 5-1a shows the metalloid concentrations for the Etowah River and Euharlee Creek on 7-31-02. The vertical line represents the inlet of Euharlee Creek to the Etowah. Metalloid concentration in ppb (µg/L) is on the y-axis. Km downstream in on the x-axis.

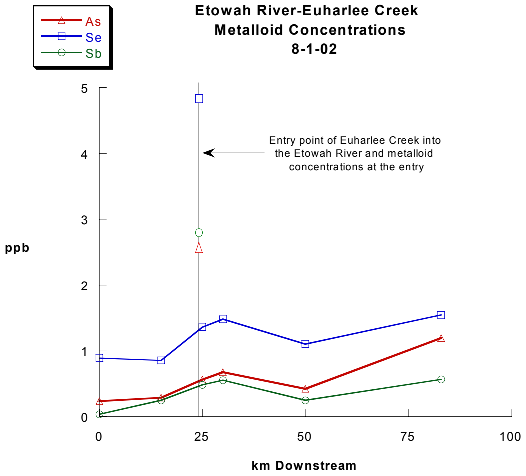

Figure 5-1b shows the metalloid concentrations for the Etowah River and Euharlee Creek on 8-1-02. The vertical line represents the inlet of Euharlee Creek the to Etowah. Metalloid concentration in ppb (µg/L) is on the y-axis. Km downstream in on the x-axis.

Table 5-1 shows the analytical data for the Etowah River upstream of Euharlee Creek. Table 5-2 shows the analytical data for the Etowah River downstream of Euharlee Creek. Cursory examination of the data shows that the average metalloid concentrations below Euharlee creek are approximately two fold higher than above Euharlee Creek. Figures 5-1a and 5-1b are metalloid profiles of the Etowah. The vertical lines show the input concentration of Euharlee Creek. On both days the metalloid levels in Euharlee Creek are well above those in the upstream Etowah. The peaks in metalloid concentration downstream of the Euharlee inlet are clear evidence of the release of ash pond effluent to the river.

Using the average mean daily flow of 36,860 L/s for 7-31 and 8-1 and the stream concentration data we can calculate riverine metalloid fluxes and their upper and lower bounds. These data are shown in Tables 5-3a and 5-3b.The flux of metalloids is higher downstream of Euharlee Creek. Figure 5-4 shows the Δ Flux across Euharlee Creek. The centric values for As, Se, and Sb are 24 mg / s, 25 mg / s, and 17 mg / s respectively. This amounts to a total release of 6.3 kg As, 6.5 kg Se and 4.5 kg Sb over the three days of the spill.

Tables 5-3a and 5-3b Euharlee Creek Metalloid Fluxes

Above Euharlee Fluxes (mg/s)			
	As	Se	Sb
Centric	9.73	32.67	4.23
Upper Bound	12.32	33.62	8.04
Lower Bound	7.15	31.71	0.53

Table 5-3a

Below Euharlee Fluxes (mg/s)			
	As	Se	Sb
Centric	33.87	57.73	21.62
Upper Bound	49.24	77.20	35.26
Lower Bound	18.49	38.26	7.97

Table 5-3b

Tables 5-3a and 5-3b show the flux data for above and below Euharlee Creek in mg / s. Upper and lower bounds are the statistical high and low estimates for the fluxes. The centric is the median value.

Table 5-4 Etowah Δ Flux

Delta Fluxes (mg/s)			
	As	Se	Sb
Centric	24.13	25.06	17.33
Upper Bound	42.09	45.49	34.73
Lower Bound	6.17	4.64	0.00

Table 5-4 shows the upper, lower, and centric estimates for the Δ Flux across Euharlee creek in mg / s.

CHAPTER 6

CONCLUSIONS

This study has established and quantified the flux of the toxic metalloids arsenic, selenium, and antimony from coal fired power plant ash ponds to local receiving waters. Calculation of metalloid escape efficiencies have show that 4.1 tons of arsenic, 1.7 tons of selenium, and 0.9 tons of antimony were released to the environment in the dissolved reactive form during the year of this study. Detailed mass balance models of metalloid fate in the riverine environment were developed. These models revealed that there is also a metalloid flux from ash ponds in the form of solid ash material. These fluxes are 10.1 tons of As, 1.4 tons of Se, and 0.1 tons of Sb released on ash material during the year of this study. Over the course of 20 years the combined dissolved and solid releases have amounted to 284 tons of As, 62 tons of Se, and 20 tons of Sb. Mass balance has shown that the primary sink of metalloids in contaminated rivers is biological uptake. Over the year of this study 8.7 tons, 1. tons, and 0.5 tons of As, Se, and Sb entered the biological system respectively. Concern has also been raised regarding the settling of metalloid laden sediment in the upper reaches of West Point reservoir.

These fluxes have been compared to the EPA Toxic Release Inventory (TRI) estimates. Comparison of escape efficiency estimates to TRI estimates has shown that TRI estimates typically underestimate metalloid release by a factor of two.

Comparison of recent data to historic data at a CFPP that has converted to a dry ash disposal system has shown the cessation of metalloid input to local surface waters. These facts combined with studies at other CFPPs that have converted to dry ash disposal have shown this method to be an effective means of stopping the contamination of surface water with metalloid elements.

While this study has quantified metalloid release from CFPPs to the Chattahoochee River, it has only touched on the downstream fates if metalloids. Detailed metalloid speciation studies downstream of the power plants would allow a more comprehensive estimate of metalloid spiraling through the biological system. Seasonal water column studies in West Point Reservoir need to be undertaken in order to assess the impact of the settling of metalloid laden sediments from CFPPs on the ecology of the reservoir and the quality of the drinking water taken from the reservoir.

APPENDIX I

These tables contain the analytical data gathered during this study. Each table represents a sampling sequence (one day or contiguous dates). In all tables the row labeled “km downstream” indicates how far downstream from the origin the sample was taken. “Time” denotes the time of day the sample was taken. In the case of the Etowah River, the origin is the outlet from Allatoona Dam below Allatoona Reservoir. For the Chattahoochee River the origin is Buford Dam below Lanier Reservoir. Specific Site location and driving directions are found in Appendix 3. In all tables “nd” denotes “not determined”.

TDC: Total dissolved concentration in ppb (µg/L) of As, Se, Sb, and Ge at each sampling location.

As, Se, Sb, Ge: Concentration of dissolved metalloids for each sampling location in µg/L

.

Nuts: Nutrient concentrations at each sampling location in µmol/L

PO_4: Dissolved reactive phosphate
NH_4: Ammonia
NO_2: Nitrite
NO_2+NO_3: Nitrite plus nitrate
Si: Dissolved silica

Solids: Suspended solids and metalloid concentrations of the solids at each sample location.

Sus. Solid: Suspended solid concentration in each river sample in mg/L
As, Se, Sb, Ge: Concentration of acid extractable metalloids in the suspended solid in µg/g

WQ: Water quality parameters for each sampling location

pH: pH (-log $\{H^+\}$)
DO (%): Percent oxygen saturation at insitu temperature
O_2 (µM): Concentration of dissolved oxygen in µmol/L
Cond: Conductivity in µS/cm
Chlor: Concentration of chlorophyll in µg/L
Turb: Turbidity of the water in normalized turbidity units (NTU)
T: Temperature of the water in degrees Celsius.

Please see Tables 1 and 2 for location of relevant sites at kilometers downstream

Table 1

Chattahoochee River	
Km downstream	Power plant
20	
96	
105	Yates
112	Wansley
129	
172	

Table 2

Etowah River	
Km downstream	Power plant
0	
11	
25	Bowen
83	
113	Hammond

5-21-2001, Monday Etowah River

	R-Number		**R-1017**	**R-1019**	**R-1020**	**R-1021**
	km downstream	**0**	**11**	**25**	**83**	**113**
Time			11:00 AM	12:45 PM	2:15 PM	2:50 PM
TDC (µg/L)	**As**	nd	0.79	0.16	0.24	0.54
	Se	nd	1.93	0.07	0.07	0.07
	Sb	nd	1.26	0.05	0.23	0.18
	Ge	nd	0.10	0.08	nd	nd
Nuts (µM)	**PO_4**	nd	nd	nd	nd	nd
	NH_4	nd	nd	nd	nd	nd
	NO_2	nd	nd	nd	nd	nd
	NO_2+NO_3	nd	nd	nd	nd	nd
	Si	nd	nd	nd	nd	nd
Sus. Solids (mg/kg)	**Sus. Solid (mg/l)**	nd	nd	nd	nd	nd
	As	nd	nd	nd	nd	nd
	Se	nd	nd	nd	nd	nd
	Sb	nd	nd	nd	nd	nd
	Ge	nd	nd	nd	nd	nd
WQ	**pH**	nd	nd	nd	nd	nd
	DO (%)	nd	nd	nd	nd	nd
	O_2 (uM)	nd	nd	nd	nd	nd
	Cond	nd	nd	nd	nd	nd
	Chlor	nd	nd	nd	nd	nd
	Turb	nd	nd	nd	nd	nd
	T	nd	nd	nd	nd	nd

5-22-2001, Tuesday Chattahoochee River

	R-Number		**R-1027**	**R-1026**	**R-1025**	**R-1024**	**R-1023**
	km downstream	**20**	**96**	**105**	**112**	**129**	**172**
Time			5:00 PM	4:15 PM	3:10 PM	2:15 PM	12:45 PM
TDC (µg/L)	**As**	nd	0.24	0.43	1.37	0.35	0.28
	Se	nd	0.95	1.10	1.40	0.96	1.02
	Sb	nd	0.22	0.32	0.61	0.35	3.99
	Ge	nd	0.70	1.22	2.31	0.95	nd
Nuts (µM)	**PO_4**	nd	nd	nd	nd	nd	nd
	NH_4	nd	nd	nd	nd	nd	nd
	NO_2	nd	nd	nd	nd	nd	nd
	NO_2+NO_3	nd	nd	nd	nd	nd	nd
	Si	nd	nd	nd	nd	nd	nd
Sus. Solids (mg/kg)	**Sus. Solid (mg/l)**	nd	nd	nd	nd	nd	nd
	As	nd	nd	nd	nd	nd	nd
	Se	nd	nd	nd	nd	nd	nd
	Sb	nd	nd	nd	nd	nd	nd
	Ge	nd	nd	nd	nd	nd	nd
WQ	**pH**	nd	nd	nd	nd	nd	nd
	DO (%)	nd	nd	nd	nd	nd	nd
	O_2 (uM)	nd	nd	nd	nd	nd	nd
	Cond	nd	nd	nd	nd	nd	nd
	Chlor	nd	nd	nd	nd	nd	nd
	Turb	nd	nd	nd	nd	nd	nd
	T	nd	nd	nd	nd	nd	nd

8-2-2001, Thursday Etowah River

	R-Number	R-1040	R-1039	R-1038	R-1036	R-1034
	km downstream	0	11	25	83	113
Time		12:50 PM	11:40 AM	10:55 AM	9:40 AM	8:00 AM
TDC (µg/L)	As	0.18	0.62	0.24	0.21	0.36
	Se	0.40	1.71	0.55	0.06	0.08
	Sb	0.04	0.99	0.10	0.06	0.41
	Ge	nd	0.10	0.44	nd	nd
Nuts (µM)	PO_4	nd	nd	nd	nd	nd
	NH_4	nd	nd	nd	nd	nd
	NO_2	nd	nd	nd	nd	nd
	NO_2+NO_3	nd	nd	nd	nd	nd
	Si	nd	nd	nd	nd	nd
Sus. Solids (mg/kg)	Sus. Solid (mg/l)	nd	nd	nd	nd	nd
	As	nd	nd	nd	nd	nd
	Se	nd	nd	nd	nd	nd
	Sb	nd	nd	nd	nd	nd
	Ge	nd	nd	nd	nd	nd
WQ	pH	nd	nd	nd	nd	nd
	DO (%)	nd	nd	nd	nd	nd
	O_2 (uM)	nd	nd	nd	nd	nd
	Cond	nd	nd	nd	nd	nd
	Chlor	nd	nd	nd	nd	nd
	Turb	nd	nd	nd	nd	nd
	T	nd	nd	nd	nd	nd

8-6-2001, Monday Chattahoochee River

	R-Number		**R-1045**	**R-1044**	**R-1043**	**R-1042**	**R-1041**
	km downstream	**20**	**96**	**105**	**112**	**129**	**172**
Time			12:05 PM	11:40 AM	10:45 AM	9:40 AM	8:20 AM
TDC (µg/L)	**As**	nd	0.28	0.71	1.89	0.60	0.82
	Se	nd	0.25	0.66	1.25	0.74	0.40
	Sb	nd	0.27	0.38	0.68	0.43	0.17
	Ge	nd	0.80	1.01	3.02	1.41	nd
Nuts (µM)	**PO_4**	nd	nd	nd	nd	nd	nd
	NH_4	nd	nd	nd	nd	nd	nd
	NO_2	nd	nd	nd	nd	nd	nd
	NO_2+NO_3	nd	nd	nd	nd	nd	nd
	Si	nd	nd	nd	nd	nd	nd
Sus. Solids (mg/kg)	**Sus. Solid (mg/l)**	nd	nd	nd	nd	nd	nd
	As	nd	nd	nd	nd	nd	nd
	Se	nd	nd	nd	nd	nd	nd
	Sb	nd	nd	nd	nd	nd	nd
	Ge	nd	nd	nd	nd	nd	nd
WQ	**pH**	nd	nd	nd	nd	nd	nd
	DO (%)	nd	nd	nd	nd	nd	nd
	O_2 (uM)	nd	nd	nd	nd	nd	nd
	Cond	nd	nd	nd	nd	nd	nd
	Chlor	nd	nd	nd	nd	nd	nd
	Turb	nd	nd	nd	nd	nd	nd
	T	nd	nd	nd	nd	nd	nd

9-15-2001, Saturday Chattahoochee River

	R-Number	**R-1051**	**R-1050**	**R-1049**	**R-1048**	**R-1047**	**R-1046**
	km downstream	**20**	**96**	**105**	**112**	**129**	**172**
Time		2:30 PM	12:05 PM	11:30 AM	10:45 AM	10:00 AM	8:30 AM
TDC (µg/L)	**As**	0.07	0.25	0.50	5.60	1.12	0.37
	Se	0.15	0.63	1.21	3.01	1.09	0.39
	Sb	0.02	0.22	0.45	1.41	0.53	0.19
	Ge	0.02	0.28	0.85	1.87	0.87	nd
Nuts (µM)	**PO_4**	nd	nd	nd	nd	nd	nd
	NH_4	nd	nd	nd	nd	nd	nd
	NO_2	nd	nd	nd	nd	nd	nd
	NO_2+NO_3	nd	nd	nd	nd	nd	nd
	Si	nd	nd	nd	nd	nd	nd
Sus. Solids (mg/kg)	**Sus. Solid (mg/l)**	nd	nd	nd	nd	nd	nd
	As	nd	nd	nd	nd	nd	nd
	Se	nd	nd	nd	nd	nd	nd
	Sb	nd	nd	nd	nd	nd	nd
	Ge	nd	nd	nd	nd	nd	nd
WQ	**pH**	nd	nd	nd	nd	nd	nd
	DO (%)	nd	nd	nd	nd	nd	nd
	O_2 (uM)	nd	nd	nd	nd	nd	nd
	Cond	nd	nd	nd	nd	nd	nd
	Chlor	nd	nd	nd	nd	nd	nd
	Turb	nd	nd	nd	nd	nd	nd
	T	nd	nd	nd	nd	nd	nd

11-9-2001, Friday Chattahoochee River

	R-Number	R-1057	R-1056	R-1055	R-1054	R-1053	R-1052
	km downstream	20	96	105	112	129	172
Time		5:00 PM	1:45 PM	12:55 PM	11:25 AM	10:00 AM	8:10 AM
TDC (µg/L)	As	0.07	0.24	0.46	3.72	0.63	0.27
	Se	0.17	0.34	1.09	2.02	1.07	0.44
	Sb	0.02	0.21	0.42	1.11	0.47	0.24
	Ge	0.01	0.25	0.76	1.16	0.53	
Nuts (µM)	PO_4	nd	1.15	1.10	0.90	0.55	0.45
	NH_4	nd	nd	nd	nd	nd	nd
	NO_2	nd	1.65	0.87	0.98	0.78	0.67
	NO_2+NO_3	nd	nd	nd	nd	nd	nd
	Si	99.05	119.41	116.48	107.50	75.93	127.00
Sus. Solids (mg/kg)	Sus. Solid (mg/l)	5.75	6.50	5.25	2.75	13.75	3.25
	As	19.10	23.20	387.37	502.89	9.79	374.24
	Se	0.00	11.25	72.48	8.77	0.00	1.10
	Sb	9.77	6.88	2.49	13.75	0.99	10.64
	Ge	nd	nd	nd	nd	nd	Nd
WQ	pH	7.07	6.89	6.92	6.95	6.90	6.70
	DO (%)	0.97	0.91	0.99	0.96	0.90	0.65
	O_2 (uM)	296	272	290	281	275	190
	Cond	511	221	227	207	194	135
	Chlor	nd	nd	nd	nd	nd	Nd
	Turb	nd	nd	nd	nd	nd	nd
	T	15.30	16.00	16.90	16.90	15.20	16.60

12-18-2001, Monday Chattahoochee River

	R-Number	R-1063	R-1062	R-1061	R-1060	R-1059	R-1058
	km downstream	20	96	105	112	129	172
Time		4:30 PM	1:15 PM	12:10 PM	10:45 AM	9:35 AM	7:15 AM
TDC (µg/L)	As	0.10	0.21	0.28	1.73	0.74	0.23
	Se	0.13	0.24	0.42	0.98	0.63	0.32
	Sb	0.05	0.16	0.21	0.52	0.35	0.56
	Ge	0.02	0.35	0.46	0.88	0.68	nd
Nuts (µM)	PO_4	0.23	1.19	1.14	0.91	0.68	0.46
	NH_4	4.29	6.01	3.42	0.49	2.75	0.28
	NO_2	0.72	2.39	2.43	1.55	1.15	0.80
	NO_2+NO_3	22.8	207.2	182.2	160.7	134.7	61.9
	Si	113	157	158	153	154	152
Sus. Solids (mg/kg)	Sus. Solid (mg/l)	28.25	53.25	130.00	30.50	29.25	18.00
	As	5.95	3.99	6.51	39.38	20.88	3.03
	Se	2.74	1.76	1.61	2.12	0.29	0.00
	Sb	0.00	0.27	0.95	0.67	4.00	0.09
	Ge	nd	nd	nd	nd	nd	nd
WQ	pH	7.52	7.35	1.37	7.47	7.45	7.28
	DO (%)	84	82	82	86	86	70
	O_2 (uM)	270	250	250	259	259	210
	Cond	0.06	0.18	0.17	0.17	0.15	0.13
	Chlor	3.53	4.42	5.32	-0.23	3.59	2.62
	Turb	100	77	149	52	228	18
	T	12.13	15.33	15.36	15.29	14.65	14.79

3-6-2002, Wednesday Chattahoochee River

	R-Number	**R-1070**	**R-1069**	**R-1068**	**R-1067**	**R-1066**	**R-1065**
	km downstream	**20**	**96**	**105**	**112**	**129**	**172**
Time		4:20 PM	2:10 PM	1:00PM	11:20 AM	10:00AM	8:10AM
TDC (µg/L)	**As**	0.30	0.22	0.31	0.40	0.27	0.25
	Se	0.03	0.22	0.71	0.64	0.49	0.34
	Sb	0.19	0.12	0.20	0.24	0.18	0.19
	Ge	nd	nd	nd	nd	nd	nd
Nuts (µM)	**PO_4**	0.13	0.27	0.31	0.31	0.31	0.12
	NH_4	nd	nd	nd	nd	nd	nd
	NO_2	0.18	1.30	0.93	0.38	0.32	0.59
	NO_2+NO_3	22.3	102.0	103.4	87.8	73.7	75.4
	Si	129	141	154	152	159	94
Sus. Solids (mg/kg)	**Sus. Solid (mg/l)**	2.75	20.50	16.00	66.00	30.25	8.75
	As	6.19	4.29	21.85	5.24	6.47	2.50
	Se	65.60	16.64	19.07	3.01	1.82	14.27
	Sb	0.00	0.00	0.00	0.04	0.00	0.00
	Ge	nd	nd	nd	nd	nd	nd
WQ	**pH**	nd	nd	nd	nd	nd	nd
	DO (%)	nd	nd	nd	nd	nd	nd
	O_2 (uM)	nd	nd	nd	nd	nd	nd
	Cond	nd	nd	nd	nd	nd	nd
	Chlor	nd	nd	nd	nd	nd	nd
	Turb	nd	nd	nd	nd	nd	nd
	T	nd	nd	nd	nd	nd	nd

5-6-2002, Monday Chattahoochee River

	R-Number	R-1084	R-1083	R-1082	R-1081	R-1080	R-1079
	km downstream	20	96	105	112	129	172
Time		4:15 PM	2:15 PM	12:45 PM	11:45 AM	10:30 AM	9:00 AM
TDC (µg/L)	As	0.145	0.320	0.406	0.937	0.628	0.254
	Se	0.183	0.242	0.450	0.560	0.482	0.358
	Sb	0.035	0.132	0.226	0.325	0.272	0.175
	Ge	nd	nd	nd	nd	nd	Nd
Nuts (µM)	PO_4	0.09	0.57	0.52	0.52	0.57	0.38
	NH_4	2.55	5.94	6.11	4.38	4.44	4.77
	NO_2	0.33	1.29	1.95	0.65	0.52	0.43
	NO_2+NO_3	24.8	100.3	98.3	74.4	62.1	61.9
	Si	104	168	164	160	147	164
Sus. Solids (mg/kg)	Sus. Solid (mg/l)	17.50	37.75	32.75	50.50	23.25	2.75
	As	4.77	5.28	14.44	19.94	21.61	3.38
	Se	8.76	9.23	9.10	8.19	19.39	13.58
	Sb	0.00	0.00	0.28	0.16	0.52	0.00
	Ge	nd	nd	nd	nd	nd	Nd
WQ	pH	nd	nd	nd	nd	nd	Nd
	DO (%)	nd	nd	nd	nd	nd	Nd
	O_2 (uM)	nd	nd	nd	nd	nd	nd
	Cond	nd	nd	nd	nd	nd	nd
	Chlor	nd	nd	nd	nd	nd	nd
	Turb	nd	nd	nd	nd	nd	nd
	T	nd	nd	nd	nd	nd	nd

6-5-2002, Wednesday Chattahoochee River

	R-Number	R-1093	R-1092	R-1090	R-1089	R-1088	R-1087	R-1086	R-1085
	km downstream	0	20	50	96	105	112	129	172
Time		7:30 PM	5:45 PM	2:10 PM	1:00 PM	11:30 AM	10:20 AM	9:20 AM	7:30 AM
TDC (µg/L)	As	0.162	0.157	0.641	0.525	2.873	5.671	1.742	0.302
	Se	0.094	0.142	0.427	0.320	1.029	1.990	0.967	0.261
	Sb	0.029	0.048	0.542	0.260	0.494	1.071	0.574	0.404
	Ge	nd	nd	nd	nd	nd	nd	nd	nd
Nuts (µM)	PO_4	0	0.00	0.30	0.75	0.89	0.45	0.21	0.11
	NH_4	0.52	0.61	7.86	4.08	1.41	1.55	2.97	6.27
	NO_2	0.077	0.18	1.60	3.10	3.14	1.31	0.78	0.99
	NO_2+NO_3	nd	nd	nd	nd	nd	nd	nd	nd
	Si	64	79	113	122	116	107	89.00	133
Sus. Solids (mg /kg)	Sus. Solid (mg / L)	1.00	0.00	29.25	95.25	5.25	10.75	24.50	9.75
	As	2.85	0.00	6.94	2.00	44.33	73.45	17.88	2.10
	Se	139.21	0.00	18.73	2.30	24.83	24.73	2.48	5.40
	Sb	39.76	0.00	3.18	0.06	0.03	0.51	0.00	0.00
	Ge	nd	nd	nd	nd	nd	nd	nd	nd
WQ	pH	nd	nd	nd	nd	nd	nd	nd	nd
	DO (%)	nd	nd	nd	nd	nd	nd	nd	nd
	O_2 (uM)	nd	nd	nd	nd	nd	nd	nd	nd
	Cond	nd	nd	nd	nd	nd	nd	nd	nd
	Chlor	nd	nd	nd	nd	nd	nd	nd	nd
	Turb	nd	nd	nd	nd	nd	nd	nd	nd
	T	nd	nd	nd	nd	nd	nd	nd	nd

APPENDIX II

This appendix contains flux calculations based on my analytical data and river flow data from the United States Geological Survey National Water Information System program. Each table represents a sampling sequence (one day or contiguous dates). Column headers are the same as Appendix I

Flow Data: River flow data collected from the USGS NWIS web site. (http://www.water.usgs.gov/usa/nwis/sw)

USGS Gaging Station: The eight-digit number used to identify the gaging stations utilized in this study. In some cases the USGS no longer maintains gaging stations at or near the sampling sites and flow must be estimated using historical data. These sites are denoted with "estimate"* in the data cell.

Flow (CFS): River flow in cubic-feet per second (ft^3/s) directly from the USGS. Data obtained directly (not estimated) from the NWIS site is the 24-hour average of the flow on date the sample was taken.

Flow (L/s): River flow Converted from CFS to L/s

$Ft^3/s \times 28.357\ L/ft^3 = L/s$

Riverine Flux: The flux of metalloids in the river in mg/s.

$\mu g/L$ (concentration) $\times 10^{-3}\ mg/\mu g \times L/s$ (flow) $= mg/s$ (flux)

As, Se, Sb, Ge: The flux of a particular metalloid element in the river at the sampling location (mg/s).

Δ Flux: The difference in upstream and downstream river flux calculated between sampling locations in mg/s . Calculated by subtracting the upstream flux from the downstream flux. A negative Δ flux indicates a net loss of metalloids from the river between the two locations. A positive flux indicates net input of metalloids into the river.

As, Se, Sb, Ge: The Δ flux of each metalloid element in the river between sampling locations (mg/s).

TRI Estimate: The metalloid flux estimate released by coal fired power plants in their Toxic Release Inventory (http://www.epa.gov/enviro/html/tris/tris_query.html) "NA" indicates an inventory of the element is required by the EPA but is not available in the TRI estimate. "NR" indicates that an inventory of the element is not required based on the peak mega-wattage rating of the power plant.

As, Se, Sb, Ge: The TRI estimate of the power plant aquatic emission of metalloid elements in mg/s.

$Lbs/year \times 1\ kg/2.2\ lbs \times 10^6\ mg/kg \times 1 year/3.15\times10^7\ s = mg/s$

* Estimated flows were determined by comparing historical flow data with recent flow data. The USGS publishes the historical data for stations that are inactive as well as those online now. Flows at inactive sites are estimated by comparing the difference between the flows for the day of the year the sample was taken, averaged over the entire history of the station, at an active station and the inactive station. The percent difference between the flows in historical data is scaled to the flow at an active station of the data the sample was taken.

Average flow for Station 1 (active) on June 15th (life of station) = 1000CFS
Average flow for Station 2 (inactive) on June 15th (life of station) = 500CFS

Difference = -50%

Daily average flow for Station 1 June 15th 2001 = 1500 CFS
Estimated flow for Station 2 June 15th 2001 = 1500 CFS x -0.5 = 750 CFS

5-21-2001, Monday Etowah River

	R-Number		R-1017	R-1019	R-1020	R-1021
	km downstream	0	11	25	83	113
Flow Data	**USGS Gaging Station**	nd	Estimate	Estimate	Estimate	2397000
	Flow (CFS)	nd	1356	1549	1587	3430
	Flow (L/s)	nd	38398	43863	44939	97127
Riverine Flux (mg/s)	**As**	nd	30	7	11	52
	Se	nd	74	3	3	7
	Sb	nd	48	2	11	18
	Ge	nd	4	3	nd	nd

Δ Flux (mg/s)	**As**	nd	nd	-24	4	42	nd
	Se	nd	nd	-71	0	4	nd
	Sb	nd	nd	-46	8	7	nd
	Ge	nd	nd	0	nd	nd	nd
Power Plants				**Bowen**		**Hammond**	
TRI Estimate (mg/s)	**As**			0		NA	
	Se			0		NR	
	Sb			NR		NR	
	Ge			NR		NR	

5-22-2001, Tuesday Chattahoochee River

	R-Number		R-1027	R-1026	R-1025	R-1024	R-1023
	km downstream	20	96	105	112	129	172
Flow Data	**USGS Gaging Station**	nd	2338000	2338000	2338000	2338000	2339500
	Flow (CFS)	nd	1850	1850	1850	1850	4230
	Flow (L/s)	nd	52386	52386	52386	52386	119781
Riverine Flux (mg/s)	**As**	nd	13	22	72	18	34
	Se	nd	50	58	73	50	122
	Sb	nd	12	17	32	19	478
	Ge	nd	37	64	121	50	nd

Δ Flux (mg/s)	**As**	nd	nd	10	49	-54	16	nd
	Se	nd	nd	8	15	-23	72	nd
	Sb	nd	nd	5	15	-13	460	nd
	Ge	nd	nd	27	57	-71	nd	nd
Power Plants				**Yates**	**Wansley**			
TRI Estimate (mg/s)	**As**			0.057	0			
	Se			NA	6.5			
	Sb			NR	NR			
	Ge			NR	NR			

8-2-2001 Thursday Etowah River

	R-Number	**R-1040**	**R-1039**	**R-1038**	**R-1036**	**R-1034**
	km downstream	**0**	**11**	**25**	**83**	**113**
Flow Data	**USGS Gaging Station**	2494000	Estimate	Estimate	Estimate	2397000
	Flow (CFS)	2250	2422	2767	2970	5910
	Flow (L/s)	63713	68584	78353	84101	167353
Riverine Flux (mg/s)	**As**	11	43	17	18	60
	Se	26	117	40	5	13
	Sb	2	68	7	5	68
	Ge	nd	7	34	nd	nd

Δ Flux (mg/s)	**As**	nd	31	-25	0	43	nd
	Se	nd	92	-77	-36	9	nd
	Sb	nd	65	-60	-3	63	nd
	Ge	nd	nd	27	nd	nd	nd
Power Plants				**Bowen**		**Hammond**	
TRI Estimate (mg/s)	**As**			0		NA	
	Se			0		NR	
	Sb			NR		NR	
	Ge			NR		NR	

8-6-2001, Monday Chattahoochee River

	R-Number		**R-1045**	**R-1044**	**R-1043**	**R-1042**	**R-1041**
	km downstream	**20**	**96**	**105**	**112**	**129**	**172**
Flow Data	**USGS Gaging Station**	nd	2338000	23380000	2338000	2338000	2339500
	Flow (CFS)	nd	2020	2020	2020	2020	3620
	Flow (L/s)	nd	57200	57200	57200	57200	102508
Riverine Flux (mg/s)	**As**	nd	16	40	108	34	84
	Se	nd	15	38	71	43	41
	Sb	nd	16	22	39	25	17
	Ge	nd	46	58	173	80	nd

Δ Flux (mg/s)	**As**	nd	nd	24	68	-74	50	nd
	Se	nd	nd	23	34	-29	-2	nd
	Sb	nd	nd	6	17	-14	-7	nd
	Ge	nd	nd	12	115	-93	nd	nd
Power Plants				**Yates**	**Wansley**			
TRI Estimate (mg/s)	**As**			0.057	0			
	Se			NA	6.5			
	Sb			NR	NR			
	Ge			NR	NR			

9-15-2001, Saturday Chattahoochee River

	R-Number	R-1051	R-1050	R-1049	R-1048	R-1047	R-1046
	km downstream	**20**	**96**	**105**	**112**	**129**	**172**
Flow Data	**USGS Gaging Station**	2335000	2338000	2338000	2338000	2338000	2339500
	Flow (CFS)	1290	2170	1270	1270	1270	741
	Flow (L/s)	36529	61448	35963	35963	35963	20983
Riverine Flux (mg/s)	**As**	3	9	18	201	40	8
	Se	5	23	43	108	39	8
	Sb	1	8	16	51	19	4
	Ge	1	17	30	67	31	nd

Δ Flux (mg/s)	**As**	nd	6	9	183	-161	-33	nd
	Se	nd	17	21	65	-69	-31	nd
	Sb	nd	7	8	35	-32	-15	nd
	Ge	nd	17	13	37	-36	nd	nd
Power Plants				**Yates**	**Wansley**			
TRI Estimate (mg/s)	**As**			0.057	0			
	Se			NA	6.5			
	Sb			NR	NR			
	Ge			NR	NR			

11-9-2001, Friday Chattahoochee River

	R-Number	R-1057	R-1056	R-1055	R-1054	R-1053	R-1052
	km downstream	**20**	**96**	**105**	**112**	**129**	**172**
Flow Data	**USGS Gaging Station**	2335000	2338000	2338000	2338000	2338000	2339500
	Flow (CFS)	977	1030	1030	1030	1030	2580
	Flow (L/s)	27666	29167	29167	29167	29167	73058
Riverine Flux (mg/s)	**As**	2	7	13	108	18	20
	Se	5	10	32	59	31	32
	Sb	1	6	12	32	14	18
	Ge	1	10	13	26	20	nd

Δ Flux (mg/s)	**As**	nd	5	6	95	-90	1	nd
	Se	nd	5	22	27	-28	1	nd
	Sb	nd	5	6	20	-19	4	nd
	Ge	nd	9	3	12	-6	nd	nd
Power Plants				**Yates**	**Wansley**			
TRI Estimate (mg/s)	**As**			0.057	0			
	Se			NA	6.5			
	Sb			NR	NR			
	Ge			NR	NR			

12-18-2001, Monday Chattahoochee River

	R-Number km downstream	R-1063 20	R-1062 96	R-1061 105	R-1060 112	R-1059 129	R-1058 172
Flow Data	**USGS Gaging Station**	2335000	2338000	2338000	2338000	2338000	2339500
	Flow (CFS)	880	3920	3870	3650	3350	1040
	Flow (L/s)	24954	111159	109742	103503	94996	29491
Riverine Flux (mg/s)	**As**	4	33	43	252	99	10
	Se	3	27	46	101	60	9
	Sb	1	18	23	54	33	17
	Ge	1	38	50	91	65	

Δ Flux (mg/s)	**As**	nd	29	10	209	-153	-90	nd
	Se	nd	24	19	56	-41	-51	nd
	Sb	nd	16	6	31	-21	-17	nd
	Ge	nd	38	11	41	-26	-65	nd
Power Plants				**Yates**	**Wansley**			
TRI Estimate (mg/s)	**As**			0.057	0			
	Se			NA	6.5			
	Sb			NR	NR			
	Ge			NR	NR			

3-6-2002, Wednesday Chattahoochee River

	R-Number km downstream	R-1070 20	R-1069 96	R-1068 105	R-1067 112	R-1066 129	R-1065 172
Flow Data	**USGS Gaging Station**	2335000	2338000	2338000	2338000	2338000	2339500
	Flow (CFS)	696	2160	2180	2190	2170	8690
	Flow (L/s)	19736	61251	61818	62102	61535	246422
Riverine Flux (mg/s)	**As**	6	13	19	25	17	61
	Se	1	13	44	40	30	84
	Sb	4	7	12	15	11	47
	Ge	nd	nd	nd	nd	nd	nd

Δ Flux (mg/s)	**As**	nd	8	6	5	-8	44	nd
	Se	nd	13	30	-4	-10	53	nd
	Sb	nd	4	5	3	-4	36	nd
	Ge	nd	nd	nd	nd	nd	nd	nd
Power Plants				**Yates**	**Wansley**			
TRI Estimate (mg/s)	**As**			0.057	0			
	Se			NA	6.5			
	Sb			NR	NR			
	Ge			NR	NR			

5-6-2002, Monday Chattahoochee River

	R-Number km downstream	R-1084 20	R-1083 96	R-1082 105	R-1081 112	R-1080 129	R-1079 172
Flow Data	**USGS Gaging Station**	2335000	2338000	2338000	2338000	2338000	2339500
	Flow (CFS)	696	2120	2130	2160	2170	996
	Flow (L/s)	19945	60753	61039	61899	62186	28542
Riverine Flux (mg/s)	**As**	3	19	25	58	39	7
	Se	4	15	27	34	30	10
	Sb	1	8	14	20	17	5
	Ge	nd	nd	nd	nd	nd	nd

Δ Flux (mg/s)	**As**	nd	17	5	33	-19	-32	nd
	Se	nd	11	13	7	-5	-20	nd
	Sb	nd	7	6	6	-3	-12	nd
	Ge	nd	nd	nd	nd	nd	nd	nd
Power Plants				**Yates**	**Wansley**			
TRI Estimate (mg/s)	**As**			0.057	0			
	Se			NA	6.5			
	Sb			NR	NR			
	Ge			NR	NR			

6-5-2002, Wednesday Chattahoochee River

<table>
<tr><td></td><td>R-Number</td><td colspan="2">R-1093</td><td colspan="2">R-1092</td><td colspan="2">R-1090</td><td colspan="2">R-1089</td><td colspan="2">R-1088</td><td colspan="2">R-1087</td><td colspan="2">R-1086</td><td colspan="2">R-1085</td></tr>
<tr><td></td><td>km downstream</td><td colspan="2">0</td><td colspan="2">20</td><td colspan="2">50</td><td colspan="2">96</td><td colspan="2">105</td><td colspan="2">112</td><td colspan="2">129</td><td colspan="2">172</td></tr>
<tr><td rowspan="3">Flow
Data</td><td>USGS Gaging Station</td><td colspan="2"></td><td colspan="2">2335000</td><td colspan="2">2338000</td><td colspan="2">2338000</td><td colspan="2">2338000</td><td colspan="2">2338000</td><td colspan="2">2338000</td><td colspan="2">2339500</td></tr>
<tr><td>Flow (CFS)</td><td colspan="2">482</td><td colspan="2">670</td><td colspan="2">3610</td><td colspan="2">2920</td><td colspan="2">2610</td><td colspan="2">2280</td><td colspan="2">2020</td><td colspan="2">877</td></tr>
<tr><td>Flow (L/s)</td><td colspan="2">13668</td><td colspan="2">18999</td><td colspan="2">102369</td><td colspan="2">82802</td><td colspan="2">74012</td><td colspan="2">64654</td><td colspan="2">57281</td><td colspan="2">24869</td></tr>
<tr><td rowspan="4">Riverine
Flux
(mg/s)</td><td>As</td><td colspan="2">2</td><td colspan="2">3</td><td colspan="2">66</td><td colspan="2">43</td><td colspan="2">213</td><td colspan="2">367</td><td colspan="2">100</td><td colspan="2">8</td></tr>
<tr><td>Se</td><td colspan="2">1</td><td colspan="2">3</td><td colspan="2">44</td><td colspan="2">27</td><td colspan="2">76</td><td colspan="2">129</td><td colspan="2">55</td><td colspan="2">15</td></tr>
<tr><td>Sb</td><td colspan="2">0</td><td colspan="2">1</td><td colspan="2">55</td><td colspan="2">22</td><td colspan="2">37</td><td colspan="2">69</td><td colspan="2">33</td><td colspan="2">23</td></tr>
<tr><td>Ge</td><td colspan="2">Nd</td><td colspan="2">nd</td><td colspan="2">nd</td><td colspan="2">nd</td><td colspan="2">nd</td><td colspan="2">nd</td><td colspan="2">nd</td><td colspan="2">nd</td></tr>
<tr><td rowspan="4">Δ
Flux
(mg/s)</td><td>As</td><td>nd</td><td colspan="2">1</td><td colspan="2">63</td><td colspan="2">-22</td><td colspan="2">169</td><td colspan="2">154</td><td colspan="2">-267</td><td colspan="2">-92</td><td>nd</td></tr>
<tr><td>Se</td><td>nd</td><td colspan="2">1</td><td colspan="2">41</td><td colspan="2">-17</td><td colspan="2">50</td><td colspan="2">53</td><td colspan="2">-73</td><td colspan="2">-40</td><td>nd</td></tr>
<tr><td>Sb</td><td>nd</td><td colspan="2">1</td><td colspan="2">55</td><td colspan="2">-34</td><td colspan="2">15</td><td colspan="2">33</td><td colspan="2">-36</td><td colspan="2">-10</td><td>nd</td></tr>
<tr><td>Ge</td><td>nd</td><td colspan="2">nd</td><td colspan="2">nd</td><td colspan="2">nd</td><td colspan="2">nd</td><td colspan="2">nd</td><td colspan="2">nd</td><td colspan="2">nd</td><td>nd</td></tr>
<tr><td colspan="2">Power Plants</td><td></td><td colspan="2"></td><td colspan="2"></td><td colspan="2"></td><td colspan="2">Yates</td><td colspan="2">Wansley</td><td colspan="2"></td><td colspan="2"></td><td></td></tr>
<tr><td rowspan="4">TRI
Estimate
(mg/s)</td><td>As</td><td></td><td colspan="2"></td><td colspan="2"></td><td colspan="2"></td><td colspan="2">0.057</td><td colspan="2">0.00</td><td colspan="2"></td><td colspan="2"></td><td></td></tr>
<tr><td>Se</td><td></td><td colspan="2"></td><td colspan="2"></td><td colspan="2"></td><td colspan="2">NA</td><td colspan="2">6.70</td><td colspan="2"></td><td colspan="2"></td><td></td></tr>
<tr><td>Sb</td><td></td><td colspan="2"></td><td colspan="2"></td><td colspan="2"></td><td colspan="2">NR</td><td colspan="2">NR</td><td colspan="2"></td><td colspan="2"></td><td></td></tr>
<tr><td>Ge</td><td></td><td colspan="2"></td><td colspan="2"></td><td colspan="2"></td><td colspan="2">NR</td><td colspan="2">NR</td><td colspan="2"></td><td colspan="2"></td><td></td></tr>
</table>

APPENDIX III

Appendix III contains specific driving direction to each sampling location. For both transects the directions start on Interstate 75-85 in downtown Atlanta and proceed to the first sample site of the sequence. Following directions are from one sample site to another.

Chattahoochee Transect (Figure 2-6)

Km marker 172 (West Point): Drive south on Interstate 75-85 and take the I-85 south split. Proceed south on I-85 to Exit 2 (GA 18). Take GA 18 west toward Alabama. Turn right immediately after the Chattahoochee River bridge into parking lot of the Interstate Telephone Company. Sample location is underneath the overpass. West Bank

Latitude-32° 52.670’ N
Longitude- 85° 10.882’ W
USGS gaging station- 02339500 (active)

Km marker 129 (Franklin): From the Interstate Telephone Company turn back onto GA 18 headed east. Turn left onto US 29 North toward La Grange. In La Grange turn onto US 27 North towards Franklin. In Franklin cross the bridge over the Chattahoochee River and make the first left after the bridge into the parking lot with the softball field. Sample from the boat dock near the bridge. West Bank

Latitude-33° 16.663’ N
Longitude- 85° 06.114’ W
USGS gaging station (inactive)

Km marker 112 (Below Wansley / Yates): Turn back onto US 27 N. Proceed north to Central Hatchee. App. 2 miles past Central Hatchee turn right at the large white sign for the concrete plant and Yellow Dirt Baptist Church. Follow this road past the four-way intersection, church and onto the dirt road. You will pass the entrance to Plant Wansley. The road ends in a boat ramp on the Chattahoochee River. Sample from this boat ramp. West Bank

Latitude-33° 23.674’ N
Longitude- 85° 02.007’ W

Km marker 105 (Between Wansley / Yates): Follow the dirt road back to the four-way intersection. At the intersection turn right. This road will lead back to US 27. Turn right onto US 27 headed north. At the intersection of GA 5 turn right (east). Proceed east until mile marker 22. Between mile marker 22 and 23 turn right into the McIntosh Reserve at McIntosh Road. Follow this road until it ends at the information center. Turn right onto the dirt path and follow it a very short distance to the bottom of the hill. Walk along the riverbank back toward the information center and sample from the rocks jutting into the river. West Bank

Latitude-33^{o} 26.403’ N
Longitude- 84^{o} 57.173’ W

Km Maker 96 (Above Wansley / Yates) Proceed back to GA 5 and turn right (east). Head east to the intersection of GA 5 and US 27 Alt. Turn right onto US 27 Alt (south). After a short distance you will cross the bridge over the Chattahoochee. Make an immediate left after the bridge. Park in the parking lot and sample from the boat ramp. East Bank

Latitude-33^{o} 28.563’ N
Longitude- 84^{o} 54.012’ W
USGS gaging station- 02338000 (active)

Km marker 20 (Holcomb Bridge): Turn back onto US 27 Alt. Headed south. Follow signs back to I-85 N through Newnan, GA. In Newnan, get on I-85 N. Follow I-85 N back through Atlanta. Merge onto I-75-85. At the I-75-85 split, follow I-85 N. Proceed north to the Clairemont Road exit. Turn left onto Clairemont Road (north) and follow it until ends at Peachtree Industrial Drive. Turn right onto Peachtree Industrial and follow it to the exit at Jimmy Carter Blvd. After the exit turn left (north) onto Jimmy Carter Blvd. Follow this road north. It will turn into Holcomb Bridge Road. At the border of Gwinnett County Holcomb Bridge Road crosses the Chattahoochee River. Turn left immediately after the bridge into the front drive of the North Atlanta Raw Water Uptake. Park and sample from the stream-bank. This is the last sample site for the Chattahoochee Transect. East Bank

USGS Gaging Station- 02335000

Etowah River Transect (Figure 2-3)

Km marker 113 (Coosa outside Rome): Drive north on Interstate 75-85. Take the 75 N split. Drive app. 40 miles north to the GA 20 West (toward Rome) exit. Take this exit. Drive through Rome towards the Alabama border. Outside Rome turn left onto GA 100 S. Cross the bridge over the Coosa River and make an immediate right. There is a small path down to the river. Sample from this shore.

Latitude-34^{o} 14.887' N
Longitude- 85^{o} 21.320' W
USGS gaging station- 02397000 (active)

Oostanuala River in Rome: Turn left onto GA 100 N. Turn right onto GA 20 E. In Rome make a right immediately before crossing the bridge over the Oostanuala River. This leads into the parking lot of the Floyd County Library. Park in the lot and sample from the river bank.

Latitude-34^{o} 15.542' N
Longitude- 85^{o} 10.170' W

Km marker 83 (The Shrimp Boat): From the library get on GA 20 E. Turn right onto North Broad Street. Navigate to East 2nd Avenue. Turn right into the Shrimp Boat Restaurant. Sample underneath the overpass.

Latitude-34^{o} 14.780' N
Longitude- 85^{o} 10.091' W

Km Marker 25 (Etowah below Euharlee Creek): Navigate back to GA 20 E. Turn onto GA 20 headed east and proceed out of Rome. At the intersection of US 411 and GA 20, take US 411 east towards Cartersville. Turn right onto Harden Bridge Road. Follow this road app. 4 miles until it intersects Chulio Road. Follow Chulio Road until it crosses the Etowah River. Make an immediate right after the bridge. On this road make the first right. This leads into a small dirt parking area by the river bank. Sample from the shore.

Latitude-34^{o} 08.859' N
Longitude- 84^{o} 55.179' W

Covered Bridge over Euharlee Creek: Turn left onto Chulio Road. Drive west to the fork that leads towards the covered bridge. Follow this road to the covered bridge, which is on the right side of the road. Turn into the parking lot. Sample at the creek underneath the bridge.

Latitude-34^{o} 08.573' N

Longitude- 84^{o} 55.934’ W

Km Marker 11 (61-113): Turn left out of the covered bridge parking lot. Make and drive south. Make the first right you come to. Follow this road past Bowen power plant and through the plant grounds. Follow this road to GA 113 and turn left (east). Proceed east until GA 61 and GA 113 merge. Continue northeast. After crossing the bridge over the Etowah River make an immediate right into a dirt parking area underneath the bridge. Sample at the stream bank.

Latitude-34^{o} 08.574’ N
Longitude- 84^{o} 50.297’ W

Km marker 0 (Allatoona Dam): Return to 61-113 headed northeast. Follow this road through Cartersville to US 41. Take US 41 South. After crossing the Etowah River, take a short spur road (GA 293) to the bank of the Etowah. Sample underneath the bridge.

Latitude-34^{o} 09.198’ N
Longitude- 84^{o} 46.310’ W
USGS gaging station- 02494000 (active)

REFERENCES

Anderson, L.C.D. and Bruland, K.W. (1991) Biogeochemistry of Arsenic in Natural Waters: The Importance of Methylated Species. *Environmental Science and Technology*. **25**, 420-427

Andreae, M.O. (1978) Distribution and Speciation of Arsenic in Natural Waters and Some Marine Algae. *Deep Sea Research*, **25**, 391-402.

Andreae, M.O. and Froelich, P.N. (1981) Determination of Germanium in Natural Water by Graphite Furnace Atomic Adsorption Spectrometery with Hydride Generation. *Analytical Chemistry*, **53**, 287-291.

Andreae, M.O. and Froelich, P.N. (1984) Arsenic, Antimony, and Germanium Biogeochemistry in the Baltic Sea, *Tellus*, **36B**, 101-117.

Andrewes, P. Cullen, W.R., Polishchuk, E. (2000) Antimony Biomethylation by *Scopulariopsis Brevicaulis*: Characterization of Intermediates and the Methyl Donor. *Chemosphere,* **41,** 1717-1725.

Baines, S.B., Fisher N.S., Doblin, M.A. Cutter, G.A. (2001) Uptake of Dissolved organic Selenides by Marine Phytoplankton. *Limnology and Oceanography*, **46**, 1936-1934.

Bhumbala, D.K. and Keefer, R.F. Arsenic Mobilization and Bioavailability in Soils. *Arsenic in the Enviroment Part I: Cycling and Characterization*. Ed. Nriagu J.O. New York: John Wiley & Sons, Inc., 1994.

Brookins, D.G. *Eh-pH Diagrams for Geochemistry*. New York: Springer-Verlag, 1988.

Byrd, J.T. and Andreae, M.O. (1982) Tin and Methyltin Species in Seawater: Concentrations and Fluxes. *Science*. **218**, 565-569.

Chowns, T.M. (1983) *Geologyof Paleozoic Rocks in the Vicinity of Rome, Georgia*. Georgia Geological Society, Georgia.

Cooke, T.D. and Bruland, K.W. (1987) Aquatic Chemistry of Selenium: Evidence of Biomethylation. *Environmental Science and Technology*. **21**. 1214-1219.

Crutchfield, J.U. (2000) Recovery of a Power Plant Cooling Reservoir From Selenium Bioaccumulation. *Environmental Science and Policy.* **3**, 145-163.

Cutter, G. A. and Bruland, K.W. (1984) The Marine Biogeochemistry of Selenium: A re-evaluation. *Limnology and Oceanography*. **29(6)**, 1179-1192.

Eisler, R. A Review of Arsenic Hazards to Plants and Animals with an Emphasis on Fishery and Wildlife Resources *Arsenic in the Enviroment Part II: Human Health and Ecosystem Effects*. Ed. Nriagu J.O. New York: John Wiley & Sons, Inc., 1994.

Filella, M., Belzile, N., and Chen , W. (2002) Antimony in the Environment: A review focused on Natural Waters I. Occurance. *Earth Science Reviews,* **57**, 125-176.

Francesconi. K.A. and Kuehnelt, D. Arsenic Compounds in the Environment. *Environmental Chemistry of Arsenic*. Ed. Frankenburger, W.T. Marcel Dekker, Inc: New York, 2002.

Grasshoff, K., Kremling, K., and Ehrhardt, M. (1999) *Methods of Seawater Analysis.* Wiley-Vich, Germany.

Hambrick, G.A., Froelich, P.N., Andrea, M.O., Lewis, B.L. (1984) Determination of Methylgermanium Species in Natural Waters by Graphite Furnace Atomic Absorption Spectrometry with Hydride Genertation. *Analytical Chemistry*, ***56***, 421-424

Klien, C. and Hulbut, C.S. (1993) *The Manual of Mineralogy*, 21st Edition. John Wiley & Sons, Inc., New York.

Le, X.C., Cullen, W.R., Reimer, K.J. (1994) Effect of Cysteine on the Speciation of Arsenic by Using Hydride Generation Atomic Absorption Spectrometry. *Analytica Chemica Acta*, **285**, 277-285.

Milne, J.B. The Uptake and Metabolism of Inorganic Selenium Species. *Environmental Chemistry of Selenium*. Ed. Frankenburger, W.T, and Engberg, R.A. Marcel Dekker, Inc: New York, 1998.

Mok, W.M. and Wai C.M. Mobilization of Arsenic in Contaminated River Waters. *Arsenic in the Enviroment Part I: Cycling and Characterization*. Ed. Nriagu J.O. New York: John Wiley & Sons, Inc., 1994.

Murphy, Riley. (1962) Analysis of Dissolved Reactive Phosphate in Natural Waters. *Analytica Chemica Acta,* **29**, 31.

Morris, Rilet, (1963) Analysis of Nitrite in Natural Waters. *Analytica Chemica Acta.* **30**, 272.

Newman, D.K., Ahmann, D., Morel, F.M.M. (1998) A Brief Review of Microbial Arsenate Respiration. *Geomicrobiology*, **15**, 255-268.

Oldfield, J.E. Environmental Implications of Uses of Selenium with Animals. *Environmental Chemistry of Selenium*. Ed. Frankenburger, W.T, and Engberg, R.A. Marcel Dekker, Inc: New York, 1998.

Ormland, R.S., Dowdle, P.R., Hoeft, S., Sharp, J.O., Schaefer, J.K., Miller, L.G., Blum, J.S., Smith, R.L., Bloom, N.S., Wallschlager, D. (2000) Bacterial Dissimilatory Reduction of Arsenate and Sulfate in Meromictic Mono Lake, California. *Geochemica et Cosmochemica Acta*, **64**, 3073-3084.

Rubin, E. (1999) Toxic Releases from Power Plants. *Environmental Science and Technology*, **33**, 3062-3067.

Ryan, Dave. *Whitman Annouces Transistion From Consumer Use of Wood Containing Arsenic*. (12 Feb. 2002): 1pp. Online. Internet. 14 Oct. 2002.

Sandelin, K. and Backman, R. (1999) A Simple Two-Reactor Method for Predicting Distribution of Trace Elements in Combustion Systems. *Environmental Science and Technology*, **33**, 4508-4513.

Sanders, J.G. (1981) Role of Marine Phytoplankton in Determining the Chemical Speciation and Biogeochemical Cycling of Arsenic. *Canadian Journal of Fisheries and Aquatic Science*. **40**, 192-196.

Sordo, M. Herrera, L.A., Ostrosky-Wegman, P., Rojas, E. (2001) Cytotoxic and Genotoxic Effects of As, MMA, and DMA on Leukocytes and Stimulated Human Lymphcytes. *Teratogenesis, Carcinogenesis, and Mutagenesis*. **21**, 249-260.

Stephens, D.W. and Waddel, B. Selenium Sources and Effects in Biota in the Green River Basin of Wyoming, Colorado, and Utah. *Environmental Chemistry of Selenium*. Ed. Frankenburger, W.T, and Engberg, R.A. Marcel Dekker, Inc: New York, 1998.

Takayanagi, K. and Wong, G.T.F. (1985) Dissolved Inorganic and Organic Selenium in the Orca Basin, *Geochemica and Cosmochemica Acta,* **49**, 539-546.

Yamauchi, H. and Fowler, B.A. (1994) Toxicity and Metabolism of Inorganic and Methylated Arsenicals. *Arsenic in the Enviroment Part II: Human Health and Ecosystem Effects*. Ed. Nriagu J.O. New York: John Wiley & Sons, Inc., 1994.

Yan, R., Gauthier, D., and Filles, G. (2001) Volatility and chemistry of trace elements in a coal combuster, *Fuel*, **80**, 2217-2226.

Yan, R., Gauthier, D., and Filles, G. (1999) Possible Interactions Between As, Se, and Hg During Coal Combustion. *Combustion and Flame*, **120**, 49-60.

Zeng, T., Sarofim, A.F., and Senior, C.L. (2001) Vaporization of Arsenic, Selenium, and Antimony during Coal Combustion, *Combustion and Flame*, **126**, 1714-1724

RESERVOIR SHORELINE EROSION AND SEDIMENTATION ANALYSIS:

Basic Information

Title:	RESERVOIR SHORELINE EROSION AND SEDIMENTATION ANALYSIS:
Project Number:	2002GA7B
Start Date:	3/1/2002
End Date:	2/28/2003
Funding Source:	104B
Congressional District:	1st, GA
Research Category:	None
Focus Category:	Sediments, Non Point Pollution, Surface Water
Descriptors:	None
Principal Investigators:	Paul A Work

Publication

1. Sebnem Elci and Paul A.Work, 2003. Numerical Modeling of Hydrodynamic Circulation and Cohesive Sediment Transport in Hartwell Lake, South Carolina/Georgia, USA. Contaminated Sediments: Characterisation, Evaluation, Mitigation/Restoration,Management Strategy Performance, ASTM STP 1442, J. Locat, R.Galvez-Cloutier, R.C. Chaney, and K. Demars, Eds., ASTM International, West Conshohocken, PA, 2003.
2. Sebnem, Elci and Paul A. Work, 2003, "Field Observations for Definition of Reservoir Shoreline Erosion and Sedimentation: Lake Hartwell, SC/GA," Georgia Water Resources Institute, Georgia Tech, Atlanta, GA., 48p.

Field Observations for Definition of

Reservoir Shoreline Erosion and Sedimentation:

Lake Hartwell, SC/GA

Şebnem Elçi and Paul A. Work

School of Civil and Environmental Engineering
Georgia Tech Regional Engineering Program
6001 Chatham Center Drive, Suite 350
Savannah, GA 31405

TECHNICAL REPORT

August 2003

Sponsored by:

Georgia Water Resources Institute

and

The U.S. Geological Survey

TABLE OF CONTENTS

LIST OF FIGURES

LIST OF TABLES

1. Abstract

A U.S. Environmental Protection Agency (EPA) “Superfund” site is located on a tributary to Hartwell Lake because of high concentrations of polychlorinated biphenyls (PCBs) in the lake sediments. In a previous study conducted by the authors, the fate of sediments introduced to the reservoir was investigated via numerical models of hydrodynamics and sediment transport (Elci and Work, 2002). The study described here involves surveying of the bathymetry of the lake and comparison of the results to the previous surveys to quantify 40 years of deposition.

The hydrodynamics of the lake were modeled using a numerical model and the results were presented in Elci and Work (2002). In this study, surface velocities are measured in the main pool of the lake to validate results of the numerical model.

With a total of 1516 erosion control structures along the lakeshores as of September 2002 (source: USACE Hartwell Office), shoreline erosion has been a significant problem for Hartwell Lake. Elci and Work (2002) developed a methodology for predicting shoreline erosion. In this study, two peninsulas with large fetches are surveyed to provide data for the shoreline erosion prediction methodology.

This report addresses the field data collection and analysis in Hartwell Lake, SC/GA. The primary goals of the study are:

1. Survey bathymetry of different transects in the main pool and compare to old surveys conducted by the U.S. Army Corps of Engineers.
2. Measure surface velocities along different transects.
3. Survey shorelines of the lake.

2. Introduction

This report describes the field data collection and analysis in Hartwell Lake, a U.S. Army Corps of Engineers (USACE) reservoir, located on the Savannah River, between Anderson, South Carolina, and Hartwell, Georgia, USA (Figure 1). The reservoir was built between 1955 and 1963, with joint goals of flood control, power production, water supply, and recreation (Elci and Work, 2002). High concentrations of polychlorinated biphenyls (PCBs) have been found in the lake and in Twelve-Mile Creek, a tributary, resulting from the operation of a capacitor manufacturing facility in the Twelve Mile Creek Watershed from 1955-1976 (EPA, 1991). In a previous project funded by the

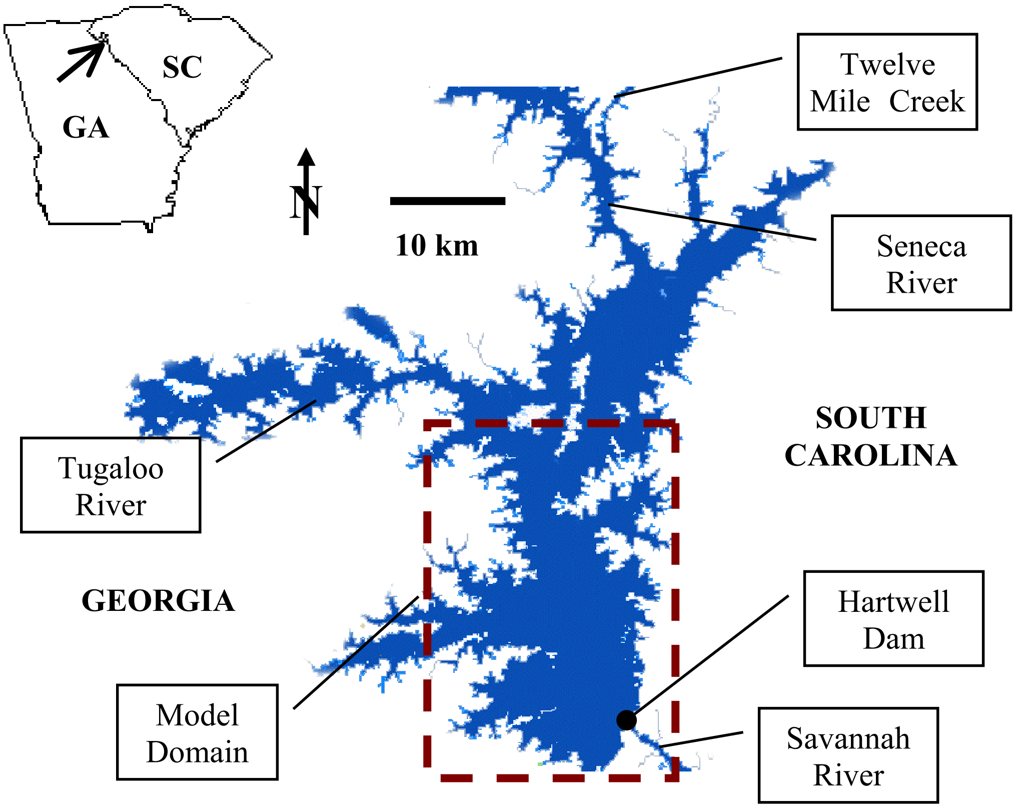

Figure 1. Map of study site. Dashed box shows the region within the main pool of the lake that was modeled (numerically) to describe the water circulation and sediment deposition patterns.

South Carolina Water Resources Center (SCWRC), the hydrodynamic circulation and sedimentation in the main pool of Hartwell Lake were investigated via 3-D numerical modeling of hydrodynamics and sediment transport (Elci and Work, 2002). For this purpose the Environmental Fluid Dynamics Code (EFDC) developed by Hamrick (1996) was applied to Hartwell Lake to simulate hydrodynamic processes in the lake. The main objective of the field data collection effort described in this report is to obtain data for validation of the results of the hydrodynamic model. This effort also yielded bathymetric survey data to quantify sediment deposition in the main pool of the lake, since the lake was last surveyed in 1970's.

Hartwell Lake has a shoreline length of 1548 km, and erosion of lakeshores has been a significant problem for homeowners. As of September 2002, there were 1123 permitted riprap installations, and 393 permitted retaining walls, for a total of 1516 erosion control structures along the lakeshores (source: USACE Hartwell Office), an indication of the magnitude of the erosion problem. Another objective realized in the previous project was to develop a methodology for estimating shoreline erosion rates. The study described in this report also resulted in new shoreline data for calibrating and testing the erosion prediction methodology.

The field data were collected February 10-14, 2003. Throughout the week, very strong winds (more than 4 times the historical average) from the southwest were observed (Figure 2). The mean water level was 199.33 m.

Hartwell Lake is an example of a warm monomictic lake, which is vertically mixed from December to March, and thermally stratified to varying degrees between April and

November. Figure 3 shows a temperature profile measured at a station near the dam in February 2002.

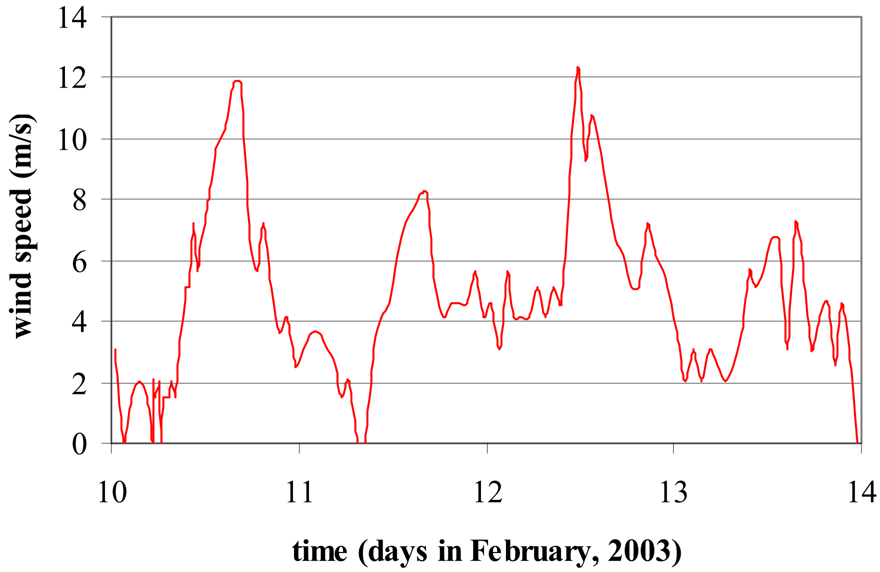

Figure 2. Hourly wind speed data obtained from Anderson County Airport, SC during field measurement campaign.

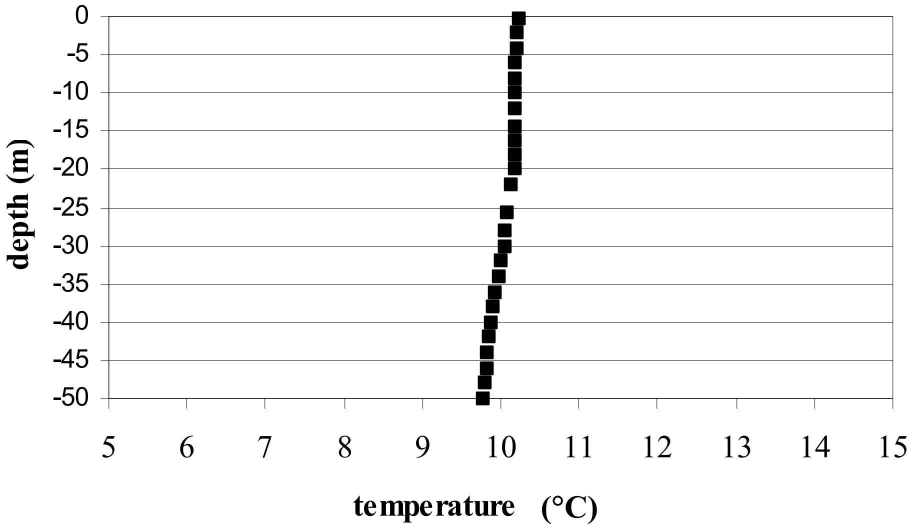

Figure 3. Measured temperature profiles at a station near dam in February 2002.

Field data collection and analysis described in this report is a continuation project to provide data to validate the results of the previous project funded by South Carolina Water Resources Center (SCWRC). For details and findings of the previous project, the reader is referred to the technical report submitted to the SCWRC by the authors (Elci and Work, 2002). In this report, the techniques to collect, bathymetric, velocity and shoreline position data are first described. Then, the results from topographic surveys conducted by USACE in the past, and the new bathymetric surveys are compared. Next, a summary of new velocity data is presented. Finally, shoreline data are presented. In the conclusion of this report, benefits associated with these two projects are stated.

3. Data Collection

This section discusses the techniques applied to collect bathymetric, velocity and shoreline position data in Hartwell Lake, SC/GA. Bathymetry data collected along several transects were compared to old surveys to quantify 40 years of deposition in the lake. Surface velocities were measured to validate the results of a numerical model used previously for simulation of the hydrodynamics in the lake. Two peninsulas along the shoreline of the lake were surveyed to provide data for validating a shoreline erosion prediction methodology previously developed by the authors.

3.1. Bathymetric Survey Data

Two sources of bathymetric data are available for the lake: data collected by the U.S. Army Corps of Engineers (USACE) in the past, and new data collected by the authors in February 2003.

i) Corps of Engineers data

Three surveys of different transects across the lake were conducted by the USACE; a topographic survey in 1959 before completion of the dam in 1963, a bathymetric survey in 1963 and another in 1973. Although the 1959 survey included several cross sections within the main pool of the reservoir, surveys from both 1963 and 1973 were available mostly for the upstream region of the main pool on the Tugaloo and Seneca Rivers. A map showing the transects surveyed by USACE is given in Figure 4. Projection, datum and mean water level data for the historical surveys are given in Table 1.

The historical surveys used the method of triangulation from known benchmarks. Concrete monuments at locations along the future shoreline were established and land was surveyed by creating a loop with level lines and turning points. The surveys were

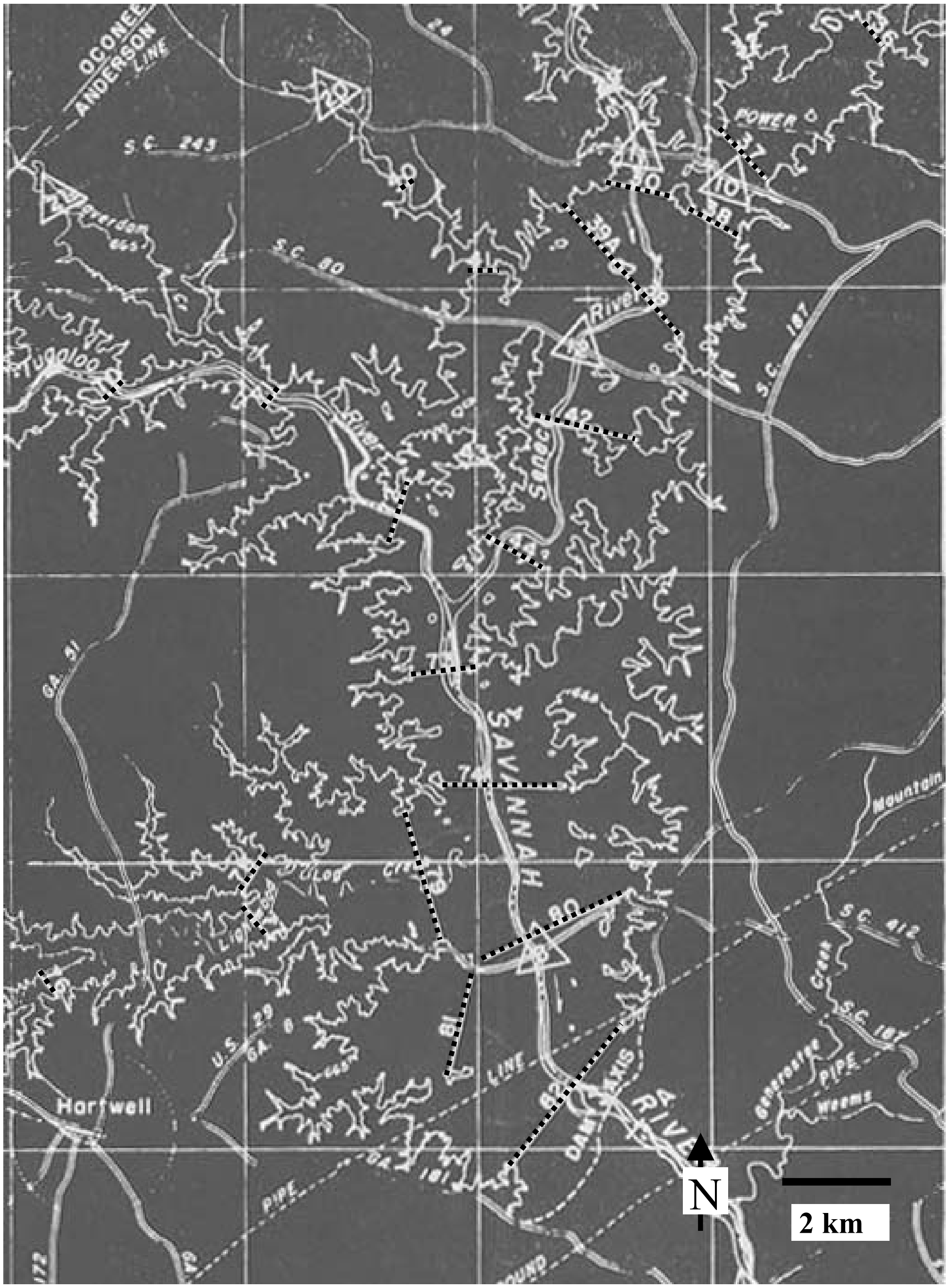

Figure 4. A map showing the transects surveyed by USACE (source: USACE, Savannah District).

Table 1. Projection, datum and mean water level data for the previous surveys.

Survey year	Mean water level	Datum	Projection
1959	-	1927 North American Datum	Plane Coordinate System based on Georgia East Zone and South Carolina North Zone
1963	200.59		
1973	201.06		

done with an accuracy of ±1.2 cm in the vertical (Jason Ward, USACE, Savannah District, pers. comm.).

The USACE provided the survey data in an analog, graphical format for each transect, with elevations plotted versus horizontal distance from the starting point of the transect. Transect 74 is shown in Figure 5 as an example. Locations of benchmarks were not precisely described. Other available transects are given in Appendix.

ArcView's Digitize extension was used for conversion of graphs to digital format. Digitizing errors are estimated as ±15 cm in vertical and ±1 m in horizontal prototype scale.

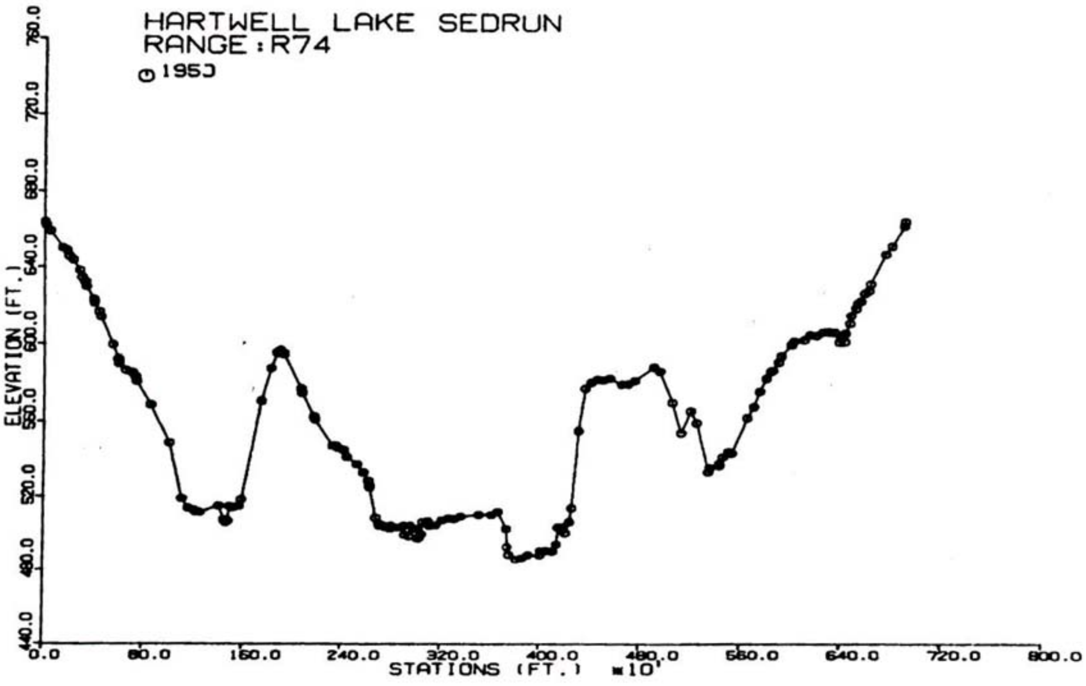

Figure 5. Bathymetric survey data from 1959 provided by USACE for transect 74.

ii) New data

A survey system shown in Figure 6 was used to collect hydrographic survey data. The survey system was mounted on a Boston Whaler 17 foot fiberglass boat. Depth data were provided by a dual frequency depth measuring system (high frequency 200 kHz, low frequency 30kHz), Digital Echo Sounder Ceestar, manufactured by Bruttour Int. Figure 7 shows the mounting of the depth sounder. Digital depth data were directly logged to a laptop computer equipped with Coastal Oceanographic's HYPACK Hydrographic Survey Software. Data were output and stored at a rate of 6 soundings / sec.

Figure 6. Boat used for data collection

.

Figure 7. Over the side mounting for dual frequency depth sounder.

Echo sounders in general determine the distance between a transducer, that converts electrical energy to sound, and dense objects such as fish or a seabed. An ultrasonic wave is transmitted through water, and as the sound wave strikes an object, it is reflected back toward the source and received by the transducer. The speed of the ultrasonic wave varies with temperature and is 1447 m/s for 10 °C fresh water. The depth of the object is then calculated by the time difference between transmission of sound wave and the reception of the reflected sound.

Dual frequency echo sounders are commonly employed in areas where soft sediments are present. High and low frequency transducers have different characteristics. High frequency transducers transmit a signal of 200 kHz and it is more directional with a smaller beam angle (Figure 8). Low frequency transducers transmit a signal of 30 kHz that penetrates to a greater depth with a wider beam angle covering a greater sea bottom area. However a sharper focus of the transmitted energy is achieved at higher frequencies. Low frequency depth measurement can be used only if the slope of the bottom is low and there are no structures nearby.

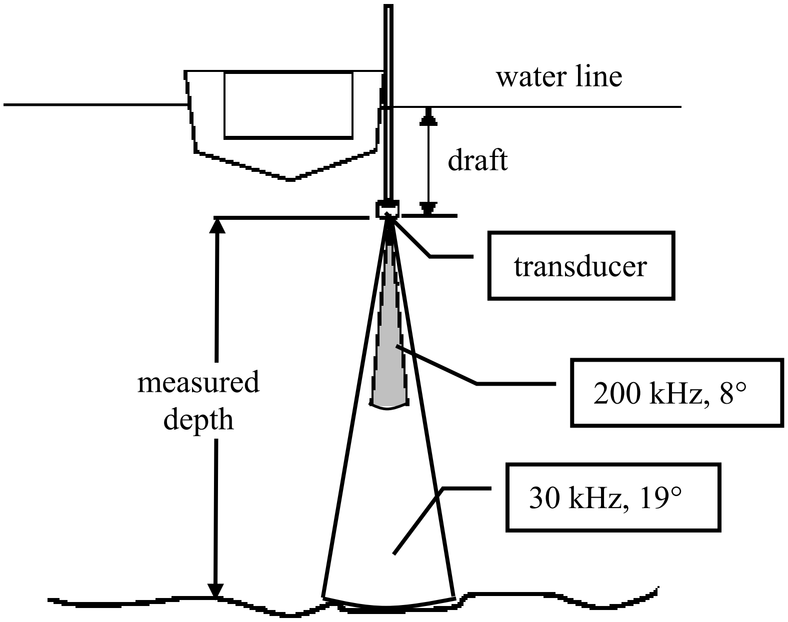

Figure 8. Representation of high and low frequency transducers (adapted from Bruttour, 2003).

The Corps of Engineers recommends that for bathymetric surveys, a horizontal positioning error should be less than 5 meters. Horizontal positional accuracy is not critical for a reservoir sedimentation survey (USACE, 2002).

The transects previously surveyed by USACE in the main pool of the reservoir were marked on the lake map provided by Mapsource software of Garmin (Figure 9). The coordinates of the two ends of transects were obtained using Mapsource software and were uploaded to the GPS as waypoints which were used to navigate during the surveys.

During the surveying of the transects shown on Figure 9, the draft for the high and low frequency transducers were 28 ± 1 cm and 20 ± 1 cm respectively. The measurements were then corrected to account for the draft. Another correction was made because of the projection and datum used in historical surveys was different then the current survey. Conversion of depth data measured using 1927 North American Datum (NAD 27) projected by the Plane Coordinate System to 1983 North American Datum (NAD 83) projected by the Universal Transverse Mercator (UTM) were made by Corpscon program provided by USACE.

The manufacturer’s rated accuracy for the depth sounder is 0.01 meter, however the prior measurements during the testing of the equipment indicated 0.10 meter accuracy. The sources of errors in old and current surveys add up to ± 27 cm and are summarized in Table 2.

Table 2. The error sources in old and current surveys.

Source	Magnitude
Depth measurement errors	± 10 cm
Draft measurement errors	± 1 cm
Errors in old survey	± 1.2 cm
Digitizing errors	± 15 cm

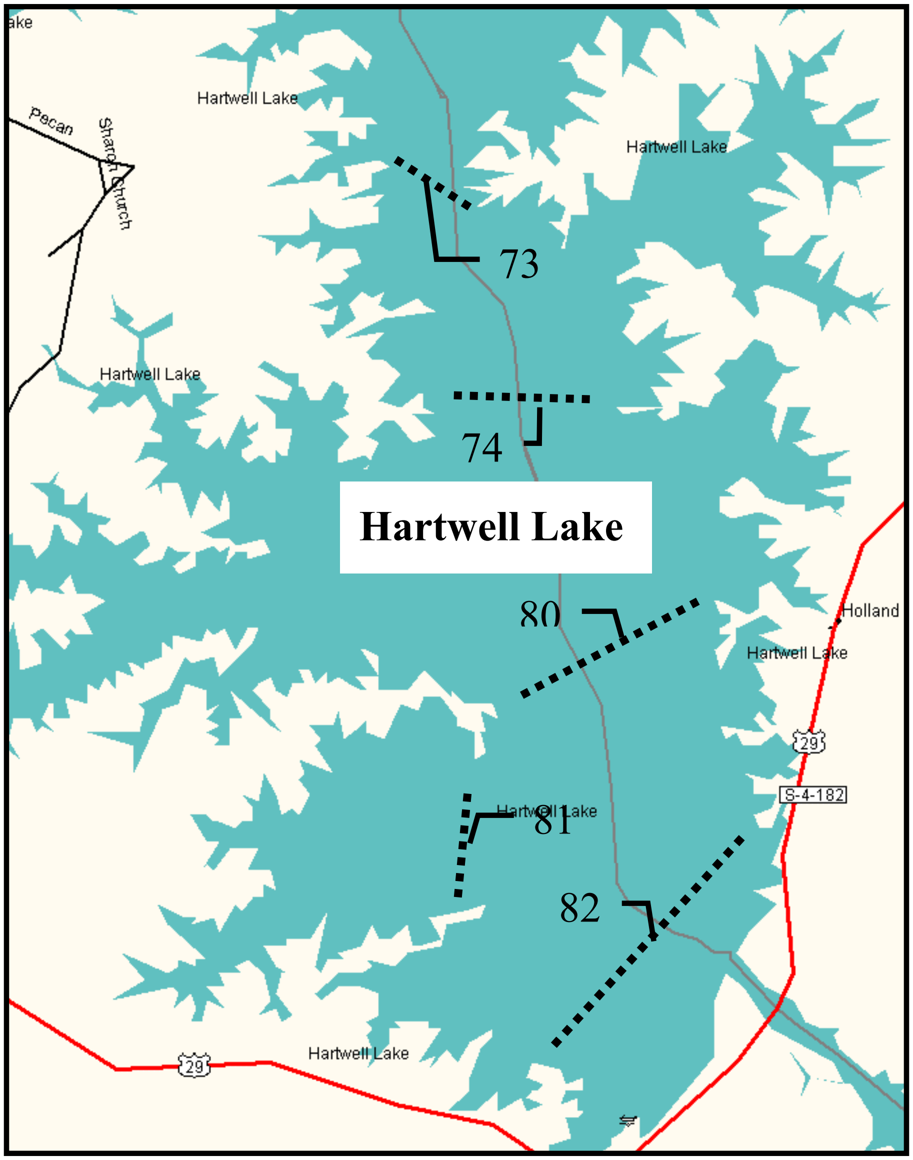

Figure 9. Transects surveyed in Hartwell Lake.

3.2. Velocity Data

Velocity measurements are made using a 1200 kHz Workhorse Sentinel Acoustic Doppler Current Profiler (ADCP) developed by RD Instruments (Figure 10). It is designed for measuring real time current profiles in ocean, near shore, harbors and lake regions. An ADCP estimates horizontal and vertical velocity as a function of depth by using the Doppler effect to measure the relative velocity between the instrument and scatterers in the ocean. The Doppler effect is a change in the observed sound frequency that results from relative motion toward or away from the sound source.

Measurement of velocities by the ADCP is described in the user's manual as follows: "An ADCP utilizes the Doppler effect by transmitting sound at a fixed frequency and listening to echoes returning from sound scatterers in the water. These sound scatterers are small particles or plankton that reflect the sound back to the ADCP. Three acoustic beams in different directions are the minimal requirement for measuring the three velocity components. A fourth beam adds redundancy and an error estimate. The ADCP

Figure 10. Over the side mounting for ADCP.

transmits a ping from each transducer element roughly once per second. The echo arrives back at the instrument over an extended period, with echoes from shallow depths arriving sooner than those from greater distances. Profiles are produced by range-gating the echo signal, which means the echo is broken into successive segments called depth bins corresponding to successively deeper depth ranges. The operator configures the length of each depth bin and the transmit pulse, which determines the degree of averaging in the vertical, depending on whether one is interested more in vertical resolution or profile penetration. The noisy velocity estimates from each ping are vector-averaged into user specified ensembles." For specifics of the instrument capabilities and configuration options the reader is referred to the user's manual (RD Instruments, 2001).

The navigation information provided by a Global Positioning System (GPS) receiver is integrated and used to obtain the relative velocities to the earth's reference frame. Data are averaged to reduce the measurement uncertainty. Velocity uncertainty includes two kinds of errors: random error and bias. Averaging reduces random error. The size of the random error depends on ADCP frequency, depth cell size, number of pings averaged, and beam geometry. External factors such as turbulence, internal waves and ADCP motion also influence error. Bias error depends on temperature, mean current speed, signal/noise ratio, and beam geometry.

For quantification of this bias error several tests were performed in a 2.5 meter deep swimming pool prior to the field trip. The ADCP was placed in the middle of the pool bottom looking upwards. The pump of the pool was turned on and off so that the velocity magnitude and direction uncertainty could be investigated. Data were averaged every 10 minutes. Depth of each cell (bin) was selected as 10 cm. Figure 11 shows the measured velocity magnitude plotted versus ensemble for bin numbers 5 and 10, corresponding to 1.16 m and 1.66 m depths. Figure 12 shows the measured direction of the currents plotted versus ensemble. The pump was turned off after 30 minutes and turned on again after 460 minutes. When the water was turned off the average noise levels observed were 1.4 cm/s at 1.16 m water depth, and 1.2 cm/s at 1.66 m water depth. The noise level of the ADCP

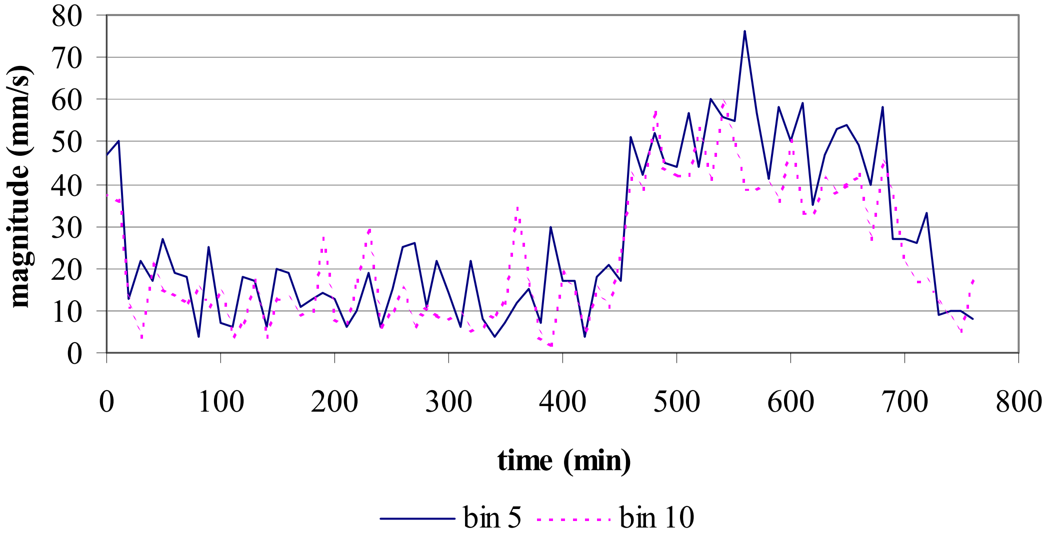

Figure 11. Measured velocity magnitude during pool tests.

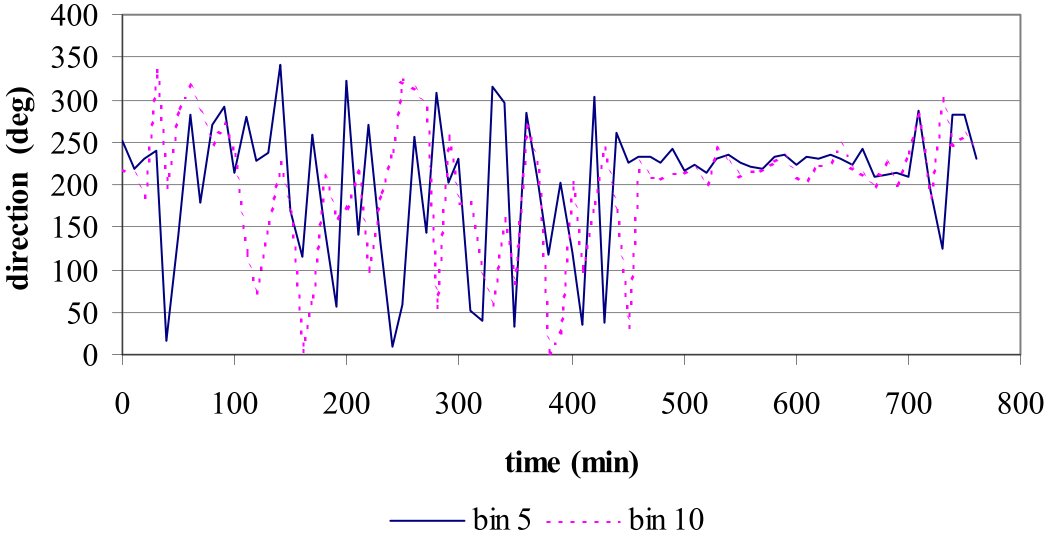

Figure 12. Measured velocity direction during pool tests.

is determined as ± 1.4 cm/s based on the pool tests.

During the collection of data in Hartwell Lake, velocity data were collected in self-contained deployment, and stored internally every 30 seconds with a bin size of 1 meter. The velocities had to be corrected for boat speed since the measurements were made while the boat was moving.

There are two options for correcting boat speed during the measurements: i) bottom-track, ii) GPS options. The primary function of bottom-track is to measure the ADCP's speed-over-bottom and detected range-to-bottom. The absolute water velocity is calculated by subtracting the boat's velocity from the relative velocity measured by the ADCP, where the cross-sectional area of the transect has to be estimated for the discharge calculation. However when the bottom is out of range or if there is a very heavy layer of suspended sediment moving along with the flow, the ADCP can falsely detect the bottom in the moving suspended sediment layer, resulting in biased measurements.

In both cases, it is necessary to have an external means for estimating the boat's velocity. GPS is used to estimate the boat's velocity while underway. During the velocity measurements in Hartwell Lake, the velocities are corrected for boat speed according to the GPS.

The errors associated with the GPS were quantified with a simple test. The GPS was left to record coordinates at a fixed location for 20 minutes, and the recorded coordinates are plotted. The average horizontal error was 1 m and the errors evolved gradually, between two consequent recordings errors were lower than the average (Figure 13). In other words errors were biased in time, decreasing the uncertainty in boat speed. This observation suggests that when the boat moves with 3.3 m/s speed in 30 seconds it covers

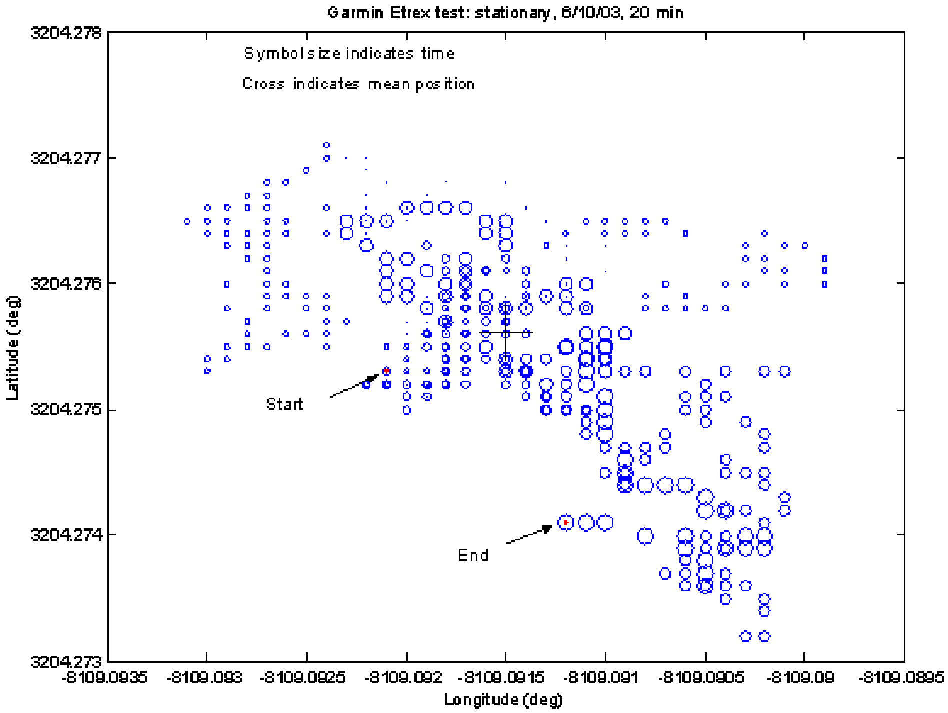

Figure 13. Evolution of Garmin Etrex errors at a fixed location. Symbol size indicates time.

100 m of distance. An average of 1 m of error between two readings causes ± 6 cm/s error in boat and water current speed.

The instrument configuration used for the velocity measurements is given in Table 3. Some of the configuration details can be summarized as follows: WF blanks out bad data close to the transducer head. WN sets the number of depth cells over which the Workhorse collects data. TP sets the minimum time between pings. It was set to 20 (hundredths of seconds). WP sets the number of pings to average in each data ensemble. WP = 150 corresponds to averaging time of 30 seconds. WL is used to lower the effects of transducer motion by averaging the velocities of a column of water and subtracting the average velocity from each of the depth cell velocities. WM selects the application – dependent profiling mode used by the ADCP. Dynamic sea state mode was selected for this application. EA is a heading alignment angle and it corrects for physical misalignment between Beam 3 and the heading reference. EB is the heading angle that counteracts the electrical bias and it corrects electrical/magnetic bias between ADCP heading value and the heading reference. EX sets the coordinate transformation. Earth coordinates were selected, however for the coordinate transformation to work properly, heading alignment and heading bias must be set correctly. Since they were not set properly correction for the velocity data direction was required. EZ selects the source of environmental sensor data. It was selected that ADCP uses data from appropriate sensor.

Table 3. Configuration of ADCP used for data collection.

Orientation	Down
Beam Angle	20 Degrees
Blank (WF)	0.44 m
Min Pgood (WG)	0
Ref Layer (WL)	1, 5 first bin, last bin
Mode (WM)	1
Bins (WN)	17
Pings/Ens (WP)	150 (30 seconds)
Bin Size (WS)	1 m
Head Align (EA)	0.00 degrees
Head Bias (EB)	0.00 degrees
Coordinate Transformation (EX)	11111
Sensor Source (EZ)	1111111
Time/Ping (TP)	00:00.20

Correction is required to account for the discrepancy between true north and magnetic north. True north is defined by the axis of rotation of the earth. Magnetic north, at the other hand, is defined by the earth's magnetism caused by the flow of electrons in its fluid metallic core in motion. The earth's magnetic poles are mobile and therefore magnetic north varies over time, as well as from place to place, on earth. The ADCP uses the compass to determine magnetic heading, and GPS uses true north. For the duration of the field trip, and location of Hartwell Lake this difference was - 5 degrees and 22 minutes (Figure 14). The velocities were corrected by adding this difference to direction.

Due to the rough weather conditions during the period of field trip, successful measurements were mostly made on the west side of the lake. The transects where the velocities were measured are shown in Figure 15.

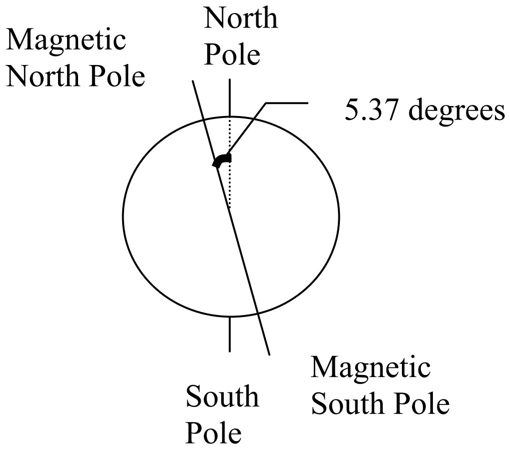

Figure 14. Representation of true north with respect to magnetic north on February 12th 2003, at Hartwell Lake.

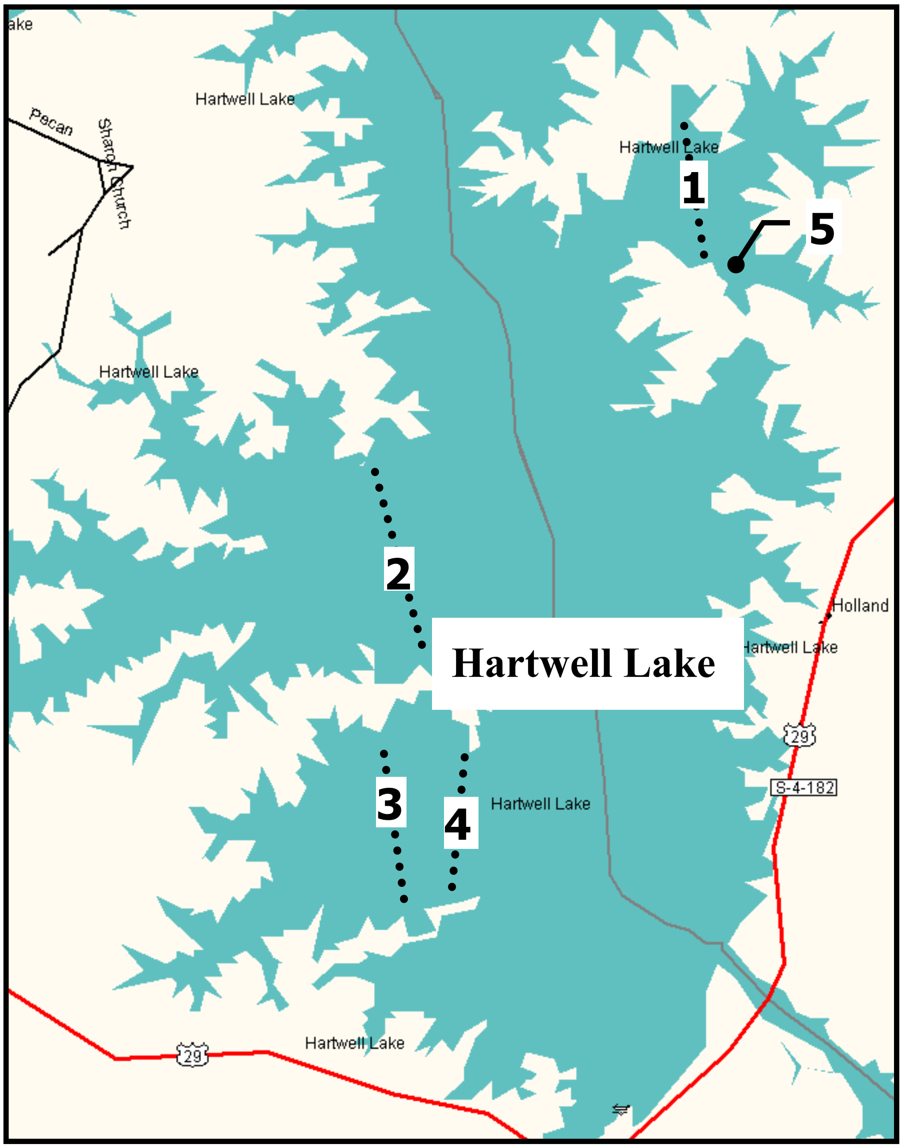

Figure 15. Transects where the current velocity vectors are measured by ADCP.

3.3. Shoreline Position Data

Horizontal positioning data defining shoreline positions were supplied using an Ashtech Z-12 model differential global positioning system (GPS). This instrument was developed for geodesy, surveying and precise navigation applications and tracks up to 12 satellites**.** This system utilizes the GPS measurement data from a stationary GPS receiver at a known site (base station) to correct for errors in the measurement data of a GPS receiver at an unknown site (remote station). For real time differential measurement, the data are transferred from the base station to rover station via a radio link. Precision is documented as ±(5mm + 1ppm) for static GPS**,** ±(10mm + 1ppm) for kinematic GPS**,** and cm-dm accuracies for baselines <100km for kinematic (resolved ambiguities). GPS accuracy depends on many factors, with the primary errors being due to satellite related errors, receiver related errors, and signal propagation errors (Work et al. 1998).

The base station was set at a National Geodetic Survey monumented benchmark located at Sadlers Creek State Park, in Anderson County, SC (Table 4, Figure 16).

Table 4. Details of benchmark used for base station.

Name, Designation	ED3754, Sadlers Creek
Coordinates	N 34 25.633 W 82 49.859
Altitude	211.53 m

Figure 16. Base station set up at Sadlers Creek State Park.

The Sadlers Creek and Longpoint Peninsulas shown in Figure 17 were surveyed. These two locations were selected since they are exposed to greater fetches which would likely result in greater erosion problems. In fact during the survey of the peninsulas it was observed that most of the shores along both peninsulas are protected by erosion control structures such as ripraps and revetments.

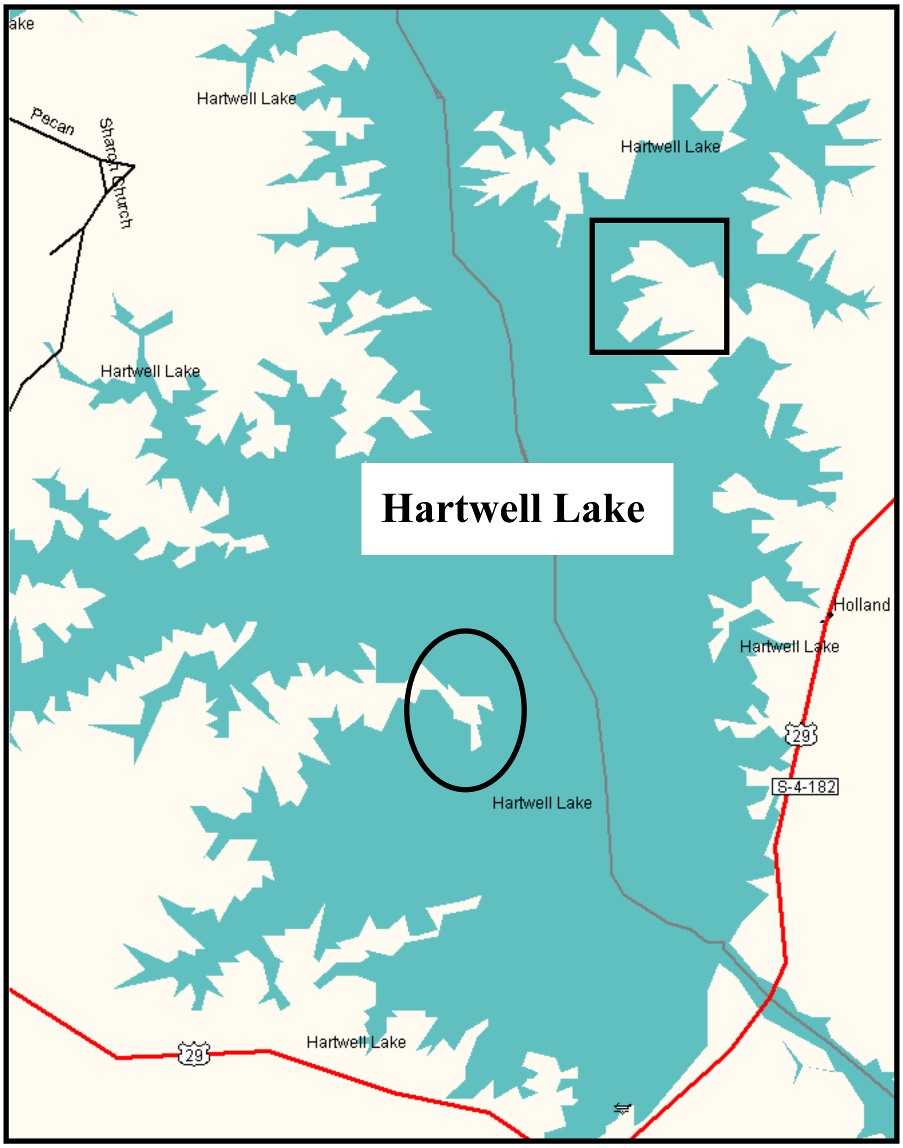

Figure 17. Peninsulas surveyed along the shores of Hartwell Lake. Sadler Creek Peninsula is shown by the rectangle, Longpoint Peninsula is shown by the ellipse.

4. Data Analysis

This section of the report discusses the analysis of the bathymetry, velocity and shoreline data. The bathymetry data are compared to the available data from historical surveys. The velocity data are analyzed and presented. The shoreline data are also presented in this section.

4.1. Comparison of Bathymetric Data to Historical Surveys

The new survey data were compared with the historical surveys after the old data were adjusted so that both data sets have the same datum and projection. Also new data sets were corrected for draft. When the data from the high and low frequency transducers were compared, the two results were generally in agreement, except in regions where strong slopes were present. All of the data presented in this section use the 1983 North American Datum (NAD 83) projected by the Universal Transverse Mercator (UTM). The 2003 data plotted in the graphs of this section are from higher frequency depth sounder if otherwise is not stated.

Figure 18 compares the survey results at transect 73. Focusing on the thalweg, up to 1.8 ± 0.27 m of deposition are observed (Figure 19). The estimated uncertainty (± 0.27 m) includes potential errors due to digitizing, draft measurement, errors in the old survey, and depth measurement as discussed in section 3.1. A topographic map of transect 73 is shown in Figure 20. Since the detailed coordinates of transects surveyed in 1959 were not provided, exactly same routes of the historical surveys could not be followed at all transects. This is tolerable since the purpose of this study is to investigate where and at what rate the deposition mostly occurred.

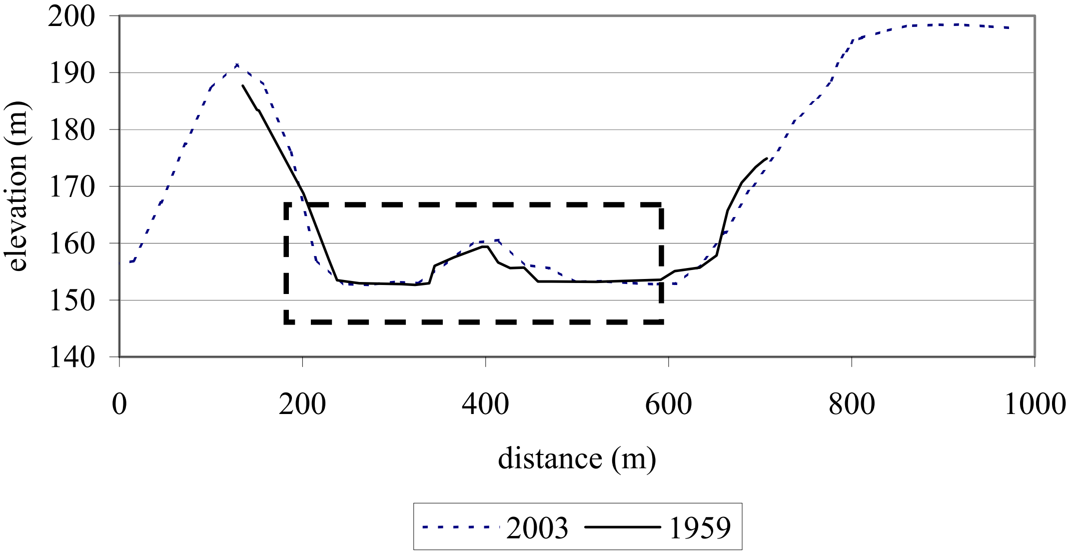

Figure 18. Comparison of survey results at transect 73, with the results of historical survey conducted in 1959. $X = 0$ corresponds to the west end of the transect. Dashed box shows the thalweg of the lake.

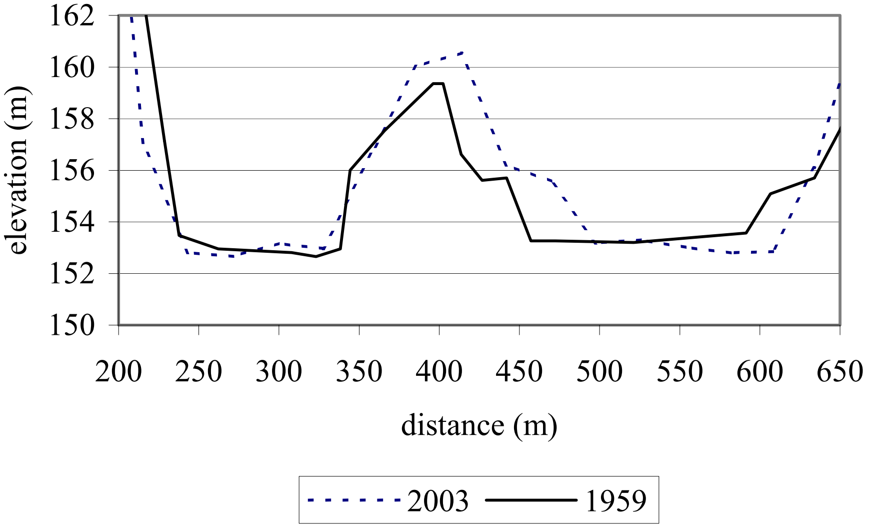

Figure 19. Comparison of survey results within the region shown by the dashed box in Figure 18 with the results of historical survey conducted in 1959.

A resurvey of transect 73 with a different route (shown by 73b in Figure 20) indicated that deviating from the route did not introduce significant errors to the thalweg elevation estimates. The survey results from two different routes are compared in Figure 21.

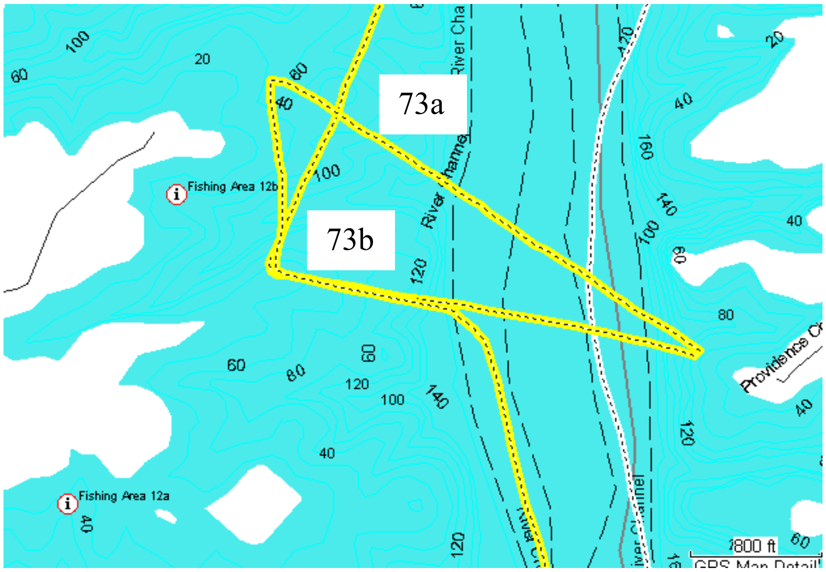

Figure 20. Topography map for transect 73.

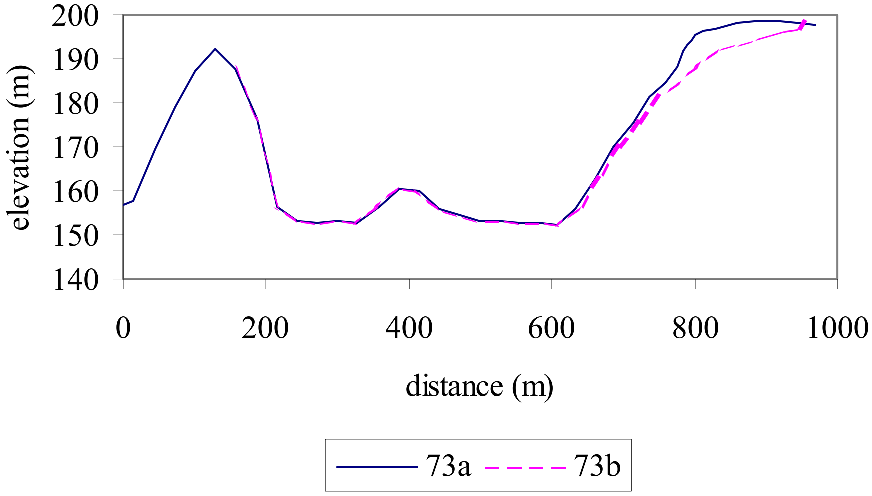

Figure 21. Comparison of surveying results from two different routes shown in Figure 20. $X = 0$ corresponds to the west end of the transect.

Figure 22 compares survey results at transect 74. Within the thalweg, 2 ± 0.27 m of deposition are observed in the deeper regions (Figure 23a). A dashed line is drawn on the topographic map to represent the probable route taken by the surveyors in 1959 (Figure 23b).

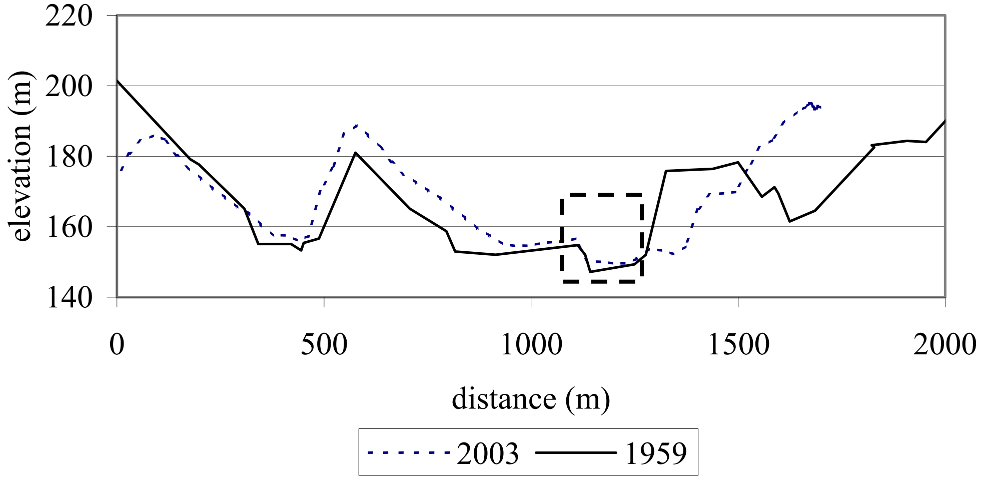

Figure 22. Comparison of survey results at transect 74, with the results of historical survey conducted in 1959. $X = 0$ corresponds to the east end of the transect. Dashed box shows the thalweg of the lake.

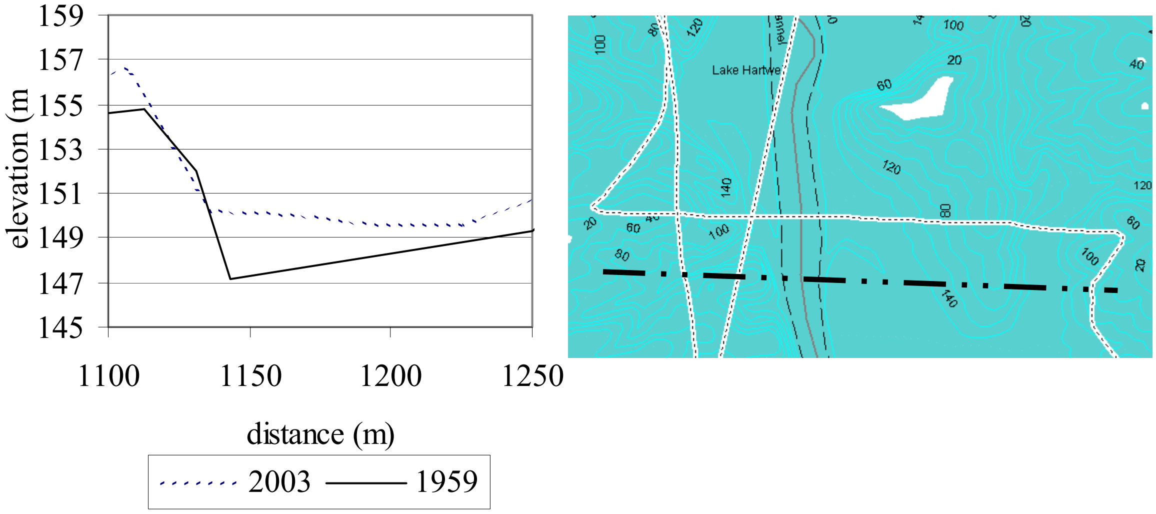

Figure 23. a) Details of survey results shown by dashed line at Figure 22. b) Topography map at transect 74. Dashed line represents the possible route taken in 1959.

Survey results for transect 80 are shown in Figure 24. Similarly, 2 ± 0.27 m of deposition is observed in the thalweg. Details of the survey are given in Figure 25a. The discrepancy between the two surveys at $x =$ 2500 m can be explained by the hill marked by a dashed circle in Figure 25b.

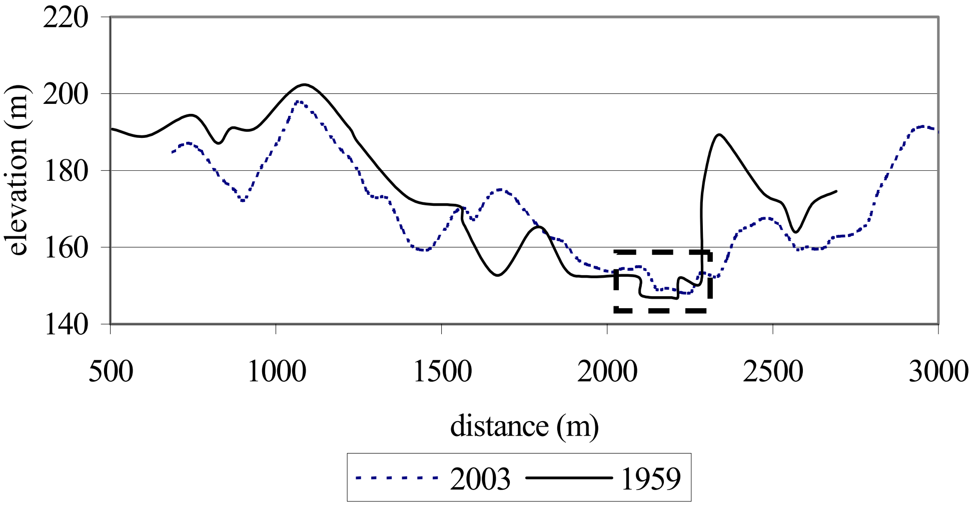

Figure 24. Comparison of survey results at transect 80, with the results of the historical survey conducted in 1959. $X = 0$ corresponds to the east end of the transect. Dashed box shows the thalweg of the lake.

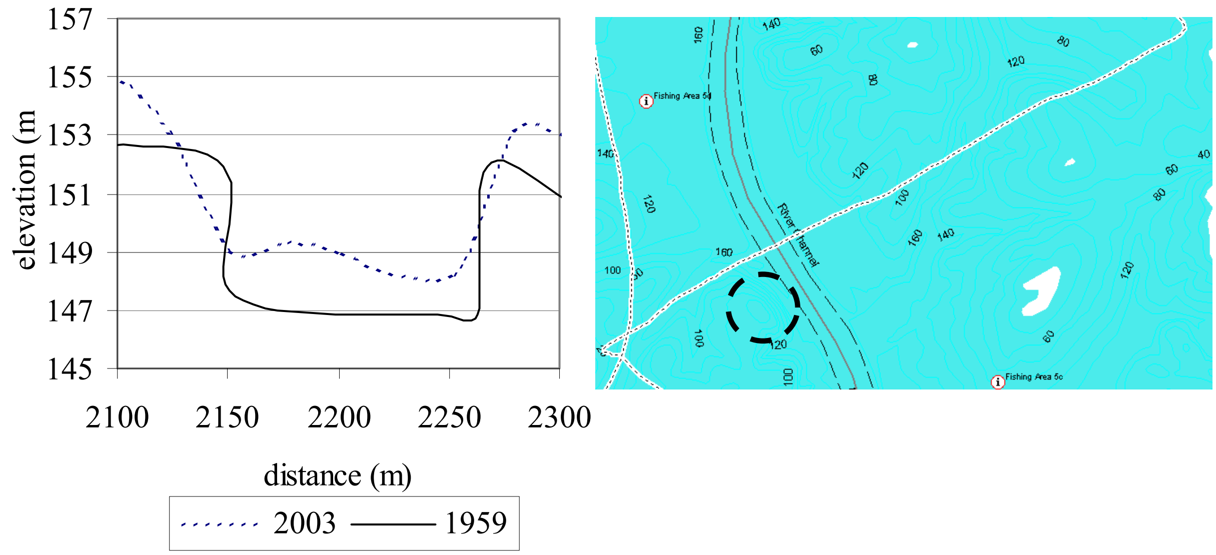

Figure 25. a) Details of survey results shown by dashed line at Figure 24. b) Topography map at transect 80. Dashed eclipse shows the hill that might cause the discrepancy at $x =$ 2500 m.

Transect 81 is the only resurveyed transect that does not pass through the thalweg. The comparison of results with the previous surveys indicated no significant deposition (Figure 26). Details of the deepest region are given in Figure 27a. The differences in the shallow region of the transect ($x \leq$ 1000 m) can be explained by a slight deviation from the route followed by the old survey (see Figure 27b).

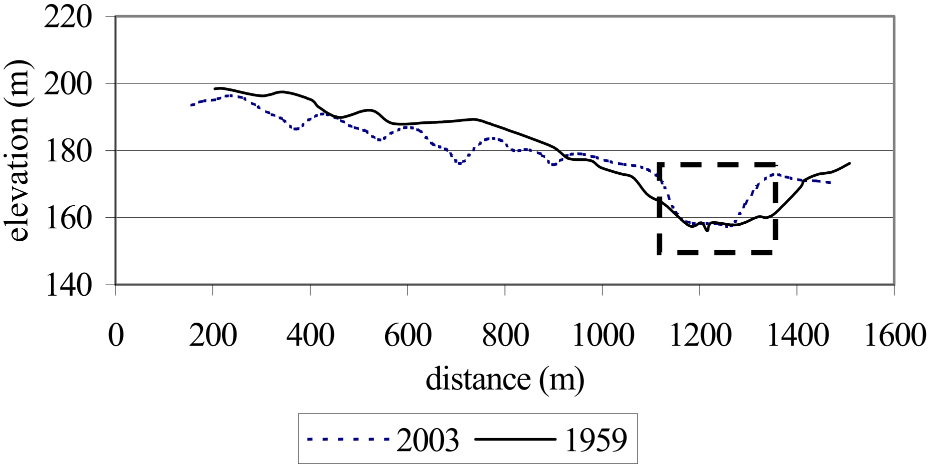

Figure 26. Comparison of survey results at transect 81, with the results of historical survey conducted in 1959. $X = 0$ corresponds to the north end of the transect. Dashed box shows the deepest region of the transect.

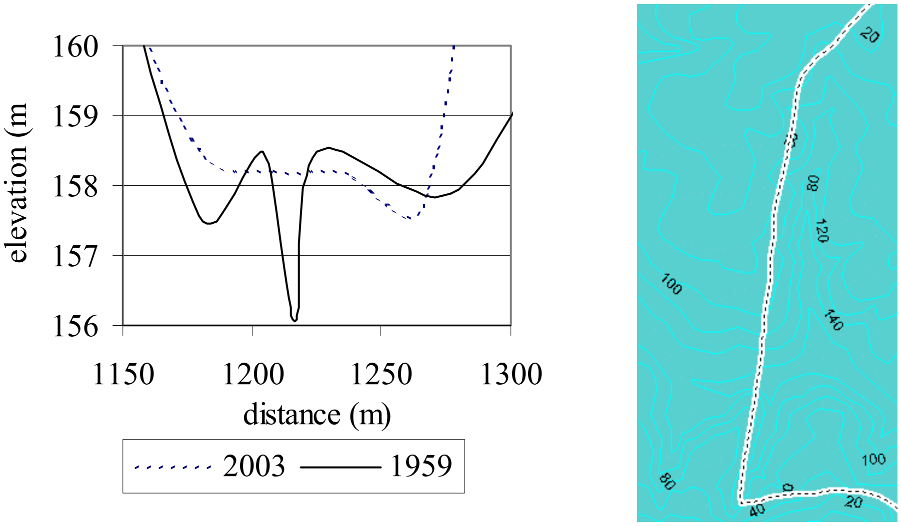

Figure 27. a) Details of survey results shown by dashed line at Figure 26. b) Topography map at transect 81.

Figure 28 shows the comparison of survey results with the previous survey for transect 82. Deposition of 2 ± 0.27 m is observed in the thalweg. Details of the thalweg are given in Figure 29.

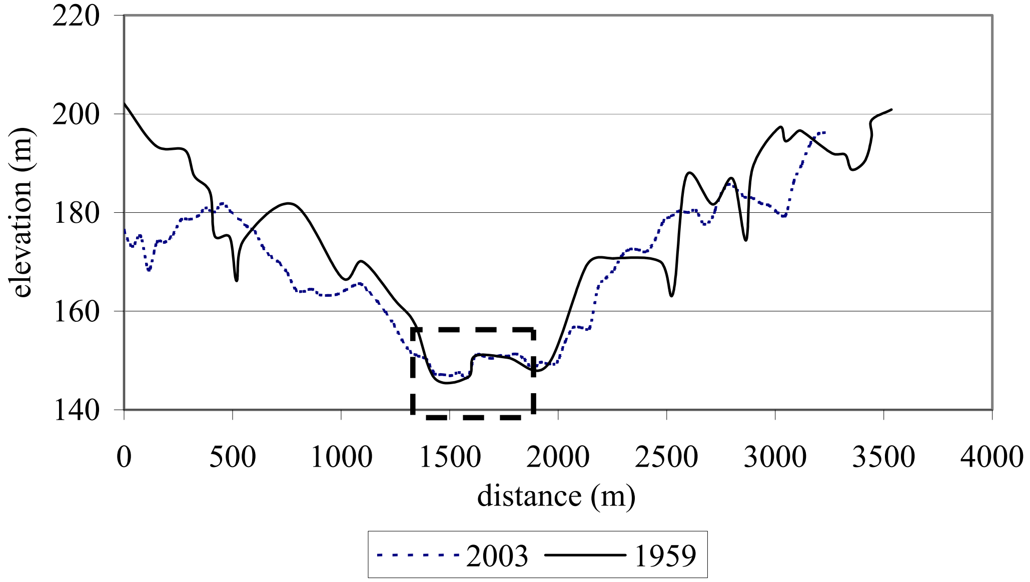

Figure 28. Comparison of survey results at transect 82, with the results of historical survey conducted in 1959. Dashed box shows the thalweg of the lake.

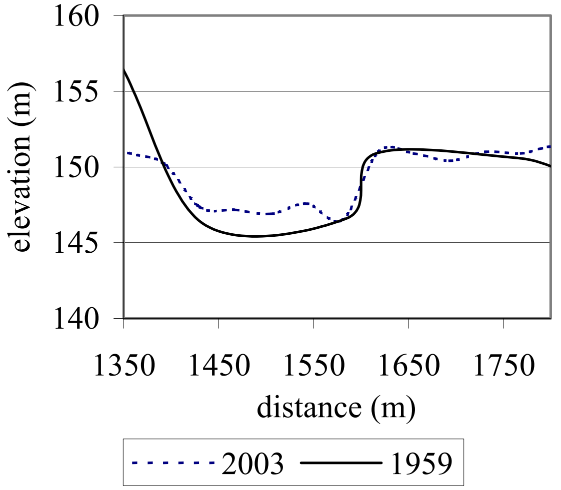

Figure 29. Details of survey results shown by dashed line at Figure 28.

4.2. Analysis of Velocity Data

Velocities at selected transects in Hartwell Lake shown in Figure 15 were measured using the ADCP with GPS speed corrections. During the measurements strong winds from the southwest were observed. Boat speed was maintained near 2.5 m/s.

Figure 30 shows the near-surface velocity vectors measured at transect 1 after correction for boat speed. At this transect maximum surface velocities were measured as 25 cm/s. The measured velocities were filtered to discard measurements for which error velocities exceeded 5 cm/s. Figure 31 shows the measured velocity profile for the same transect before the filtering process. Velocity profiles showing east, north and error velocities captured at an ensemble are given in Figure 32.

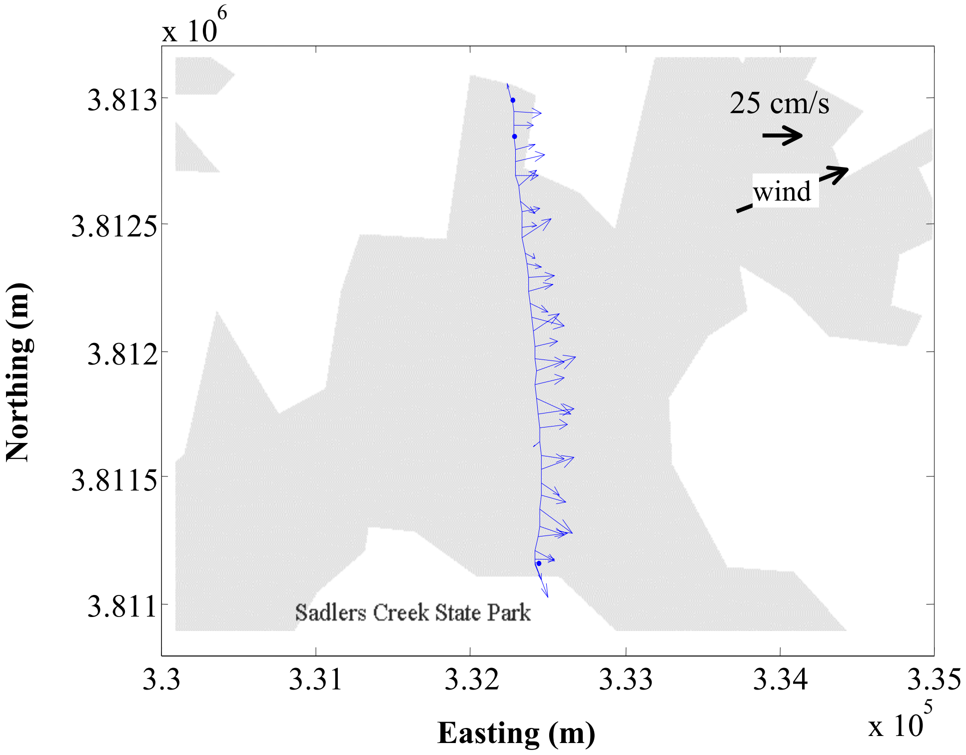

Figure 30. Near-surface velocity vectors measured at transect #1 shown in Figure 15.

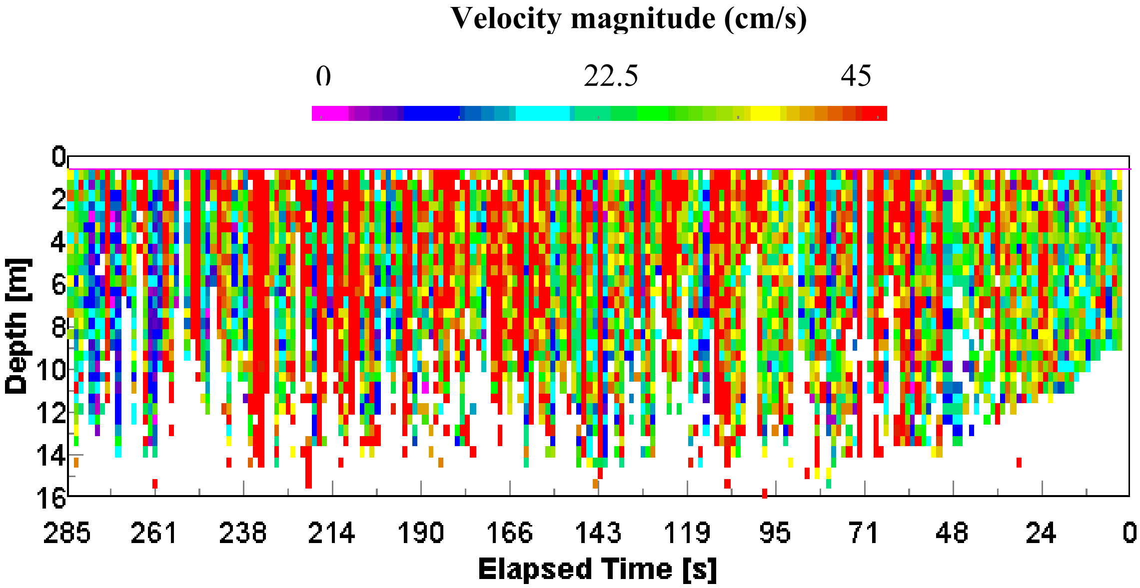

Figure 31. Measured velocity profiles for transect#1.

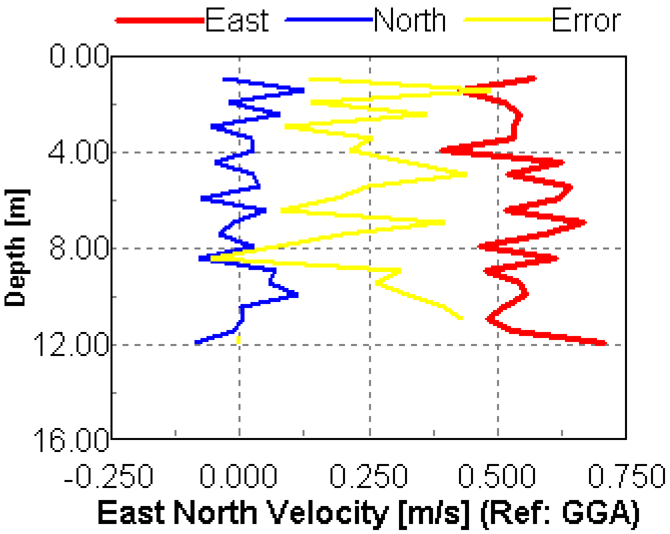

Figure 32. Measured velocity profiles showing east, north and error velocities at an ensemble (*time* = 209 seconds) for transect#1.

Measured near-surface velocities at the other three transects (#2, #3, and #4) are shown in Figures 33, 34 and 35 respectively. In all three cases, maximum measured velocities are ~50 cm/s and average velocities are ~25 cm/s. One rule of thumb for wind-driven currents in open water is 3% of wind speed. During the field measurement period wind was blowing from the southwest at ~10 m/s magnitude, which gives roughly 30 cm/s of surface currents in agreement with the measurements.

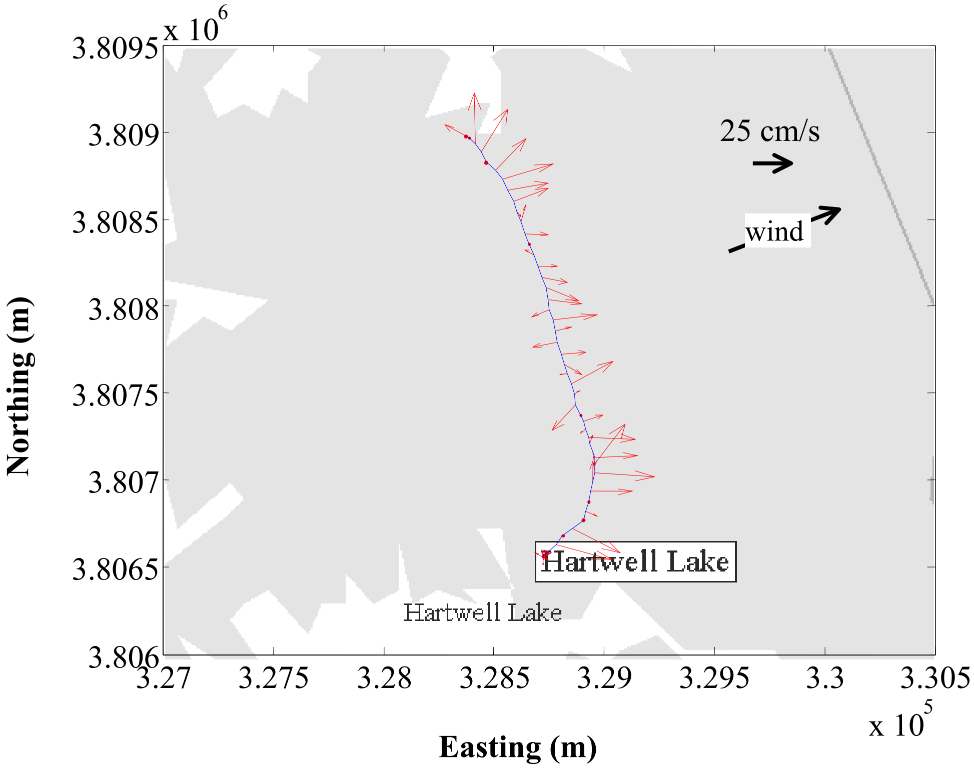

Figure 33. Near-surface velocity vectors measured at transect #2 shown in Figure 15.

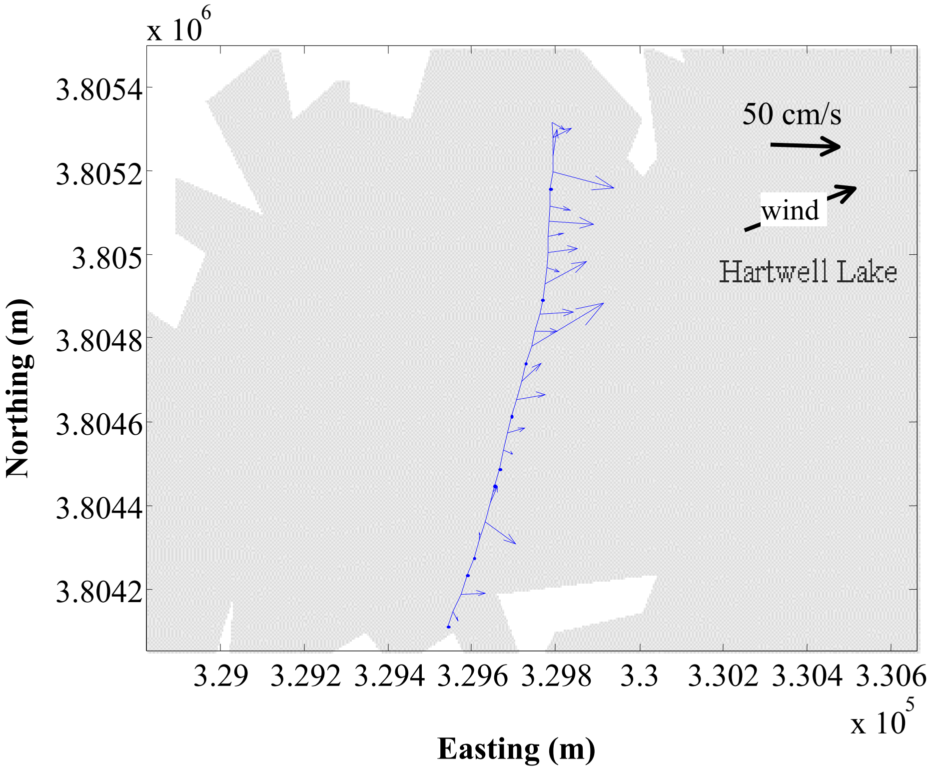

Figure 34. Near-surface velocity vectors measured at transect #3 shown in Figure 15.

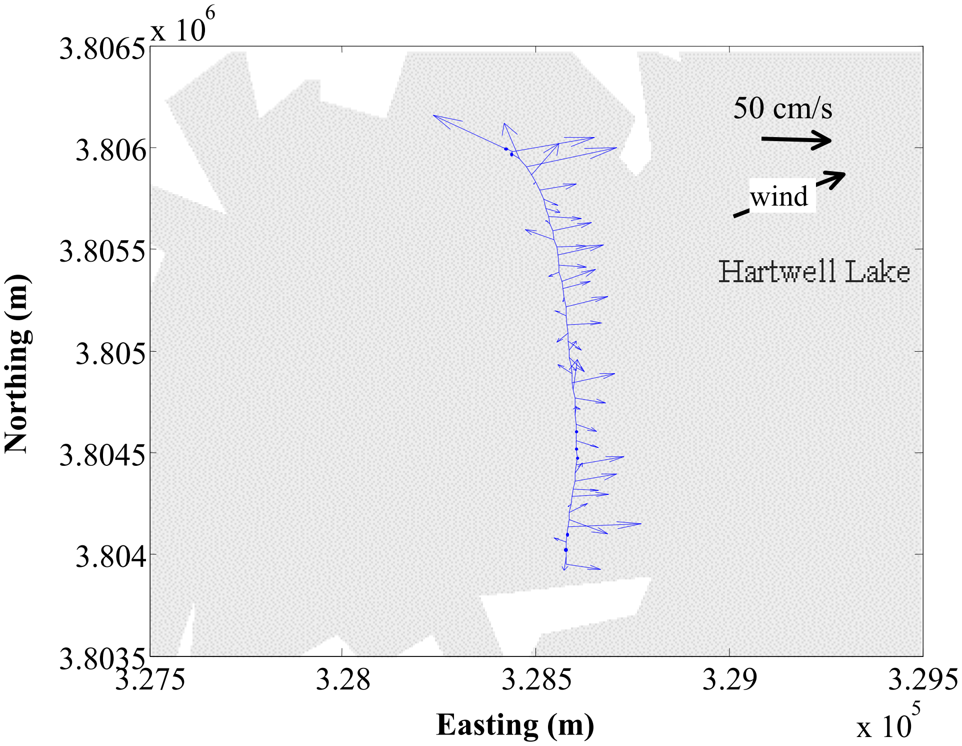

Figure 35. Near-surface velocity vectors measured at transect #4 shown in Figure 15.

Point measurements of velocities were also made at a location shown by (5) in Figure 15. The boat was anchored during the measurement period. Point 5 is located behind Sadler's Creek peninsula and has a small fetch of ~ 500 meters (one tenth of the others). The measured east and north velocities are thus much smaller (about three tenth of the average) than the measured velocities at the four other transects (Figure 36).

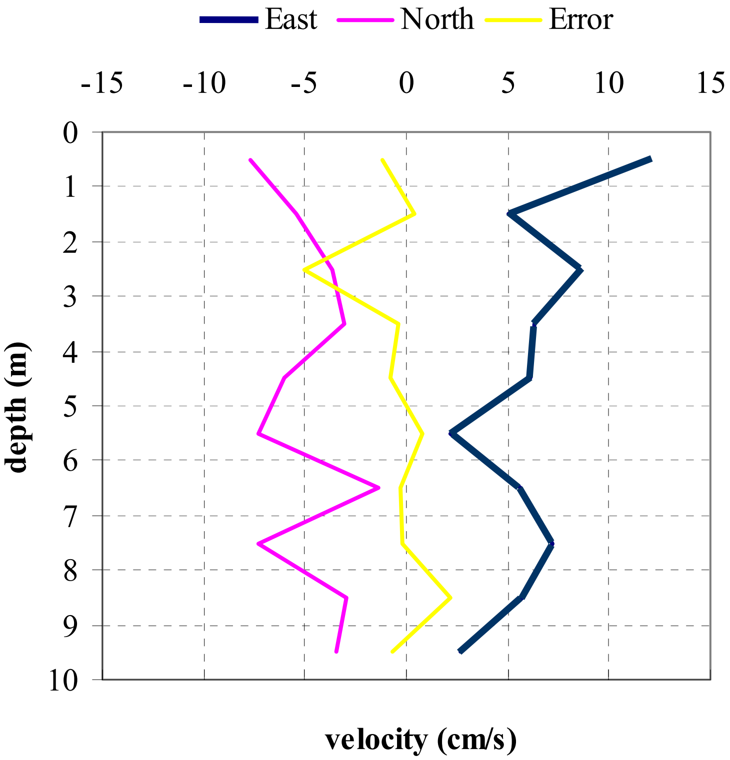

Figure 36. Measured velocity profiles showing east, north and error velocities at point #5 shown in Figure 15.

4.3. Analysis of Shoreline Data

The two peninsulas along the shores of Hartwell Lake, Sadlers Creek and Longpoint Peninsulas, shown in Figure 17 are surveyed. Figure 37 shows the horizontal coordinates of the survey plotted on an aerial photo of the Sadlers Creek Peninsula. The photo was taken on February 25th 1994, and each pixel in the images represents 1 meter × 1 meter of earth. The survey was conducted on February 14th 2003. The mean water levels on both days are given in Table 5. During the surveys both the high water line which is determined where the color changes between the wetted beach and the dry beach, and the low water line, where the shore meets the waters of the lake were followed. Figure 38 shows the 3D geometry of the peninsula. Similarly, horizontal coordinates on an aerial photo of Longpoint Peninsula and 3D geometry of the peninsula are given in Figures 39 and 40 respectively.

Table 5. Comparison of mean water levels during the survey period with the date on which digital aerial photo was taken.

Data	Date	Mean water level
Aerial photo	2/25/94	199.63
Survey	2/14/2003	199.33

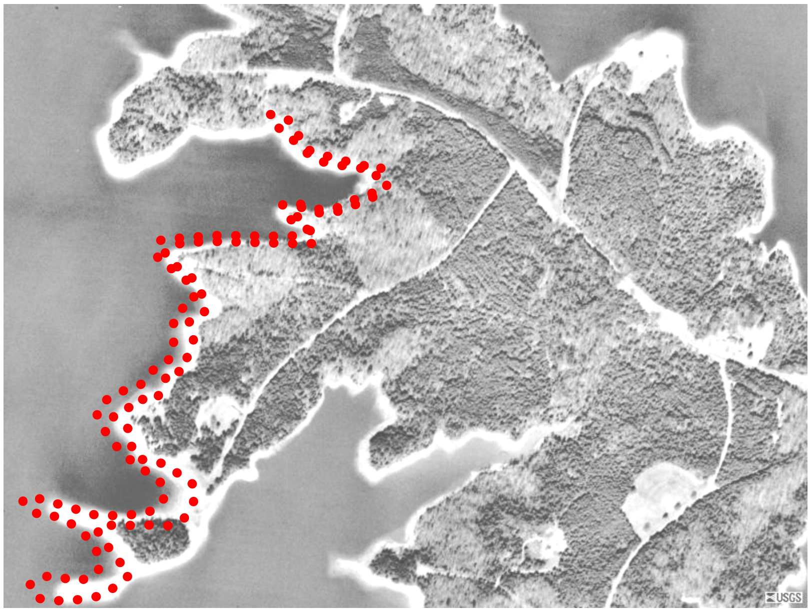

Figure 37. The surveyed transect shown on aerial photo of the Sadlers Creek Peninsula.

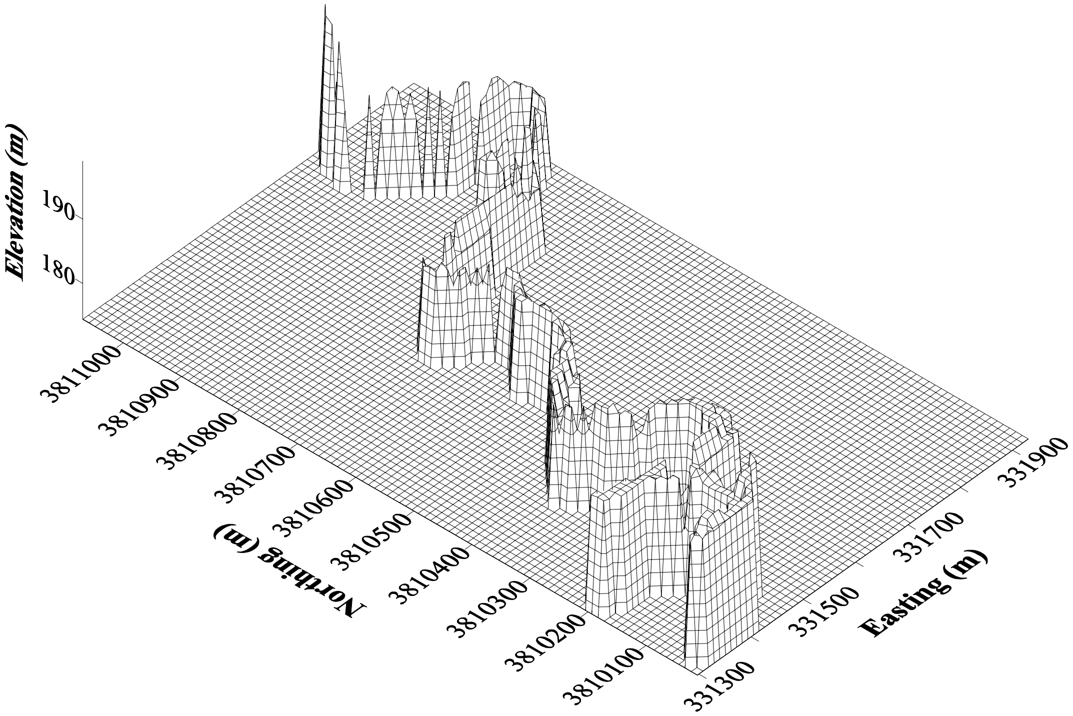

Figure 38. 3D view of the survey results on Sadlers Creek Peninsula.

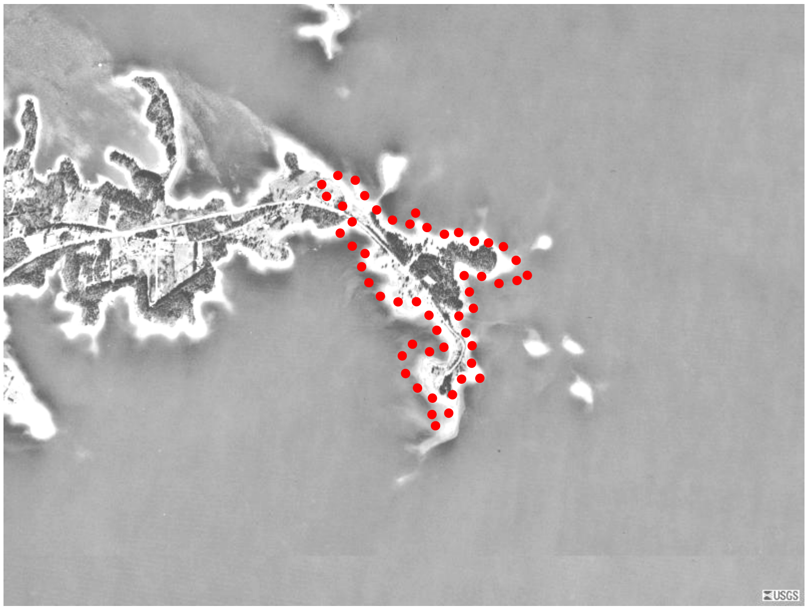

Figure 39. The surveyed transect shown on aerial photo of the Longpoint Peninsula.

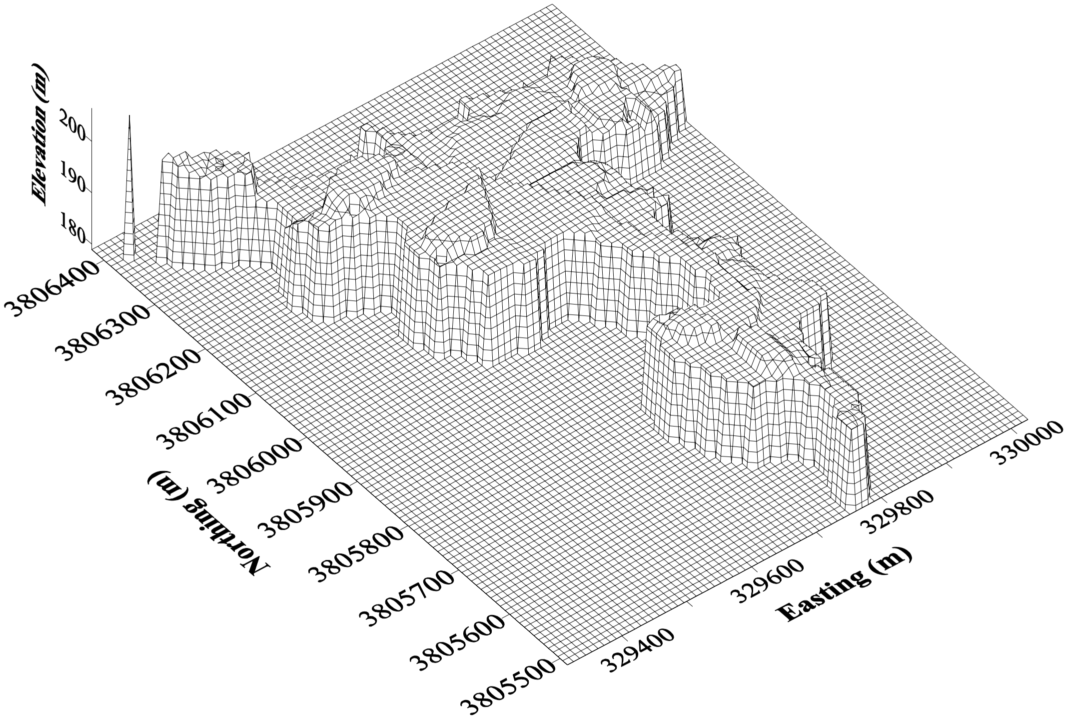

Figure 40. 3D view of the survey results on Longpoint Peninsula.

5. Conclusions

Field data are necessary to provide data for numerical modeling studies and for validation of the results. This report discusses the techniques for data collection in Hartwell Lake and presents the analyzed data. Three types of data were collected in Hartwell Lake between February 10th and February 13th, 2003: bathymetry, velocity and shoreline position data. . Depth data were collected using a dual frequency depth measuring system. Velocity data were measured using a 1200 kHz Acoustic Doppler Current Profiler (ADCP), and shoreline data were provided by a differential global positioning system (GPS). During the bathymetric surveys and velocity measurements a handheld GPS was also integrated with the devices for navigation.

Comparison of bathymetric surveys to previous surveys provided by USACE indicated approximately 2 ± 0.27 meters of deposition over 40 years within the thalweg. The uncertainty arises due to errors in historical surveys, digitizing errors, draft measurement and depth measurement errors. Another main source of error is due to the different routes followed by the authors and the surveyors from USACE. Since the coordinates of old surveys were not available to the authors, exact routes could not be followed. However the interest of the project is deposition at the thalweg, therefore errors due to the deviation from the route are acceptable.

Strong winds (more than 4 times the historical average) from the southwest were observed during the measurement period. Maximum measured surface velocities at several transects were ~50 cm/s and average velocities were ~25 cm/s. The main source of error in measured velocities was due to the boat speed, which calculated by handheld GPS. A ± 6 cm/s error in boat speed thus in water current speed is estimated.

Shoreline data collected at two selected peninsulas are also discussed in this report. The main source of error in the surveys is the precision of GPS (± 10mm).

The data collection techniques and analyzed data for Hartwell Lake are presented in this report. Future work will include simulation of climate and flow conditions in Hartwell Lake for the period of field trip and validation of model results with the measured values. Also, application of the shoreline erosion methodology to the surveyed peninsulas is planned.

6. References

Bruttour, 2003. *Ceestar User Guide for Dual Frequency Digital Survey Echo Sounder*, published by Bruttour International.

Elci, S. and Work, P.A., 2002. Prediction of shoreline erosion and sedimentation in Hartwell Lake, SC/GA. *Technical Report No. GTREP-CEE/2002-1.*

RD Instruments, 2001. *WorkHorse Sentinel User's Guide*, published by the RD Instruments.

Work, P.A., Hansen, M., and Rogers, W.E., 1998. Bathymetric surveying with GPS and heave, pitch, and roll compensation. *J. Surv. Eng., ASCE* , 124(2), 73-90.

Investigation of Chlorination and Ozonation of Antibiotics Detected in Georgia Waters

Basic Information

Title:	Investigation of Chlorination and Ozonation of Antibiotics Detected in Georgia Waters
Project Number:	2002GA11B
Start Date:	3/1/2002
End Date:	2/28/2003
Funding Source:	104B
Congressional District:	5th
Research Category:	None
Focus Category:	Treatment, Water Quality, Waste Water
Descriptors:	None
Principal Investigators:	Ching-Hua Huang, Ching-Hua Huang

Publication

1. Huang, Ching-Hua, 2003, "Investigation of Chlorination and Ozonation of Antibiotics Detected in Georgia Waters," Georgia Water Resources Institute, Georgia Tech, Atlanta, GA., 12p.
2. Dodd, M. C. and Ching-Hua Huang, 2003, "Oxidation of Aquatic Antibiotic Microcontaminants by Free and Combined Chlorine. 1. Kinetics," Environ. Sci. Technol. 2003, in preparation.
3. Dodd, M. C. and Ching-Hua Huang, 2003, "Oxidation of Aquatic Antibiotic Microcontaminants by Free and Combined Chlorine. 2. Products and Reaction Pathways," Environ. Sci. Technol. 2003, in preparation.
4. Dodd, M. C. and Ching-Hua Huang, 2003, " Chemical Oxidation of Aquatic Antibiotic Microcontaminants by Free and Combined Chlorine, in proceedings of the AWWA Water Quality and Technology Conference, Philadelphia, PA.

Investigation of Chlorination and Ozonation of Antibiotics Detected in Georgia Waters

Final Report

September 1, 2003

Principle Investigator

Ching-Hua Huang

Assistant Professor
School of Civil and Environmental Engineering
Georgia Institute of Technology
Atlanta, GA 30332

Sponsored by:

Georgia Water Resources Institute
790 Atlantic Drive
Atlanta, GA 30332

Executive Summary

This study investigates kinetics and degradation pathways for the reactions between sodium hypochlorite (free available chlorine – FAC) or chloramines (combined chlorine – CC) and substrate compounds representative of three commonly prescribed and environmentally prevalent classes of antibiotics: fluoroquinolones, sulfonamides, and dihydrofolate reductase (DHFR) inhibitors. Pseudo-first-order kinetics was observed for oxidation of the fluoroquinolone antibiotic enrofloxacin (EF), sulfonamide antibiotic sulfamethoxazole (SMX), and DHFR inhibitor trimethoprim (TMP) by FAC. Second-order rate constants for reactions involving EF, SMX, and TMP were calculated from observed pseudo-first-order constants, on the assumption that concentration of oxidant remained essentially constant throughout the monitoring periods of each kinetic experiment. EF, SMX, and TMP were directly oxidized by FAC at varying rates, where second-order rate constants for reaction with FAC at pH 7 were measured as 4.80×10^{2} $\mathrm{M}^{-1}\mathrm{s}^{-}1$, 1.53×10^{3} $\mathrm{M}^{-1}\mathrm{s}^{-1}$, and 4.74×10^{1} $\mathrm{M}^{-1}\mathrm{s}^{-1}$, respectively. In contrast, significantly lower second-order rate constants (9.6×10^{-1} $\mathrm{M}^{-1}\mathrm{s}^{-1}$, 2.5×10^{-1} $\mathrm{M}^{-1}\mathrm{s}^{-1}$, and 6.0×10^{-2} $\mathrm{M}^{-1}\mathrm{s}^{-1}$ for EF, SMX, and TMP, respectively) were measured for reaction with CC at pH 7.

Solution pH exhibited a marked influence on reaction rates for all three antibiotic classes. Consideration of predominant antibiotic species and corresponding reaction rates at specific pH values allowed a preliminary determination of reactive sites within the antibiotics. Compounds representing the hypothesized reactive and non-reactive portions of each antibiotic class were utilized to verify the proposed location(s) of reactivity. LC/MS and H^{1}-NMR were used where applicable to identify reaction products and to assess product evolution during each reaction time course. Product characterization of CF reaction mixtures indicates the formation of a number of products, represented primarily by four major degradates corresponding to m/z 263, 297, 306, and 340 (corresponding to full or partial dealkylation of the piperazine ring, and – in two cases – substitution of Cl on the quinolone structure's aromatic ring). The relatively rapid oxidation of SMX is accompanied by what appears to be a unique radical-chain cleavage of the S-N sulfonamide bond to yield 3-amino-5-methylisoxazole and an unknown product. S-N bond cleavage, combined with N-chlorination of the aniline functional group, also appears to lead to the formation of relatively stable dimers and a number of lower mass products. Chlorination of TMP yields primarily stable, multiply-halogenated products – with the parent compound undergoing relatively minor structural modification.

The results of this investigation indicate that representative members of these three antibiotic classes are substantially degraded under conditions simulating chlorination of water supplies during disinfection processes, yielding a wide variety of lower and higher mass degradates.

Research Objectives

The proposed objective of this project was to determine the removal efficacy of chlorination and ozonation treatment processes for antibiotic compounds that had been commonly detected in Georgia waters with the aim of elucidating reaction kinetics and mechanisms. Studies were carried out to meet the research objective with a focus on oxidation of antibiotics by free chlorine and combined chlorine. Oxidation of antibiotics by ozone was not investigated in this study. The modification of the research objective was necessary based on several factors including new publications of ozonation of antibiotics by other research groups at the early stage of this project [1], high level of complexity of the reactions between antibiotics and chlorine that warranted a more detailed investigation, and the relatively short period of one year for this project.

Research Results

Significant progress has been made to meet the modified research objective. Results of this study have demonstrated that representative members of three common antibiotic classes are substantially degraded under conditions simulating chlorination of water supplies during disinfection processes. Reaction kinetics have been successfully described using a modified second-order kinetic model. Evaluation of the pH-dependencies of the reaction kinetics, kinetic results of an array of structurally-related compounds, and characterization of reaction products have elucidated the reactive sites of the antibiotic compounds and aided determination of reaction pathways. The research results are summarized in the following sections. This study has yielded several publications [2-4], in which more details of the investigation can be found.

Antibiotics and Related Compounds in this Study

A range of antibiotics including ciprofloxacin (CF), enrofloxacin (EF), flumequine (FLU), sulfamethoxazole (SMX) and trimethoprim (TMP) were examined in this study (see Table 1 for their structures). These antibiotics represent three commonly prescribed classes of modern antibiotics: fluoroquinolones, sulfonamides, and dihydrofolate reductase (DHFR) inhibitors. These three classes of antibiotics were also frequently detected in environmental occurrence studies in recent years [5-7]. The investigation was undertaken with the intent of quantifying reaction kinetics and clarifying reaction pathways involved in oxidative degradation of antibiotics by free available chlorine (FAC) and combined chlorine (CC) under conditions associated with chlorine-based municipal wastewater and drinking water disinfection processes. Structurally-related compounds (Table 1) that correspond to either the hypothesized reactive or inactive portions of each antibiotic class were also examined for their oxidation by FAC in order to verify the site(s) of reaction.

Table 1. Selected Antibiotic Compounds and Associated Structures

Compound	Structure	Molecular Weight	pK_a
Ciprofloxacin (CF)	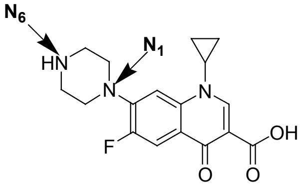	331.35	$pK_{a1}=6.43$, $pK_{a2}=8.49$ [18]
Enrofloxacin (EF)	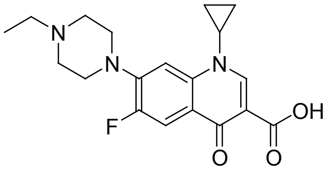	359.39	$pK_{a1}=6.06$, $pK_{a2}=7.7$ [18]
Flumequine (FLU)	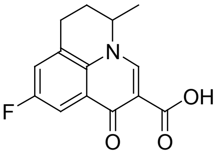	261.25	$pK_{a1}=6.42$ [19]
Sulfamethoxazole (SMX)	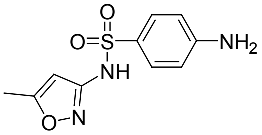	253.28	pKa1=1.83, pKa2=5.57 [20]
3,5-dimethylisoxazole (DMI)	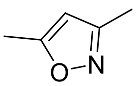	97.12	NA
3-amino-5-methylisoxazole (AMI)	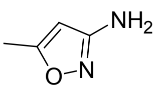	98.1	$pKa_1=2.63$ [21]
4-aminophenyl methyl sulfone (APMS)	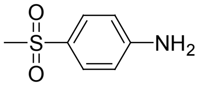	171.22	$pKa_1=1.48$ [22]
4-methyl-N-(5-methyl-isoxazol-3-yl)-benzenesulfonamide (MMIB)	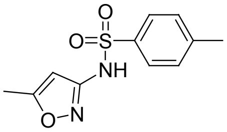	252.29	$pKa_1=10.58$ [21]
Trimethoprim (TMP)	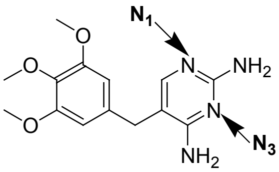	290.32	pKa1=1.32 [23], pKa2=7.45 [24]
2,4-diamino-5-methyl pyrimidine (DAMP)	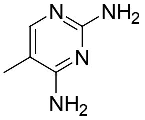	124.14	$pKa_1=5.15$, $pKa_2=7.54$ [21]

2,4-dichloro-5-methylpyrimidine (DCMP)	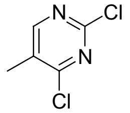	163.00	NA
3,4,5-trimethoxytoluene (TMT)	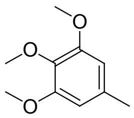	182.22	NA

Materials and Methods

Chemical Reagents. Sulfamethoxazole (SMX), ciprofloxacin (CF) hydrochloride, enrofloxacin (EF), and flumequine (FLU) were obtained from ICN Biomedicals (Irvine, California). Trimethoprim (TMP), 2,4-dichloro-5-methylpyrimidine (DCMP), 3,4,5-trimethoxytoluene (TMT), 3,5-dimethylisoxazole (DMI), 3-amino-5-methylisoxazole (AMI), and 4-aminophenyl methyl sulfone (APMS) were purchased from Sigma-Aldrich (St. Louis, MO). 2,4-diamino-5-methylpyrimidine (DAMP) was purchased from Daniels Fine Chemicals (Edmonton, Alberta, Canada). 4-methyl-N-(5-methyl-isoxazol-3-yl)-benzenesulfonamide (MMIB) was purchased from ASINEX (Moscow, Russia). All chemical standards were of reagent grade and were used without further purification. All reagent solutions (e.g., buffers, stocks, oxidants, quenching agents) were prepared using Barnstead Nanopure© water (Dubuque, IA). 100 mg/L stock solutions of all compounds (for use in kinetic experiments) were prepared in 10% methanol.

Aqueous sodium hypochlorite solutions (~7%) from Fisher Scientific (Pittsburgh, PA) were diluted to ~100 mg/L FAC for use in kinetic experiments. FAC stocks were periodically standardized iodometrically [8]. N,N-diethyl-*p*-phenylenediamine (DPD) was used through either DPD colorimetry or DPD-FAS titrimetry to measure free chlorine residual concentrations after completion of kinetic experiments [8].

Pre-formed chloramine stocks were prepared at pH values of 4.5, 5, 6, 7, 8, and 9 in 0.1 M acetate (pH ≤ 5), 0.1 M phosphate (6 ≤ pH ≤ 8), and 0.025 M borate (pH 9) buffers, with modifications to the methods of Chapin [9]. Solutions of NH_4Cl and FAC were combined at 25°C under completely-mixed conditions to produce ~100 mg/L of CC, at 2:1 NH_4Cl:FAC molar ratios. CC stocks were prepared prior to each experiment, temporarily stored at <5˚C, and used within 24 hours of generation. CC concentrations were standardized using DPD-FAS titrimetry.

Reaction Kinetics Monitoring. Temperature was maintained at 25˚C in all experiments using a recirculating water bath connected to an acrylic water tank. Reaction solutions were partially immersed in the water tank and stirred with Teflon-coated stir bars using a 15-position magnetic stir-plate. 0.01 M acetate (pH 4, 4.5, 5), phosphate (pH 6, 7, 8), and borate (pH 9) buffers were used to maintain pH. Reactions were initiated by addition of appropriate volumes of FAC or CC stock (to achieve 10:1 oxidant:substrate ratio) to solutions containing 500 µg/L of substrate and 0.01 M buffer, under completely-mixed conditions, at 25˚C. Reactions involving oxidation of SMX and TMP by CC were monitored by HPLC with ultraviolet detection immediately after sampling, without quenching. All other reactions were monitored by quenching 1-mL samples of each reaction solution with either NH_4Cl/tris-hydroxymethyl aminomethane (THAM) or sodium thiosulfate (NH_4Cl/THAM for SMX, TMP, APMS, and DAMP; $Na_2S_2O_3$ for all other compounds) at appropriate time intervals and analyzing by HPLC with fluorescence or ultraviolet detection. An Agilent 1100 series HPLC system equipped with a 5 μm particle-diameter, 4.6 mm × 250 mm Zorbax RX-C18 column, a fluorescence detector and a UV/Vis diode-array detector was used to monitor parent compounds and product formation during the oxidation reactions.

Reaction of an antibiotic or surrogate compound with chlorine oxidant can be described as a bimolecular reaction: Substrate + Oxidant → Products. At least a 10-fold excess of chlorine oxidant with respect to substrate was always employed in the kinetic experiments in this study to ensure pseudo-first-order conditions. Therefore, using an approach similar to that used by von Gunten and Oliveras [10], oxidant concentration was assumed to be constant and used to determine the second-order rate constant according to equation (1):

$$-\frac{d[\text{substrate}]_{\text{T}}}{dt} = k_{app}^{'}[\text{substrate}]_{\text{T}} = k_{app}^{''}[\text{oxidant}]_{\text{T}}[\text{substrate}]_{\text{T}} \qquad (1)$$

where $k_{app}^{'}\ (\text{in S}^{-1}) = k_{app}^{''}[\text{oxidant}]_{\text{T}}$ or $k_{app}^{''}(\text{in M}^{-1}\text{S}^{-1}) = \dfrac{k_{app}^{'}}{[\text{oxidant}]_{\text{T}}}$

Kinetic experiments involving EF, SMX and TMP were conducted in triplicate, whereas those involving all other compounds were conducted in duplicate. 95% confidence limits were calculated and reported with all rate constants as error bars in relevant graphs.

Product Characterization. LC/MS was used to analyze unquenched reaction solutions of CF, SMX, and TMP. An Agilent 1100 series HPLC system equipped with a 4.1 μm particle-diameter, 2.1 mm × 150 mm Zorbax SB-C18 column, a UV/Vis DAD, and an 1100 series quadrupole mass spectrometer was used in the characterization of reaction products. In order to identify peaks observed in HPLC chromatograms, LC/MS was also utilized to analyze appropriate fractions collected from samples initially resolved via HPLC. Fractions were collected (using an ISCO Foxy, Jr. fraction collector) for each major product peak. These dilute fractions were subsequently reconcentrated by evaporating under nitrogen gas at ~50°C and analyzed by LC/MS to verify their identity. H^1-NMR was utilized to provide structural information for an unknown oxidation product of SMX. One-dimensional and 2-D COSY H^1-NMR spectra were obtained using a Bruker AMX 400 NMR instrument.

Results and Discussion

Kinetics of Reactions with Free Chlorine. Solution pH strongly affects the speciation of free chlorine oxidant and antibiotic substrate, where relevant antibiotic speciation patterns are shown in Figure 1. Second-order rate equations incorporating pH-dependent speciation of both substrate and free chlorine oxidant have been utilized previously to model observed pH-dependent kinetics [11,12]. A similar kinetic model has been developed in this investigation to help explain variations in rate constants for degradation of antibiotics by FAC at different pH values. Six individual sub-reactions (comprised of the six possible combinations amongst the three antibiotic and two oxidant species) may be considered as contributing to the overall reactions between free chlorine and the antibiotic compounds. These six sub-reactions can be incorporated into the second-order kinetic expression as shown in equation (1).

$$\frac{d\left[substrate\right]_T}{dt} = -k_{00}[HOCl][H_2A] - k_{10}[OCl^-][H_2A] - k_{01}[HOCl][HA] - k_{11}[OCl^-][HA] - k_{02}[HOCl][A] - k_{12}[OCl^-][A] \qquad (1)$$

where $k_{00\text{-}12}$ represent the specific second-order rate constants corresponding to each combination of reactant species.

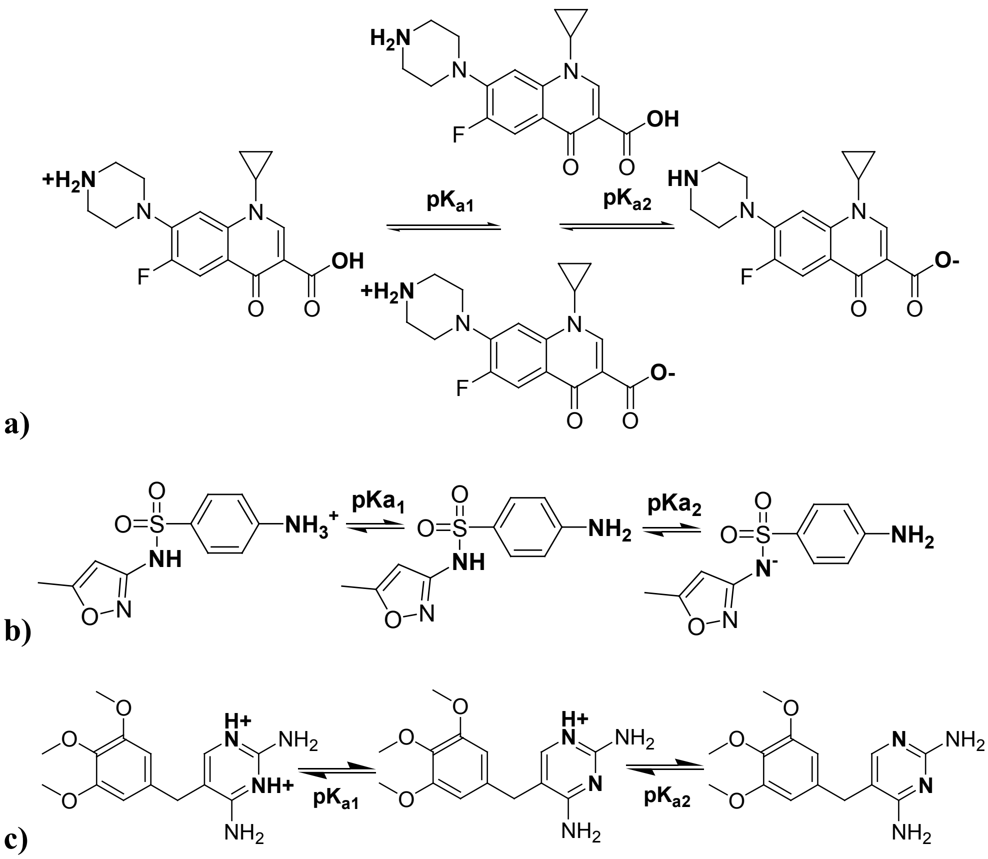

Figure 1. Speciation patterns of: a) CF, b) SMX, and c) TMP

Application of principal component analysis (PCA) [13] to the linear systems formulated with this equation allows simplification to yield less complex models for each antibiotic compound. The revised models for oxidation of EF, SMX, and TMP by FAC can be represented by equations (2), (3), and (4), respectively:

$$\frac{d\left[\mathrm{EF}\right]_{\mathrm{T}}}{dt} = -k_{00}\alpha_0[\mathrm{ox.}]_{\mathrm{T}}\alpha_0^{'}[\mathrm{sub.}]_{\mathrm{T}} - k_{01}\alpha_0[\mathrm{ox.}]_{\mathrm{T}}\alpha_1^{'}[\mathrm{sub.}]_{\mathrm{T}} - k_{02}\alpha_0[\mathrm{ox.}]_{\mathrm{T}}\alpha_2^{'}[\mathrm{sub.}]_{\mathrm{T}} \qquad (2)$$

$$\frac{d[\mathrm{SMX}]_\mathrm{T}}{dt} = -k_{00}\alpha_0[\mathrm{ox.}]_\mathrm{T}\alpha'_0[\mathrm{sub.}]_\mathrm{T} - k_{01}\alpha_0[\mathrm{ox.}]_\mathrm{T}\alpha'_1[\mathrm{sub.}]_\mathrm{T} \tag{3}$$

$$\frac{d[\mathrm{TMP}]_\mathrm{T}}{dt} = -k_{00}\alpha_0[\mathrm{ox.}]_\mathrm{T}\alpha'_0[\mathrm{sub.}]_\mathrm{T} - k_{01}\alpha_0[\mathrm{ox.}]_\mathrm{T}\alpha'_1[\mathrm{sub.}]_\mathrm{T} - k_{02}\alpha_0[\mathrm{ox.}]_\mathrm{T}\alpha'_2[\mathrm{sub.}]_\mathrm{T} - k_{12}\alpha_1[\mathrm{ox.}]_\mathrm{T}\alpha'_2[\mathrm{sub.}]_\mathrm{T} \tag{4}$$

The apparent rate constants, k_{ij}, for reaction between hypochlorous acid/hypochlorite and each individual substrate species can be calculated from experimental data using a matrix algebra routine written in MATLAB. Using equations (2), (3), and (4), the overall apparent second-order rate constant, k''_{app}, can be determined from the reaction-specific constants, k_{ij}, for EF, SMX, or TMP at any pH value within the range considered. An example of measured second-order rate constants and fitted curves based on the simplified models is shown in Figure 2, for reaction of EF with FAC.

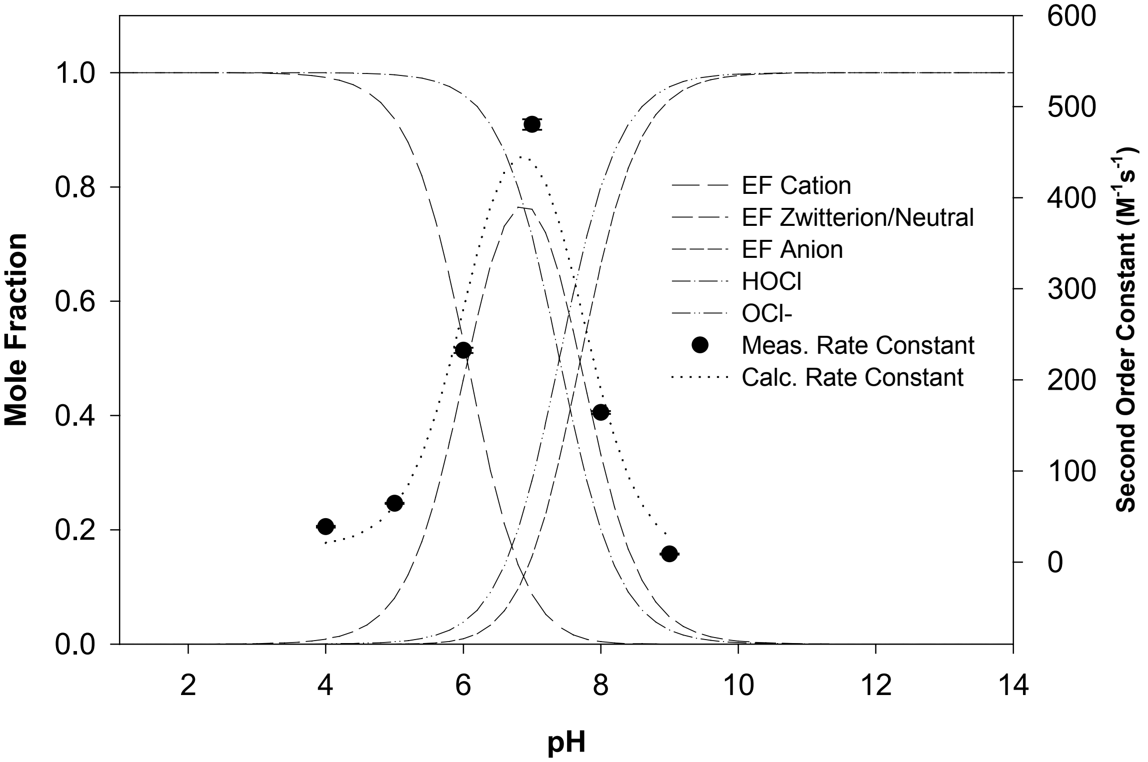

Figure 2. pH-dependency of apparent second order rate constants for reaction of FAC with EF

The second-order pH-dependency model serves as a useful qualitative tool in evaluating the importance of each antibiotic and oxidant species in the overall oxidation reactions. This can in turn aid in identification of the sites of free chlorine attack on the antibiotics. Experimental data suggest that attack of EF, SMX, and TMP by free chlorine is tied to protonation and deprotonation of basic or acidic nitrogen groups within each compound, as well as of the oxidant species.

Oxidation of EF appears to occur at the N_6 nitrogen of the compound's piperazine ring (Table 1), as evidenced by the decrease in reactivity with FAC for pH below ~7, which corresponds to a decrease in neutral/Zwitter ionic EF and an increase in cationic (protonated) EF. Attack of SMX appears to occur at the compound's amido nitrogen, as shown by a decrease in reactivity below pH ~5.6, corresponding to an increase in concentration of the neutral SMX relative to the deprotonated anionic SMX. However, additional experimental data is necessary to verify this seemingly unlikely mechanism. TMP appears to undergo oxidative attack on the compound's diaminopyrimidine moiety, as indicated by a drop in reactivity below pH ~7.7, corresponding to an increase in concentration of monoprotonated TMP relative to neutral TMP. However, TMP also appears to undergo attack at another site, as indicated by the sharp increase in reactivity for pH < 5. This additional site of oxidative attack on the TMP structure is likely located on its trimethoxy moiety, which could be expected to exhibit higher susceptibility to FAC oxidation with increasing acidity [14]. The validity of these conclusions has been further investigated through the use of various antibiotic substructures and structural surrogates in additional oxidation experiments, in conjunction with structural characterization of reaction products, as will be discussed below.

Kinetics of Reactions with Combined Chlorine. Reactions between CC and EF, SMX, or TMP were extremely slow compared to those with FAC, as typified by measured second-order rate constants of 9.6×10^{-1} $M^{-1}s^{-1}$, 2.5×10^{-1} $M^{-1}s^{-1}$, and 6.0×10^{-2} $M^{-1}s^{-1}$ for reaction of EF, SMX, and TMP, respectively, with CC at pH 7. In contrast, measured reaction rate constants for reaction of EF, SMX, and TMP with FAC were 4.80×10^{2} $M^{-1}s^{-}1$, 1.53×10^{3} $M^{-1}s^{-1}$, and 4.74×10^{1} $M^{-1}s^{-1}$, respectively, at pH 7. In fact, TMP exhibited discernible reactivity toward chloramines only at pH 7, after nearly 40 hours of reaction time.

Reactions of Substructures and Structural Surrogates with FAC. Additional kinetic studies – in which substructures or structural surrogates of each antibiotic were subjected to application of FAC – were performed in order to verify the locations of proposed reaction sites. FLU, DMI, MMIB, and DCMP (Table 1) were all unreactive toward FAC. Oxidation studies involving fluoroquinolones and their substructure FLU – which represents a fluoroquinolone lacking the characteristic piperazine ring – show that the reactive portion of the fluoroquinolone antibiotics is located on the piperazine ring, presumably at the N_6 amino nitrogen, as indicated by kinetic results for EF. Oxidation studies involving DMI, coupled with those involving APMS (which contains the aniline amino-nitrogen but no sulfonyl amido-nitrogen) and MMIB (which contains the sulfonyl amido-nitrogen, but not the aniline amino-nitrogen), show that direct oxidative attack of the SMX structure occurs on its amino-nitrogen. However, as noted in the pH-dependency of apparent kinetic rate constants for reaction of SMX with FAC, overall oxidation of the SMX structure is further modulated by protonation of the compound's amido nitrogen via an effect that is not completely clear at the current stage. Oxidation studies involving TMP and its substructures verify that reaction rates are influenced primarily by speciation of the 2,4-diaminopyrimidinyl moiety for pH ≥ 5, while interactions with the 3,4,5-trimethoxybenzyl moiety predominate for pH < 5. This indicates that oxidative attack of the TMP structure occurs primarily on the 3,4,5-trimethoxybenzyl ring under highly acidic conditions, and on the 2,4-diaminopyrimidine moiety for mildly acidic to basic conditions.

Product Characterization and Proposed Degradation Pathways

Ciprofloxacin. CF was chosen as a representative FQ in product characterization studies as it is essentially a template common to all other FQs (Table 1). LC/MS analyses of oxidation products generated by reaction of CF with FAC revealed a number of transient products, which appear to be N-chlorinated intermediates: m/z 352 (1 Cl), 366 (1 Cl), 374 (2 Cl), and 408 (3 Cl). The number of chlorines assigned to each compound was based on relative abundance of Cl isotopic peaks. The intermediates with m/z 366, 374, and 408 exhibited spontaneous rearrangement to stable products corresponding to m/z 306, 263 and 297, respectively, over a time-span of several hours. The products with m/z 306 and 263 correspond to partial dealkylation (removal of a single ethylene group) and complete dealkylation (removal of both ethylene groups and the amino group) of the piperazine ring of CF, respectively. The m/z 297 product corresponds to a chlorinated analogue of m/z 263, in which one chlorine substitution occurs on the quinolone ring. Temporal distribution of these products indicated that m/z 297 is likely a terminus in the degradation of CF and other fluoroquinolones. Products identified by LC/MS for the reactions between CC and CF were the same as those detected for reactions involving FAC. Thus, similar degradation pathways are expected to apply in the case of FQ oxidation by CC.

Sulfamethoxazole. Mass chromatograms corresponding to oxidation products of SMX yielded a number of distinct, stable peaks, corresponding primarily to lower mass degradates (e.g., m/z 99 and 190) and higher mass dimers (e.g., m/z 501 and 503). Two transient peaks, both corresponding to m/z 288, appear to be a N-chloro intermediate and a transient ring-chlorinated SMX molecule. A prominent, early-eluting peak in HPLC and LC/MS chromatograms was identified as 3-amino-5-methylisoxazole (AMI) through comparison to a pure standard. Another prominent product peak detected by way of its UV absorption in kinetic experiments failed to ionize in either APCI or ESI modes during LC/MS analyses. H^1-NMR analysis of this unknown product revealed that cleavage at the sulfonyl amido nitrogen of SMX had taken place, indicating that this particular site somehow participated in the chlorination reaction. Additionally, generation of AMI was detected at roughly the same reaction time as the unknown product throughout the reaction time course, indicating that cleavage of the SMX structure yields both AMI and the unknown contemporaneously. Despite the above evidence, lack of a definite m/z value for the unknown product prevents identification of its chemical structure at this point.

Taking into account all available kinetic data and product characterization results, the reaction between FAC and SMX can be envisioned as one in which initial attack of the SMX structure occurs at its amino-nitrogen [15], followed by subsequent attack of sulfonamide S-N bonds – possibly by aminium radicals generated through initial oxidation of amino-nitrogens – to yield a number of products resulting from cleavage of the sulfonamide S-N bond. Support for generation of aminium radicals in the absence of metal or photolytic chain initiators can be found in studies conducted on oxidation of amines (via hypochlorous acid and chlorine dioxide) by the U.S. Army Edgewood Arsenal Research Laboratories [16]. Oxidation product distributions generated by reaction of SMX with CC are very similar to those observed for reaction of SMX with FAC.

Trimethoprim. Reaction mixtures obtained from the oxidation of TMP by FAC at pH ≥ 5 yield considerably more complex chromatograms than reactions involving SMX. One stable product was identified as containing four Cl atoms (with molecular ion of 445), indicating that Cl substitution can occur in numerous locations on the TMP structure. Fragmentation of this compound was minimal. Unstable products which appeared to be intermediates exhibited mass spectra corresponding to: m/z 377 (2 Cl) and m/z 411 (3 Cl). A fragment ion peak with m/z 181 in TMP product mass spectra apparently corresponds to the 3,4,5-trimethoxytoluene fragment of the molecule, cleaved from the parent ion during LC/MS analysis, at the aliphatic carbon bridging it to the 2,4-diaminopyrimidine moiety. The parent TMP does not yield such a fragment upon ionization, indicating that chlorine somehow sensitizes TMP to fragmentation at the aliphatic carbon. Experiments conducted at pH < 5 also yielded relatively complex mixtures of halogenated products, for which LC/MS analyses indicated very low abundances of fragment ions exhibiting m/z 181, but significant quantities of ions with m/z 215 or 249 (which represent mono- and dichlorinated 3,4,5-trimethoxytoluene fragments, respectively).

TMP oxidation by FAC at pH ≥ 5 can be envisioned as proceeding through initial attack on TMP at one of its exocyclic amino nitrogens to yield an iminoquinone methide intermediate [17] (in which the antibiotic's aliphatic carbon participates in resonance with the aromatic heterocyclic ring of the 2,4-diaminopyrimidine), followed by subsequent Cl attack on the TMP structure's aliphatic carbon, then by Cl substitution at various positions on the 2,4-diaminopyrimidine moiety to yield singly- and multiply-halogenated products. TMP oxidation at pH < 5 appears to proceed primarily through direct attack of the TMP structure's 3,4,5-trimethoxy moiety to yield singly- and multiply-halogenated products, where Cl substitution occurs on the benzene ring of the 3,4,5-trimethoxy moiety. As mentioned earlier, TMP did not exhibit any appreciable degradation in the presence of CC, even after 40 hours.

Literature Cited

1. Huber, M. M.; Canonica, S.; Park, G.-Y.; von Gunten, U. " Oxidation of Pharmaceuticals during Ozonation and Advanced Oxidation Processes", *Environ. Sci. Technol.* **2003**, *37*, 1016-1024.
2. Dodd, M. C. "Chemical Oxidation of Aquatic Antibiotic Microcontaminants by Free and Combined Chlorine" **2003**, MS thesis, School of Civil and Environmental Engineering, Georgia Institute of Technology, Atlanta, Georgia.
3. Dodd, M. C.; Huang, C.-H. "Oxidation of Aquatic Antibiotic Microcontaminants by Free and Combined Chlorine. 1. Kinetics", *Environ. Sci. Technol.* **2003**, in preparation.
4. Dodd, M. C.; Huang, C.-H. "Oxidation of Aquatic Antibiotic Microcontaminants by Free and Combined Chlorine. 2. Products and Reaction Pathways", *Environ. Sci. Technol.* **2003**, in preparation.
5. Kolpin, D. W.; Furlong, E. T.; Meyer, M. T.; Thurman, E. M.; Zaugg, S. D.; Barber, L. B.; Buxton, H. T. "Pharmaceuticals, Hormones, and Other Organic Wastewater Contaminants in U.S. Streams, 1999-2000: A National Reconnaissance" *Environ. Sci. Technol.* **2002**, *36*, 1202-1211.
6. Golet, E. M.; Alder, A. C.; Hartmann, A.; Ternes, T. A.; Giger, W. " Trace Determination of Fluoroquinolone Antibacterial Agents in Urban Wastewater by Solid-Phase Extraction

and Liquid Chromatography with Fluorescence Detection." *Anal. Chem.* **2001**, *73*, 3632-3638.

7. Hirsch, R.; Ternes, T.; Haberer, K.; Kratz, K.-L. "Occurrence of Antibiotics in the Aquatic Environment" *Sci. Total Environ.* **1999**, *225*, 109-118.
8. *Standard Methods for the Examination of Water and Wastewater*; 20 ed.; APHA, AWWA, WPCF: Washington, 1998.
9. Chapin, R. M. " The Influence of pH upon the Formation and Decomposition of the Chloro Derivatives of Ammonia" *J. Org. Chem.* **1929**, *51*, 2112-2117.
10. von Gunten, U.; Oliveras, Y. " Kinetics of the Reaction between Hydrogen Peroxide and Hypobromous Acid: Implication on Water Treatment and Natural Systems" *Water Res.* **1997**, *31*, 900-906.
11. Lee, G. F. "Kinetics of Reactions between Chlorine and Phenolic Compound" In *Rudolfs Research Conference*; Faust, S. D., Hunter, J. V., Eds.; John Wiley & Sons, Inc.: Rutgers University, 1967; pp 54-74.
12. Gallard, H.; von Gunten, U. "Chlorination of Phenols: Kinetics and Formation of Chloroform" *Environ. Sci. Technol.* **2002**, *36*, 884-890.
13. Minitab Statistical Software v.13.32. Minitab, Inc., 2000.
14. Langvik, V.-A.; Hormi, O.; Tikkanen, L.; Holmbom, B. *Chemosphere* **1991**, *22*, 547-555.
15. Uetrecht, J. P.; Shear, N. H.; Zahid, N. " N-Chlorination of Sulfamethoxazole and Dapsone by the Myeloperoxidase System" *Drug Metab. Dispos.* **1993**, *21*, 830-834.
16. Hull, I. A.; Giordano, W. P.; Rosenblatt, D. H.; Davis, G. T. " Oxidations of Amines. VIII. Role of the Cation Radical in the Oxidation of Triethylenediamine by Chlorine Dioxide and Hypochlorous Acid" *J. Phys. Chem.* **1969**, *73*, 2147-2152.
17. Lai, W. G.; Zahid, N.; Uetrecht, J. P. " Metabolism of Trimethoprim to a Reactive Iminoquinone Methide by Activated Human Neutrophils and Hepatic Microsomes" *J. Pharmacol. Experimental Therapeutics* **1999**, *291*, 292-299.
18. Barbosa, J.; Barron, D.; Jimenez-Lozano, E.; Sanz-Nebot, V. *Anal. Chim. Acta* **2001**, *437*, 309-321.
19. Barbosa, J.; Barron, D.; Cano, J.; Jimenez-Lozano, E.; Sanz-Nebot, V.; Toro, I. *Journal of Pharmaceutical and Biomedical Analysis* **2001**, *24*, 1087-1098.
20. Lin, C.-E.; Lin, W.-C.; Chen, Y.-C.; Wang, S.-W. *J. Chromatogr., A* **1997**, *792*, 37-47.
21. Weber, E. J.; Kenneke, J. F. SPARC (http://www.epa.gov/athens/research/projects/sparc), US EPA, National Exposure Research Laboratory: Athens, GA.
22. Pankratov, A. N.; Uchaeva, I. M.; Doronin, S. Y.; Chernova, R. K. *Journal of Structural Chemistry* **2001**, *42*, 739-746.
23. Cao, J.; Cross, R. F. *J. Chromatogr., A* **1995**, *695*, 297-308.
24. Cocco, L.; Roth, B.; Temple, C., Jr.; Montgomery, J. A.; London, R. E.; Blakley, R. L. *Arch. Biochem. Biophys.* **1983**, *226*, 567-577.

Scientific and Educational Contributions

Results of this study indicate that representative members of three environmentally relevant antibiotic classes - fluoroquinolones, sulfonamides, and dihydrofolate reductase (DHFR) inhibitors - are substantially degraded under conditions simulating chlorination of water supplies during disinfection processes, yielding a wide variety of lower and higher mass degradates. These results are important in facilitating a better risk assessment for these compounds in the aquatic environment. Results of this study also indicate that evaluation of the toxicity of the chlorination products of antibiotics is necessary. The mechanistic understanding of the reactions between chlorine and these three antibiotics classes provides a critical basis for predicting the fate of related antibiotics and pollutants in the chlorination disinfection processes.

This project has provided significant training for a master student in experimental, problem solving and communication skills. A master thesis has been completed from this study and received an outstanding master thesis award within the School of Civil and Environemntal Engineering of Georgia Tech. In addition, two journal publications, one conference proceedings, and at least two conference presentations as listed below are also products of this study, providing avenues of sharing the research results with scientific community and water industry.

Products of this investigation:

Publications:

1. Dodd, M. C. "Chemical Oxidation of Aquatic Antibiotic Microcontaminants by Free and Combined Chlorine" **2003**, MS thesis, School of Civil and Environmental Engineering, Georgia Institute of Technology, Atlanta, Georgia.
2. Dodd, M. C.; Huang, C.-H. "Oxidation of Aquatic Antibiotic Microcontaminants by Free and Combined Chlorine. 1. Kinetics", *Environ. Sci. Technol.* **2003**, in preparation.
3. Dodd, M. C.; Huang, C.-H. "Oxidation of Aquatic Antibiotic Microcontaminants by Free and Combined Chlorine. 2. Products and Reaction Pathways", *Environ. Sci. Technol.* **2003**, in preparation.
4. Dodd, M. C.; Huang, C.-H. " Chemical Oxidation of Aquatic Antibiotic Microcontaminants by Free and Combined Chlorine", proceedings of the AWWA Water Quality and Technology Conference, November 2-5, **2003,** Philadelphia, PA.

Conference Presentations:

1. Huang, C.-H. "Factors Affecting the Concentrations of Antibacterial Agents Released to the Aquatic Environment", AWWA Georgia/South Carolina Conference, September 25-26, **2003**, Savannah, GA.
2. Dodd, M. C.; Huang, C.-H. " Chemical Oxidation of Aquatic Antibiotic Microcontaminants by Free and Combined Chlorine", AWWA Water Quality and Technology Conference, November 2-5, **2003,** Philadelphia, PA.

Developing a Regional Water Management and Planning Initiative Model: Using Regional Leadership Summits to Address Water Resource Challenges in the Flint River Watershed, GA

Basic Information

Title:	Developing a Regional Water Management and Planning Initiative Model: Using Regional Leadership Summits to Address Water Resource Challenges in the Flint River Watershed, GA
Project Number:	2002GA12B
Start Date:	3/1/2002
End Date:	2/28/2003
Funding Source:	104B
Congressional District:	USHS 02
Research Category:	None
Focus Category:	Management and Planning, None, None
Descriptors:	None
Principal Investigators:	Elizabeth R. Blood

Publication

“Developing a Regional Water Management and Planning Initiative Model: Using Regional Leadership Summits to Address Water Resource Challenges in the Flint River Watershed, GA.”

Executive Summary

Submitted by: Mary Newcomb, Project Manager
Southwest Georgia Water Resource Task Force, Inc.
November 2003

1. Overview

1.1 Southwest Georgia Water Resources Task Force

The members of the Southwest Georgia Water Resources Task Force, Inc., are volunteers who work together to encourage and facilitate dialog among those interested in regional water issues. Our group neither promotes, nor endorses agendas. The goal of the Task Force is to encourage citizens, groups, regulators, and elected officials to participate in open discussion on water resources issues pertinent to Southwest Georgia.

The Task Force assumes a position of neutrality on all legislative actions. Through educational Water Summits, the Task Force provides an unbiased forum for Southwest Georgian’s to exchange ideas and opinions with elected officials, and state and federal agency staff in a neutral setting. This facilitated dialog builds mutual understanding which benefits the region.

The major focus of the Southwest Georgia Water Resources Task Force is to provide unbiased education through water summits that will lead to the empowerment of regional leadership, stewardship, and conservation ethic. The Task Force does not advocate agendas, nor does the Task Force make any effort to shape policy.

The goals of the SWGA Water Resources Task Force are to:

- Educate leaders and citizens about water issues through sponsorship of water leadership summits since 1999;
- Develop leadership stewardship and a conservation ethic in citizens of all ages; creating a society in which each person understands the importance of his actions and chooses to act to conserve water resources; and
- Facilitate the process whereby southwest Georgian’s can formulate and implement a self-determined regional plan for equitable and sustainable use of water resources that will benefit all stakeholders, provide incentives for water conservation, and effectively deal with the challenges of increased water demand.

The summits are broadly attended by regional leaders, elected officials, representatives from other regions in the state, state and federal agencies, non governmental organizations, and other interested parties. Leaders in agriculture, industry, commerce, health, municipal and county governments, conservation and recreation form a 30 county region of Southwest Georgia participate. From these summits have emerged educated citizens, stakeholders and a regional leadership; a basic knowledge of water issues; a regional awareness, identity, voice and vision; collaborations, partnerships; and interconnected networks; and an understanding of the importance of citizen responsibility and participation in governance and management.

1.2 Project Activities

This project included the following two activities:

Activity I: June 20, 2002
Water Summit VIII: *Taking Charge of our Future*
Regional Leadership Makes Comprehensive Planning Happen
Date: June 20, 2002

Activity II: October 1, 2002
A ONE HOUR TELEVISED FORUM
GEORGIA'S WATER UPDATE

2. Activity I: Water Summit VIII

"Taking Charge of our Future: Regional Leadership Makes Comprehensive Planning Happen"

June 20, 2002 • 8:30 a.m. until 4:15 p.m.
Darton College Building J
2400 Gillionville Road, Albany, Georgia

2.1 Presentations

Water Summit VIII featured guest speaker Dr. Doug Kenney, Natural Resources Law Center, University of Colorado School of Law. Dr. Kenney spoke about the general goals and principles that should be the foundation of a water management program, and focused on how a "watershed-based" and "stakeholder-oriented" element fits into this strategy. Discussion included key design issues, potential problems or dangers, etc.

Doug Kenney BIO:
Dr. Doug Kenney is a Research Associate at the Natural Resources Law Center, located within the University of Colorado School of Law (Boulder). In that capacity, he designs and implements a comprehensive research agenda examining a variety of public policy issues associated with natural resources, with a particular emphasis on water. He has written extensively

on several water-related issues, including river basin and watershed-level planning, the design of institutional arrangements, and alternative strategies for solving complex resource issues. Recently, he served as a consultant to the Western Water Policy Review Advisory Commission, authoring a special report for the Commission, and co-authoring the final report of the Commission: Water in the West: Challenge for the Next Century. Before beginning his current position with the Natural Resources Law Center, he served as a principal technical consultant to the Apalachicola-Chattahoochee-Flint and Alabama-Coosa-Tallapoosa (ACT/ACF) Comprehensive Study, assisting Alabama, Florida, and Georgia in the development of two interstate water compacts. Dr. Kenney has a B.A. in biology from the University of Colorado, a M.S. in Natural Resources Policy and Administration from the University of Michigan, and a Ph.D. in Renewable Natural Resource Studies from the University of Arizona.

Additional speakers included:

Woody Hicks
Hydrologist
Joseph W. Jones Ecological Research Center
Update: Water Resources Conditions

Dr. David Stookesbury
Georgia State Climatologist
Climate & Drought

Dr. Elizabeth R. Blood
Education & Outreach Ecologist, Joseph W. Jones Ecological Research Center

Dr. Doug Kenney
Natural Resources Law Center, University of Colorado School of Law
Regional Water Resources Planning

Nap Caldwell & Harold Reheis
EPD Efforts

2.2 Summary of Facilitated Discussion:

What elements do you suggest be part of SWGA's water management strategy?

What blocks would build on the drought working committees' reports?

Management structure defined from the bottom-up

ACF basin could use a management authority to administer water conservation, permitting and related issues. Suggest using an ACF water management authority that administers the entire basin w/ 4 to 6 water management districts overseeing the actions in GA

Local input/control at a regional level

Monitoring of water use is imperative (ground and surface), w/ fees for certain types and amounts of usage in a manner similar to the way municipal electric, gas, and water are regulated (compensation for use of a public resource)

Some kind of entity defined from bottom up

Water management agency with local control + state/local funding

State funding w/ local contribution

Water management district managed by elected representatives of each stakeholder groups:

- Funding would be provided by taxation.
- District would have authority to manage area's water resources under
- guidelines developed by the district and GA EPD Jointly.
- GA EPD would participate as member of WMD board.
- WMD would conduct independent monitoring program separate from GA EPD.
- Water use permit would be issued or rescinded based on specific set of criteria: 1) existing density of water use; 2) capacity of the aquifer to meet additional pumping (water use); 3) connectivity of the aquifer to local streams specific to the area where the additional withdrawal is requested; 4) other criteria such as intended water use (public supply should be highest priority), water quality constraints, pending climatic conditions, etc.

Water management district concept:

- Selected representation by stakeholder group
- Need government authority for taxation, land use planning, enforcement
- (basin-wide management)
- Strong professional staff
- Data-based decisions
- No blanket, region-wide application of policies: look at data in a
- specific area
- Florida model without bureaucracy

Conservation

- Make water use more efficient: a) old irrigation systems; b) industry
- procedures; c) household procedures

- Ascending water rates: M+I
- Certification process for farmers (all new permits) for water conservation
- BMPs
- Efficiency for new and existing irrigation systems
- Require new industries to implement conservation measures
- Water conservation plans during all conditions for health, municipal
- Incentives
    - Cost share to upgrade agricultural equipment for water conservation
    - CRP or similar program to take marginal land out of production
    - Incentives for industry to reuse/recycle/conserve water
    - Incentives to retire marginal land from farming (CRP and other programs)
    - and to retain undeveloped high recharge land in open space (Chickasawhatchee
    - Swamp, etc.)
    - State cost-share program or other incentives to conserve water (ag,
    - industrial, municipal, residential)
    - Water conservation cost-share program for ag (and other efficiencies)

Monitoring and research

- Monitoring of surface/ground water and aquatic species
- Better information – research
- Intermediate flow targets alone entire lengths of rivers to ensure
- protection of rivers for benefit and use of stakeholders

Financial compensation

- Financial protection for those who give up water
- Retirement of water rights as available w/ compensation

Manage water quality and quantity

- Include water quality and quantity
- Protection of recharge areas
- Increase land uses that conserve surface and groundwater while improving
- soil moisture and groundwater recharge potential to maintain base flows in
- streams

Need to be proactive in evaluating existing rules and existing problems which, though small now, could escalate. Need to implement land use controls and incorporate into state rules requirements which recognize the special conditions karst geology presents and define more stringent safeguards to prevent groundwater, as well as surface water, degradation. Have a prevention orientation vs. a reactive one.

Drought planning

- Define "drought conditions" (indicators)
- Drought plan approved before drought

Education

- Educate the population
- Education at all levels
- Education before enforcement for all stakeholder groups

Miscellaneous

- No interbasin transfers
- Vision for the river

Full group discussion: Suggested elements for SW GA's water/drought management strategy

Need local autonomy.

Establish a water management district of some sort, with all stakeholders represented and agribusiness having a higher proportion of representation given the proportion of agricultural water use.

Ensure a bottom-up definition of whatever we create: an entity defined by local citizens not imposed by the state. And, whatever the entity is, it needs to have authority (i.e., have some teeth).

Need an organization with local control, local input, teeth to speak for the people, and with good science to act upon. We don't want to be in the middle without a voice.

But, we need more complete information before putting such authority in place.

A district would (or could) allow the collection of revenue to fund the science needed to make decisions.

Note that communication among interested parties can make a formal district unnecessary.

If established, a district should have some commonality to be successful. Look at existing studies to establish the boundaries: use information from existing studies to identify common-sense boundaries based on resource characteristics and resource use rather than political boundaries.

"Commission" or decision making body: how will it be chosen?

Possibilities include gubernatorial appointees, elected commissioners, commissioners selected by each stakeholder group. Participants expressed preferences for one of the latter two options.

One table suggested the commission include a representative from EPD.

Funding sources (short-term and long-term):

How will this organization be funded in a way that maintains local control?

Some participants felt people in the region will have to pay for it, and should be willing to pay for it as an acceptable cost of local control. Costs should be allocated equitable and any taxes or fees should apply to all property owners, not just farmers. A tax may not have to be very large (e.g., $100 annual tax bill for a water management district in Florida). But, we must think carefully about imposition of local taxation, fees, etc. to support a local program. The burden of additional costs on farmers, in particular, should be considered.

Other participants suggested it should be a mix of state, local, and other funds, because areas up and downstream will benefit from this effort in a variety of ways.

Don’t make decisions about management districts until more meetings like this have been held and the data being collected demonstrate a need for them.

As an interim step, perhaps a commission could be established to guide EPD’s five-year study.

Provide incentives for water conservation in all stakeholder sectors (agricultural, business, residential): incentives for farmers to increase irrigation efficiency; incentives to retire marginal land, shift dry land to tree farming, and protect recharge areas.

Clearly make links between the "district" and other planning entities (e.g., RDCs) and link our activities with other plans.

Provide financial protection for all stakeholders who give up water use (e.g., industry and municipal users, not just agriculture users).

Must balance human use with environmental needs: how much water is available for human use after meeting ecosystem requirements? Need good science to answer this question.

Need to demonstrate efficient, reliable use of water (can help forestall imposition of more heavy-handed regulation).

Funding for small communities to meet any mandates, requirements.

Need a regional, multi-state vision for the Flint River should look like in 40-50 years.

Provide education about water use, conservation across all sectors (e.g., BMPs).

Pay attention the economic base of local communities: balance so that decisions don't destroy the economic base.

Recognize that local control may have to make ugly decisions locally – a "district" may not be just a lobbying organization. But, we need to put a positive spin on this; also recognize the benefits an organization can provide and the ways it can help us take advantage of opportunities.

Funding is needed from the state for data collection so that science can be done to head off some of the "ugly" decisions, to take a more positive approach.

In Florida, the water management districts put some farmers out of business and are seen as taking over control in some counties.

Invite speakers from existing water management districts to help educate us: this may or may not be the right approach for this region. But, either way, we shouldn't reinvent the wheel.

Where do we go from here?

Need to have more meetings like this, and more information, before we move to decisions about forming a district, a commission, or whatever. That doesn't necessarily mean wait for EPD to finish their five-year Flint River Water Development and Conservation Plan. But, it does mean we should continue laying the groundwork for these decisions and not act before the necessary information is available.

At the same time, we need to be aware that things are already happening and we can't wait too long before making decisions.

Note that funding is available for two summits in the next year.

Find out if legislative authority or impediments to regional water management exist. Is there legislation that provides the authority for an entity like that under discussion? If not, that should be established.

Need to face the hard questions: continue the drought working committees; extend current models to look at periods of shortfall; talk about what must be done.

If this is to be a multi-county entity, how do you get buy-in from all counties, from all stakeholders?

Need to get buy-in from this group and then talk about how to build support and buy-in across the region.

We need a community/watershed vision (economy, quality of life, etc.) before we can get to the point of making proposals.

Ultimately, the General Assembly must deal with the question of who owns the water. You can't make allocation decisions until there is legislation that answers this question.

We need to realize that there are other groups in the state who are making decisions, who have a sense of urgency about water: "he who has the money or the votes will get the water."

Next steps

- Set up a group to work with the Task Force and with the stakeholder
- committees to develop a proposal for completing a regional water management
- strategy in way that: 1) builds on the results of the drought working
- committees and 2) follows the direction provided by this and preceding
- summits. This expanded group will put together a strawman for a 1-5 year
- process and bring it to the next summit for review and revision.
- Get information about existing legislative authority and/or impediments. At
- the same time, pursue a resolution from Governor and/or General Assembly to
- formally recognize this effort and provide a window of opportunity.
- Pursue funding sources

3. Activity II: Georgia's Water Update

WHO: WALB –TV & The SWGA Water Resources Task Force, Inc.
WHAT: A one hour televised forum
WHEN: October 1, 2002 -   TIME: Tuesday, 7:00 P.M. – 8:00 P.M.
WHERE: WALB-TV Studio, Stuart Avenue, Albany, GA
WHY: To facilitate the opportunity to provide the public with a forum in which questions can be asked regarding state compact negotiations

3.1 Segment 1: Bob Kerr & Woody Hicks

TOPIC FOR THIS SEGMENT: ACF/ACT NEGOTIATIONS: WATER WARS Robert (Bob) Kerr, Chief Negotiator, ACT & ACF Compact (Robert Kerr represents Governor Barnes as the chief negotiator in the ACT & ACF Compact) and Woody Hicks, Hydrologist, Joseph W. Jones Ecological Research Center answered questions on the Apalachicola-Chattahoochee Flint Compact Allocation Negotiations and how they could affect you.

3.2 Segment 2: Harold Reheis & Dr. Elizabeth Blood

TOPIC FOR THIS SEGMENT: JOINT COMNPREHENSIVE WATER PLAN STUDY COMMISSION REPORT: MANAGING GEORGIA'S WATER – IS THERE ENOUGH TO LAST? Harold Reheis, Director of the Georgia Environmental Protection Division & Dr. Elizabeth Blood, Ecologist with the Joseph W. Jones Ecological Research Center answered questions on the recently completed Joint Study Committee's sweeping recommendations for Georgia Water Planning.

3.3 Segment 3: Napolean Caldwell, Georgia EPD & Murray Campbell

TOPIC FOR THIS SEGMENT: REGIONAL WATER PLANNING: DETERMINING OUR OWN FUTURE. Nap Caldwell, GA Environmental Protection Division & Murray Campbell, Mitchell County Farmer & Owner/Operator of CoveyRise Plantation answered questions about how you and other citizens in SWGA can have a say in your water future.

3.4 Segment 4: Dr. Elizabeth Blood, Woody Hicks, Murray Campbell & Susan Reyher (Director of Environmental Health, Dougherty County)

TOPIC FOR THIS SEGMENT #4: (LOCAL IMPACT SEGMENT) WATER WRAP UP: SUMMATION - Creating a Water Management Plan for the State.

Mid Infrared Water Quality Sensors for the detection of organic pollutants

Basic Information

Title:	Mid Infrared Water Quality Sensors for the detection of organic pollutants
Project Number:	2002GA30G
Start Date:	9/1/2002
End Date:	9/1/2004
Funding Source:	104G
Congressional District:	5th District John Lewis
Research Category:	Not Applicable
Focus Category:	Water Quality, Surface Water, Toxic Substances
Descriptors:	
Principal Investigators:	Boris Mizaikoff

Publication

1. Mizaikoff, Boris, 2003, "Mid Infrared Water Quality Sensors for the Detection of Organic Pollutants," Georgia Water Resources Institute, Georgia Tech, Atlanta, GA., 15p.

PROF. DR. BORIS MIZAIKOFF

Georgia Institute of Technology, School of Chemistry and Biochemistry, Applied Sensors Laboratory

Atlanta, Georgia 30332-0400, U.S.A.

Phone: (404) 894 4030, Fax: (404) 894 7452, Email: boris.mizaikoff@chemistry.gatech.edu

http://asl.chemistry.gatech.edu

Project: **2002GA30G**

(U.S.G.S., WATER RESOURCES RESEARCH GRANT PROPOSAL)

Mid Infrared Water Quality Sensors for the Detection of Organic Pollutants

Technical Report, Year 1

Research Activities September 01, 2002 – July 31, 2003

Boris Mizaikoff (PI)

Atlanta, September 28, 2003

1 TITLE:

MID-INFRARED WATER QUALITY SENSORS FOR THE DETECTION OF ORGANIC POLLUTANTS

2 PROBLEM AND RESEARCH OBJECTIVE

Increasing pollution of water resources has stimulated the development of sensor systems capable of screening organic pollutants in the aquatic environment. Especially in urban areas, increasing concentration of volatile organic compounds in surface and ground water threaten primary sources of drinking water. Hence, there is a substantial demand for in-situ, continuously operating and reliable analysis methods emphasizing selective determination of abundant pollutants, such as chlorinated hydrocarbons (CHCs), pesticides or the broad class of endocrine disrupting compounds (EDCs).

The main goal of this research project is the optimization, application and validation of infrared chemical sensor systems for the determination of organic pollutants such as chlorinated hydrocarbons, pesticides or endocrine disrupting compounds in the Rottenwood Creek stream, an urban stream located in the metro Atlanta area. This stream is affected by residential, commercial and industrial land use. Synthetic sensing interfaces ('biomimetics') based on sol-gels and imprinted polymers emphasizing selective analyte recognition will be combined with existing infrared sensor systems already established by our research group. Following optimization of the instrument in the laboratory and validation with real-world samples, measurements at Rottenwood Creek are envisaged as representative example of an urbanized water resource.

3 METHODOLOGY

The methodology of this study is divided into three workpackages (**WPs**), which are described in the following sections:

- **WP 1: Development of novel chemical recognition layers ("biomimetics") for optical waveguides based on sol-gels and molecularly imprinted polymers.**

Sol-gel Chemistry

The sol-gel process represents a method of preparing glasses and ceramics at low temperatures by hydrolysis and polymerization of organic precursors and provides a promising platform for creating thin films at optical waveguide surfaces. Particularly, properties such as high chemical and mechanical stability and tunability of porosity and polarity make these materials attractive for sensing applications in harsh environments. By introducing organically modified siloxanes (Ormosils) as novel sol-gel precursors, reactive functional groups can be incorporated in the sol-gel matrix enabling the formation of improved chemical recognition elements. These chemical recognition elements are integrated with mid-infrared (mid-IR) waveguides serving both, as enrichment membrane and as protective layer. Two different kinds of IR transparent waveguides have been applied for developing intrinsic *evanescent field sensing systems*: ZnSe ATR crystals and silver halide fibers. Utilizing attenuated total reflection (ATR) techniques the environmentally relevant group of organophosphates has been targeted.

Molecularly Imprinted Polymers

Molecularly imprinted polymers are based on utilizing the functionalities of a target molecule (template) to assemble its own recognition cavity by forming interactions with ‘complementary’ functional groups of appropriate functional monomers. These interactions are either provided by cleavable covalent bonds or non-covalent interactions, which are then “frozen” in position by polymerization carried out in the presence of a high concentration of cross-linker. Subsequent removal of the template creates binding pockets within the polymer matrix memorizing the spatial arrangement of functional groups and the size and shape of the target molecule. Ideally, highly selective recognition of the imprinted analyte molecules is thereby ensured, which favors reversible re-binding and selective retention of the templated compound within the biomimetic recognition matrix.

First experiments have been performed to create highly selective separation materials for the endocrine disrupting compound (EDC) 17β-estradiol. HPLC columns packed with either molecularly imprinted stationary phase material or control (non-imprinted) material have been prepared and compared concerning their separation performance.

• WP 2: Optimization and testing of a fiber optic evanescent wave sensor prototype for measuring organic pollutants in the aquatic environment.

A prototype mid-infrared sensor system for the determination of volatile organic pollutants in ground and surface waters was developed and tested. The sensor comprises a portable Fourier transform infrared spectrometer, coupled to the sensor head via mid-infrared transparent silver halide fibre optic cables. A 10 cm unclad middle section of the 6 m long fibre is coated with ethylene propylene copolymer (E/PCo), in order to enrich the analytes within the penetration depth of the evanescent field protruding from the fibre sensor head. Alternatively, polymer coated ATR crystals are used. Mixtures of benzene, toluene and xylene isomers (BTX) at concentrations down to the low ppb region were successfully qualitatively and quantitatively investigated. All analytes could be simultaneously discriminated ; with LODs in the low ppb concentration range.

• WP 3: Alternative sensing concept for water analysis using an IR hollow waveguide gas sensing module combined with a supported capillary membrane sampler.

Following the proposed time schedule and work plan (see Figure 1) research was mainly focused on **WP 1** and **WP 2**.

4 PRINCIPLE FINDINGS AND SIGNIFICANCE

A major part of **WP 1** was dedicated to the development and investigation of organically modified sol-gel membranes as physico-chemical recognition element in chemical mid-IR evanescent field sensing systems [1,2]. In summary, following major parameters were studied: (i) influence of various organoalkoxysilanes on the membrane formation behavior for two different waveguides (planar ZnSe ATR crystals; silver halide optical fibers) and their resulting surface polarity, (ii) properties of sol-gel based membranes for water exclusion from the analytical volume probed by the evanescent field, (iii) response of the sensing system towards aromatic compounds containing nitro-functional groups with focus on the detection of organophosphate pesticides, (iv) characterization of the sensing system concerning response time, sensitivity, reproducibility and stability, and (v) processing approaches enabling tunability of membrane porosity.

Due to significant IR absorption features of the sol-gel membranes below 1200 cm^{-1} the mid-IR fingerprint region (1200-600 cm^{-1}) is not accessible when applying sol-gel coated IR waveguides. Hence, during the first year of **WP 2** ethylene/propylene co-polymer coatings have been used to simultaneously quantify benzene, toluene and xylenes in water as these chlorinated hydrocarbons show molecule specific absorption features in the mid-IR fingerprint region [3].

Molecular imprinting procedures for the analyte 17β-estradiol have been developed and evaluated with the final goal of producing separation materials with improved selectivity for this specific analyte.

4.1 Organically Modified Sol-Gel Membranes as Physico-Chemical Recognition Element in Mid-Infrared Evanescent Field Sensing Systems

A Bruker IFS 66 research FT-IR spectrometers was used in the course of this work. The instrument was controlled via a desktop PC and equipped with a sample compartment for conventional ATR measurements and an external beam port for fiberoptic measurements. The mid-IR waveguides were coated with sol-gel membranes (1-10 μm thick) via spin- or drop-coating techniques and mounted into flow-through cells for analyte enrichment and detection studies. Exemplary sol-gel processing compositions for both, acid- and base-catalyzed approaches are presented in Table 1 and the common sol-gel processing procedures are described as follows:

Acid-catalyzed approach. The sol solution was prepared by acid-catalyzed co-polymerisation of a 3:1 mixture of PTMOS and TMOS in ethanol/water (molar ratio 4:3). 1.4 ml of PTMOS, 0.37 ml of TMOS, 1.5 ml of EtOH, 0.35 ml of H_2O and 0.5 ml of HCl (pH =1.7) were mixed, stirred at room temperature for 3 hours and aged overnight.

Base-catalyzed approach. In a typical synthesis 0.15 ml of CTAC (cetyltrimethylammonium chloride, 25 wt %) and 0.13 ml of 25 % aqueous NaOH solution were added to 2.5 ml of deionized water under stirring followed by addition of 0.127 ml of PTMOS. The vial was then sealed, stirred at room temperature for 2 hours and aged overnight.

4.1.1 Proof of Principle

Three organophosphates have been selected as target analytes for detection in an aqueous environment: parathion, fenitrothion and paraoxon (see Table 2). These compounds represent suitable test analytes due to their IR specific absorption features caused by the nitro-group. While IR spectra of pure organophosphates reveal a multitude of IR spectral features, the most noticeable mid-infrared spectral absorptions, when using sol-gel coated waveguides, are the asymmetric and symmetric stretching vibrations of the nitro group at 1522 cm^{-1} and 1347 cm^{-1} as these are located within the characteristic IR spectral window for sol-gel membranes. Besides, as depicted in Figure 2, the sensing system arrangement is capable of performing organophosphate detection in the lower ppm range.

4.1.2 Sensing Performance: Comparison of Sol-Gel Coated Waveguides to Conventional Polymer Coated Waveguides

Figure 3 shows a comparison of the sensor response after 60 min using an (a, c) uncoated, (b) Teflon AF, and (d) sol-gel coated ZnSE waveguide to 2.5 ppm and 40 ppm parathion, respectively. It can be derived that neither the uncoated nor the Teflon coated waveguide are able to detect 2.5 ppm parathion with sufficient accuracy. A 40 ppm parathion solution measured with an uncoated crystal results in a clearly visible absorbance band, which shows approx. the same peak area as 2.5 ppm parathion detected with a sol-gel coated crystal. Hence, with respect to a bare ZnSe waveguide an enrichment factor of at least 20 is achieved in this example due to the sol-gel film. The fact that Teflon coated waveguides are not suitable for detection of these organophosphate analytes is probably related to the substantially higher hydrophobicity of Teflon. While Teflon is known to readily enrich chlorinated hydrocarbons, such as tricholoroethylene [4], sorption can be hindered in case of parathion by the polar character of the nitro-group. The additional advantage of sol-gel coated waveguides is that they require a significantly shorter sensor equilibration time in aqueous media (see Figure 4). Sol-gel membranes prepared from different organically modified precursors have also been analyzed in respect to their properties suppressing the water background. This feature is of particular importance for optical sensors based on mid-IR evanescent field spectroscopy as water is a strong IR absorber itself and would cause major interferences. The two graphs in Figure 5 demonstrate the ability of organically modified sol-gels to efficiently exclude water from the sensing region. The left part of the graph indicates that the surface polarity is not the only factor of influence in water suppression, otherwise the pure PTMOS coating should show the lowest water up-take. Membrane homogeneity and thickness certainly play an important role, which is demonstrated in the right graph, revealing that thicker coatings result in better water suppression. In the following, sol-gel membranes with thicknesses of about 1700 nm were used for further investigations. Although thicker films would additionally decrease interference by spectral water absorptions, thinner coatings were selected reducing the sorption time of the analyte and consequently providing shorter sensing response times.

4.1.3 Reproducibility

In order to investigate the reproducibility of the performed measurements with sol-gel coated sensing elements, repeated concentration series of two organophosphates, parathion and fenitrothion were analyzed. Results of three independent measurements of samples containing organophosphate concentrations between 0.5 ppm and 2.5 ppm are presented in Figure 6. The mean and standard deviation of repeated measurements at each enrichment time was determined and plotted vs. the input concentrations.

The results show that all peak area values fit a linear regression function and that the slopes of the linear fits increase with increasing enrichment times. These linear relationships were consistent for all measurement series as well as the fact that increased enrichment time corresponds to higher sensitivity. In particular, small error bars indicated in the right graph of Figure 6 demonstrate the reproducibility of this measurement technique. As the organophosphates reveal relatively long enrichment times into the sol-gel membranes different evaluation methods have been tested in respect to their applicability of analyzing the signal prior to the equilibrium state. Particularly, a chemometric approach using principle component regression (PCR) shows potential of evaluating the sorption curve before reaching the equilibrium, as already after 16 min the enrichment curve can be evaluated with similar accuracy to evaluation after 88 min. Improved algorithms currently developed in our laboratory will enable even faster evaluation of the sensor response.

4.1.4 Real World Measurements

In order to simulate real-world measurements, river water samples were collected from Peachtree Creek, an urban stream located in Atlanta, GA. Without any filtration or purification steps, the river water samples were spiked with 1 ppm and 10 ppm parathion, respectively. As a reference spectrum pure deionized water was used and a peristaltic pump assured a constant flow rate of 3 ml/min. In Figure 7 the response of a 1.7 µm acid catalyzed sol-gel coated ATR waveguide after 15 minutes is shown.

Both parathion concentrations are readily distinguished from the background signal indicating the feasibility of using sol-gel recognition layers for investigation of organophosphates at elevated concentration levels in a real-world aqueous environment.

As a concentration of 1 ppm is not a realistic environmental level for this type of pesticides the sensing system at the current development stage is not competitive with biosensors, which have limits of detection down to the sub µM (low ppb) concentration range [5]. However, as the sol-gel coated ATR system exhibits reliable performance and no degradation of the coating properties or optical behavior, it enables much longer operation times (up to several months) compared to biosensors. Strategies towards enhanced limits of detections for these optical sensing systems involve approaches aiming at improved control over porosity and hydrophobicity (see section 4.1.6).

4.1.5 Sol-Gel Coated Silver Halide Fiberoptic Waveguides

In the following, the use of silver halide fibers coated with porous sol-gels as mid-IR evanescent field sensing element for detection of nitro-based aromatic compounds is described. Due to the significantly lower costs of the chemical and lower toxic impact nitrobenzene was selected as model analyte in order to investigate potential and limitations of such sensing systems with respect to response behavior, reversibility of enrichment and reproducibility.

In order to ensure that the coating procedure provides a homogeneous film, scanning electron microscopy (SEM) images of the coated waveguide surface have been recorded and are presented in Figure 8. Derived from the SEM images and the known diameter of the fibers (700 µm) it can be estimated that the film thickness is in the range of 5 to10 µm for acid-catalyzed sol-gel membranes.

Results in Figure 9 demonstrate that nitrobenzene can be entirely removed after one enrichment process within 5 to 10 minutes of washing with the 10 % aqueous EtOH solution. Subsequent washing with water equilibrates the system for the next measurement. In the upper right corner of the left graph in Figure 9 desorption of the target analyte is shown applying only water during the regeneration step. The result clearly indicates that water extracts analytes slower from the sol-gel membrane due to the lower solubility of nitrobenzene in water compared to ethanol/water mixtures. Upon one hour of purging with water still a significant amount of nitrobenzene remains within the membrane. The left graph of Figure 9 also depicts the repeatability of the measurement procedure with a calculated RSD of 4.5 %. This value corresponds to similar ranges reported in literature (RSD of 2.5 % for poly(isobutylene)-coated sensor systems for reversible enrichment of tetrachloroethylene) [6]. Repeatability could be further improved by recording a new reference spectrum before each measurement. Herein reported experiments proof that no accumulation of analyte molecules ('memory effect') is evident within the sol-gel matrix even after several measurement cycles.

In order to further investigate reproducibility and to determine the limit of detection (LOD) of the applied method various concentrations of aqueous nitrobenzene solutions were prepared, pumped through the sensor flow cell and spectroscopically analyzed after an enrichment time of 10 min. The mean and standard deviation of repeated measurements in a concentration range of 40 ppm – 100 ppm were determined and plotted vs. input concentrations (see right graph of Figure 9). All peak height values fit a linear regression function with a correlation coefficient of 0.9951. The LOD for nitrobenzene is 10 ppm, which corresponds to a signal 3 times higher than the standard deviation of the background noise. Longer enrichment times result in lower LODs, e.g. sorption times of 60 min improve the LOD by a factor of approximately 2.

4.1.6 Approach to Influence Porosity of Thin Sol-Gel Membranes

So far, only acid-catalyzed sol-gel recognition layers have been reported for mid-IR applications [7] as usually crack-free thin films are obtained. However, as sol-gel materials are tunable in pore size distribution and porosity depending on the choice of catalyst, it is of great interest to compare acid- and base-catalyzed sol-gel layers with respect to their enrichment behavior.

Figure 10 depicts the comparison of enrichment properties of HCl- and NaOH-catalyzed sol-gels when exposed to aqueous parathion solutions in the lower ppm concentration range. The left graph shows data obtained with AgX fibers and results for ZnSe crystals as waveguides are shown in the right graph. The base-catalyzed material yields significantly better enrichment and faster penetration into the sol-gel membrane reaching the t_{90} value (90 % of enrichment) after approximately 40 min (AgX fibers) and after approximately 120 min (ZnSe crystals), respectively, while in case of the acid-catalyzed type the sorption process does not reach equilibrium even after 120 min of enrichment time. This effect is consistent with larger pores and higher porosity of base-catalyzed sol-gel materials reported in literature [8]. Furthermore, collapse and shrinkage of the pore channels during the drying process is usually less pronounced than for the acid catalyzed sol-gels, which would enhance access for the analyte parathion.

4.1.7 Summary

Thin film membranes with a thickness of a few µm have been fabricated at the surface of planar ATR crystals and silver halide fibers using mixtures of the precursor tetramethoxysilane (TMOS) and low molecular weight organoalkoxysilanes with various functionalities. The 3:1 molar mixture of phenyltrimethoxysilane and tetramethoxysilane yields films of high homogeneity with comparatively hydrophobic properties confirmed by water contact angle measurements. This approach results in excellent water suppression, which is a prerequisite for successful IR measurements in aqueous environments. The organophoshates parathion, fenitrothion and paraoxon were detected in the low ppm and sub-ppm concentration range using acid-catalyzed sol-gel films. High stability and reproducibility was demonstrated, however, contrasted by enrichment times of several hours. Hence, a variety of kinetic signal evaluation methods were investigated to minimize the response time of the sensing system. Multivariate concentration evaluation methods based on multivariate linear regression and principle component regression proved advantageous over conventional linear regression models enabling reliable signal evaluation after approx. 30 min. Real world measurements of parathion spiked river water samples indicated the feasibility of such an *in situ* sol-gel based chemical IR sensing system especially for field screening applications which are not sensitive to the response time and for expected concentration ranges in the sub-ppm region. For the first time the combination of sol-gel based membranes with mid-IR transparent silver halide fibers was demonstrated, which is particularly important as such robust sol-gel materials significantly improve the lifetime of these delicate fiber materials. In addition, evanescent field spectroscopy enables *in situ* monitoring of the sol-gel coating, drying and aging process. Reversible enrichment of nitrobenzene for multiple measurement cycles was shown and linear relationship between peak height of selected absorption bands and input concentrations was obtained. When comparing acid- and base-catalyzed sol-gel membranes faster response time and enhanced enrichment are yielded for the environmentally relevant pesticide parathion, which corroborates the theory of larger pores and higher porosity for base-catalyzed sol-gels.

4.2 Simultaneous Quantitative Determination of Benzene, Toluene and Xylenes in Water Using Mid-Infrared Evanescent Field Spectroscopy

Attenuated total reflection mid-infrared (ATR-IR) spectroscopy using ZnSe ATR crystals is applied for simultaneous detection and quantification of the environmentally relevant analytes benzene, toluene, and the three xylene isomers (BTX). The analytes are enriched into a thin ethylene/propylene co-polymer membrane coated onto the surface of the internal reflection waveguide, which is exposed to the aqueous sample. As shown in Figure 11 linear relationships between characteristic absorption peak areas vs. input concentrations with R^2-values > 0.99 have been obtained for each analyte along with high reproducibility for 5 consecutive measurements. Detection limits lower than 20 ppb (v/v) have been achieved for all xylene isomers and of approx. 80 ppb (v/v) for benzene and 50 ppb (v/v) for toluene, respectively. Equilibrium conditions for this diffusion based sensor were achieved within approx. 18 min. At the present stage of development the sensor system is suitable as analytical device for online, in-situ process monitoring of multiple organic components at low ppb concentrations.

4.3 Molecularly Imprinted Polymers Selective For β-Estradiol

Experimental. The polymers were prepared using bulk polymerization by initially dissolving the template molecule 17β-estradiol in a mixed solvent (9 ml acetonitrile with 3 ml acetone). Upon the successive addition of the functional monomer (MAA), the cross-linker (EDMA), and the initiator (0.381 mmol) the reaction mixture was degassed by sonication and saturated with argon for 5 min. Afterwards, the tubes were sealed under argon and the pre-polymerization mixture were thermally polymerized at 60 ^{o}C for 16 h. Subsequently, the bulk polymers were dried at 40 ^{o}C in an oven and each polymer was ground with a mechanical mortar and sieved in acetone to yield a fraction with a particle size < 25 μm. Fine particles were removed by repeated sedimentation in acetone. The polymer particles were slurry-packed into a stainless steel HPLC column (250×4.6 mm) and the template was extracted by washing with methanol-acetic acid (85:15, v/v) for 6 h. The control polymer was prepared in exactly the same way without adding the template molecule.

Results. The results of the chromatographic separation of 17α-estradiol and 17β-estradiol using imprinted polymer and control polymer as stationary HPLC phases are presented in Figure 12. While HPLC runs using control polymers as stationary phase did not result in a separation of these structurally very similar analytes, separation can be achieved when applying imprinted polymers as stationary phase. These results indicate the existence of 17β-estradiol selective recognition sites and can be seen as a first step towards the formation of highly selective separation materials for the endocrine disrupting compound (EDC) 17β-estradiol.

5 WORKING PLAN FOR THE 2nd YEAR

- Continued development of sol-gel chemistry towards better control on porosity and surface termination for increased sensitivity.
- Continued MIP development for (i) sensing applications and (ii) suspension polymerization strategies for the development of MIP beads for SPE and HPLC applications.
- Collaboration with USGS Atlanta to coordinate real-world measurements at Rottenwood Creek with accompanying validation.
- Field measurements at Rottenwood Creek.
- Prototype IR evanescent field sensor for in-situ chlorinated hydrocarbon analysis.
- Hollow waveguide based IR sensor for VOC analysis.

6 FIGURES AND TABLES

	1ST YEAR (QUARTERS)				2ND YEAR (QUARTERS)			
	1	*2*	*3*	*4*	*1*	*2*	*3*	*4*
WP 1	Development of chemical recognition layers based on sol-gels							
			Implementation of sol-gels as coating materials for the fiber optic evanescent wave sensor system					
	Molecular imprinting strategies for selected organic pollutants							
			Characterization of molecularly imprinted polymers and their application as novel recognition layers					
WP 2	Optimization of the FT-IR based fiber optic evanescent wave sensor prototype							
		Measurement of real-world samples						
					Field measurements at Rottenwood Creek			
WP 3			Alternative sensing concept based on IR hollow waveguide sensor combined with capillary membrane sampler					

Figure 1: Time schedule and work plan

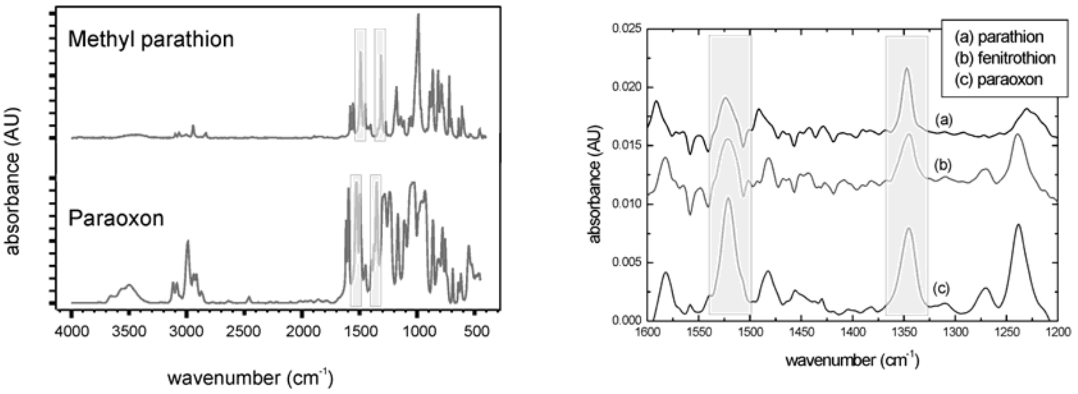

Figure 2: (left) Pure IR spectra of methyl parathion and paraoxon obtained from the Bio-Rad Sadtler IR database, (right) ATR spectra of 2.5 ppm parathion, 2.5 ppm fenitrothion, and 3 ppm paraoxon, 1.7 µm acid catalyzed PTMOS/TMOS sol-gel coated ZnSe ATR crystal, gray areas indicate the wavenumber region suitable for concentration evaluation by peak area integration.

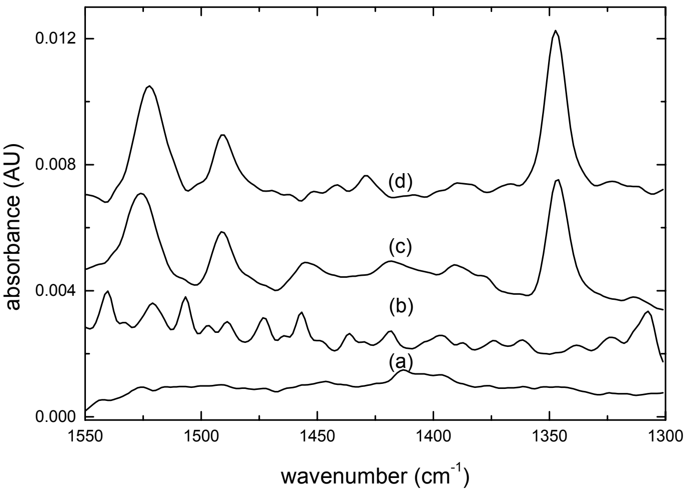

Figure 3: Response to the organophosphate parathion produced after 60 minutes by ZnSe waveguide sensors mounted in a flow-through cell. Spectra are shifted in the y axis for better illustration. (a) uncoated waveguide purged with 2.5 ppm parathion (b) an Teflon AF coated waveguide purged with 2.5 ppm parathion (c) uncoated waveguide purged with 40 ppm parathion (d) sol-gel coated waveguide purged with 2.5 ppm parathion.

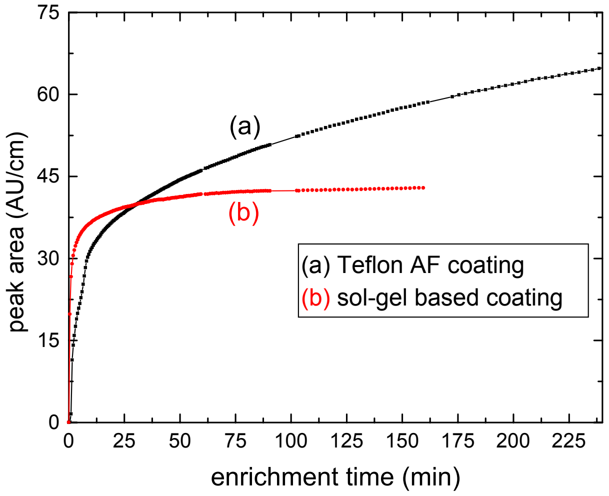

Figure 4: Comparison of water up-take of coatings based on Teflon AF (3 µm thick) and PTMOS/TMOS sol-gels (2 µm thick) on ZnSe crystals, monitored via ATR FT-IR spectroscopy.

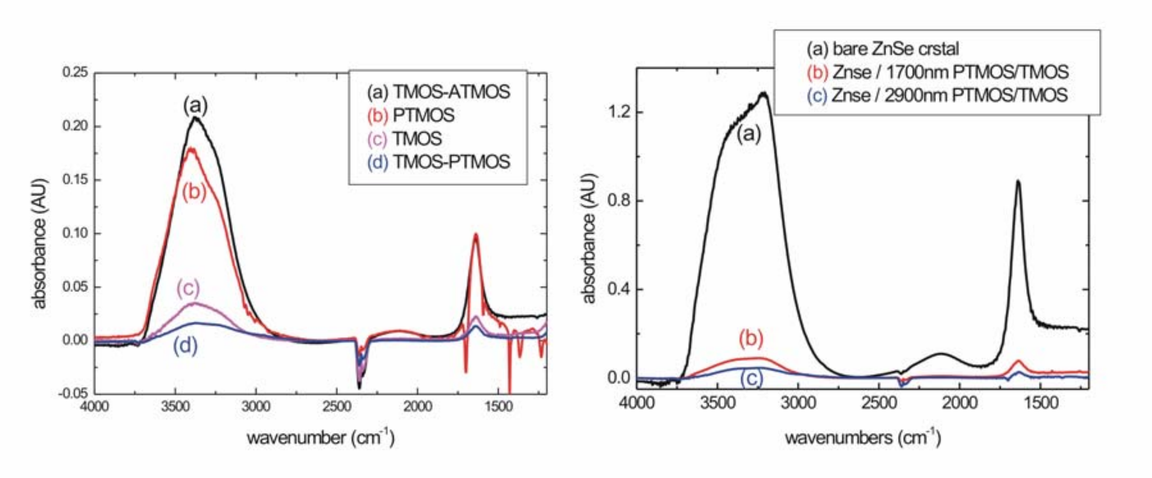

Figure 5: IR absorption caused by water up-take of sol-gel membranes on ATR crystals: (right) influence of various sol-gel precursors on the water suppression, (left) comparison of the water spectrum recorded using a bare crystal with sol-gel coated ATR elements of different membrane thicknesses.

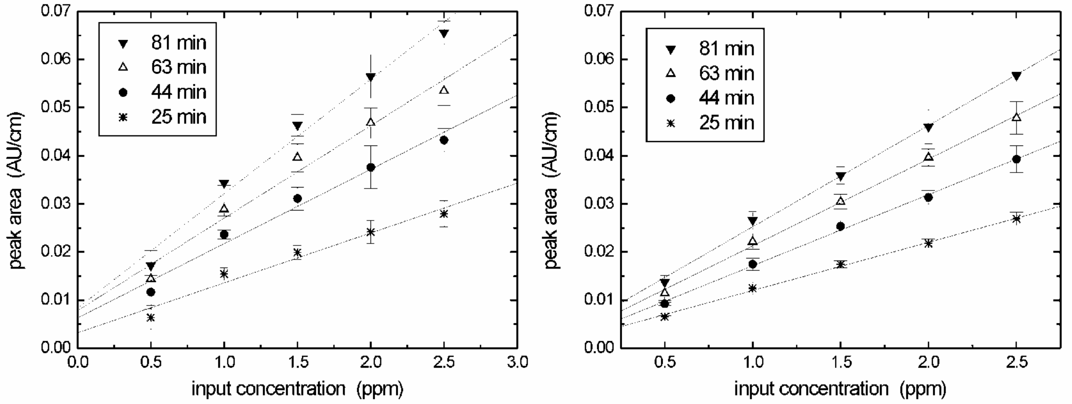

Figure 6: Calibration curve of fenitrothion (left) and parathion (right) over the concentration range of 0.5 – 2.5 ppm evaluated at different times during the enrichment process (error bar on the highest concentration point of the 81 minute data point for parathion is missing due to only two available data points).

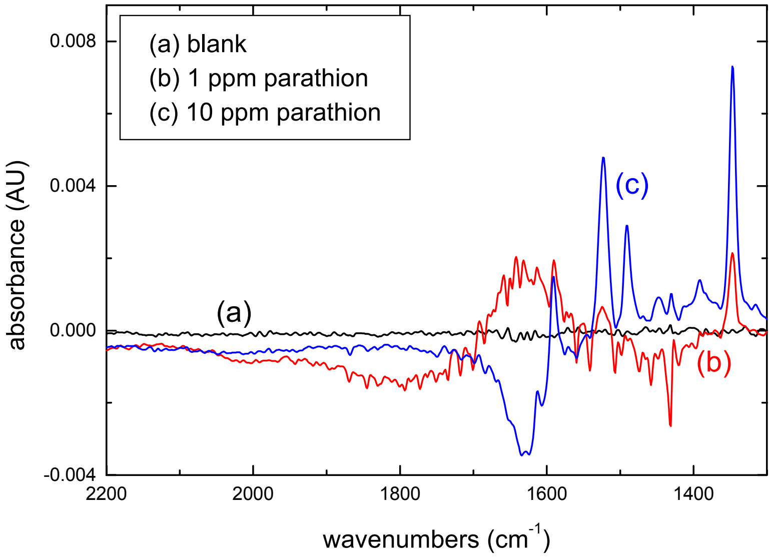

Figure 7: Sensor response after 15 minutes to 1 ppm and 10 ppm parathion spiked river water.

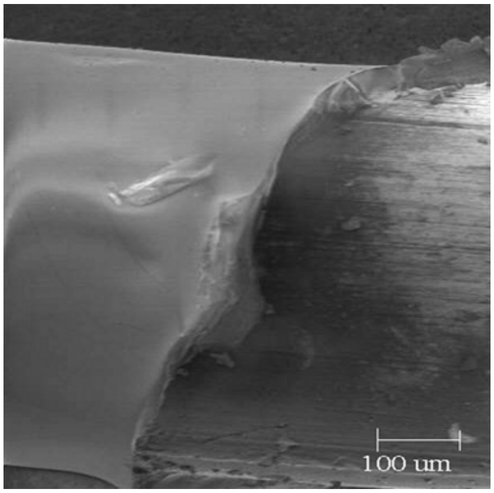

Figure 8*:* SEM images of sol-gel coated silver halide fibers. The right section of each fiber was protected with tape before application of the sol-gel coating.

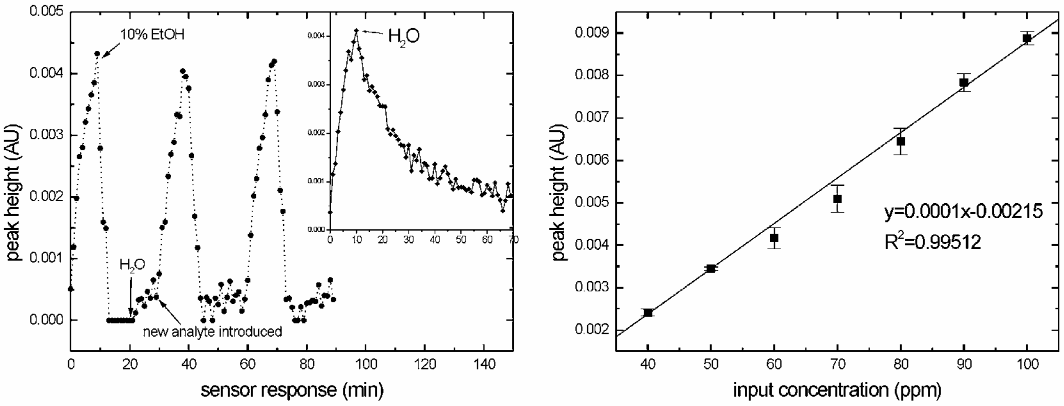

Figure 9*:* (left): Enrichment and desorption of a 50 ppm nitrobenzene solution using acid-catalyzed sol-gel coating, (right): Calibration curve of nitrobenzene over the concentration range of 40 – 100 ppm using acid-catalyzed sol-gel coating and performing three consecutive measurements.

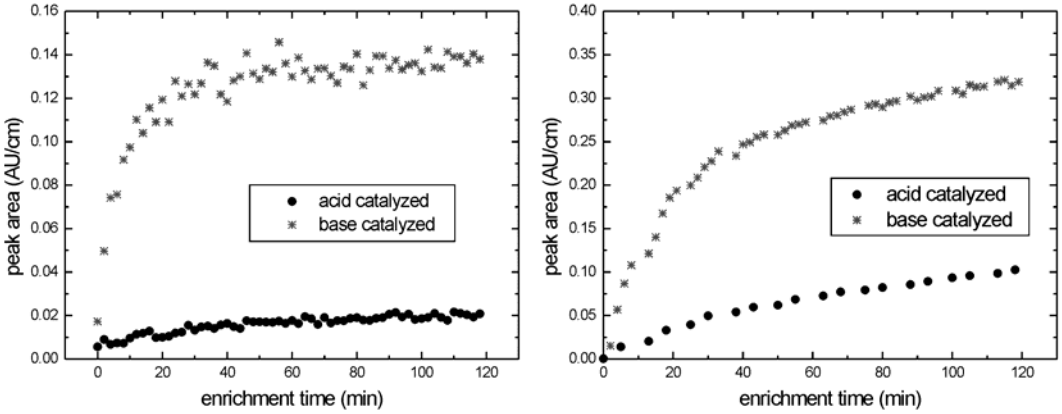

Figure 10: Comparison of enrichment behavior of acid- and base-catalyzed sol-gels, (left) using AgX fibers and a 50 ppm parathion solution; (right) using ZnSe crystals and a 2.5 ppm parathion solution.

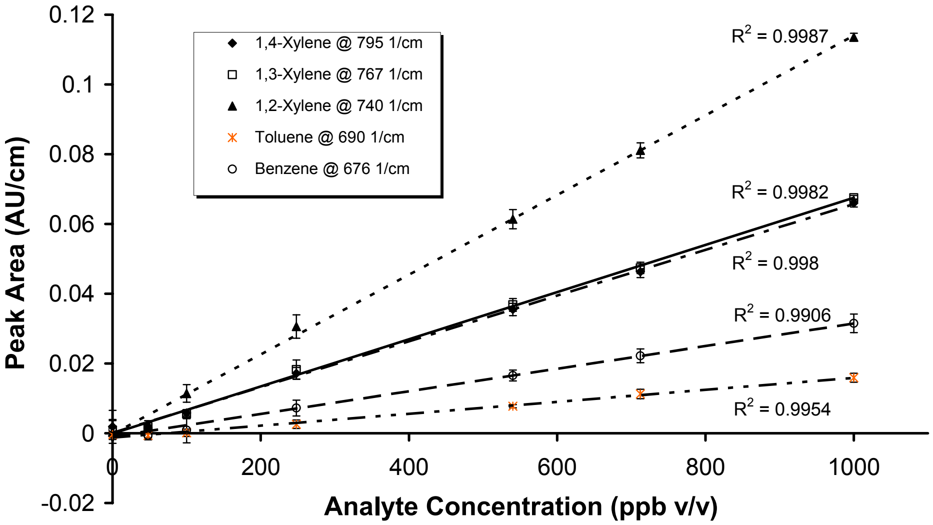

Figure 11: Calibration graphs for benzene, toluene and the xylene isomers in the concentration range of 0 – 1000 ppb (v/v) based on peak area integration. The error bars represent the standard deviation of five subsequent measurements.

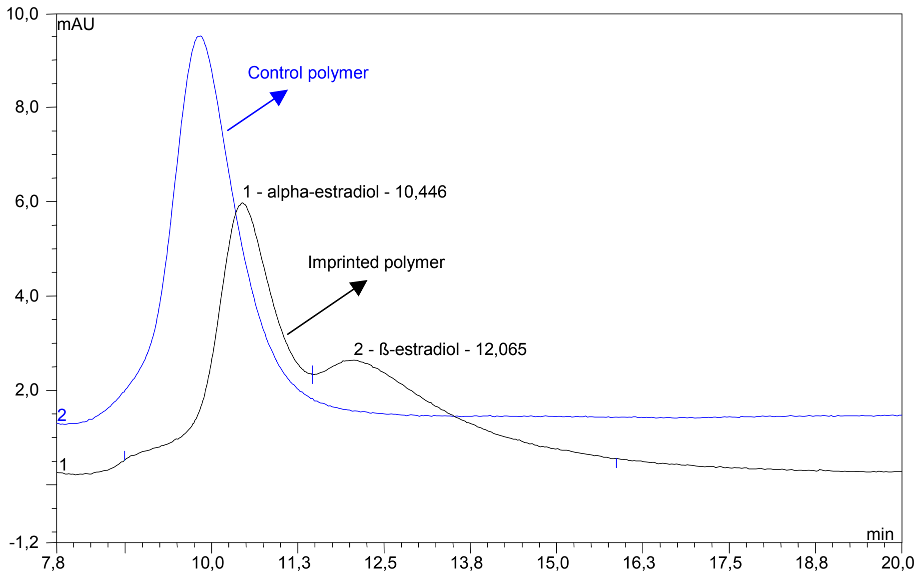

Figure 12: Chromatographic separation of 17α-estradiol and 17β-estradiol (1×10^{-2} µg each) using imprinted polymer, and control polymer as stationary phase. 250×4.6 mm stainless steel columns were used. Acetonitrile containing 1% acetic acid was applied as mobile phase at a flow rate of 0.6 ml/min.

Table 1: Composition of pre-polymerization sol-gel mixture for acid and base catalyzed approaches.

		acid catalyzed (ml)	base catalyzed (ml)
sol-gel precursor	PTMOS	1.4	0.127
	TMOS	0.37	
catalyst	HCl	0.5	
	25% NaOH		0.065
	H_2O	0.35	2.5
solvent	EtOH	1.5	
surfactant	cetyltrimethyl-ammonium chloride		0.15

Table 2*: Selected organophosphates including their chemical structure and properties*

	Chemical structure	Comments
Parathion	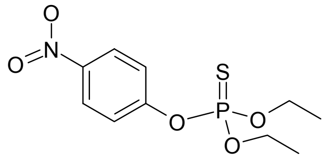	rapidly hydrolyses at alkaline conditions (pH>10); hydrolytically stable under sterile conditions at pH 4 – 9; very toxic to aquatic organisms; may cause long-term effects in the aquatic environment; classified as a Restricted Use Pesticide (RUP)
Fenitrothion	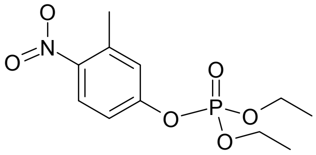	less toxic than parathion; heavily used in countries, such as Japan where parathion has been banned
Paraoxon	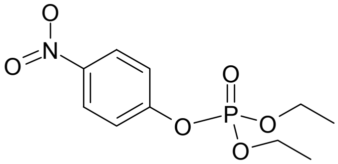	active metabolite of parathion; inhibits cholinesterase and is further metabolized to compounds, such as para-nitrophenol

7 REFERENCES

1. M. Janotta, M. Karlowatz, F. Vogt, B. Mizaikoff, *Sol-gel Based Mid-Infrared Evanescent Wave Sensors for Detection of Organophosphate Pesticides in Aqueous Solution*, in press, Anal. Chim. Acta (2003).
2. M. Janotta, A. Katzir, B. Mizaikoff, *Sol-gel coated fiber–optic sensors for the mid-IR,* Appl. Spec., **57(7)**, 823-828, (2003)
3. M. Karlowatz, M. Kraft, B. Mizaikoff, *Simultaneous Quantitative Determination of Benzene, Toluene and Xylenes in Water Using Mid-Infrared Evanescent Field Spectroscopy,* submitted, Anal. Chem. (2003)
4. R. Krska, K. Taga, R. Kellner, *New IR fiber-optic chemical sensor for in situ measurements of chlorinated hydrocarbons in water*, Appl. Spec., **47**, 1484-1487 (1993)
5. M. Trojanowicz, *Determination of pesticides using electrochemical enzymatic biosensors*, Electroanalysis, **14(19-20)**, 1311-1328 (2002)
6. J. E. Walsh, B. D. MacCraith, M. Meany, J. G. Vos, F. Regan, A. Lancia, S. Artjushenko, *Sensing of chlorinated hydrocarbons and pesticides in water using polymer coated mid-infrared optical fibers*, Analyst, **121**, 789-792 (1996)
7. F. G. Haibach, A. Sanchez, J. A. Floro, T. M. Niemczyk, *Extended spectral range surface-modified sol-gel coated infrared waveguide sensors*, Appl. Spec., **56(3)**, 398-400 (2002)
8. C.J. Brinker, G.W. Scherer, Sol-Gel Science: *The physics and chemistry of sol-gel processing,* Academic Press, Inc.: New York, (1990)

Nile Decision Support System

Basic Information

Title:	Nile Decision Support System
Project Number:	2002GA28O
Start Date:	7/1/2001
End Date:	6/30/2003
Funding Source:	Other
Congressional District:	11
Research Category:	Climate and Hydrologic Processes
Focus Category:	Agriculture, Hydrology, Water Use
Descriptors:	Information and Decision Tools for River Basin Management
Principal Investigators:	Aris P. Georgakakos

Publication

1. Georgakakos, A., and K. Georgakakos, 2003, Value of Climate and Hydrologic Forecasts for River Basin Planning and Management, Key Note Address, GEWEX Workshop, IUGG Conference, Saporo, Japan.
2. Georgakakos, A., and H. Yao, 2002, "Implications of Climate Variability and Change for Water Resources Management, The Climate Report, 3(4), 9-13.

Nile Decision Support Tool: Executive Summary

1. Introduction and Overview

The Nile River Basin is spread over ten countries covering an area of about 3.1 million km^2, or approximately 10 percent of the African continent. The river discharge per unit drainage area is relatively small, and almost all of the Nile water is generated from 20 percent of the basin, while the remainder is in arid or semi-arid areas. The Nile Basin encompasses five main regions (Figure 1): (a) the Equatorial Lake sub-basin within the countries of Uganda, Tanzania, Kenya, Rwanda, Burundi, and Congo, (b) the Sudd, the Bahr el Ghazal, and the Sobat River Basin (in Sudan and Ethiopia), (c) the White Nile (in Sudan) connecting the Sudd with the Blue Nile, (d) the Blue Nile and Atbara Rivers draining parts of Ethiopia, Eritrea, and Sudan, and (e) the Main Nile flowing through Northern Sudan and Egypt. Each region has distinct hydrologic features, water use requirements, and development opportunities.

The Nile Decision Support Tool has been developed as part of the Nile Basin Water Resources Project (GCP/INT/752/ITA) in collaboration with the Nile focal point institutions. The model purpose is to assess the benefits and tradeoffs associated with various basin wide water development and management options. The guiding principles for the development of the Nile DST are outlined below:

- The *data of the Nile DST should be shared and agreed upon* by the Nile Basin nations;

- The Nile DST should be based on *sound and current scientific and engineering approaches* able to handle the Nile Basin size, natural complexity, and range of development and management options; It should also include functionalities useful for users of varying technical backgrounds and experience, from novice to advanced;

- The Nile DST should be a *neutral* decision support tool; Thus, its overriding purpose should be to objectively assess the benefits and tradeoffs associated with various water development and sharing strategies that may interest the Nile Basin partners individually or as an interdependent community of nations;

- The Nile DST should be *sustainable and adaptable* as future needs arise; The implications of this are twofold: First, the Nile DST should be based on *widely supported* computational technology and should be *expandable* to incorporate new data and applications; Second, *effective technology and know-how building* mechanisms should be implemented during the Nile DST development as well as for the long term.

The Nile DST includes six main components: database, river simulation and management, agricultural planning, hydrologic modeling, remote sensing, and user-model interface. Each component has been described in detail in separate technical reports and user manuals. The purpose of this report is to provide an executive summary of these documents. The report is organized in 7 sections. Sections 2 to 6 outline the project accomplishments and future opportunities with respect to each Nile DST component. Section 7 provides a longer term vision of potential Nile DST benefits and impacts.

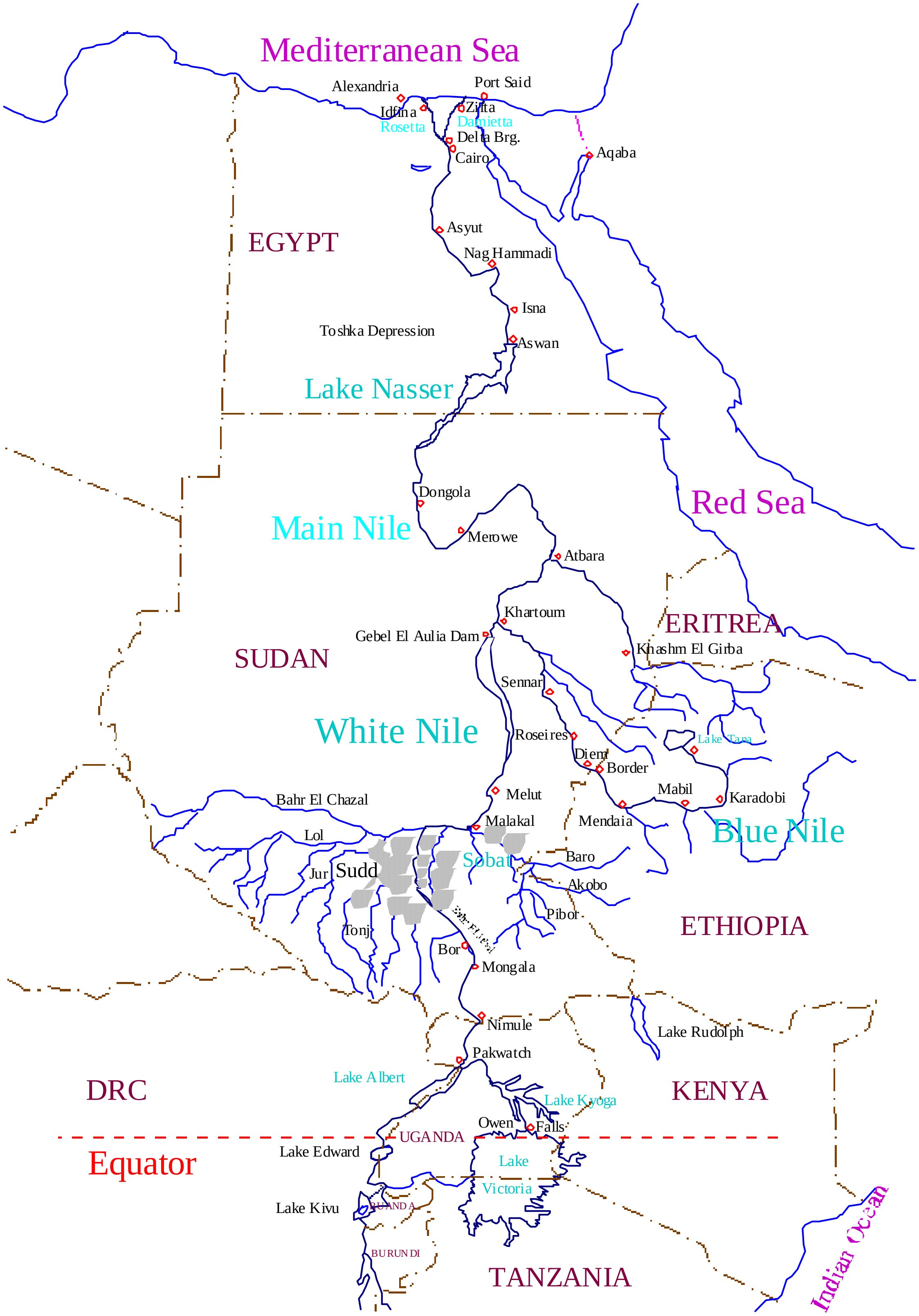

Figure 1: The Nile River

2. Database

2.1 Nile DST Database: Accomplishments

Flexible and Expandable Database Design

The Nile DST database is an object-oriented, databasing structure developed to (**1**) house all types of data (existing as well as future) required by a comprehensive water resources decision support tool and (**2**) to optimize data entry, access, visualization, and analysis. It is important to emphasize that to support the process of water resources planning and management, the data base is designed with the ability to grow, namely, to accept new data, regardless of its type and size. Further, this tool is capable of visualizing and analyzing the data in efficient and meaningful ways.

Database Contents

The Nile DST database is of considerable size. In fact, it is not one but many databases. Each of the Nilotic countries has painstakingly provided an MS Access database of station data with measurements of more than 30 parameters. In addition to this, the project has compiled some 3 years of remotely sensed data that covers the entire basin. The temporal resolution of the remotely sensed data is 30 minutes, and the special resolution is approximately 5 km x 5 km. Derived data products are also included in the database including climatic zone data that is based on the original station data and is used in the Nile DST agricultural planning module. Finally, the entire database used in the Lake Victoria Decision Support System has been incorporated in the Nile DST database. All together, this data represents some 37 GB of information, the largest such collection ever compiled for the Nile Basin.

Data Visualization

The data visualization tool in the Nile DST provides a seamless system to look at all of the databases. At its heart is a tree-style exploring tool (data tree) that at once shows the entire contents of the Nile DST database and, equally importantly, allows the user to navigate down to greater and greater levels of detail. Due to the database's sheer size, the data tree is necessary to promote user awareness and understanding of the database. Each database in the tool has a geo-referenced component and time series component. The geo-referenced data is viewed in the mapping tool, which holds a geographic information system (GIS). The mapping tool incorporates the ESRI Inc. Map Objects mapping plug in to ensure compatibility of the system with industry standard GIS files. The time series data is viewed in the charting tool, which features a powerful chart and aggregation and statistics calculators. Together, the charting tool, mapping tool, and the data tree work seamlessly to provide the user with an ability to view any piece of information in the system quickly and meaningfully.

Data Analysis

The data analysis tool provides powerful data manipulation capabilities for current and future applications. The user can instruct the Nile DST to take information from its databases in user specified forms, operate on the data, and construct maps of the output. One example of this is the generation of mean areal precipitation (MAP) estimates over user-specified areas. This process requires spatially defining the watershed of interest, defining a grid that covers this watershed, deriving from stations a time series for each of the grid cells in the watershed, and then aggregating each of the time series into one time series that represents the precipitation for the entire watershed. Traditionally, this process takes a spreadsheet program, a database program, and a GIS program, and a user who understands how to transfer data between them. The data analysis tool brings all of this together into one graphical map. The benefits of this tool are wide ranging. First, the tool greatly reduces error and processing time. More importantly, the MAP process described above is but one example in an extensive set of analyses that a user can build. Finally, the tool allows the user to save the graphical map of the analysis, which is a built-in method of journaling analyses, a task rarely done well in water resources planning.

Training

To this point, there have been two training workshops on the database. The first took place in Dar es Salaam, Tanzania in June, 2002. The workshop concentrated on describing the design principles of the database. Participants were lead through database principles to final database design. An alpha version of the software was displayed to show the implementation of the design. The second workshop took place in Entebbe, Uganda in February, 2003. In that workshop, the beta version of the software was installed on computers, and the participants went through extensive and realistic exercises of data access, visualization, and general manipulation. Since the second training workshop, significant database capabilities have been added to the Nile DST software. The opportunity to provide training on the recent database features has not yet realized.

Technical Report and Manual

A detailed technical report and manual describing the methods used, application range, and software usage have been developed and provided as part of the final deliverables.

2.2 Nile DST Database: Future Opportunities

The Nile DST database system is a technical tool that the Nile water professionals can use to comprehensively compile, quality control, and analyze existing and future data sets. Some of the future opportunities and recommendations are listed below:

- *Training*: As mentioned earlier, new important database features have recently been added to the Nile DST on which the national modelers have not yet received training. These features include (**1**) the Data Analysis Tool and (**2**) a versatile and user-friendly data entry system. As described in the "Accomplishments" section, the data analysis tool represents a powerful component of the database system that enables the Nile water professionals to perform extensive and complex data-related functions. The data entry system facilitates adding data to existing stations, adding new stations within a database, and even adding new databases.

- *Database extension:* The Nile DST database contains all data provided to Georgia Tech during the project tenure. However, due to time constraints, very useful hydro-meteorological data (a good part of which exist in digital form) have not been provided and are not included in the Nile DST. It is recommended that this data be compiled and added to the Nile DST database to insure their preservation and beneficial use.

- *Data Quality Control:* There is a clear need to systematically quality control the data in the national data bases and in the Nile DST. The reader is referred to Georgia Tech's reports on "Remote Sensing" and "Hydrology" where these issues are discussed at length. Data quality control would have to be done primarily by the countries with Georgia Tech or other experts establishing systematic protocols and procedures. Country engineers, knowledgeable in the history of data collection, would provide the only sound basis for data infilling and verification. The Nile DST database system would provide an effective tool to consistently implement the quality control process.

3. River Simulation and Management

3.1 Nile DST River Simulation and Management: Accomplishments

The Nile DST River Simulation and Management system aims at simulating the Nile response under different hydrologic, development, and management scenarios. Thus, its overriding purpose is to objectively assess the benefits and tradeoffs associated with various water development, sharing, and management strategies that may interest the Nile Basin partners individually or as an interdependent community of nations. Tradeoffs exist among water uses in the same country and across the Nile countries. The river basin planning and management Nile DST component has several unique features:

Data

The database of this module includes extensive data in five major categories: (**a**) River network configuration, (**b**) river hydrology, (**c**) existing and planned hydro facilities, (**d**) water use, and (**e**) reservoir/lake regulation rules. Data can be viewed, added, or modified as necessary through a user-friendly interface. The actual river system is represented by a network of river nodes, reaches, and reservoirs, each with its own attributes. River nodes represent locations of local inflow and/or water withdrawals and returns. River reaches represent physical river segments and their water transport characteristics. Reservoirs represent man-made or natural lakes that may support various water uses including water supply, flood control, drought management, hydropower, and others.

Models

The Nile-DST river simulation and management model simulates the flow of water through the various system nodes, reaches, and reservoirs. In keeping with its planning purpose, the model time resolution is 10-days. The simulation model includes a routing model for each river reach and regulation rules for each reservoir. Two types of reservoir regulation rules are included: (**1**) Simple static rules and (**2**) dynamic multi-reservoir coordination rules. Simple reservoir regulation rules define reservoir release as a function of reservoir elevation, inflow, irrigation demand, time of the year, or some combination of these parameters. The Nile-DST user can select and define any of these options. These regulation rules are very common, but they are simple because they relate reservoir release to a few parameters of the same reservoir and, possibly, of nearby reservoirs. Dynamic multi-reservoir coordination rules are also possible and are available through the system optimization model. System optimization encompasses four sub-models pertaining to (**a**) streamflow forecasting, (**b**) river and reservoir simulation, (**c**) reservoir optimization, and (**d**) scenario assessment.

Selected Applications

The Nile-DST river simulation and management model can be used to provide answers to various important questions. Typical applications are listed below:

- Value of various regulation, hydro-power, and irrigation projects along the White, Blue, and Main Nile branches; Such assessments could quantify the incremental benefits from individual development projects as well as the combined benefits from various project configurations;
- Implications of reservoir regulation rules for local, upstream, and downstream riparians;
- Marginal value (gain or loss) of irrigation with respect to hydropower at various basin locations;
- Irrigation versus hydropower tradeoffs for each nation, region, and the entire basin.

The Nile-DST utilizes several assessment criteria of possible interest to the Nile Basin nations. These criteria include

(i) severity and frequency of shortages with respect to user-specified water supply targets;
(ii) water withdrawals and losses over user-selected regions and times of the year;
(iii) reservoir and lake level drawdown and spillage statistics;
(iv) in-stream flow availability at user-selected river nodes and reaches;
(v) flood and drought severity and frequency;
(vi) annual and firm energy generation statistics.

Training

As with the rest of the Nile DST, there have been two training workshops on the river simulation and management model. The training in Dar es Salaam, Tanzania (June, 2002) concentrated on methods for river flow forecasting, routing, and simulation, and on reservoir regulation. The workshop in Entebbe, Uganda (February, 2003), was a hands-on training experience where the national modelers defined and run various scenario assessments. At the end of the workshop, the national modelers presented their assessments to the first evaluation mission and demonstrated good command of the model functions. However, following the last workshop, additional optimization features have been added to the Nile DST.

Technical Report and Manual

A detailed technical report and manual describing the methods used, application range, and model usage have been developed and provided as part of the final deliverables.

3.2 Nile DST River Simulation and Management: Future Opportunities

The river simulation and management model is the centerpiece of the Nile DST as it is designed to support water sharing policy debates with factual information. Although the model is presently able to perform this function, its value for the Nile countries can be maximized with additional training and the inclusion of more data.

- *Training*: Two national modelers have been trained from each country and have demonstrated good understanding of model capabilities. However, the model can assess a plethora of development scenarios, water sharing strategies, and management options and there has not been enough time to cover all of its features and capabilities. Furthermore, the purpose of the Nile DST is to convert data and models into information and understanding of the issues, and this requires systematic model usage by several competent individuals. There is a clear need to continue the training and capacity building process until a large enough human resources pool has been created that can adequately support the information needs of the decision makers.

- *Additional Data:* All Nile river reaches have been modeled to the extent that the data have allowed. However, additional data clearly exist that can easily be incorporated to increase the model spatial resolution and assessment range. To this end, a better representation of the Sobat river and its tributaries, the Blue Nile in Ethiopia, and the Main Nile in Egypt would add simulation accuracy and perhaps reveal more interesting water sharing options and strategies.

4. Agricultural Planning

4.1 Nile DST Agricultural Planning: Accomplishments

The Nile DST Agricultural Planning module has been developed as an integrative tool useful for various analyses relevant to crop production and irrigation in the Nile Basin. The main purpose of this component is to assess the crop yield potential and irrigation needs at different locations within the Nile basin. This information can be used to define meaningful scenarios for the assessment by the river simulation and management model. The software integrates several different technologies into a user-friendly form. These technologies include databases, geographic information systems, advanced crop growth models, optimization techniques, and agricultural management tools. In its present form, the Agricultural Planning module can be used for the following applications:

Applications

- Crop growth and production can be simulated for 11 crops at any point in the Nile Basin based on historical meteorology;
- The optimal quantitative relationship between crop yield and irrigation (the "crop-water production function") can be determined as a continuous function from rainfed to fully irrigated conditions;
- Optimized irrigation schedules can be found for all points on the crop-water production function;
- By simulating for multiple years of climatic data, variability of crop yield and irrigation needs can be determined;
- Irrigation management for individual farms or irrigation districts can include information on yield-irrigation relationships, irrigation schedules, and sensitivity to other parameters provided by the module; and
- Long-term planning decisions can include agricultural assessment results for questions of water availability and sharing.

Training

Training relevant to the Nile DST Agricultural Planning module has been conducted during both training workshops in June 2002 (Tanzania) and February 2003 (Uganda). Training in Tanzania included the following methodological aspects:

- Physical science of soil-plant-water systems,
- Physiologically based crop models,
- Irrigation planning and management techniques,
- Optimization of irrigation systems, and
- Vulnerability of agricultural systems under climate variability.

Training in Uganda included hands-on usage of the model to develop crop water production functions and perform sensitivity analysis on parameters affecting crop yield. Such parameters were related to hydro-meteorological data, soil types, and planting dates.

Technical Report and Manual

A detailed technical report and manual describing the methods used, typical applications, and model usage have been developed and provided as part of the final deliverables.

4.2 Nile DST Agricultural Planning: Future Opportunities

- *Training:* Previous training aimed to engage the national modelers most of whom have a water resources and hydrology background. While these professionals are interested in the water aspects of the model, the Nile DST Agricultural Planning system is a tool with functions especially meaningful to agricultural engineers and scientists. Availing the model to agricultural professionals would increase its utility and impact. It is recommended that a training strategy be developed to engage agricultural professionals in the training process. In time, these professionals would enhance the model application range to local crop varieties and conditions and ensure its sustainability.

- *Data:* The Agricultural Planning module has been developed to use the Nile DST Database as fully as possible. In some cases, important meteorological data have not been available in the database, and a system of climatic zones was developed to fill in average regional values for unavailable parameters. Continued additions of meteorological data, from both the past and future, will allow for more accurate and comprehensive assessments. Furthermore, results from crop experiments have been used when available to verify the crop models. Continued collection of this data from agricultural experiment stations in the region will allow for continued calibration and verification of model parameters.

- *Model Extensions:* In its present form, the Agricultural Planning module is capable of producing results for many types of analyses. Further tools can be added to increase its capabilities. Particularly, an economic valuation module can be included to analyze net profits from agricultural operations by considering factors such as crop prices, costs of water and other inputs, profit goals, and risk analysis.

5. Hydrologic Modeling

5.1 Nile DST Hydrologic Modeling: Accomplishments

Data, Models, and Applications

Hydrologic watershed models provide the means to describe the response of river basins (streamflow and soil moisture) to different conditions of rainfall and temperature. A hydrologic model has been developed in a generic form and has been applied to selective Nile sub-basins where data allowed. A detailed technical report has been provided describing the modeling method, the input data preparation process (step by step), and the model outputs. The model applications are particularly instructive, showing the significance and necessity of good quality hydrologic and hydro-meteorological data.

Thus, including other existing data and the need for data quality control are clearly illustrated. Notwithstanding data limitations, the hydrologic model is applicable to any basin for which suitable data can be assembled.

Training

Hydrologic training has been provided at the two training workshops, with methods emphasized in the first and model usage in the second. However, due to workshop time limitations, the time allotted to this module has been insufficient to cover all software features and hydrologic modeling issues.

Technical Report and Manual

A detailed technical report and manual describing the hydrologic model, typical applications, and software usage have been developed and provided as part of the final deliverables.

5.2 Nile DST Hydrologic Modeling: Future Opportunities

- *Training and Nile DST Ownership:* As mentioned above, the national modelers would benefit from additional hydrologic model training. However, the hydrologic model also presents an excellent opportunity to develop model "ownership" on the part of the national experts. This is because the development of valid hydrologic models requires that the national modelers and their agency colleagues systematically review and assess all relevant data, basin-by-basin. This process would be tedious but would provide full appreciation of the existing data quality and their importance in modeling applications. The Nile DST data analysis tool can be used to facilitate this process.

- *Data Monitoring Based on Modeling Needs:* To this point, no real connection has been established between the two major project components of data monitoring and model development. The hydrologic model (as well as the remote sensing model to be discussed next) presents an excellent opportunity to assess where data is needed from a modeling standpoint. This connection is crucial and it will help prioritize monitoring needs with the highest payoff or maximize the value of monitoring investments.

6. Remote Sensing

6.1 Nile DST Remote Sensing: Accomplishments

Data, Models, and Applications

A fairly comprehensive remote sensing data set was availed to the project only recently. In spite of these delays, a remote sensing component has been developed and is included in the Nile DST. Two remote sensing rainfall estimation procedures have been calibrated and validated, and a comprehensive assessment has been made for all regions of the Nile Basin. The results are very interesting (**1**) demonstrating the value of remote sensing information for rainfall estimation, and (**2**) delineating the areas of the Nile Basin where estimation accuracy is fairly reliable (e.g., Lake Victoria basin, Ethiopia) and those where better ground data are clearly needed. An application over the Lake Victoria and its watershed shows that remote sensing can enhance the value of conventional data and support water resources assessments and management.

Training

Training on this model has been limited to remote sensing methodologies during the first training workshop in Dar es Salaam, Tanzania (June 2002). Due to data delivery delays, the model was not part of the Nile DST at the time of the second training workshop in Uganda (February, 2003).

Technical Report and Manual

A detailed technical report and manual describing the remote sensing method, comprehensive data quality control, basin-wide assessments, and model usage have been developed and provided as part of the final deliverables.

6.2 Nile DST Remote Sensing: Future Opportunities

The remote sensing model and its value for the countries has shown to have significant promise and can be improved in the following ways:

- *Training:* Detailed review of the assessments and hands-on training has not been conducted and is recommended.

- *Data Availability and Quality:* First, important gaps in the already acquired satellite data can be filled with data obtained directly from Eumetsat, the management agency of the Meteosat satellites. These are voluminous data, and their acquisition may a few months. However, compiling a long data base of satellite images (e.g., 1980 to present) would enable very useful long term assessments and the development of hydrologic models in rain gage scarce areas. Second, rain gage data availability and poor quality affect model calibration, especially in regions featuring strong variations in precipitation patterns. Any further improvement of the remote sensing rainfall estimation procedures will depend strongly on quality control and expansion of the available data. These data needs can only be filled by a concerted effort of the national agencies.

- *Modeling Improvements:* Such improvements can potentially include (1) seasonal re-calibration of the remote sensing parameters based on extended data records and (2) implementation of more sophisticated remote sensing methods such as the Georgia Tech Remote Sending procedure that also incorporates information from the TRMM (tropical rainfall measuring mission) satellite.

7. Conclusions

This report provides an executive summary of the Nile DST development work conducted under the Nile Basin Water Resources Project (GCP/INT/752/ITA) consistent with the project terms of reference. Much has been achieved under this project, despite its limited time and resources. The Nile DST is not only a tool that can provide scientifically valid facts and information to the Nile Basin decision makers, but it also represents a foundation for further developments as well as vehicle for capacity building.

Further Assessment Capabilities: At its present form, the Nile DST assessments are expressed in quantities of river flow, water supply, food production, and energy generation. Building on these developments, it is now possible to introduce the next layer of assessment capabilities that can translate these physical outputs into economic and social benefits and impacts. Furthermore, a water quality component can be added to enable fully integrated assessments.

Long Term Capacity Building: While the purpose of the above-mentioned training activities is to ensure that a core modeling group has sufficient expertise to effectively use the Nile-DST, long term capacity building aims at steadily expanding this human resource pool in size as well as in scientific and engineering knowledge. Although the Nile-DST is a useful tool for the Nile Basin countries, its most important impact could be as an educational and capacity building instrument. As described earlier, the Nile DST incorporates several science and engineering disciplines, from database and software development to meteorology, hydrology, agricultural science, remote sensing, and policy assessment, and represents an extensive knowledge base upon which to build formal college and professional education programs.

In this regard, engaging existing or planned water resources centers (e.g., centers that may be established under NBI) represents an excellent follow-up opportunity. These centers could include country professionals from agencies, universities, NGO’s, etc., and could take on the responsibility to maintain and continue to develop these technical tools and data bases. Center personnel would be knowledgeable in data analysis, quality control, and the theory and use of the modeling tools. As new data and models are developed, center engineers and scientists would release new versions to the country agencies, perform the installations, and conduct training for the national professionals.

In collaboration with the universities in the region, Georgia Tech and other institutions of higher learning could contribute courses and seminars (on-site or via distance learning means); educate scientists and engineers at the Masters and Ph.D. levels (abroad as well as in the region); establish joint degree programs in meteorology, hydrology, water resources, agricultural planning, environmental science, and socio-economics; and bring to bear a lasting mechanism for capacity building and the continuous development of technical professionals. In time, the centers would provide valuable services to the Nile Basin countries and would produce the human resources necessary to develop sound and sustainable water sharing and management policies.

INFORM: Integrated Forecast and Reservoir Management System for Northern California

Basic Information

Title:	INFORM: Integrated Forecast and Reservoir Management System for Northern California
Project Number:	2002GA29O
Start Date:	7/1/2002
End Date:	6/30/2005
Funding Source:	Other
Congressional District:	11
Research Category:	Climate and Hydrologic Processes
Focus Category:	Hydrology, Management and Planning, Surface Water
Descriptors:	Integrated Forecast-Decision Systems for River Basin Management
Principal Investigators:	Aris P. Georgakakos, Konstantine P. Georgakakos

Publication

1. Georgakakos, A., and K. Georgakakos, 2003, Value of Climate and Hydrologic Forecasts for River Basin Planning and Management, Key Note Address, GEWEX Workshop, IUGG Conference, Saporo, Japan.
2. Georgakakos, A.P. and H. Yao, 2003, Climate Variability and Change Assessments for the ACR and ACT River Basins, in Proceedings of the 2003 Georgia Water Resources Conference, April 23-24, 2003, at University of Georgia. Kathryn J. Hatcher, editor, Institute of Ecology, University of Georgia, Athens, GA.

Information Transfer Program

Georgia Water Resources Conference, March 2003

Basic Information

Title:	Georgia Water Resources Conference, March 2003
Project Number:	2002GA24B
Start Date:	4/24/2003
End Date:	4/25/2003
Funding Source:	104B
Congressional District:	11
Research Category:	Not Applicable
Focus Category:	Water Quantity, Water Quality, Management and Planning
Descriptors:	Biennial statewide conference
Principal Investigators:	

Publication

2003 Georgia Water Resources Conference

GWRI is a co-sponsor of the Georgia Water Resources Conference. In FY 2002, as part of a GWRI initiative, conference proceedings were electronically compiled and distributed on CD's. Furthermore, the proceedings have been incorporated in and are publicly accessible through the GWRI website. Conference proceedings can be searched through the hyperlinked table of contents, from which papers can be accessed to view and print. Currently, GWRI is in the process of converting into electronic format past Georgia Water Resources Conference proceedings. The outline of 2003 GWRC proceedings is included below.

CONFERENCE TRACKS

TABLE OF CONTENTS

KEYNOTE SPEAKERS

TRACK I. GEORGIA WATER POLICY AND PLANNING

GEORGIA WATER POLICY - I
IS WATER A PUBLIC RESOURCE OR PRIVATE COMMODITY?
Moderator: Peter Appel, UGA School of Law

GEORGIA WATER POLICY - II

TRACK II. METRO NORTH GEORGIA WATER ISSUES

METRO AREA WATERSHED MANAGEMENT

Moderator: Kevin Green, Metro Atlanta Chamber of Commerce

SOURCE WATER PROTECTION

-Moderator: Jim Patterson, Columbus Water Works

GRIFFIN STORMWATER MANAGEMENT PROGRAM

Moderator: Brant Keller, City of Griffin

STORMWATER MANAGEMENT

-Moderator: Bob Donaghue, DNR Pollution Prevention Assistance Division

TRACK III. NONPOINT SOURCES AND BUFFERS

SEDIMENT MANAGEMENT

-Moderator: Terry Sturm, Civil and Env. Engineering, Georgia Tech

RIPARIAN BUFFERS AND FORESTRY

-Moderator:

RIPARIAN BUFFER MANAGEMENT

-Moderator:

GREENSPACE AS 404B MITIGATION

Moderator: Keith Parsons, Georgia Environmental Protection Division

TRACK IV. RESTORATION AND SAVANNAH RIVER

AQUATIC ECOLOGY

Moderator: Alan Covich, UGA Institute of Ecology

SAVANNAH RIVER BASIN COMPREHENSIVE STUDY ....

Moderator: Leroy Crosby, USACE Savannah District

SAVANNAH RIVER ECOSYSTEM FLOWS

Session Organizer: Judy Meyer, Institute of Ecology, University of Georgia
Moderator: Kim Lutz, The Nature Conservancy

SAVANNAH HARBOR AND COAST

TRACK V. MONITORING AND FLINT RIVER

FLOODS AND STORMS

FLOODS AND DROUGHTS

STREAM MONITORING

FLINT RIVER ISSUES

TRACK VI. GROUNDWATER, COAST AND ALTAMAHA RIVER

COASTAL AQUIFER SALT INTRUSION

COASTAL WATER SUPPLY

COASTAL WATER CONSERVATION

GROUNDWATER SUPPLY IN PIEDMONT

ALTAMAHA RIVER AND ESTUARY

COASTAL WATER ISSUES

GROUNDWATER AT S.R.S.

GROUNDWATER CONTAMINATION
-Moderator:

POSTER SESSION

Hydrologic Engineering for Dam Design

Basic Information

Title:	Hydrologic Engineering for Dam Design
Project Number:	2002GA25O
Start Date:	10/15/2002
End Date:	10/16/2002
Funding Source:	Other
Congressional District:	11
Research Category:	Engineering
Focus Category:	Hydrology, Floods, Water Supply
Descriptors:	Continuing Education Course
Principal Investigators:	, Bert Holler

Publication

Nile Decision Support Tool Software Training Workshops

Basic Information

Title:	Nile Decision Support Tool Software Training Workshops
Project Number:	2002GA26O
Start Date:	6/1/2002
End Date:	6/30/2002
Funding Source:	Other
Congressional District:	11
Research Category:	Climate and Hydrologic Processes
Focus Category:	Hydrology, Water Supply, Irrigation
Descriptors:	Decision Support, River Basin Planning and Management, Remote Sensing, Hydrology, Agricultural Planning, Hydropower
Principal Investigators:	Aris P. Georgakakos, Stephen Bourne, Carlo De Marchi, Amy C. Tidwell, Huaming Yao

Publication

Nile Decision Support Tool Software Training Workshops

Basic Information

Title:	Nile Decision Support Tool Software Training Workshops
Project Number:	2002GA27O
Start Date:	2/15/2003
End Date:	2/28/2003
Funding Source:	Other
Congressional District:	11
Research Category:	Engineering
Focus Category:	Hydrology, Irrigation, Water Use
Descriptors:	Information and modeling systems, databases, river models, reservoir management
Principal Investigators:	Aris P. Georgakakos, Stephen Bourne, Huaming Yao

Publication

Nile Decision Support Tool Software

Basic Information

Title:	Nile Decision Support Tool Software
Project Number:	2002GA30O
Start Date:	7/1/2001
End Date:	6/30/2003
Funding Source:	Other
Congressional District:	11
Research Category:	Climate and Hydrologic Processes
Focus Category:	Agriculture, Hydrology, Water Use
Descriptors:	Decision support systems, river basin planning and management
Principal Investigators:	, Aris P. Georgakakos

Publication

1. Georgakakos, A., H. Yao, K. Brumbelow, C. Demarchi, S. Bourne, A. Tidwell, L. Visone, 2003, Nile Decision Support Tool : 1) Executive Summary, 2) Database, 3) River Basin Planning and Management, 4) Agricultural Planning, 5) Hydrology, 6) Remote Sensing . Georgia Water Resources Institute Technical Reports, School of Civil and Environmental Engineering, Atlanta, GA.
2. Georgakakos, A., H. Yao, K. Brumbelow, C. Demarchi, S. Bourne, A. Tidwell, L. Visone, 2003, Nile Decision Support Tool Software and Manual (Alpha Version Jul. 2002, Beta Version Feb. 2003, Version 1.0 Jun. 2003). Georgia Water Resources Institute Technical Report, School of Civil and Environmental Engineering, Atlanta, GA.

Nile Decision Support Tool Software

This decision support system combines extensive hydro-climatic data bases with state of the science hydrologic, agricultural, and water resources models to assess the merits and impacts of alternative development and management policies for the Nile Basin. The Nile DST software and associated reports (6 volumes) and user manuals (6 documents) has been developed and provided to the Nile Basin countries (Burundi, Congo, Egypt, Ethiopia, Eritrea, Kenya, Rwanda, Sudan, Tanzania, and Uganda). Training and technology transfer activities are taking place with all water related Nile Basin country agencies (i.e., Ministries of Water and Environment, Ministries of Agriculture, Ministries of Energy, and Hydro-Meteorological Services, among others).

GWRI Website Upgrade

Basic Information

Title:	GWRI Website Upgrade
Project Number:	2002GA31S
Start Date:	7/1/2001
End Date:	6/30/2002
Funding Source:	Supplemental
Congressional District:	11
Research Category:	Not Applicable
Focus Category:	None, None, None
Descriptors:	Information dissemination, web site
Principal Investigators:	Aris P. Georgakakos, Stephen Bourne

Publication

GWRI Website Upgrade

Introduction:

During FY 2002, the GWRI website at www.gwri.org has been re-designed to better inform the academic and professional communities of on-going research activities and technology transfer and educational opportunities. The website provides comprehensive information on research projects, investigators, publications, software, proceedings of the Georgia Water Resources Conferences, continuing education and employment opportunities, useful links to water related and partner organizations, and a calendar of important water resources events in Georgia.

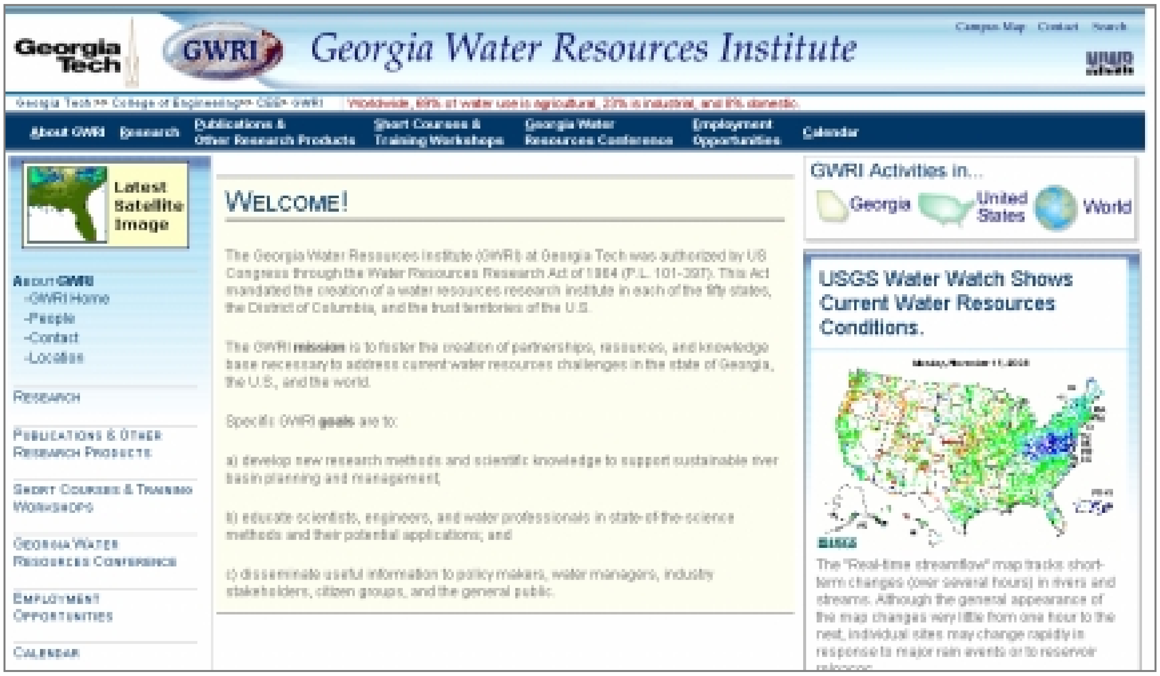

WELCOME!

The Georgia Water Resources Institute (GWRI) at Georgia Tech was authorized by US Congress through the Water Resources Research Act of 1984 (P.L. 101-397). This Act mandated the creation of a water resources research institute in each of the fifty states, the District of Columbia, and the trust territories of the U.S.

The GWRI **mission** is to foster the creation of partnerships, resources, and knowledge base necessary to address current water resources challenges in the state of Georgia, the U.S., and the world.

Specific GWRI **goals** are to:

a) develop new research methods and scientific knowledge to support sustainable river basin planning and management;

b) educate scientists, engineers, and water professionals in state-of-the-science methods and their potential applications; and

c) disseminate useful information to policy makers, water managers, industry stakeholders, citizen groups, and the general public.

USGS Water Watch Shows Current Water Resources Conditions.

The "Real-time streamflow" map tracks short-term changes (over several hours) in rivers and streams. Although the general appearance of the map changes very little from one hour to the next, individual sites may change rapidly in response to major rain events or to reservoir

Structure and Features:

The GWRI website is organized into the following sections:

1. **About** – This section holds information on the establishment, location, and contact information for GWRI. Further, it contains listings of the GWRI Advisory Board, staff, and associated faculty. Each person associated with GWRI is listed with a short description of his or her research interests and a link to a more in-depth personal web page. Vitae web pages for GWRI staff members are housed on the site and describe in detail their work at GWRI.

2. **Research** – The research section describes the research projects conducted by GWRI staff and associated faculty since 1997. Projects are subcategorized according to whether they were conducted by GWRI staff or were sponsored by GWRI and conducted by associated faculty. The GWRI staff projects are further sub-categorized according to their geographic focus: Georgia, the United States,

or the World. An archive of all GWRI research projects since 1964 is planned and will be online soon.

3. **Publications & Other Research Products** – GWRI's research and technology transfer activities produce many different research products including journal articles, conference proceedings, student theses, project technical reports, and software. This section of the website provides access to all of these products in a concise and dynamic listing format.

4. **Short Courses & Training Workshops** –This section lists the educational GWRI efforts. Through the Georgia Tech Continuing Education Department, GWRI offers many professional short courses. Past and proposed courses are listed and described in detail. To help tailor the course offerings, the website hosts a survey that gathers information about which courses are desired in the professional community. Also described in this section are GWRI's technology transfer workshops in the US and abroad.

5. **Georgia Water Resources Conference** - GWRI is a co-sponsor of the Georgia Water Resources Conference, which brings together water resources researchers, professionals, and citizen groups to discuss important water resources issues for Georgia. This section of the website provides news about the upcoming conference as well as archives of past conference proceedings.

6. **Employment Opportunities** – The Employment opportunities section lists academic and professional employment opportunities in water resources related fields in Georgia. Those interested in posting a position can do so through an online form.

7. **Calendar** – The calendar section lists interesting upcoming water resources events in Georgia, the United States, and the world.

Online Products – In addition to the sections above, the web site provides online products such as remotely sensed infrared radiation images of the southeastern US collected at the GWRI Satellite Data Acquisition Facility.

Technology:

The GWRI website is based on a comprehensive database that enables the majority of the site's pages to be dynamically generated at user request.

MYSQL/PHP Database Driven Design:

The relational database contains information about all of GWRI staff and associated faculty, the projects they have worked on and their research interests. Further, the database contains a table of all research projects, publications, short courses, training workshops, and employment opportunities. These items contain attributes such as the associated investigators, geographic focus, and sponsor. Customized lists of items pertaining to each GWRI activity are automatically generated using the database structure.

Cross-referenced items can be tied together so the website user can conveniently view all activities associated with the project in which they are interested. For example, a given research project page will generate a project description, any associated journal articles, technical reports, software, and any other related items. When a project page is generated, the website queries the database and finds all associated entries with the item being viewed. The resulting web page contains links to all related items.

Standardized Formatting (CSS):

Through standardized formatting (implemented with Cascading Style Sheets), the appearance of the website is both uniform and easily updated. This uniformity is important as the website is designed to follow the general Georgia Tech format. This technology facilitates future website updates and enhancements. This is an important feature in light of future and past projects and activities.

Student Support

Student Support					
Category	**Section 104 Base Grant**	**Section 104 RCGP Award**	**NIWR-USGS Internship**	**Supplemental Awards**	**Total**
Undergraduate	0	0	0	0	0
Masters	3	0	0	0	3
Ph.D.	5	1	1	0	7
Post-Doc.	1	0	0	0	1
Total	9	1	1	0	11

Notable Awards and Achievements

Publications from Prior Projects

None